Western Graduate&PostdoctoralStudies

Western University
Scholarship@Western

Electronic Thesis and Dissertation Repository

8-24-2016 12:00 AM

Martian Gully Formation and Evolution: Studies From the Local to Global Scale

Tanya Nicole Harrison
The University of Western Ontario

Supervisor
Gordon Osinski
The University of Western Ontario Joint Supervisor
Livio Leonardo Tornabene
The University of Western Ontario

Graduate Program in Geology
A thesis submitted in partial fulfillment of the requirements for the degree in Doctor of Philosophy
© Tanya Nicole Harrison 2016

Follow this and additional works at: https://ir.lib.uwo.ca/etd

 Part of the Geology Commons, and the Geomorphology Commons

Recommended Citation

Harrison, Tanya Nicole, "Martian Gully Formation and Evolution: Studies From the Local to Global Scale" (2016). *Electronic Thesis and Dissertation Repository*. 3980.
https://ir.lib.uwo.ca/etd/3980

This Dissertation/Thesis is brought to you for free and open access by Scholarship@Western. It has been accepted for inclusion in Electronic Thesis and Dissertation Repository by an authorized administrator of Scholarship@Western. For more information, please contact wlswadmin@uwo.ca.

Abstract

Gullies in the mid- and high-latitudes of Mars were first observed in Mars Global Surveyor (MGS) Mars Orbiter Camera (MOC) images in 1997. Appearing to be geologically young, they quickly became a feature of interest due to the implication of liquid water in their formation based on distinct morphological characteristics including incised channels, many exhibiting features indicative of fluid flow. However, the temperature and pressure conditions on the surface of Mars during its most recent geologic era have not been conducive to sustaining water in the liquid phase for extended periods of time; therefore, a number of "wet" (water-related) and "dry" (driven by CO_2 gas or granular flow) gully formation mechanisms have been proposed. The goal of this thesis is to conduct a large-scale study of gullies on Mars in order to determine how they are likely to have formed and evolved. I begin with a comprehensive global inventory of martian gullies to determine how their geographic distribution correlates with the effects of past and present climate conditions based on recent models, as well as thermophysical properties of the surface. Then I move to a regional focus in Utopia Planitia in Mars' northern mid-latitudes, using gullies as a stratigraphic marker for the relative timing of formation of other mid-latitude landforms found in the region. Lastly, I take a localized approach within Gasa Crater, a particularly active gully site in the southern mid-latitudes, to investigate methods of looking for recent changes in martian gullies.

Keywords

Mars, landslide processes, mass movement processes, fluvial processes, Earth analogues

Dedication

To my grandfather Jack, and the Ph.D. he never got the chance to complete.

Co-Authorship Statement

Chapter 2: All data collection and processing was completed by Tanya Harrison. Manuscript was written by Tanya Harrison. Comments and editing were provided by Gordon Osinski, Livio Tornabene, and Eriita Jones.

Chapter 3: Data were collected and processed by Tanya Harrison. Manuscript was written by Tanya Harrison. Cassie Stuurman provided SHARAD-related elements for Figure 3.22 and some clarifying text in reference to her SHARAD work. Comments and editing were provided by Gordon Osinski, Livio Tornabene, and Cassie Stuurman.

Chapter 4: The concept behind this paper grew from a discussion with co-author Susan Conway while going over the null results of a previously attempted study by T. Harrison looking at the thermal inertia of gullied vs. non-gullied slopes within craters. Data collection, processing, and manuscript writing were completed by Tanya Harrison. Comments and editing were provided by Gordon Osinski and Livio Tornabene.

Acknowledgments

Thank you to my advisors, Drs. Gordon Osinski and Livio Tornabene, for your guidance and bringing me into such a fantastic group of people at CPSX. I've been extremely lucky to have an amazing support network here in our not-so-little group—something I've not really had before. Huge thanks to, in no particular order, Annemarie Pickersgill, Alexandra Pontefract, Cassandra Marion, Marianne Mader, Emily McCullough, Bhairavi Shankar, Haley Sapers, Christy Caudill, Jared Shivak, and Mike Craig for all of your advice, words of encouragement, and for generally being amazing. Thanks are also due to Tim Haltigin, Phil McCausland, and Robbie Flemming for (perhaps sometimes unknowingly) saying the right things at the right time. And thank you to the members of the Seattle chapter of The Mars Society/National Space Society for getting me started on this path, and for encouraging me along the way.

I also owe a huge debt of gratitude to Nina Lanza, for helping me find both my inner strength and inner extrovert, and for helping me become a better scientist over the past decade. I am confident I wouldn't be where I am today without your encouragement, advice, and support over the years.

To Cassie Stuurman, for being a constant source of inspiration and support in the relatively short period during which our orbits have crossed, and for being there during the best and worst of times.

To Jenna Wakenight—for everything, no matter how many miles are between us.

And lastly to Don Fay, for encouraging me to change my life to a path where I would be happier than the path on which I'd been. Without your love and support, I might have remained complacent and unhappy. Instead, a whole new world of opportunities opened up to me, and I was finally able to smile again. For that, I am truly grateful.

Table of Contents

List of Tables

Chapter 1:

Chapter 2:

Chapter 4:

List of Figures

Chapter 1:

Chapter 2:

Chapter 3:

Chapter 4:

Chapter 5:

List of Appendices

List of Abbreviations

CCF	Concentric crater fill
CRISM	Compact Reconnaissance Imaging Spectrometer for Mars
CTX	Context Camera
DEM	Digital elevation model
FCCF	Frost-coated clast flow
GCM	Global circulation model
GRS	Gamma-Ray Spectrometer
HiRISE	High Resolution Imaging Science Experiment
HRSC	High Resolution Stereo Camera
JPL	Jet Propulsion Laboratory
LDM	Latitude-dependent mantle
LVF	Lineated valley fill
MEPAG	Mars Exploration Program Analysis Group
MEX	Mars Express
MGS	Mars Global Surveyor
MOC NA	Mars Orbiter Camera (narrow angle)
MOLA	Mars Orbiter Laser Altimeter
MRO	Mars Reconnaissance Orbiter
MSSS	Malin Space Science Systems
MY	Mars Year
NASA	National Aeronautics and Space Administration
OMEGA	Obervatoire pour la Minéralogie, l'Eau, les Glaces et l'Activité
PDS	Planetary Data System
RSL	Recurring slope lineae
SDBT	Scalloped depression bearing terrain
SHARAD	Shallow Radar
TES	Thermal Emission Spectrometer

THEMIS VIS	Thermal Emission Imaging Spectrometer (visible subsystem)
THEMIS IR	Thermal Emission Imaging Spectrometer (infrared subsystem)
UA	University of Arizona
USGS	United States Geological Survey

Chapter 1: Background & Literature Review

1.1 Introduction

On Earth, gullies are defined as incised channel features carved by overland flow, seepage erosion, landsliding, and/or subsurface flow [e.g., *Montgomery and Dietrich*, 1988; *Bull and Kirkby*, 1997]. Features resembling terrestrial gullies were first observed on the walls of martian craters, valleys, and massifs in images from the Mars Global Surveyor (MGS) narrow-angle Mars Orbiter Camera (MOC NA) acquired in 1999 [*Malin and Edgett*, 2000a]. As described by Malin and Edgett [2000a], martian gullies typically consist of three characteristic features: A head alcove, a set of main and secondary channels, and a depositional apron (Figure 1.1). The head alcove represents the main area of slope failure, providing the source material for the depositional apron located at the base of the slope. The main and secondary channels extend from within the alcove downslope, terminating at the upper portion of the depositional apron. The channels often exhibit streamlined features, terraces [e.g., *Schon and Head*, 2012], and braided/anastomosing patterns [e.g., *Levy et al.*, 2009a; *Gallagher et al.*, 2011], decreasing in order as they progress downslope, and occur on slopes higher than the angle of repose—all of which are highly suggestive of formation by erosion involving fluid in some capacity. The depositional aprons generally lack superimposed landforms and crosscutting features such as aeolian dunes and impact craters, implying that martian gullies are geologically youthful ($\lesssim$1 Ma). This suggests the possibility of flowing water on the surface of Mars in the geologically recent past, and thus these features have generated significant interest in the scientific community.

Another observation with the initial discovery of gullies on Mars, subsequently confirmed by later surveys, was the confinement of gullies to latitudes poleward of ~30° in both hemispheres [*Malin and Edgett*, 2000a; *Heldmann and Mellon*, 2004; *Balme et al.*, 2006; *Bridges and Lackner*, 2006; *Heldmann et al.*, 2007; *Kneissl et al.*, 2010; *Harrison et al.*, 2015]. Mass movement features similar in size to gullies on slopes equatorward of 30° latitude have morphologies distinctly different from gullies, as they

lack incised channels (although some authors have inappropriately classified these as "gullies" [*Treiman*, 2003; *Shinbrot et al.*, 2004]) (Figure 1.2). Gullies were also initially found (based on very areally limited data) to occur predominantly on pole-facing slopes [*Malin and Edgett*, 2000a]. The combination of this pole-facing dominance and latitudinal restriction led authors to suggest that climate and insolation played key roles in gully formation [e.g., *Mellon and Phillips*, 2001; *Costard et al.*, 2002], furthering the possibility that flowing water was involved. Malin and Edgett [2000a] attributed the formation of martian gullies to seepage and runoff from shallow subsurface aquifers. However, the temperature and pressure conditions on the surface of Mars during its most recent geologic era have not been conducive to sustaining water in the liquid phase for extended periods of time [e.g., *Carr*, 1983; *Martínez and Renno*, 2013]. Because of this, a number of "wet" and "dry" gully formation mechanisms have been proposed: release of liquid water/brine from shallow [*Malin and Edgett*, 2000a; *Mellon and Phillips*, 2001] or deep aquifers [*Gaidos*, 2001]; liquid CO_2 aquifers [*Musselwhite et al.*, 2001]; melting of near-surface ground ice [*Costard et al.*, 2002; *Gilmore and Phillips*, 2002]; melting snowpacks [*Hartmann et al.*, 2002; *Lee*, 2002; *Christensen*, 2003; *Williams et al.*, 2009]; melting of seasonal frost [*Kossacki and Markiewicz*, 2004]; frosted granular flow [*Hugenholtz*, 2008]; CO_2-gas-fluidized flows [*Hoffman*, 2002; *Cedillo-Flores et al.*, 2011], and dry granular flow [*Treiman*, 2003; *Shinbrot et al.*, 2004; *Pelletier et al.*, 2008; *Kolb et al.*, 2010]. The details of each of these proposed mechanisms will be described in Section 1.2.

Thanks to the MGS MOC, Mars Odyssey Thermal Emission Imaging System (THEMIS) visible subsystem (VIS) [*McConnochie et al.*, 2006], Mars Express (MEX) High-Resolution Stereo Camera (HRSC) [*Jaumann et al.*, 2007], and Mars Reconnaissance Orbiter (MRO) Context Camera (CTX) [*Malin et al.*, 2007] and High Resolution Imaging Science Experiment (HiRISE) [*McEwen et al.*, 2007], there are nearly 20 years of continuous observations of the martian surface (March 1997 to the present), permitting investigations of changes over time. Routine gully monitoring efforts by the MOC [*Malin et al.*, 2006], CTX [*Harrison et al.*, 2009a], and HiRISE

teams [e.g., *Dundas et al.*, 2010, 2012, 2015] revealed that ~40 gullies are active today. Observed activity ranges from the movement of a few boulders [*Dundas et al.*, 2012] to distinctive new apron deposits [e.g., *Malin et al.*, 2006; *Harrison et al.*, 2009a; *Dundas et al.*, 2012, 2015]. This means that whatever process initially formed gullies on Mars may still be active today, and therefore this needs to be taken into consideration when analyzing proposed formation mechanisms.

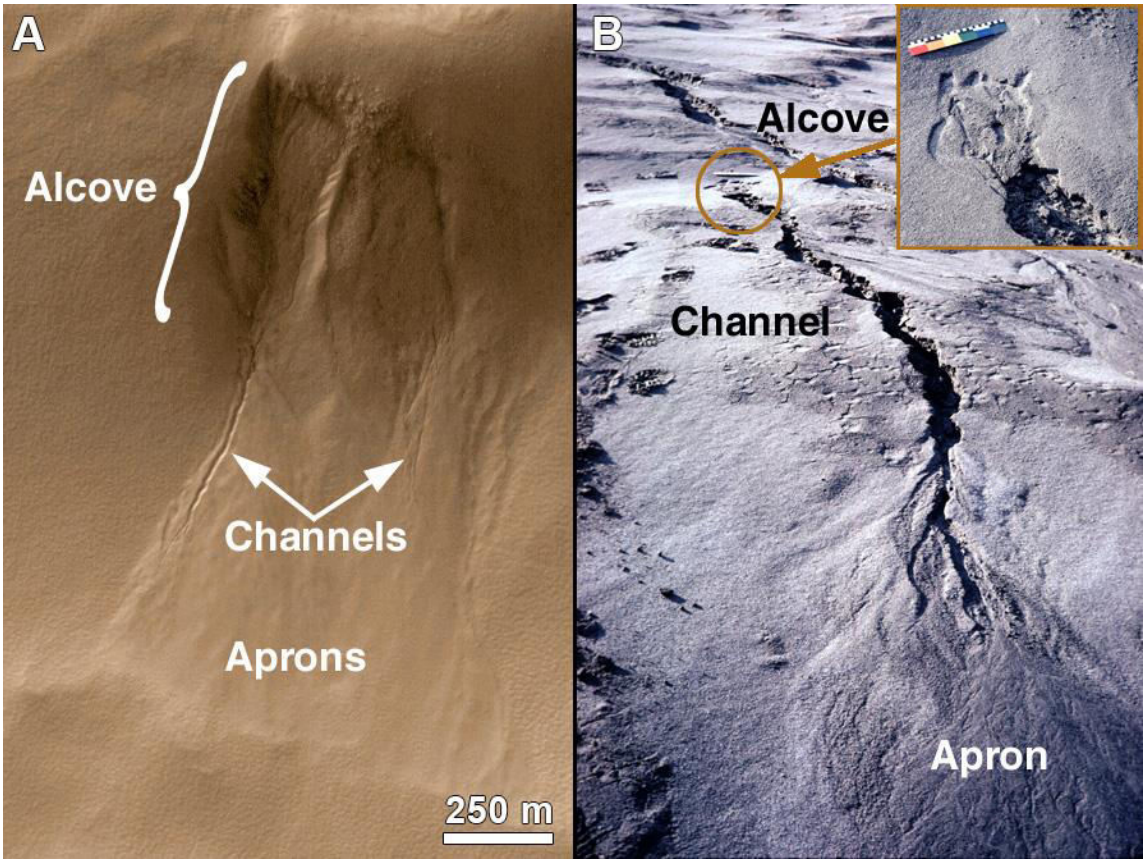

Figure 1.1. (A) Gullies in the southern mid-latitudes (54.5°S, 17.5°E) of Mars with the three characteristic features labelled: alcove, channels, and aprons. Subframe of MOC NA M03-00537. North is to the upper right. **(B)** Gully at Mount St. Helens, Washington, imaged by Michael C. Malin. Coloured bar is 30 cm long. Modified from MGS MOC Release No. MOC2-234, http://www.msss.com/mars_images/moc/june2000/labeled/.

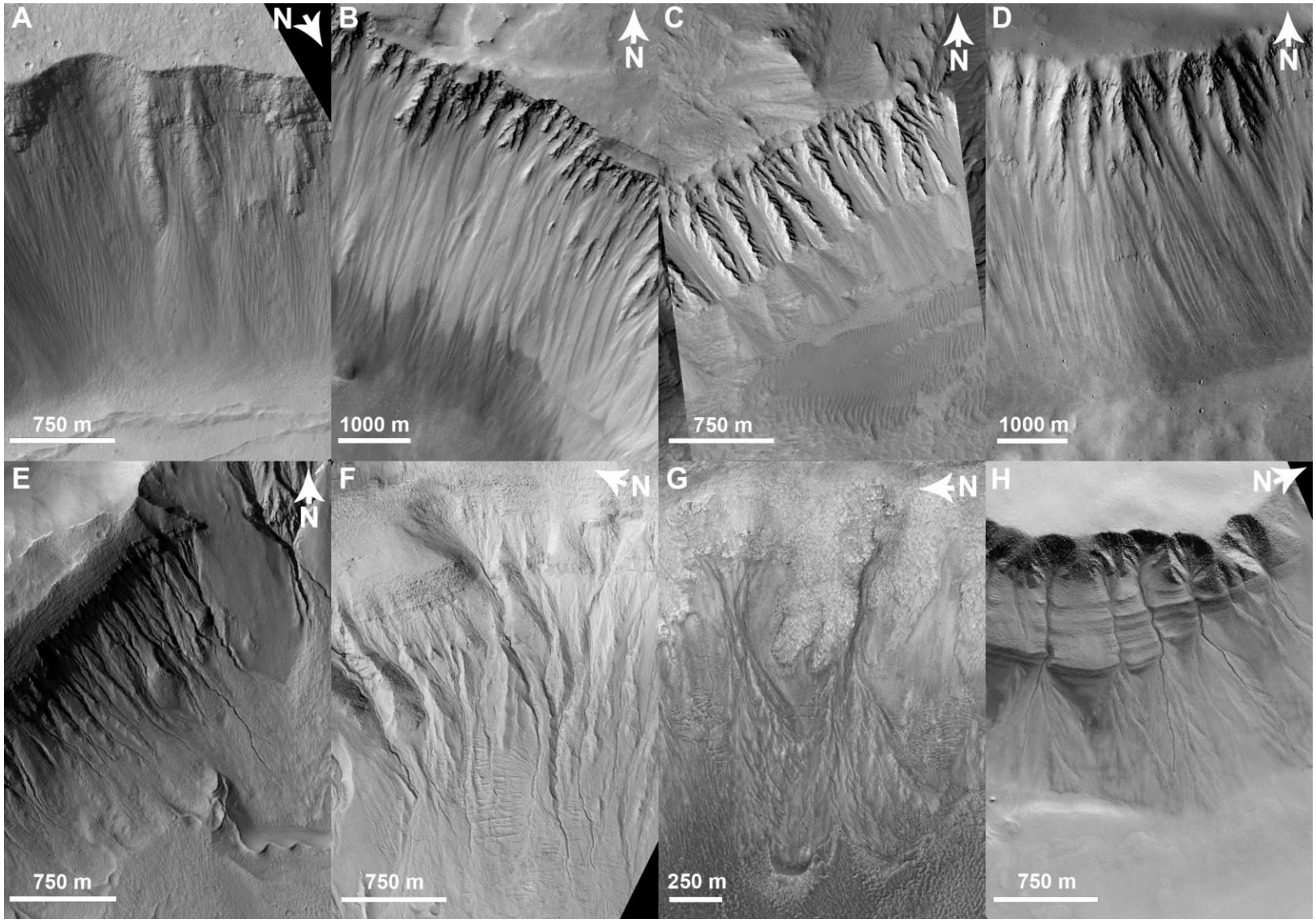
A
N
750 m
B
N
1000 m
C
N
750 m
D
N
1000 m
E
N
750 m
F
N
750 m
G
N
250 m
H
N
750 m

Figure 1.2. Comparison of equatorial mass movement features (A–C cited as gullies by Treiman (2003), D cited as gullies by Shinbrot et al. (2004)) and mid- to high-latitude gullies (E–H). Note the lack of sinuous, deeply incised channels in the equatorial features, which are characteristic of martian mid- to high-latitude gullies. **(A)** Northern wall of the Tharsis Tholus caldera, 13.94°N, 90.92°W, subframe of MOC E03-01974. **(B)** Northwestern wall of the Olympus Mons caldera, 18.64°N, 133.94°W, subframe of HiRISE PSP_004821_1985. **(C)** Northern wall of the Pavonis Mons caldera, 0.85°N, 112.81°W, subframe of MOC M18-01192. **(D)** Mass movement chutes on light-toned layered material in East Candor Chasma, 7.25°S, 69.04°W, subframe of MOC M11-02514. **(E)** Gullies on the northeastern wall of Niquero Crater, 39.05°S, 166.12°W, subframe of MOC E11-04033. **(F)** Gullies on the eastern wall of a crater southwest of Acidalia Mensa, 44.59°N, 26.22°W, subframe of HiRISE PSP_006953_2245. **(G)** Gullies on the northeastern wall of a crater in Newton Crater, 41.83°S, 157.83°W, subframe of HiRISE PSP_005943_1380. **(H)** South polar pit gullies near Sisyphi Cavi, 68.65°S, 358.79°W, subframe of HiRISE ESP_013585_1115.

The goal of this thesis is to conduct a large-scale study of gullies on Mars in order to determine how they are likely to have formed and evolved, and if they are still active today. This study begins with conducting a comprehensive global inventory of martian gullies. This survey of gullies is used to determine how their geographic distribution correlate with the effects of past and present climate and seasonal conditions based on recent models, as well as thermophysical properties of the surface. Then I move to a regional focus on Utopia Planitia in Mars' northern mid-latitudes, using gullies as a stratigraphic marker for the relative timing of formation of other mid-latitude landforms found in the region. Lastly, I take a localized approach within Gasa Crater, a particularly active gully site in the southern mid-latitudes, to investigate methods of looking for recent changes in martian gullies.

1.2 Mars climate history

Over the past 10 Ma, Mars has undergone large obliquity shifts, ranging up to ~60° [*Laskar et al.*, 2004]. On shorter timescales, however, Mars experiences smaller and shorter-duration obliquity changes (Figure 1.3). Its current obliquity is ~25°, but over the past 2.1–2.5 Ma the planet has undergone 15–20 shifts to obliquities >30° with a periodicity of ~120,000 years [*Mischna*, 2003; *Laskar et al.*, 2004]. These shifts result

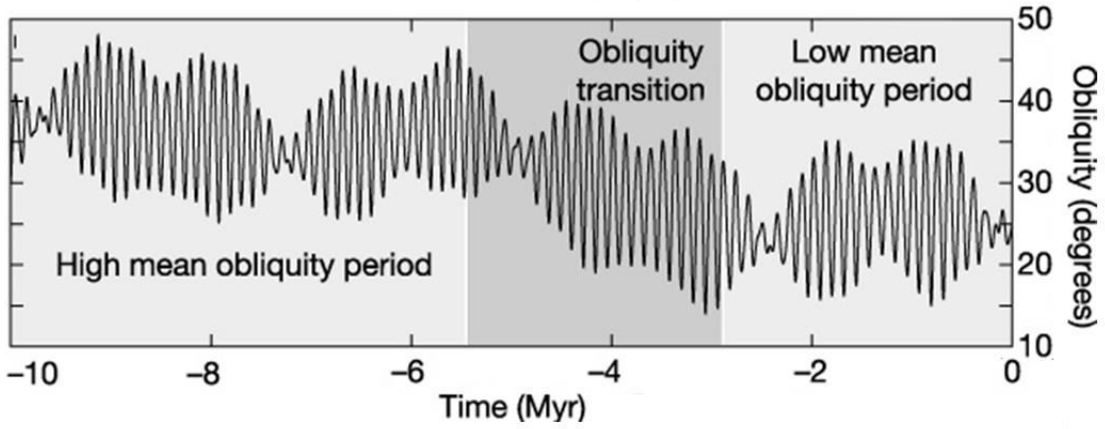

Figure 1.3. Obliquity variations (in degrees) over the past 10 Myr as modelled by Laskar et al. [2004]. The main obliquity periodicity is ~120,000 Earth years. From Levrard et al. [2004].

in changes in the latitudinal range of surface water-ice stability, leading to redistribution of ice from the (current) poles to the mid-latitudes [*Mischna*, 2003; *Levrard et al.*, 2004; *Forget et al.*, 2006; *Madeleine et al.*, 2009] (Figure 1.4). Evidence of this redistribution of ice includes inference of subsurface ice in the mid-latitudes based on the detection of hydrogen from the Mars Odyssey Gamma-Ray Spectrometer (GRS) [*Boynton*, 2002; *Feldman*, 2004], the detection of subsurface interfaces with dielectric properties consistent with that of water ice in parts of the mid-latitudes by the MRO Shallow Radar (SHARAD) instrument [e.g., *Stuurman et al.*, 2013, 2014; *Bramson et al.*, 2014], the observation of subsurface water-ice by the Phoenix lander [*Smith and the Phoenix Science Team*, 2009], and the present-day excavation of subsurface water ice by newly-formed impact craters in the mid-latitudes as observed by MRO CTX, HiRISE, and Compact Reconnaissance Imaging Spectrometer for Mars (CRISM) [*Byrne et al.*, 2009; *Dundas and Byrne*, 2010]. Additional evidence is inferred based on a suite of landforms unique to the mid-latitudes of Mars whose morphologies are suggestive of the current and/or former presence of water-ice, such as concentric crater fill, lineated valley fill, debris covered glaciers (formerly known as “lobate debris aprons” [e.g., *Squyres*, 1978, 1979; *Squyres and Carr*, 1986]), and crater wall mantling (“pasted-on”) material [*Christensen*, 2003]. In the case of debris covered glaciers, results from SHARAD

indicate the features are composed of nearly pure water ice protected by a layer of dust [*Holt et al.*, 2008; *Plaut et al.*, 2009].

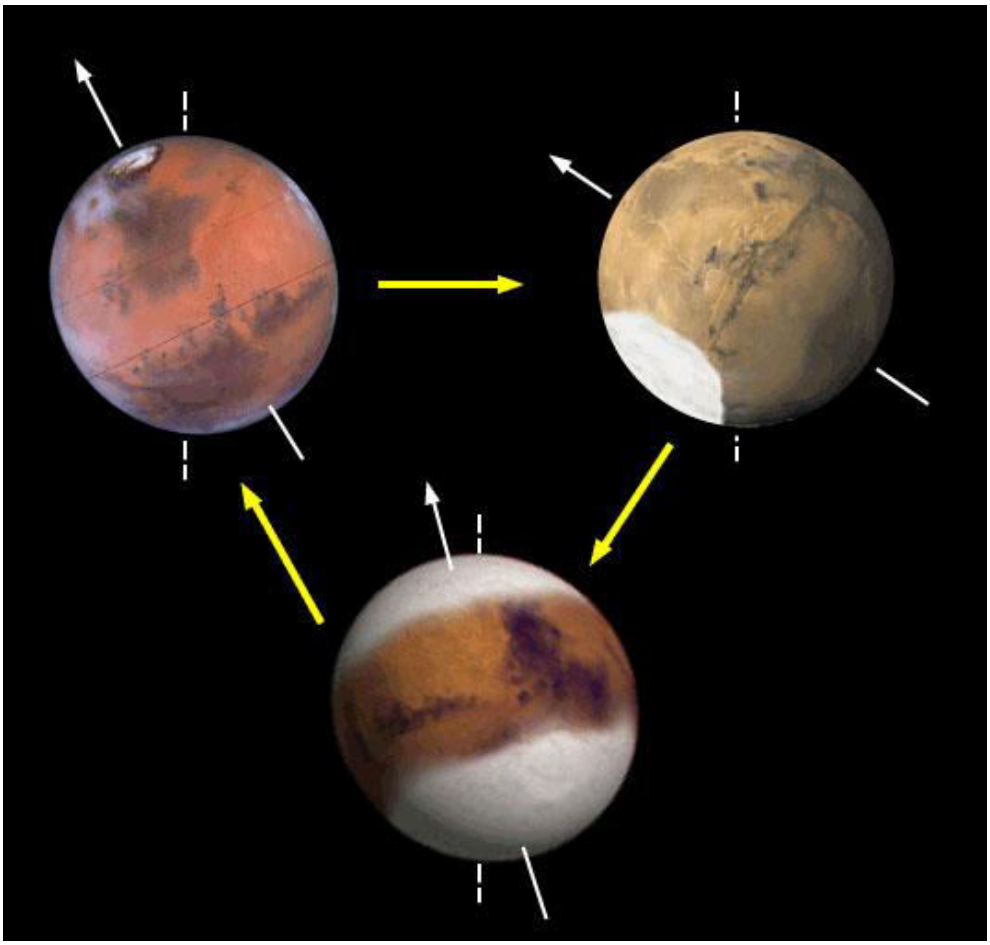

Figure 1.4. Illustration of surface ice distribution on Mars at current obliquity (upper left), high obliquity (upper right), and low obliquity (lower). *Image credit: ASD/IMCCE-CNRS, after Jim Head/Brown University and NASA/JPL-Caltech.*

Another feature unique to the mid-latitudes of Mars is a morphologic unit known as the latitude-dependent mantle (LDM). This unit drapes the middle and high latitudes of Mars, discontinuously from ~30°–45° and continuously at latitudes >45° in both hemispheres [*Kreslavsky and Head*, 2000; *Mustard et al.*, 2001; *Head et al.*, 2003; *Milliken and Mustard*, 2003]. The LDM is interpreted to be composed of a mixture of

ice and dust deposited over the course of multiple obliquity shifts based on the presence of features such as:

1. Polygonal terrain, interpreted to be thermal contraction polygons analogous to those found in periglacial environments on Earth [e.g., *French*, 2007; *Levy et al.*, 2009b];
2. Smooth terrain that gradationally transitions to dissected/highly degraded, pitted terrain, interpreted to be sublimation pits indicative of desiccation of the LDM [*Mustard et al.*, 2001; *Milliken and Mustard*, 2003; *Kostama et al.*, 2006; *Schon et al.*, 2009];
3. Crater size-frequency statistics indicating a geologically recent exposure age* (0.1–1 Ma), supporting the desiccation hypothesis [*Kostama et al.*, 2006; *Schon et al.*, 2012];
4. Metre-scale layering within the LDM traceable up to several kilometres in lateral extent, supporting the role of variations in climate with respect to their deposition [*Schon et al.*, 2009].

Obliquity cycling is expected to have resulted in multiple cycles of deposition and removal of the LDM over the past few million years [*Head et al., 2003*], coinciding with the period during which martian gullies formed [e.g., *Reiss et al.*, 2004; *Schon and Head*, 2012]. Gullies are often observed incising into the LDM, draped on the walls of craters, massifs, mesas, and valleys [*Christensen*, 2003; *Head et al.*, 2008; *Schon et al.*, 2009; *Raack et al.*, 2012; *Conway et al.*, 2015b; *Dickson et al.*, 2015]. This has led some authors to suggest that gully formation is intimately linked to the LDM, by which the LDM may provide a source for meltwater with which gullies are carved [e.g., Christensen, 2003]. Evidence for multiple generations of gullies forming during the repeated cycles of LDM deposition and erosion has been observed in the southern mid-

* On rocky planetary surfaces, crater size-frequency (measure of the number of craters of a given diameter per square kilometre) is used to estimate the "crater retention age" of the surface [e.g., *Hartmann and Neukum*, 2001; *Neukum et al.*, 2001]. In general, an area is interpreted to be older the more craters (and the greater number of large craters) it hosts. However, the crater size-frequency is affected by factors such as the occurrence of secondary impact craters [*McEwen and Bierhaus*, 2006] and the resistance to erosion of the surface materials [*Edgett*, 2009]. The latter means that a geologic unit may be much older than its crater retention age suggests if it is composed of a readily erodible material, as visible evidence of impact craters (and small craters preferentially) will be removed. Thus, the term "exposure age" is more appropriate as it represents how long the current surface that we see today has been exposed at the surface.

latitudes in the form of partially buried, exhumed, and inverted sinuous ridge features occurring on the same slopes as more pristine gullies, all within LDM deposits [Dickson et al., 2015] (Figure 1.5). The latitudinal restriction and apparent correlation of gullies with the LDM lends support to the hypothesis that climate and insolation play key factors in their formation.

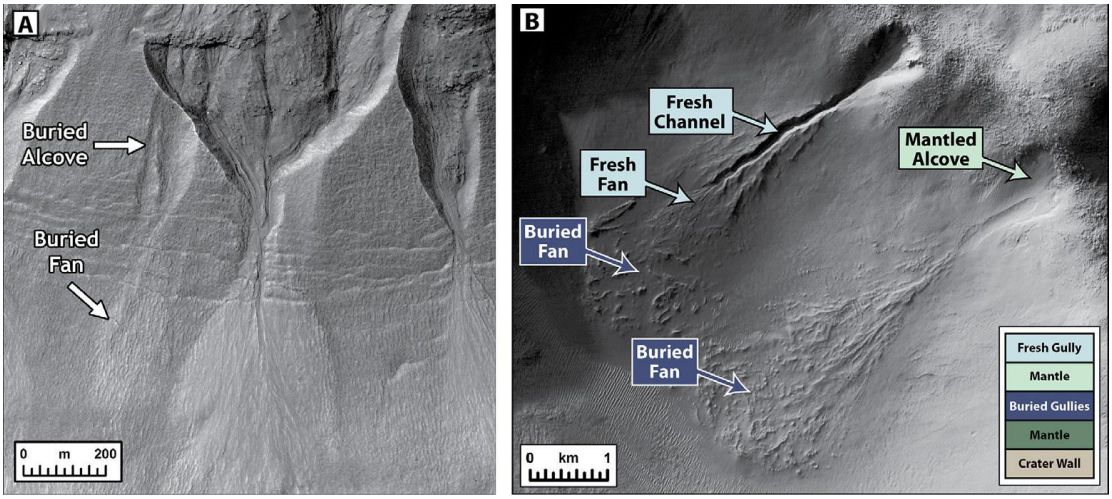

Figure 1.5. Examples of multiple generations of gullies on the same slope from Dickson et al. [2015]. **(A)** Gullies within pasted-on LDM deposits on a pole-facing wall in Harmakhis Vallis at 39.3°S, 91.7°E. Subframe of HiRISE ESP_021770_1405. **(B)** Gullies within pasted-on deposits on a pole-facing crater wall at 48.0°S, 253.5°E. Subframe of CTX P18_008077_1317.

1.3 Defining the term "gully"

The term "gully" describes a type of incised channel morphology, but not a specific geologic process. On Earth, gullies typically form and evolve through multiple mass movement (landslide) processes. Hungr et al. [2001] refined the definitions of flow-type landslides initially defined by Varnes [1978], classifying them based on grain size, water content, and velocity (Table 1.1). These definitions are used here to maintain consistency with terrestrial landslide literature.

Table 1—Classification of landslides of the flow type from Hungr et al. [2001]

Material	Water Content	Special Condition	Velocity	Name
Silt, Sand, Gravel, Debris (talus)	Dry, Moist, or Saturated	-No excess pore pressure -Limited volume	Various	Non-liquefied sand (silt/gravel/debris) flow
Silt, Sand, Debris, Weak rock	Saturated at rupture surface content	-Liquefiable material -Constant water	Extremely rapid	Sand (silt/debris/rock) flow slide
Sensitive clay	≥Liquid limit	-Liquefaction, *in situ* -Constant water content	Extremely rapid	Clay flow slide
Peat	Saturated	-Excess pore pressure	Slow to very rapid	Peat flow
Clay or Earth	Near plastic limit	-Slow movements -Plug flow (sliding)	<Rapid	Earth flow
Debris	Saturated	-Established channel -Increased water content	Extremely rapid	Debris flow
Mud	≥Liquid limit	-Fine-grained debris flow	>Very rapid	Mud flow
Debris	Free water present	-Flood	Extremely rapid	Debris flood
Debris	Partly or fully saturated	-No established channel -Relatively shallow, steep source	Extremely rapid	Debris avalanche
Fragmented rock	Various, mainly dry	-Intact rock at source -Large volume	Extremely rapid	Rock avalanche

1.3.1 Debris flows

Hungr et al. [2001] define debris flows as "a very rapid to extremely rapid flow of saturated non-plastic debris in a steep [established] channel," such as a gully (Figure 1.6). Terrestrial debris flows are typically initiated by overland flow and/or saturation of hillslopes, leading to sliding of overlying unconsolidated material [*Montgomery and Dietrich*, 1994]. The characteristic channels are formed by scouring [*Stock and Dietrich*, 2006] or by self-channelization of the flow within its levees [*Whipple and Dunne*, 1992]. Pore pressure is the key factor in debris flow initiation; increased pore pressure in soil decreases the effective stress and reduces the shear strength of the soil, leading to slope failure [*Brand*, 1981; *Brenner et al.*, 1985].

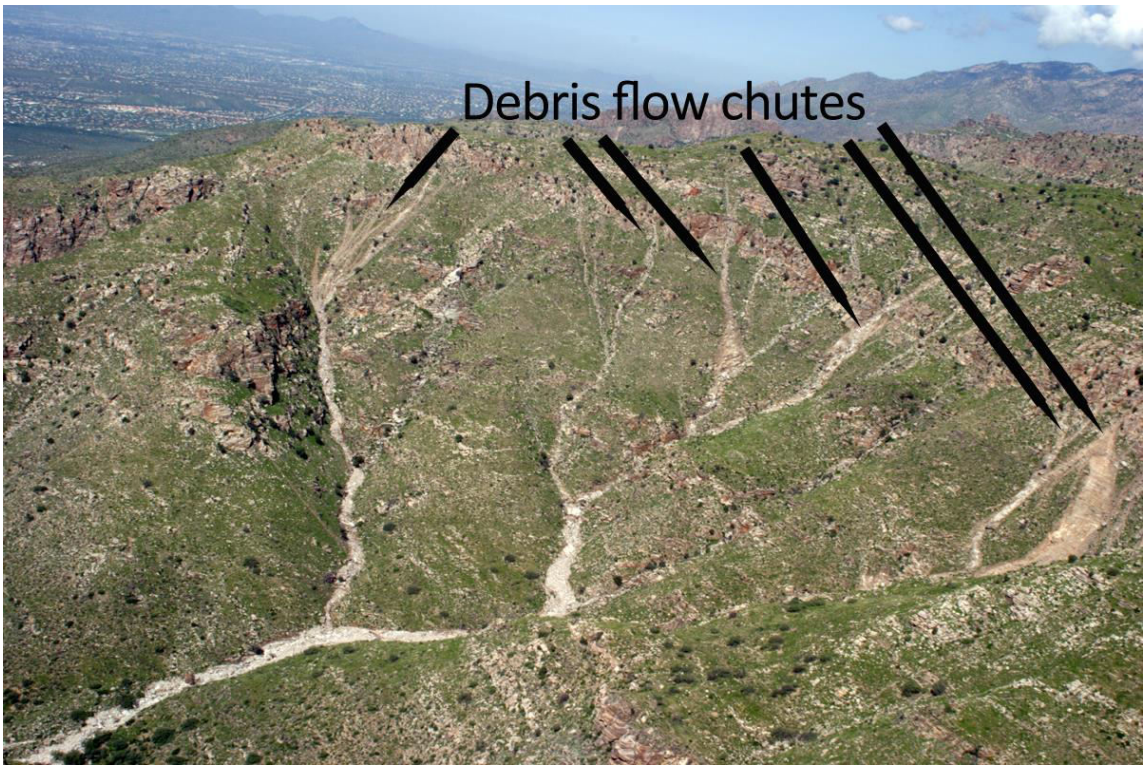

Figure 1.6. Debris flow chutes (gullies) within Soldier Canyon in the Santa Catalina Mountains, north of Tucson, Arizona. *Image credit: Arizona Geological Survey*

There are two types of debris flows: transport-limited and supply-limited [*Bovis and Jakob*, 1999; *Glade*, 2005; *Jakob et al.*, 2005]. Transport-limited debris flows occur when a sufficient amount of water enters a gully where a high volume of sediment is available that may be readily entrained. Supply-limited debris flows on the other hand require time for sediment to build up in the gully channel via erosion, and a flow occurs when both sufficient sediment and water are present. The amount of sediment present in the channel, channel gradient, angle of entry, and initial failure volume are the dominant factors in determining whether a landslide will become a debris flow [*Brayshaw and Hassan*, 2009]. While steeper slopes aid in slope failure, steep slopes are not required for debris flows to propagate once they have been initiated, after which they are able to travel over slopes as low as 1–6° [*Rodine and Johnson*, 1976; *Stock and Dietrich*, 2006]. Poor sorting within the flow leads to a reduction in the effective normal stresses between grains, reducing the apparent friction and allowing the flow to be very dense without any

interlocking grains [*Rodine and Johnson*, 1976]. The flow front is generally (but not always) the thickest part of the flow due to acquiring large clasts as the flow progresses downslope, and kinetic sieving, in which small grains slip through voids in the flow, accumulating larger grains as a residue at the flow surface and front [*Iverson et al.*, 1997]. However, evidence of these flow fronts is often poorly preserved, as they tend to be overtopped and subsequently obscured by the liquefied debris that had been previously confined by the gully channel and/or flow levees (Figure 1.7) [*Iverson et al.*, 2010]. Once the flow is no longer confined by the pre-existing channel, lobate deposits form as the flow loses kinetic energy and comes to a rest. Rough beds promote levee growth by aiding in grain size segregation, helping to channelize flows [*Iverson et al.*, 2010]. Channelization plays a key role in determining runout length, while bed roughness and velocity have little effect; identical channelized material will flow the same distance over rough and smooth beds irrespective of velocity [*Iverson et al.*, 2010]. However, rough bedding also leads to an increase in the angle of repose [*Iverson et al.*, 2010]. Experiments by Iverson et al. [2010] in the 95-m-long USGS Debris-Flow Flume [*Iverson et al.*, 1992] also showed that for any given combination of bed roughness and debris flow composition, the morphology of the flow deposit was very reproducible. Flows consisting of sand, gravel, and loam over rough beds resulted in longer and thinner (~0.1 m thick) flows than the same material flowing over a smooth bed and mixtures of sand and gravel without loam over rough and smooth beds. Levees in these flows were readily overtopped by the liquefied debris and were hence not well preserved. The minimum thickness of debris flow fronts is ~0.1 m (with flow thickness increasing with grain size) as accumulation of unliquified material provides sufficient resistance to inhibit further thinning of the deposit [*Denlinger and Iverson*, 2001]. Coarse-grained surges within the body of the debris flow while in motion increase flow resistance as well, leading to lateral flow instability resulting in digitate deposits ("fingering") [*Pouliquen et al.*, 1997]. The USGS Debris-Flow Flume experiments of Iverson et al. [2010] also showed that deposit morphology is sensitive to channel conditions upslope, with many of their experimental flows predominantly curving or

exhibiting at least one flow lobe curving to the left after exiting the flume ("channel") due to a slight leftward tilt in the flume bed. The mobility of debris flows is largely determined by the proportion of fine-grained material entrained in the flow, as it determines how much water can be retained [*Whipple and Dunne*, 1992] and how quickly the pore pressures are dissipated within the flow, with dissipation time increasing with increasing fine particle content [*Iverson et al.*, 1997, 2010; *Wang and Sassa*, 2003].

Studies of terrestrial debris flows indicate that a sudden influx of water (relative to the *in situ* soil) is required to initiate a flow. Debris flows are commonplace in Iceland, where they are well-studied as they pose a serious threat to many towns and villages [e.g., *Decaulne et al.*, 2005; *Decaulne and Sæmundsson*, 2007]. Field observations have shown that long-term saturation of loose debris from snowmelt is not enough to cause debris flows; rather, a sudden rise in temperature over a short period (hours) or significant amount of rain atop snow is required to initiate a debris flow [*Decaulne and Sæmundsson*, 2007]. A similar relationship is also seen in snow avalanches, where a small increase in liquid water content (<0.5%) does not typically lead to avalanching, but heavy rainfall atop snow will reduce shear strength to the point of slope failure [*Conway and Raymond*, 1993]. Decaulne et al. [2005] observed a series of debris flows in the Gleiðarhjalli area in northwestern Iceland, near the town of Ísafjörður on 10–12 June 1999. The flows were instigated by a temperature increase of up to 17°C in the span of a single day, causing rapid snowmelt to flow through pre-existing gully channels via overland flow. Subsurface flow of meltwater also occurred along an impermeable layer of basalt, resulting in the water emerging within the pre-existing gullies as mid-slope "springs." The estimated denudation rate for this event was 0.29 mm/km^2.

Figure 1.7. Example of a debris flow overtopping its levees. This experimental flow, conducted at the 95 m long USGS debris flow flume, was composed of 66% gravel, 33% sand [*Iverson et al.*, 2010], and some added boulders. Time elapsed since initiation of the flow is expressed in seconds in the lower left corner of each image. Note the occurrence of multiple surges in the first two frames, followed by overtopping of the levees by the liquefied (lighter-toned) material, resulting in digitate deposits. Video available from Logan and Iverson [2013].

In extremely dry climates, such as the Atacama Desert, debris flows can occur after rare rain events. Near the Angofasta research station, 0.25 mm of rainfall fell on 25 April 2005 [*Heldmann et al.*, 2010], resulting in thin flows in pre-existing channels (termed "mudflows" by Heldmann et al. [2010]). The flows were lighter-toned than their surroundings, but were spectrally indistinct from the surrounding material except for an increase in reflectance, indicating that grain size or porosity was responsible for the relative tone of the flow [*Heldmann et al.*, 2010].

Roesli and Schnidler [1990] studied debris flows in the Swiss Alps and found that an increase of only ~3–4-wt% in the water content of the soil was enough to move the material on a slope from the plastic to the liquid flow regime and initiate debris flows. Therefore, multiple terrestrial locations have demonstrated that a relatively small amount of water can produce sizeable debris flows, provided the influx of that water is rapid enough and the amount is sufficient to increase pore pressures to the point of slope failure.

It is important to note that lab-scale debris flow experiments do not scale well to the real world due to disproportionately large influences of viscosity, grain inertia, and yield strength at small scales compared to flows in nature [*Iverson et al.*, 2004, 2010]. Lab-scale experiments also exhibit little effect from pore pressure, which in nature is a key driver for debris flow initiation [*Iverson et al.*, 2004, 2010]. For example, natural flows with a high percentage of fine grains tend to be more mobile than those comprised of predominantly large grains, but small-scale experiments [e.g., *Johnson*, 1970; *O'Brien and Julien*, 1988; *Coussot and Proust*, 1996; *Parsons et al.*, 2001] inaccurately indicate that fine grains increase flow yield strength and viscosity, resulting in increased flow resistance [*Iverson et al.*, 2010]. This scaling issue is what prompted the construction of the aforementioned USGS Debris-Flow Flume.

1.3.2 Dry granular flow

Dry sand/silt/weak rock/debris flow, herein collectively referred to as "dry granular flow" (Figure 1.8), is defined as the flow-like movement of loose dry granular material without significant excess pore pressure [*Hungr et al.*, 2001]. These landslides are typically initiated by shallow planar sliding at or above the angle of repose and tend

to be low in velocity and volume [*Hungr et al.*, 2001]. They often have short, abruptly-ending runout with wider flows that are more coherent than those observed in debris flows. Highly mobile dry silt flows can be initiated due to the collapse of steep cliffs, imparting enough energy to flow on slopes as low as 28° with no excess pore pressure (indicating that they are entirely dry) [*Hungr et al.*, 2001]. However, the angle of repose for dry materials is strongly affected by the thickness of the flow over a rough bed, increasing with decreasing thickness [*Pouliquen and Renaut*, 1996]. For example, Manzella and Labiouse [2007] found that the angle of repose for Hostun sand (0.3–0.8 mm, from the Hostun region of France) varied from ~34°–40° depending on flow thickness. This effect arises because grains in thinner flows have to dilate more to overcome the geometric interlocking between adjacent grains in order to shear [*Pouliquen and Renaut*, 1996] (Figure 1.9). For grains on the order of ~0.001–2 mm, electrostatic forces have an effect, and for grains smaller than 0.1 mm (fine-grained sand and smaller), Van der Waals forces become important, enhancing cohesion between grains [*Johnson et al.*, 1971; *Derjaguin et al.*, 1975; *Alexander et al.*, 2006]. The Van der Waals forces between these grains are several orders of magnitude larger than the weight of the grains themselves, leading to flow behaviours like that of a liquid as the Van der Waals forces at the grain-scale mimic the capillary forces that are usually responsible for cohesion in wet materials [*Valverde et al.*, 2000]. The transition in grain behaviour occurs when the Van der Waals forces equal the weight of the grains [*Valverde et al.*, 2000; *Alexander et al.*, 2006].

The morphology of dry granular landslides varies depending on the thickness of the flow. Daerr and Douady [1999] and Douady et al. [2002] found that flows of thin layers of material resulted in triangular flow morphologies, such as those typically seen in loose snow avalanches [*McClung and Schaerer*, 2006] and in many martian slope streaks (Figure 1.10). Thick flows on the other hand caused headward growth of the avalanche, resulting in an inverted teardrop shape that is more reminiscent of the alcoves of sand dune avalanches (i.e., Figure 1.8A). As in debris flows, traveling over rough beds leads to enhanced channelization in dry granular flows [*Wieland et al.*, 1999]. These flows also undergo kinetic sieving similar to debris flows, with larger grains concentrated at the flow front and sides, thereby forming levees. If relatively large irregular grains are

present in the flow, size segregation and flow resistance can lead to flow front instability and result in distal fingering [*Pouliquen et al.*, 1997; *Pouliquen and Vallance*, 1999]. Fingering is not often seen in sand dune avalanches (i.e., Figure 1.8) as the grains are typically well-rounded and the grain size range is relatively small, whereas fingering likely arises in snow avalanches due to the irregular nature of the grains of snow (i.e., Figure 1.10).

Figure 1.8. Examples of dry granular flow in sand on Earth. (**A**) A slow, dry sand flow on the lee slope of a sand dune in the Namib Desert. Photo courtesy of G. D. Plage via O. Hungr. (**B**) Fingering in a dry sand flow due to flow being redirected by underlying topography in Dubai. Photo courtesy Loveson Antony.

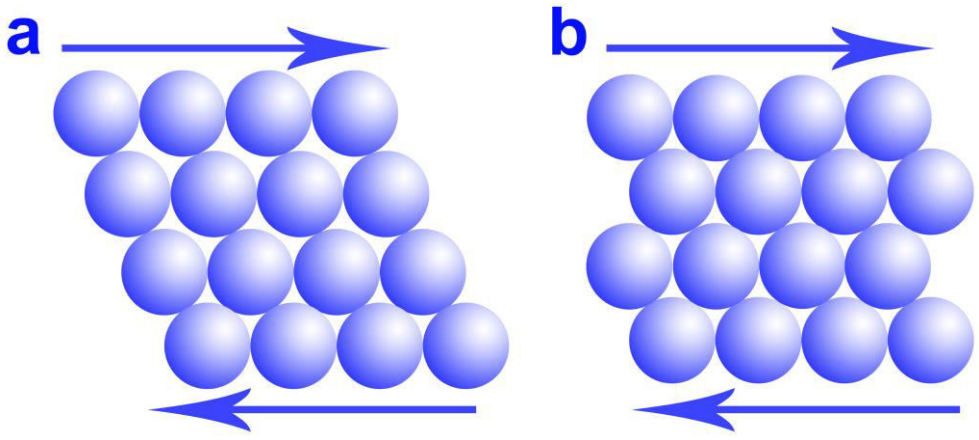

Figure 1.9. Grain dilation in dry flows. (**A**) Dilatent shearing grains. (**B**) Interlocking static grains. After Collins and Melosh [2003].

1.3.2.1 Low-gravity behaviour of dry granular flows.

Another important factor in granular flows is the Froude number, which is material-dependent and describes bulk flow characteristics by relating inertia and gravity [e.g., *Crosby et al.*, 2009]. The dimensionless Froude number F is defined as:

$$F = \frac{V}{\sqrt{gl}} \qquad (1)$$

$F = 1$ for critical flow

$F < 1$ for rapid flow

$F > 1$ for slow flow

where V is a characteristic velocity, g is the force of gravity, and l is a characteristic length. As F increases, so does the coefficient of friction between materials (in the case of dry granular flows, the friction between the sliding mass and the underlying slope material) [*Patton*, 1987]. Experiments of dry granular flow under variable gravity conditions (0-1.8g) aboard the NASA KC-135 aircraft by Klein and White [*Klein and White*, 1988; *White and Klein*, 1990] showed that the dynamic angle of repose is not a material constant, but rather varies with $\sqrt{g}$, implying that granular flows in low gravity would have higher angles of repose, shorter runout distances, and thicker shearing layers. For well-rounded glass beads (1.35 mm grain diameter) they found that the angle of repose increased from 30° at 1g to ~34° at ~0.38g (g = 9.81 m/s^2; see Figure 10 in Klein and White [1988]). Brucks et al. [2007] conducted experiments of granular flows under gravities ranging from 1–25g and found the same scaling of the angle of repose with $\sqrt{g}$ as Klein and White, but their experiments indicated that flow thickness is independent of g. Williams et al. [2008] also conducted experiments aboard the KC-135 aircraft at 0.16g (lunar), 0.38g (martian), 1.0g, and 1.8g. They noted decreased fluidization at lower gravities in their experiments, with flow behaviour transitioning from clumping with no flow, to avalanching, and then to free flow with increasing gravity; this effect has also been noted by Walton et al. [2007]. Crosby et al. [2009] conducted experiments similar to those of Klein and White aboard the NASA KC-135 aircraft using lunar soil simulants under both ambient atmospheric pressure (1 atm) and in near-vacuum conditions, and found no variation in the angle of repose with atmospheric pressure. Furthermore,

variable gravity experiments conducted during parabolic flights by Kleinhans et al. [2011] found that the presence or absence of interstitial water had no significant effect on the angle of repose either.

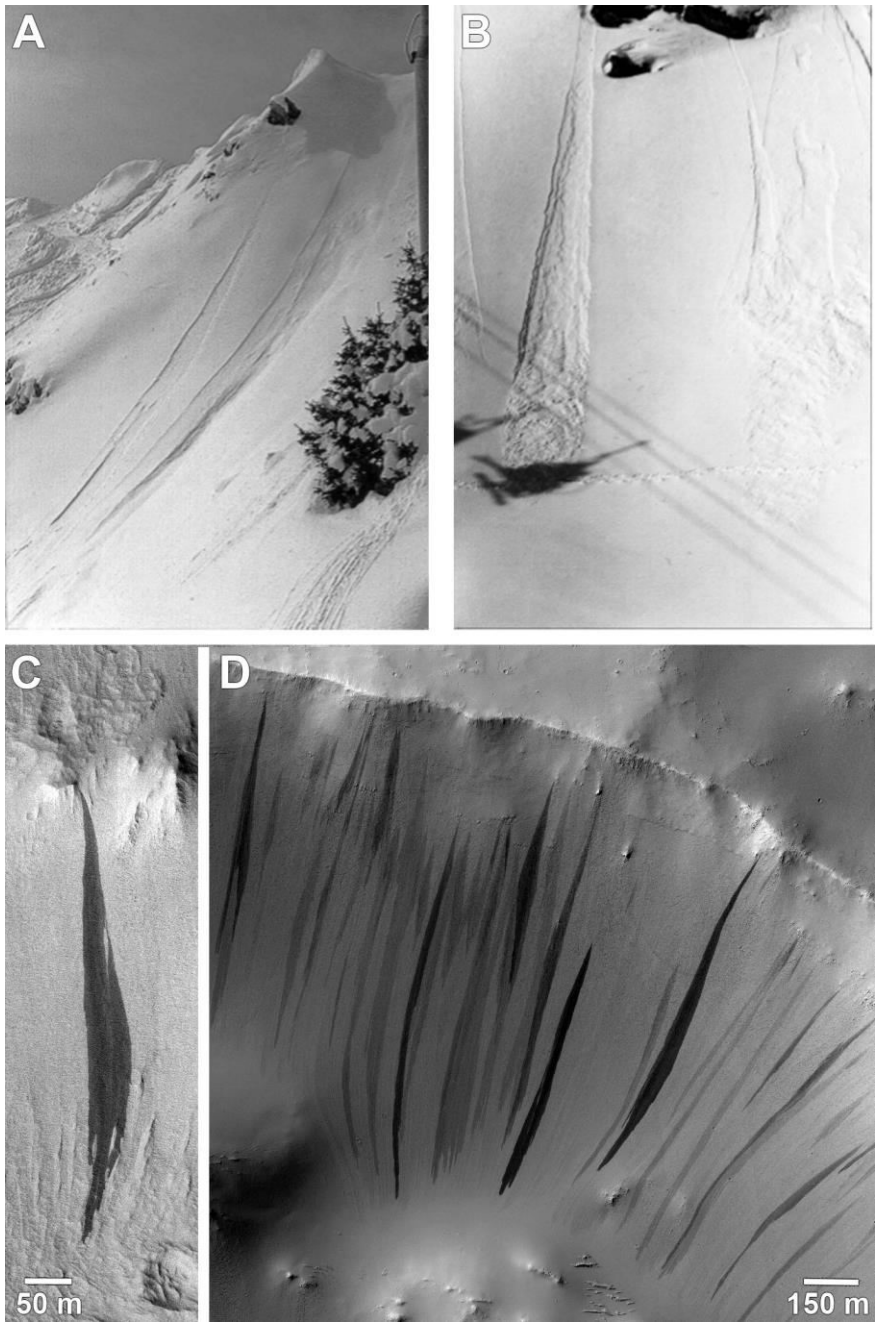

Figure 1.10. Thin triangular mass movements. (**A**) and (**B**) show loose snow avalanches. Photos by A. Daerr (modified from Daerr [2000]). (**C**) Slope streak in Lycus Sulci, Mars. Subframe of HiRISE ESP_012482_2110. (**D**) Numerous slope streaks in a crater in Arabia Terra, Mars. Subframe of HiRISE PSP_008322_1865.

The effect of gravity on the angle of repose is due to increased resistance to sliding/flow as gravity decreases, leading to a higher static angle of repose [*Walton et al.*, 2007]. This is described by Walton et al. [2007] as increased "cohesive behaviour", but this is purely descriptive in that cohesion is not dependent on gravity. Grains on the order of ~1 mm can behave as cohesive powders in low-gravity environments [*Walton et al.*, 2007], much larger than the 0.1 mm grain size required for dominance of Van der Waals forces on Earth to result in fluid-like behaviour of dry materials [*Johnson et al.*, 1971; *Derjaguin et al.*, 1975; *Geldart and Wong*, 1984; *Alexander et al.*, 2006]. This effect is well known in industrial applications, where increased effective gravity is often required for fine powders to flow uniformly [*Walton et al.*, 2007].

In contrast to the aforementioned experiments, Kleinhans et al. [2011] suggest that landslides in lower gravity conditions would be *larger* than those on Earth based on the reduction in the dynamic angle of repose observed in their variable gravity flight experiments. Kleinhans et al. [2011] hypothesized that the dynamic angle of repose decreases with decreasing gravity because a moving granular flow becomes more dilated under lower gravity conditions. They state that their results differ from those of White and Klein [1990] based on different experimental setups: The setup of White and Klein [1990], reanalyzed by Walton [2007], was found to only capture the dynamic angle of repose and in a continuous avalanching mode. The Kleinhans et al. [2011] experiments, in contrast, captured both static and dynamic angles of repose through discrete avalanching, which would be a more accurate representation of avalanche behaviour in nature. This could explain the longer than expected runout lengths observed in some large martian landslides [e.g., *Lucas and Mangeney*, 2007].

1.3.3 Rock avalanches

Rock avalanches (Figure 1.11) are defined as "extremely rapid, massive, flow-like motion of fragmented rock from a large (>10,000 m^3) rock slide or rock fall" [*Hungr et al.*, 2001], in contrast to a "rock fall," which applies to rolling, falling, and bouncing (as opposed to flowing) of distinct rock fragments whose behaviour depends on the failure mechanism. The initial failure mechanism of rock avalanches is poorly understood, but they may be mobilized by entraining and liquefying saturated soil along the path of the

avalanche [*Hungr et al.*, 2001]. Rock avalanches always conform to local topography [e.g., *Heim*, 1932; *Abele*, 1974; *Nicoletti and Sorriso-Valvo*, 1991] and can travel upslope [e.g., *Hsu*, 1975; *Hutchinson*, 1988], meander in gullies [*McClung and Schaerer*, 2006], and make large changes in direction with little loss in velocity [*Moore and Matthews*, 1978]. The effective friction in rock avalanches tends to be roughly inverse to the avalanche volume [*Heim*, 1932], resulting in longer runout distances for larger volumes of material. Multiple explanations have been proposed for the anomalous mobility of large landslides; for discussion see referred texts: lubrication by an air layer trapped beneath the sliding mass [*Shreve*, 1966, 1968]; acoustic fluidization [*Melosh*, 1979]; dispersive forces exerted by powder-sized grains resulting in fluid-like behaviour [*Hsu*, 1975]; mechanical fluidization [*Davies*, 1982; *Campbell et al.*, 1995; *Straub*, 2001]; melting of portions of the flow from the huge energy of the slide [*Erismann*, 1979]; lubrication by increased vapour pressure due to heat generated by the slippage (this mechanism requires water [*Habib*, 1975; *Gougel*, 1978] and is only possible if the permeability of the landslide is very small and the water content is sufficiently high [*De Blasio*, 2007]); and shearing from a thin basal layer of highly active particles that suspend the sliding mass off the ground [*Campbell*, 1990].

Figure 1.11. Example of a terrestrial rock avalanche. This massive avalanche, the Frank Slide, occurred on the east side of Turtle Mountain in Alberta in 1903. The avalanche

buried the entire town of Frank, killing at least 70 people. Note houses on right for scale. *Photo by Mike Bovis, courtesy of the Geological Survey of Canada.*

1.4 Previous Martian Gully Surveys

Multiple authors have made partial maps of the distribution of gullies on Mars. The very first map, created by Malin and Edgett [2000a], incorporated MOC NA data (~1–12 m/pixel resolution) from the beginning of the MGS mission through January 2000. Due to the limited areal coverage of the small MOC NA footprint (<1–3 km across, with highly variable lengths ranging from a few to hundreds of km), images often only cover a small fraction of a given landform (e.g., craters, massifs, etc.); because of this, surveys utilizing MOC NA images often reported their results in terms of the number of images containing gullies or the number of individual gullied slopes observed. In their survey, Malin and Edgett [2000a] found 160 images containing gullies covering ~120 separate gullied locales. Approximately one-third of these were crater interior walls, one-quarter occurred in the south polar pits (Sisyphi Cavi and Cavi Angusti), and one-fifth were found along the walls of the large Dao and Nirgal Vallis valley networks. They also noted concentrations of gullies on the walls of the Sirenum Fossae troughs and the nearby mesas of Gorgonum Chaos, as well as on the walls and central peaks of the Hale, Maunder, Newton, and Rabe impact basins. All gullies in both hemispheres, with the exception of those in Nirgal Vallis (~27–30°S), were found poleward of 30° latitude. They also observed a poleward-facing preference for gullies in both hemispheres, where gullies were ~2.5x more abundant on poleward-facing walls than equator-facing. The majority of gullies observed occurred in the southern hemisphere.

Edgett et al. [2003] reported updated "key observations" of gully inventory efforts with MGS MOC utilizing data through September 2002, although a map of the global distribution was not included. They stated that with this expanded dataset, they no longer observed any orientation preference for gullies except in localized cases—for example, all of the gullies within Nirgal Vallis were found on poleward-facing slopes. The observation of regional clusters of gullies, reported in the original Malin and Edgett [2000a] paper, still held true. This report also made the first mention of a gully

monitoring effort, stating that they were actively re-imaging dune gullies to look for changes, but none had been observed at that point.

Heldmann and Mellon [2004] created a revised map of gully distribution in the southern hemisphere of Mars from 30°–72°S using MOC NA data acquired through August 2000. They found 139 images containing "well-defined" gully features, with occurrence steadily declining with increasing latitude until reaching a minimum at 60°–63°S before increasing again. Crater wall gullies were more dominant than in the Malin and Edgett [2000a] survey, hosting 48% of the observed gullies. They noted a distinct lack of gullies within the Hellas and Argyre impact basins. Utilizing elevation data from the MGS Mars Orbiter Laser Altimeter (MOLA), they found that southern hemisphere gullies were restricted to an elevation range of approximately -5 to +2 km, with most occurring between -1 to +2 km. Gullies were found to have a poleward-facing preference in the 30°–44°S and 58°–72°S latitude ranges, but equator-facing between those two ranges, in disagreement with the Edgett [2003] survey (which utilized >10x the number of images than the Heldmann and Mellon [2004] survey). They also noted a correlation between gullies and areas of low albedo and high thermal inertia relative to global trends, although these areas were not distinct relative to non-gulled regions across other portions of the southern highlands.

Bridges and Lackner [2006] combined MOC NA images through 2001 with any available overlapping or "close" THEMIS VIS (18 m/pixel) images to map the gully distribution across portions (0–180°W and 240–360°W from 30–65°N) of the northern hemisphere. They found 72 MOC images containing gullies or "gully-like features." The majority of these (72%) occurred on crater walls. Gully concentration was found to decrease with increasing latitude. No statistically significant orientation preference with latitude was observed, in contrast to the southern hemisphere [*Heldmann and Mellon*, 2004].

Balme et al. [2006] used a combination of MOC NA through September 2003 and MEX HRSC (~10–50 km/pixel) data from orbits 1–1500 to conduct a survey of gullies from -10°S to -80°S. They found 943 individual gullied slopes in MOC NA images and 382 in HRSC. They note that while gully alcoves are resolved with HRSC, the

channels—required for definitive identification of a gully—are often not. This is not only due to the lower resolution of HRSC, but also illumination and contrast issues that arise from the highly variable observation geometry resulting from the non-circular orbit of MEX (see Figure 8 of Kneissl et al. [2010] for a comparison). Because of this, they detected ~10x fewer gullied slopes per square kilometre with HRSC than MOC. As with previous surveys, the majority of gullied slopes (62%) were found within craters. They found the concentration of gullies decreased with increasing latitude, with the exception of the increase near the south pole due to the gullied south polar pits, in agreement with previous surveys. They also found no gullies within the Hellas or Argyre impact basins, consistent with Heldmann and Mellon [2004]. Gully orientations had a poleward-facing preference from ~30–40°S latitude, with orientations varying more at higher latitudes, also consistent with Heldmann and Mellon [2004], but in contrast with Edgett et al. [2003].

Heldmann et al. [2007] expanded upon the previous work of Heldmann and Mellon [2004], this time covering the northern hemisphere. They inspected all MOC NA images from the beginning of the MGS MOC mission through March 2004 covering 30–90°N and found 137 containing gullies. The majority of these (84%) were found within impact craters, consistent with previous studies in both hemispheres. Clusters of gullies were observed in Acidalia, Utopia, and Arcadia Planitiae, and Tempe Terra. Gully concentration decreased with increasing latitude, with no gullies observed poleward of 72°N. Gullies were found at elevations ranging from -5.4 km to +0.8 km. A preference for gullies to occur on equator-facing slopes was observed in the mid-latitudes (30–58°N), with this preference becoming more pronounced with increasing latitude. Poleward of 58°N, gullies were found to be almost equally distributed on pole-facing and equator-facing slopes. In contrast with their southern hemisphere study, they found gullies to be correlated with areas of low thermal inertia and high albedo relative to global trends.

Kneissl et al. [2010] conducted the northern hemisphere equivalent of Balme et al.'s [2006] MOC NA+HRSC survey. Their survey utilized MOC NA data from the beginning of the MGS mission through March 2005 from 0–90°N and 230 HRSC nadir images covering 30–90°N (due to the complete lack of gullies observed in MOC NA

images south of 30°N while completing the survey). With MOC, they found 3195 gullies in 311 images spanning 30–76.6°N. Clusters of gullies were observed in Acidalia and Utopia Planitiae, with localized clusters in Tempe Terra and Arcadia Planitia as observed by Heldmann et al. [2007]. Consistent with previous studies in both hemispheres, gully concentration was found to decrease with increasing latitude, dropping off significantly at ~55°N. The vast majority of gullies (~81%) were found on crater walls. Gully orientation was found to have a pole-facing preference from 30–40°N, shifting to equator-facing preference north of 40°N. With HRSC, they were able to identify 2293 gullies in 50 images. As with the MOC NA dataset, the majority of these were found within craters (65.5%). The latitude range, orientation preference, and regional clustering results from HRSC were consistent with those from MOC NA.

1.5 Proposed Martian Gully Formation Mechanisms

Multiple models have been put forth in an attempt to explain how geologically youthful gully features could have formed on Mars. Our view of martian gullies has improved over time since their initial discovery thanks to long-term monitoring and higher resolution data. Therefore, the types of models that have been put forth have evolved over time as well. In order to best understand this progression, the potential formation mechanisms will be summarized below in chronological order of their proposition. Additional discussion of the evidence for and against each model is presented in Chapter 2.

1.5.1 Release of groundwater from shallow aquifers

The shallow aquifer hypothesis was first proposed by Malin and Edgett [2000a], and then expanded upon by Mellon and Phillips [2001]. This model involves an aquifer confined by an impermeable rock layer and dry overlying regolith (to provide thermal insulation) lying upslope from a ridge. At a point close enough to the surface toward the ridge where ground ice is stable, an ice plug forms. Obliquity-induced freeze-thaw cycles lead to increased fluid pressure within the aquifer, eventually fracturing the ice plug and

allowing water from the aquifer to burst out of the side of the slope and run downhill, forming a gully. Liquid water has been shown by multiple authors to have a residency time of up to a few hours on the martian surface under the temperature and pressure conditions of both the present and the geologically recent past [e.g., *Carr*, 1983; *McKay and Davis*, 1991; *Haberle et al.*, 2001; *Hecht*, 2002; *Heldmann*, 2005]. This model is consistent with many observations. Mellon and Phillips [2001] found that ground ice is only stable poleward of 30°, consistent with the latitudinally restricted extent of gullies. They also found that the 273 K isotherm underwent the least amount of change over obliquity cycles between ~60°S and 65°S and therefore predicted a relative lack of gullies in this latitude range, consistent with results from gully surveys [*Bridges and Lackner*, 2006; *Heldmann et al.*, 2007; *Kneissl et al.*, 2010]. Aquifers also provide an explanation for the observed regional clusters of gully occurrence, with some clusters appearing to have a common rock layer from which gullies originate (e.g., Hale Crater, Nirgal Vallis [*Gilmore and Phillips*, 2002], although these observations were made with MGS MOC; higher resolution imaging with HiRISE has discounted this observation [*McEwen et al.*, 2007]) and gully orientations in local clusters appearing to be affected by the local topography [*Márquez et al.*, 2005; *Allen et al.*, 2008]. Hartmann [2003] proposes a shallow aquifer formed by localized geothermal melting (not significant enough to have any surface expression, as no signs of geologically recent volcanic activity have been observed on Mars with any spacecraft [*Edgett et al.*, 2010]) of ground ice. Debris flows are then triggered either by direct rapid release of water to the surface or by saturation-induced failure. This also provides an explanation for the recharge of shallow aquifers. Gully activity from water traveling along impermeable layers in the subsurface and then exiting at a cliff face has been directly observed in Iceland [*Hartmann et al.*, 2003; *Decaulne et al.*, 2005], demonstrating that the phenomenon does occur in nature.

Heldmann and Mellon [2004] found that if the regolith overlying the aquifer were icy, the 273 K isotherm would be 4–8 km deep, inconsistent with the depths of the gully alcoves in their study region. Icy permafrost overburden is also not supported by the observations, as the depth of gully heads would be expected to increase with decreasing latitude, which is not the case [*Gilmore and Phillips*, 2002]. If the overburden were dry, however, 79% of the gully alcoves measured by Heldmann and Mellon [2004] fell within

the liquid H_2O regime, assuming constant thermal conductivity in the overlying regolith. Heldmann and Mellon [2004] used thermal conductivity values in the range of 0.007–0.893 W/mK, consistent with material composed of rock and loosely consolidated soil and with the experimental values of soil conductivities under martian atmospheric pressures by Presley and Christensen [1997]; however, Márquez et al. [2005] state that these conductivities are too low to represent the materials forming the aquifer, citing conductivities for the "most likely geologic materials hosting the aquifer" ranging from 0.1 (dry sand) to 5.33 (basalt) W/mK. Using these higher thermal conductivities, the 273 K isotherm would not occur at depths shallow enough to account for gullies.

While hydrated salts have not been detected in association with new light-toned gully flows [*Barnouin-Jha et al.*, 2008; *Núñez et al.*, 2016] (in contrast to the initial prediction of Malin et al. [2006])—possibly suggesting they did not form via briny flows—salts are not the only mechanism through which the freezing point of water can be depressed. Water in a porous medium can have freezing points as low as 233 K (-40°C) [*Cahn et al.*, 1992; *Maruyama et al.*, 1992] without excessive salinity due to the presence of a kinetic barrier, preventing crystallization in pore spaces where the kinetic energy is considerably lowered [*Morishige and Kawano*, 2000]. Highly concentrated acidic water, such as that suggested by results from the MER-A and B rovers, can also result in a freezing point much lower than that of pure water [e.g., *Squyres et al.*, 2006].

The shallow aquifer model however does not easily explain the occurrence of gullies on isolated central peaks and massifs. Also, neither the MEX Mars Advanced Radar for Subsurface and Ionosphere Sounding (MARSIS) nor SHARAD have detected evidence for shallow aquifers on Mars. MARSIS has a vertical resolution of 50–100 m and can penetrate up to 5000 m through the subsurface [*Picardi et al.*, 2004], while SHARAD has a vertical resolution of ~10 m and can penetrate to depths of 300–1000 m [*Seu et al.*, 2004]. However, it has been hypothesized that SHARAD is only capable of deeply penetrating the youngest units on Mars [*Stillman and Grimm*, 2009] and White and Stofan [2010] calculated that MARSIS cannot detect aquifers at depths greater than ~400 m. Based the observations that Mars is heavily layered to depths up to 10 km [*Malin*, 1998; *Malin and Edgett*, 1999; *Mcewen et al.*, 1999] and substantial burial and exhumation via erosion have occurred throughout martian history [*Malin and Edgett*,

2000b], it is not unreasonable to assume that any sizeable aquifers on Mars would be ancient and therefore buried deeply in the subsurface.

1.5.2 Release of groundwater from deep aquifers

A model proposed by Gaidos [2001] offers cryovolcanism as the origin of the liquid water required to form martian gullies (Figure 1.12). In this model, a deep aquifer is confined by an impermeable rock layer on the bottom and the cryosphere [*Clifford*, 1993] on the top. Decreasing heat flow in the subsurface leads to expansion of the cryosphere, pressurizing the confined aquifer to the point of fracturing the cryosphere. The liquid water from the aquifer then travels upward through the fractures due to increased pore pressure until low vertical stresses or failure of the surrounding rock occur, at which point the water begins moving laterally and a sill of liquid water forms. If the sills reach the surface on a slope, the water is expelled and gullies form.

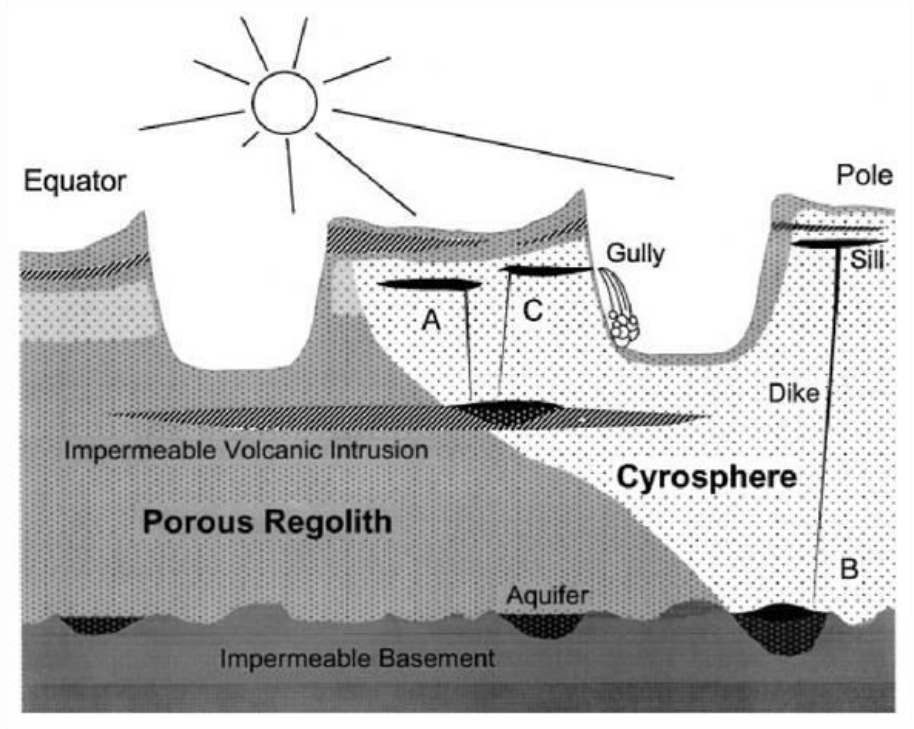

Figure 1.12. Cryovolcanic (deep aquifer) model for gully formation. See text for detailed description. From Gaidos [2001].

This model explains the lack of gullies equatorward of 30° due to the lack of a confining cryosphere, but does not explain the decrease in the number of gullies moving poleward from 30°S to 60°S and the lack of gullies from 60°S to 65°S. It also does not explain why cryovolcanic features are not observed on flat surfaces where the water would never encounter low vertical stresses or failure of the surrounding rock on its journey to the surface, and therefore never spread laterally to form a sill in the subsurface. A poleward-facing preference for gullies is invoked in this model, with this preference decreasing closer to the poles, consistent with the observations in the southern hemisphere but not in the north as previously mentioned in the shallow aquifer case.

1.5.3 Release of liquid CO_2 from shallow aquifers

Musselwhite et al. [2001] proposed that martian gullies formed via the outbreak of liquid CO_2 from near-surface "aquifers" (Figure 1.13). In this model, similar to the shallow groundwater model of Malin and Edgett [2000a], liquid CO_2 builds up in an aquifer behind a dry ice "dam" that forms at the point in the subsurface where liquid CO_2 is no longer stable. Seasonal and/or obliquity cycle driven heating weakens the dry ice "dam", eventually resulting in the rapid release of liquid CO_2 to the surface. Upon reaching the surface, the CO_2 would rapidly vaporize, forming a gas-supported flow that entrained rock and clathrate-hydrate ice, carving a gully as it moved downhill. The authors argue for CO_2 over H_2O as the gully-carving agent on Mars as CO_2 is the most abundant volatile on the planet. This model was quickly dismissed due to the difficulty in both accumulating and sustaining significant amounts of either condensed CO_2 or CO_2 clathrate-hydrate in the martian crust [*Stewart and Nimmo*, 2002]. Gas-supported flows of this nature would have velocities much too high to create morphologies observed in martian gullies, and would be expected to result in forms more like terrestrial pyroclastic flows than the fluvial/debris flow forms of gullies [*Stewart and Nimmo*, 2002].

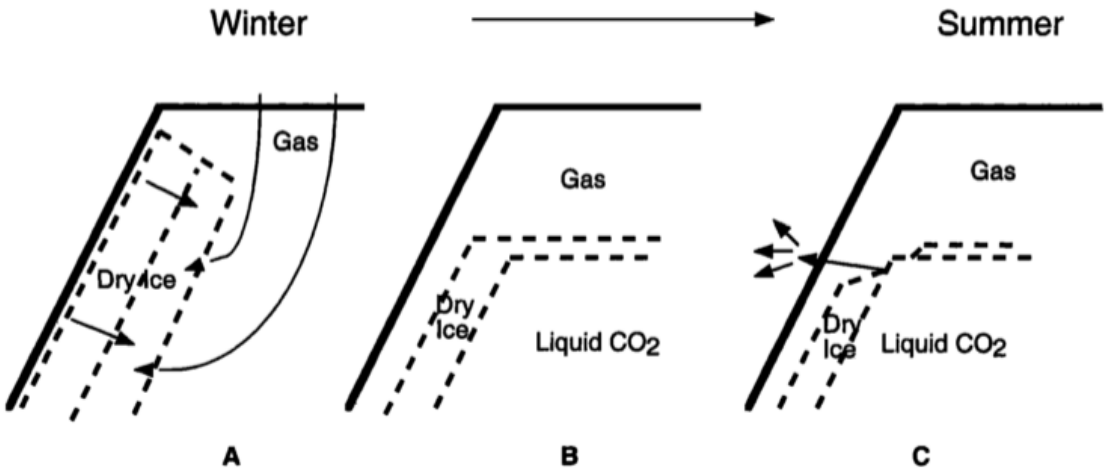

Figure 1.13. Liquid CO_2 release model for gully formation. **(A)** In winter, dry ice forms upon a slope face and extends into the slope. **(B)** As temperature and pressure increases in spring, liquid CO_2 forms behind a dam of still-frozen CO_2 ice. **(C)** When the CO_2 ice layer becomes thin enough, the pressured liquid CO_2 behind it rapidly vaporizes, generating a suspended flow of rock and clathrate-hydrate ice that flows downslope and carves a gully. From Musselwhite [2001].

1.5.4 Melting of near-surface ground ice

A few different models of melting of near-surface ground ice to produce gullies have been proposed. In the model of Costard et al. [2002], warming at high obliquity melts the ice, saturating the regolith and producing debris flows once critical sheer stress is reached. This model finds that the only locations on Mars that would experience daily mean temperatures higher than the melting point for ice (273 K) are the mid to high latitudes on poleward-facing slopes, and therefore this is where gullies tend to occur. Gilmore and Phillips [2002] on the other hand propose a model where water from melting ground ice percolates through the regolith until encountering an impermeable layer, at which point it travels laterally along the layer until it exits at the surface where the layers are exposed, such as in a crater or valley wall (Figure 1.14). Snowmelt/melting ice hypotheses have gained popularity recently with data from SHARAD suggesting there are large amounts of subsurface water ice in the mid-latitudes at present [*Holt et al.*, 2008; *Plaut et al.*, 2009], and northern mid-latitude newly-formed impact craters discovered with CTX have been found by CRISM and HiRISE to have excavated subsurface water ice [*Byrne et al.*, 2009]. Some authors have noted the presence of

"patterned" or polygonal terrain associated with some gullies and point to it as a possible indication of subsurface ice [*Bridges and Lackner*, 2006; *Levy et al.*, 2008, 2009a; *Lanza et al.*, 2010]. For all of these models however, modelling by Mellon and Phillips [2001] shows that the depth of the 273 K isotherm is always above the depth of any near-surface ground ice that might exist at these latitudes, even at high obliquity. Mellon and Phillips [2001] also found that temperatures high enough to melt ice would only be attained if the ice were composed of 15–40% salts, but CRISM has not detected any traces of hydrated minerals in association with gullies [*Barnouin-Jha et al.*, 2008; *Núñez et al.*, 2016]. Melting due to the presence of salts is also inconsistent with the latitudinal distribution of gullies, as they would be expected to form at all latitudes over a range of obliquity regimes in this case [*Mellon and Phillips*, 2001]. Melting of snow or ground ice also does not explain the regional clustering of gullies that is observed unless localized geothermal heating were involved. If the process that initially formed gullies is responsible for the activity we observe today, the Costard et al. [2002] model cannot be invoked as gullies are active at Mars' current obliquity. Any models involving melting at or near the surface would also imply that gully activity would be expected in summer (as is the case for terrestrial snowmelt-initiated debris flows in Iceland, which peak in the summer [*Decaulne and Sæmundsson*, 2007]), and the L_s constraints of all of the new gully flows known to have formed within a single Mars year demonstrate that they are forming in autumn, winter, or very early spring [*Harrison et al.*, 2009b; *Diniega et al.*, 2010; *Dundas et al.*, 2010, 2012, 2015]. If the present-day activity in gullies is separate from their initial formation mechanism however, then these issues do not pose a problem for the ground ice model.

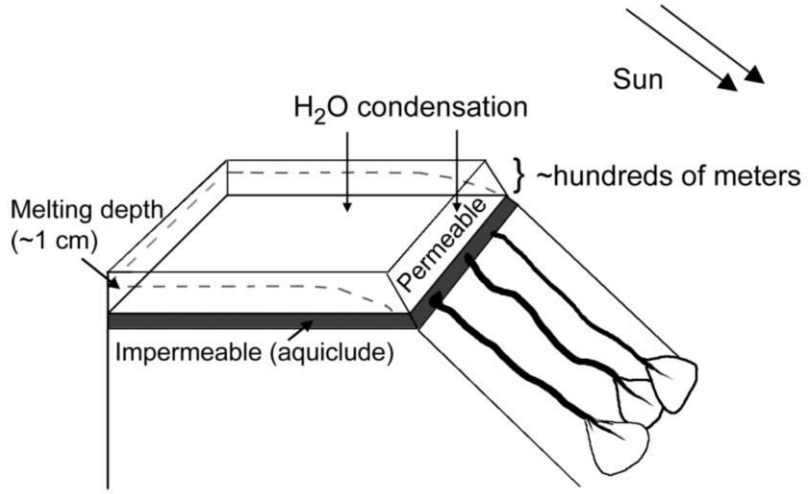

Figure 1.14. Near-surface ground ice model of gully formation from Gilmore and Phillips [2002]. In this model, ground ice melts and percolates downward until it hits an impermeable layer, where it then travels laterally until it exits at a slope (assuming the layer dips toward a slope face). If no impermeable layer is present, gullies do not form.

1.5.5 Melting of snow

Melting snow as the genesis of gullies was first proposed by Lee et al. [2002] and Hartmann et al. [2002, 2003] based on the resemblance of martian gullies to those on Devon Island and Iceland, respectively, created by snowmelt. Christensen [2003] (later detailed by Williams et al. [2009]) invoked snowmelt by proposing that the gullies formed due to melting of dust-covered snowpacks formed at high obliquity, remnants of which are preserved as LDM deposits (often informally referred to as "pasted on" material) on gullied crater walls today. Head et al. [2008] also proposed a model involving surface meltwater, in which the last glaciation of Mars resulted in debris-covered glaciers forming against the poleward-facing walls and on the floors of mid-latitude craters. When the climate changed, the glaciers stopped accumulating and flowing, leaving alcoves exposed on the crater walls. Residual surface ice and snow in these alcoves then melted to form gullies. Schon et al. [2012] advocates this model as well based on the correlation between the calculated age of one particular gully they studied and the emplacement time of dust-ice covered mantling deposits. The support and caveats of these models are the same as those discussed in the previous section on melting of ground ice.

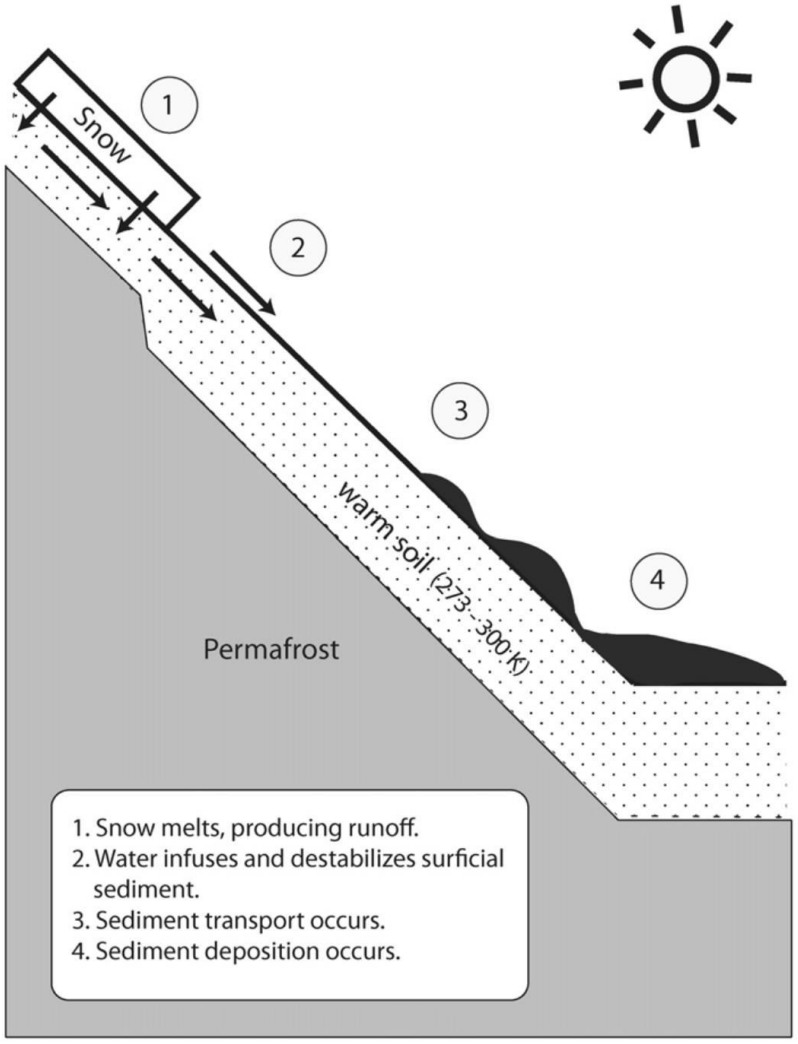

Figure 1.15. Proposed mechanism for gully formation via snowmelt-induced debris flows from Williams et al. [2009]. Arrows indicate direction of meltwater flow.

1.5.6 Dry granular flow

Treiman [2003] proposed entirely dry flow as the agent behind martian gully formation based on the difficulty of sustaining liquid water under recent climate conditions. However, he also proposed this mechanism based on classifying some equatorial features as gullies, such as alcoves with aprons in the calderas of the Tharsis volcanoes and the light-toned layered mounds in Candor Chasma. These equatorial features lack incised channels—a key morphological component of a gully—and more closely resemble dry mass movement chutes (Figure 1.2). Shinbrot et al. [2004] also supported a dry granular flow model based on a claimed resemblance of gullies to dry

mass movement features on sand dunes. Again, the sand dune features lack the incised, banked and sinuous channels characteristic of martian (and terrestrial) gullies (e.g., Figures 1.2 and 1.8). Banked and sinuous channel morphologies, as well as terraces and streamlined features observed in some martian gullies, are inconsistent with dry flow.

Gullies are morphologically distinct from dry mass movement features elsewhere on Mars and Earth. Flows that divert around an obstacle and re-integrate after passing it (i.e., the braided morphology observed in some gully channels, and the morphology of some of the newly formed gully flows) require sufficient volume and fluidity. Dry granular flows do not behave in this manner unless they are sufficiently thick and fine-grained such that Van der Waals forces are many orders of magnitude larger than intergranular friction and grain weight [*Johnson et al.*, 1971; *Derjaguin et al.*, 1975; *Campbell*, 1990]. The dry granular flow arguments of Treiman [2003] reference snow avalanche morphology; however, McClung and Shaerer [2006] note that "dry snow avalanches tend to travel in straight lines rather than being deflected by topography, such as gullies." There is also disagreement in terrestrial literature as to whether dry granular flow models are valid for snow avalanches [e.g., *Naaim et al.*, 2003; *Hutter et al.*, 2005; *Platzer et al.*, 2007; *Gauer et al.*, 2008]. Treiman [2003] asserts that gullies occur in areas where global circulation models (GCM) predict sediment deposition from the atmosphere due to deceleration of winds in the 30–50°S latitude range, accounting for regional clustering, but the complex regional gully orientation trends [*Márquez et al.*, 2005] make this model unlikely unless local variations in wind flow are considered [*Heldmann and Mellon*, 2004]. Many gullies also occur on slopes well below the angle of repose for dry material [*Heldmann and Mellon*, 2004]. The general consensus among the Mars gully community today is that gullies do not form via an entirely dry granular flow mechanism, although dry mass movement processes do occur within pre-existing gullies today [*Harrison et al.*, 2015].

1.5.7 Melting of H_2O frost

Kossacki and Markiewicz [2004] investigated whether gullies could have formed from seasonal melting of accumulated H_2O frost under favourable pressure and wind

speed conditions. In this model, H_2O frost transitions to the liquid phase after the complete removal of the overlying CO_2 frost layer (which deposits atop H_2O frost seasonally on Mars). CO_2 frost can remain on crater walls into late spring. Once insolation conditions reach a certain point (late spring/early summer), the CO_2 frost quickly warms, resulting in rapid melting of the underlying H_2O frost. The presence of salts within the water ice could aid in lowering the melting temperature. The maximum volume of liquid generated by this melting was <0.2–0.55 kg/m^2 depending on latitude, which Kossacki and Markiewicz [2004] state is not enough to generate any surface flow, but could affect the cohesive properties of the surface layer of the slope. With an average water vapour abundance of only ~10 precipitable micrometres in the current martian atmosphere [*Jakosky and Farmer*, 1982; *Jakosky and Barker*, 1984], other authors have also argued that frost accumulation and subsequent melting would not likely be significant enough to saturate the regolith to the point of slope failure, but rather the dampening would lead to increased cohesion [e.g., *Dundas et al.*, 2015]. However, water vapour abundance is highly variable, dependent upon the time of day, season, and locality [e.g., *Tamppari and Lemmon*, 2014]. Kossacki and Markiewicz [2004] found that the condensation rate of H_2O ice onto the surface is strongly dependent on partial pressure P_{H2O} and wind speed. They used a very conservative wind speed of 5 m/s in their model. Average wind speed varies as a function of L_s and depends on both the regional and local setting; average wind speeds recorded by the Phoenix lander ranged from ~2–12 m/s from L_s 75–150° [*Holstein-Rathlou et al.*, 2014], and the Viking landers recorded average wind speeds at times of 20 m/s daytime gusts up to 26 m/s [*Ryan and Henry*, 1979]. Regional circulation models have predicted slope winds as high as 40 m/s [*Rafkin et al.*, 2002]. Higher wind speeds would result in a greater amount of water ice condensation onto the surface, and therefore a greater amount of meltwater availability to potentially initiate slope instability. This model however cannot explain the formation of gullies on equator-facing slopes that are never deeply shadowed, as frost would not accumulate there [*Schorghofer and Edgett*, 2006].

1.5.8 CO_2 frost avalanches

Ishii and Sasaki [2004] proposed that avalanches of solid CO_2 frost could gradually carve gullies over time by "scratching" into the surface as chunks of frost fell during periods of sublimation (i.e., spring into summer). Frost avalanches have been favoured as gully formation/evolution mechanisms by some authors based on HiRISE observations of frost-dust avalanches on a north polar scarp [*Russell et al.*, 2008] and the hypothesis of Costard et al. [2007] that "dark streaks" observed over frost in gullies are dry avalanches (although Costard et al. [2007] do not favour dry flow as the initial formation mechanism for gullies). This model has many of the same issues as the dry granular flow model; particularly, the banked and sinuous channels observed in gullies are difficult to explain with frost avalanches. Present-day CO_2 frost avalanches on scarps of the northern polar layered deposits have also not been observed to form any gully-like features [*Russell et al.*, 2008].

Sublimation-induced CO_2 ice avalanching has been suggested as the formation mechanism behind linear dune gullies, such as those on the dunes in Russell Crater ([*Diniega et al.*, 2013]. In this model (originally proposed by Hansen et al. [2011] for mass movement features on the north polar erg of Mars), blocks of CO_2 ice dislodge from the top of the dune in springtime due to sublimation from heating. The blocks then travel downslope, carving leveed linear "channels." This morphology is very distinct from that of most crater wall gullies (except those that incise into sand dunes superposing crater walls; see Chapter 2 for a discussion of the effects of substrate properties on gully morphology), leading some to suggest that dune gullies and crater/valley/massif/etc. wall gullies may not have the same formation mechanism. The timing of present-day gully activity in dunes and crater wall gullies is similar however [*Diniega et al.*, 2010, 2013; *Dundas et al.*, 2012, 2015], which could suggest a common control on at least recent activity.

1.5.9 Frosted granular flow

Hugenholtz [2008] proposes frosted granular flow as a gully formation mechanism on Mars. Frosted granular flow is a rare type of landslide on Earth where clasts are lubricated by thin frost coatings, facilitating downslope movement. They tend

to occur in the fall and spring when the air temperature oscillates around freezing (273 K) at times of relatively high humidity on snow-free surfaces [*Hétu et al.*, 1994; *Hétu and Gray*, 2000]. Hétu et al. [1994] noted four conditions required for frosted granular flow: (1) unconsolidated sediment easily mobilized downslope, (2) a slope gradient at or near the angle of repose in the source region, (3) frost accumulation on the unconsolidated grains, and (4) a trigger for mass movement (such as a rockfall [*Hétu et al.*, 1994], point-source defrosting [*Costard et al.*, 2007], vapour-induced instability [*Hoffman*, 2002], or avalanching of CO_2 frost [*Ishii and Sasaki*, 2004] in the case for Mars). Locations of repeated flows typically either follow pre-existing channels or, when diverted by obstacles, create new "channels." Grains ranging in size from fine-grained sand (~0.0007 cm) to large clasts (20 cm) can be mobilized by these flows on slopes as low as ~25°; however, frosted granular flows predominantly transport gravel-sized grains [*Hétu and Gray*, 2000; *Hugenholtz*, 2008]. As in debris flows, kinetic sieving results in large clasts accumulating at the flow margins and surface. Frosted granular flows also exhibit levees, straight to sinuous channels, concave profiles, and digitate termination [*Hétu et al.*, 1994; *Hétu and Gray*, 2000], similar to debris flows. Seasonal H_2O frost accumulates as far north as 13°S in the winter [*Vincendon et al.*, 2010b], and early morning frost has been observed on the ground by the Opportunity rover at 2°S [*Landis*, 2007], covering the entire latitude range where gullies are found in the southern hemisphere. Hugenholtz [2008] proposes that CO_2 frost rather than water ice frost may be the lubricating mechanism for frosted granular flows on Mars. However, CO_2 frost has not been detected at latitudes lower than ~34°S [*Vincendon et al.*, 2010a]. Additionally, frost does not accumulate in the mid- to high-latitudes in areas that are never deeply shadowed at any point in the year [*Schorghofer and Edgett*, 2006], and gullies are found on equator-facing slopes where frost would not accumulate. The morphology of frosted granular flow "channels" and deposits is also very different from that of gullies (see Chapter 2 for an example (Figure 2.15) and further discussion).

1.5.10 CO_2 gas-fluidized flow

Hoffman [2002] and Cedillo-Flores et al [2011] proposed that gullies in at least Mars' polar regions, such as those in the south polar pits of Sisyphi Cavi, formed by

fluidization of aeolian sediment deposited atop CO_2 frost once the frost begins to sublime in springtime (Figure 1.16). This model requires a slope covered with CO_2 frost, which is then subsequently mantled by sediment, sand, or dust via aeolian transport from adjacent non-frosted slopes. The frost layer rapidly sublimes due to heating of the overlying lower-albedo material. This introduces instability to the slope, triggering mass movement. Mechanical heating as the material moves downslope generates more CO_2 vapour, acting as a lubricant to allow the mass to behave like a fluid and carving a channel. This model differs from that of Musselwhite et al. [2001] in that it only invokes surface CO_2 ice based on the aforementioned thermodynamic difficulty in sustaining CO_2 ground ice on Mars.

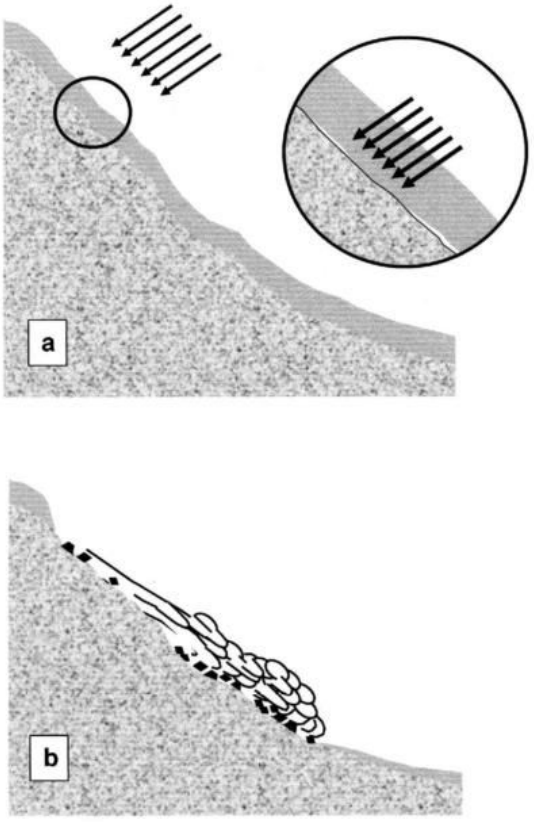

Figure 1.16. CO_2 gas-lubricated flow model from Hoffman [2002]. **(A)** Sunlight (black arrows) penetrates through the surface CO2 frost and warms the underlying regolith. This causes the frost layer to sublimate at its base, destabilizing the slope and generating an avalanche. **(B)** A mixture of the CO2 frost, gas, and entrained debris move downslope, with the frost continuing to degas and generating a vapour-lubricated flow.

Avalanches that appear to be dry based on their morphology have been observed within some gullies, coinciding with periods of defrosting [*Hoffman*, 2002; *Costard et al.*, 2007]. This suggests defrosting is capable of initiating mass movement. Hoffman [2002] suggests that the closest terrestrial analogue to this sort of gas-fluidized flow is a density flow, and presents submarine turbidity channels for their morphological similarity to martian gullies. However, laboratory experiments of fluidization of dry material with CO_2 gas by Cedillo-Flores et al. [2008] produced features much more morphologically similar to dry sand flows on terrestrial dunes than gullies (Figure 1.17).

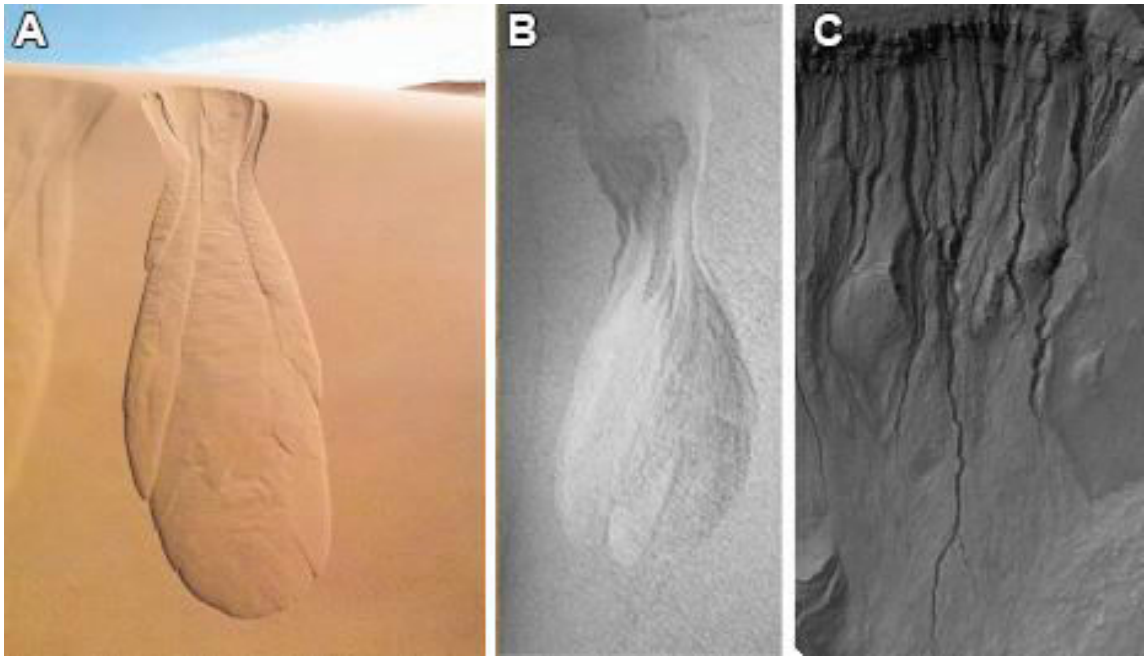

Figure 1.17. Dry granular flow on terrestrial sand dunes from Hungr et al. [2001] **(A)** compared to the laboratory experiments of Cedillo-Flores et al. [2008] **(B)** and gullies on Mars in Niquero Crater **(C)**. Niquero gullies are a subframe of HiRISE ESP_020685_1410 and scene is ~700 m wide. Scale unknown for **A** and **B**.

It is worth noting that Sisyphi Cavi may represent a special case for gully formation, and therefore it might not be a good site for extrapolating formation processes to the rest of martian gullies. Sisyphi Cavi lies within the seasonal south polar cap; as such, it experiences ~1 m of CO_2 frost accumulation in winter—significantly more than lower latitude gullies [*Hoffman*, 2002]. The gullies here are also morphologically distinct from lower latitude gullies [e.g., *Conway et al.*, 2015a], occur on all slopes without a

preferential orientation [*Hoffman*, 2002; *Harrison et al.*, 2015], and exhibit a high amount of gully activity relative to other active gully sites on Mars [*Dundas et al.*, 2015; *Raack et al.*, 2015].

Pilorget and Forget [2016] propose a model where CO_2 ice condenses onto the surface in autumn, with some subliming at the base due to differential solar heating of the underlying regolith as the ice is relatively transparent to sunlight. Some of the resulting CO_2 gas diffuses into the regolith, trapped between impermeable permafrost and the overlying CO_2 ice. In mid-winter, CO_2 ice begins to condense in pore spaces within the upper few centimetres of the underlying regolith due to the temperature gradient between the regolith at the surface and at depth from solar heating. Pressure builds up to a point where the CO_2 gas ruptures the overlying ice, forming jets of CO_2 (the same process that has been proposed for the formation of south polar "spiders" [*Piqueux et al.*, 2003]) gas that could destabilize the slope and cause a "fluidized debris flow." As in the previous model, the authors describe this type of gas-supported flow as being akin to a terrestrial pyroclastic flow. They note that not every "eruption" of CO_2 gas would be expected to generate a gully, but multiple eruptions in the same place could occur due to re-condensation, leading to repeated events within an individual gully system. In fact, in the case of the Russell Crater dune gullies, their model predicts eruptions on a daily basis from L_s 150–205°.

Pilorget and Forget [2016] state that their model explains why there are no gullies on non-pole-facing walls in the 30–45° latitude range. However, this model would be expected to produce the same morphology as the aforementioned gas-supported flow experiments of Cedillo-Flores et al. [2008], which does not resemble martian gullies. It does however produce morphologies similar to some mass movement features on the north polar erg [*Hansen et al.*, 2011, 2013; *Allen et al.*, 2016; *Diniega et al.*, 2016] (referred to as "gullies" in some of the literature, but they typically only exhibit alcoves and aprons without incised channels and should therefore likely not be classified as such), and this model could explain the formation of those features.

Based on the timing of observed present-day gully activity (coinciding with periods of defrosting), Dundas et al. [2010, 2012, 2015] favour a CO_2-based process for

gully formation. A CO_2-frost-related process is supported by the observation of the highly active south polar pit gullies relative to those in the mid-latitudes, as more frost would be deposited on slopes at higher latitudes. However, CO_2 frost has not been detected spectroscopically at latitudes equatorward of ~34°S [*Vincendon et al.*, 2010a], and present-day gully activity has been observed at latitudes as low as 29°S. While incision of new small channel segments has been observed, no entire new gully systems have been detected to date [*Dundas et al.*, 2015]; this may suggest the initial gully-forming process is no longer active today. Dundas et al. [2015] do note that CO_2 frost processes might simply be the dominant driver of activity within pre-existing gullies today, and not the process by which they initially formed.

1.6 Gullies and recurring slope lineae (RSL)

Recurring slope lineae (RSL) (Figure 1.18) were first described by McEwen et al. [2011]. They are dynamic features occurring on slopes near the angle of repose for dry material, which are observed to incrementally lengthen downslope in warmer seasons (250–300 K) and gradually fade in colder seasons over multiple years. They are typically found on equator-facing slopes. RSL are much smaller than mid-latitude gullies, at only ~0.5–5 m in width, and do not cause any topographic changes, although they are often found in occurrence with fine-scale channels [*McEwen et al.*, 2011, 2014]. However, these channel features are much smaller than middle and high latitude gullies (1–50 m wide) and are only clearly resolvable in HiRISE images. Most RSL are found in gullied latitude bands, with the exception of a high number observed within Coprates and Melas Chasma in Valles Marineris [*McEwen et al.*, 2014]. Sites where RSL are observed appear to be more likely to have active gullies [*Dundas et al.*, 2015], but gullies and RSL are rarely observed on the same slopes [*McEwen et al.*, 2011]

The initial hypothesis for RSL formation involved transient flow of briny water during periods of warming [*McEwen et al.*, 2011, 2014]. This hypothesis was bolstered by the spectral detection of hydrated chlorate and perchlorate salts with CRISM in association with RSL source regions [*Ojha et al.*, 2015] (in contrast, gullies are either spectrally indistinct from their surroundings or show the same composition as the

(probable source) material upslope [*Núñez et al.*, 2016]). The origin of this water is still under debate. Aquifers are unlikely due to the observation of RSL on isolated peaks, such as the central peaks of Horowitz and Hale craters. In the case of the equatorial RSL, ground ice should not be present to melt, although the MEX Obervatoire pour la Minéralogie, l'Eau, les Glaces et l'Activité (OMEGA) spectrometer has detected surface water ice (i.e., frost) in Coprates Chasma [*Vincendon et al.*, 2010b]. Ojha et al. [2015] propose deliquescence, a process where salts absorb atmospheric water to the point of forming a solution. This process is observed in the hyperarid Atacama Desert—an oft-cited analogue for Mars—and provides water for the survival of microbial communities there [*Aharon et al.*, 2014].

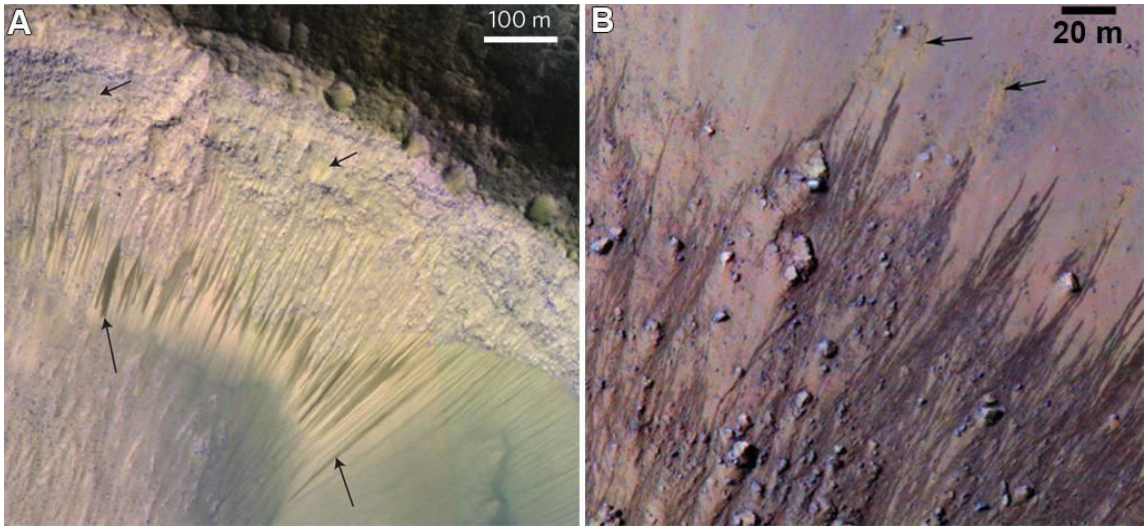

Figure 1.18. HiRISE IRB colour views of recurring slope lineae (RSL). **(A)** RSL (dark streaks, some denoted with black arrows) in a crater on the floor of Melas Chasma. Subframe of ESP_031059_1685, from McEwen et al. [2014]. **(B)** RSL on the central peak of Horowitz Crater. Black arrows denote orange streaks, which may be faded RSL. Subframe of PSP_005787_1475, from McEwen et al. [2011]. North is up in both images.

Massé et al. [2016] propose a possible hybrid wet + dry mechanism for RSL activity, and potentially for gullies as well. They conducted laboratory experiments of the behaviour of ice blocks sitting on sandy unconsolidated 30° slopes under martian temperature and pressure conditions (6.5 and 9 mbar, and 293 K). In their experiments, the ice first began to melt, percolating into the sandy substrate. This resulted in darkening of the sand as the meltwater moved downslope. However, under martian conditions, this

meltwater is metastable, and began to boil away. The boiling action led to saltation of sand grains, generating slope instability and triggering dry granular flows ahead of the saturated sand. This mechanism would seemingly be viable under conditions where a martian slope was frosted and then subsequently heated. The flows in their experiments did carve a very small "channel," but on a scale of tens of centimetres. Whether this process would scale to nature may require more study, and may be affected by the aforementioned issues in scaling debris flow behaviour from the lab to nature scale [*Iverson et al.*, 1992, 1997].

References

Abele, G. (1974), Bergstürze in den Alpen. *Wissenschaftliche Alpenvereinshefte, 25*, 230 pgs.

Aharon, O., R. E. Bardavid, and L. Mana (2014), Perchlorate and halophilic prokaryotes: Implications for possible halophilic life on Mars, *Extremophiles*, *18*, 75–80.

Alexander, A. W., B. Chaudhuri, A. Faqih, F. J. Muzzio, C. Davies, and M. S. Tomassone (2006), Avalanching flow of cohesive powders, *Powder Technol.*, *164*, 13–21, doi:10.1016/j.powtec.2006.01.017.

Allen, A., S. Diniega, and C. Hansen (2016), Gully and aeolian activity within the "Tleilax" dune field in the Olympia Undae, Mars, in *47th Lunar and Planetary Science Conference*, abstract 1759.

Allen, T. L., M. B. Wilhelm, J. L. Heldmann, and S. J. Allen (2008), Correlation of regional topography and martian gully orientation, in *Workshop on Martian Gullies: Theories and Tests*, abstract 8018.

Balme, M., N. Mangold, D. Baratoux, F. Costard, M. Gosselin, P. Masson, P. Pinet, and G. Neukum (2006), Orientation and distribution of recent gullies in the southern hemisphere of Mars: Observations from High Resolution Stereo Camera/Mars Express (HRSC/MEX) and Mars Orbiter Camera/Mars Global Surveyor (MOC/MGS) data, *J. Geophys. Res.*, *111*(E5), E05001, doi:10.1029/2005JE002607.

Barnouin-Jha, O. S., A. McGovern, D. Buczkowski, K. Seelos, F. Seelos, S. L. Murchie, B. L. Ehlmann, and CRISM Team (2008), Martian gullies as seen by the Compact Reconnaissance Imaging Spectrometer for Mars (CRISM), in *American Geophysical Union, Fall Meeting 2008*, abstract P32B–04.

De Blasio, F. V. (2007), Production of frictional heat and hot vapour in a model of self-lubricating landslides, *Rock Mech. Rock Eng.*, *41*, 219–226, doi:10.1007/s00603-007-0153-8.

Bovis, M. J., and M. Jakob (1999), The role of debris supply conditions in predicting debris flow activity, *Earth Surf. Process. Landforms*, *24*, 1039–1054.

Boynton, W. V. (2002), Distribution of hydrogen in the near surface of Mars: Evidence for subsurface ice deposits, *Science*, *297*(5578), 81–85, doi:10.1126/science.1073722.

Bramson, A. M., S. Byrne, N. E. Putzig, J. J. Plaut, and J. W. Holt (2014), Thick excess water ice in Arcadia Planitia, Mars, in *45th Lunar and Planetary Science Conference*, abstract 2120.

Brand, E. W. (1981), Some thoughts on rain-induced slope failures, *Proc. Int. Conf. Soil Mech. Found. Eng.*, *3*, 373–376.

Brayshaw, D., and M. A. Hassan (2009), Debris flow initiation and sediment recharge in gullies, *Geomorphology*, *109*(3-4), 122–131, doi:10.1016/j.geomorph.2009.02.021.

Brenner, R. P., H. K. Tam, and E. W. Brand (1985), Field stress path simulation of rain-induced slope failure, *Proc. Int. Conf. Soil Mech. Found. Eng.*, *3*, 991–996.

Bridges, N. T., and C. N. Lackner (2006), Northern hemisphere Martian gullies and mantled terrain: Implications for near-surface water migration in Mars' recent past, *J. Geophys. Res.*, *111*(E9), E09014, doi:10.1029/2006JE002702.

Brucks, A., T. Arndt, J. Ottino, and R. Lueptow (2007), Behavior of flowing granular materials under variable g, *Phys. Rev. E*, *75*(3), 032301, doi:10.1103/PhysRevE.75.032301.

Bull, L. J., and M. J. Kirkby (1997), Gully processes and modelling, *Prog. Phys. Geogr.*, *21*(3), 354–374, doi:10.1177/030913339702100302.

Byrne, S. et al. (2009), Distribution of mid-latitude ground ice on Mars from new impact craters, *Science*, *325*(5948), 1674–1676.

Cahn, J. W., J. G. Dash, and F. Haiying (1992), Theory of ice premelting in monosized powders, *J. Cryst. Growth*, *123*, 101–108.

Campbell, C. S. (1990), Rapid granular flows, *Annu. Rev. Fluid Mech.*, *22*, 57–92, doi:10.1146/ annurev.fl .22.010190.000421.

Campbell, C. S., P. W. Cleary, and M. Hopkins (1995), Large-scale landslide simulations: Global deformation, velocities and basal friction, *J. Geophys. Res.*, *100*(B5), 8267, doi:10.1029/94JB00937.

Carr, M. H. (1983), Stability of streams and lakes on Mars, *Icarus*, *56*, 476–495, doi:10.1016/0019-1035(83)90168-9.

Cedillo-Flores, Y., H. J. Durand-Manterola, and R. A. Craddock (2008), Martian gullies created by fluidization of dry material, *Workshop on Martian Gullies: Theories and Tests*, abstract 8019.

Cedillo-Flores, Y., A. H. Treiman, J. Lasue, and S. M. Clifford (2011), CO_2 gas fluidization in the initiation and formation of Martian polar gullies, *Geophys. Res. Lett.*, *38*(L21202), doi:10.1029/2011GL049403.

Christensen, P. R. (2003), Formation of recent martian gullies through melting of extensive water-rich snow deposits, *Nature*, *422*(6927), 45–48, doi:10.1038/nature01436.

Clifford, S. M. (1993), A model for the hydrologic and climatic behavior of water on Mars, *J. Geophys. Res.*, *98*(E6), 10973–11016, doi:10.1029/93je00225.

Collins, G. S. (2003), Acoustic fluidization and the extraordinary mobility of sturzstroms, *J. Geophys. Res.*, *108*(B10), 1–14, doi:10.1029/2003JB002465.

Conway, H., and C. F. Raymond (1993), Snow stability during rain, *J. Glaciol.*, *39*(133), 635–642.

Conway, S. J., M. R. Balme, M. A. Kreslavsky, J. B. Murray, and M. C. Towner (2015a), The comparison of topographic long profiles of gullies on Earth to gullies on Mars: A signal of water on Mars, *Icarus*, *253*, 189–204, doi:10.1016/j.icarus.2015.03.009.

Conway, S. J., M. R. Balme, and R. J. Soare (2015b), Using gullies to estimate the thickness of the latitude dependent mantle on Mars, *46th Lunar Planet. Sci. Conf.*, abstract 2964.

Costard, F., F. Forget, N. Mangold, and J. P. Peulvast (2002), Formation of recent martian debris flows by melting of near-surface ground ice at high obliquity, *Science*, *295*(5552), 110–113, doi:10.1126/science.1066698.

Costard, F., N. Mangold, D. Baratoux, and F. Forget (2007), Current gullies activity: Dry avalanches at seasonal defrosting as seen on HiRISE images, *Seventh International Conference on Mars*, abstract #3133.

Coussot, P., and S. Proust (1996), Slow, unconfined spreading of a mudflow, *J. Geophys. Res.*, *101*(B11), 25217–25229, doi:10.1029/96JB02486.

Crosby, K. M., I. Fritz, S. Kreppel, E. Martin, C. Pennington, B. Frye, and J. H. Agui (2009), Scaling relations for repose angles of lunar mare simulants, *2009 Annu. Meet. Lunar Explor. Anal. Gr.*, abstract 2009.

Daerr, A. (2000), Dynamique des Avalanches, University of Paris VII Denis Diderot.

Daerr, A., and S. Douady (1999), Two types of avalanche behaviour in granular media,

Nature, *399*(6733), 241–243, doi:10.1038/20392.

Davies, T. R. H. (1982), Spreading of rock avalanche debris by mechanical fluidization, *Rock Mech.*, *15*(1), 9–24.

Decaulne, A., and P. Sæmundsson (2007), Spatial and temporal diversity for debris-flow meteorological control in subarctic oceanic periglacial environments in Iceland, *Earth Surf. Process. Landforms*, *32*, 1971–1983, doi:10.1002/esp.

Decaulne, A., Þ. Saemundsson, and O. Petursson (2005), Debris flow triggered by rapid snowmelt: A case study in the Gleiðarhjalli area, Northwestern Iceland, *Geogr. Ann.*, *87A*, 487–500.

Denlinger, R. P., and R. M. Iverson (2001), Flow of variably fluidized granular masses across three-dimensional terrain: 2. Numerical predictions and experimental tests, *J. Geophys. Res.*, *106*(B1), 553, doi:10.1029/2000JB900330.

Derjaguin, B. V., V. M. Muller, and Y. P. Toporov (1975), Effect of contact deformations on the adhesion of particles, *J. Colloid Interface Sci.*, *115*, 131–143.

Dickson, J. L., J. W. Head, T. a. Goudge, and L. Barbieri (2015), Recent climate cycles on Mars: Stratigraphic relationships between multiple generations of gullies and the latitude dependent mantle, *Icarus*, *252*, 83–94, doi:10.1016/j.icarus.2014.12.035.

Diniega, S., S. Byrne, N. T. Bridges, C. M. Dundas, and A. S. McEwen (2010), Seasonality of present-day Martian dune-gully activity, *Geology*, *38*(11), 1047–1050, doi:10.1130/G31287.1.

Diniega, S., C. J. Hansen, J. N. McElwaine, C. H. Hugenholtz, C. M. Dundas, A. S. McEwen, and M. C. Bourke (2013), A new dry hypothesis for the formation of martian linear gullies, *Icarus*, *225*, 526–537, doi:10.1016/j.icarus.2013.04.006.

Diniega, S., A. Allen, T. Perez, and C. J. Hansen (2016), Tracking gully activity within the north polar erg, Mars, *47th Lunar and Planetary Science Conference*, abstract 1740.

Douady, S., B. Andreotti, A. Daerr, and P. Cladé (2002), From a grain to avalanches: On the physics of granular surface flows, *Comptes Rendus Phys.*, *3*(2), 177–186, doi:10.1016/S1631-0705(02)01310-5.

Dundas, C. M., and S. Byrne (2010), Modeling sublimation of ice exposed by new impacts in the martian mid-latitudes, *Icarus*, *206*, 716–728,

doi:10.1016/j.icarus.2009.09.007.

Dundas, C. M., A. S. McEwen, S. Diniega, S. Byrne, and S. Martinez-Alonso (2010), New and recent gully activity on Mars as seen by HiRISE, *Geophys. Res. Lett.*, *37*(7), L07202, doi:10.1029/2009GL041351.

Dundas, C. M., S. Diniega, C. J. Hansen, S. Byrne, and A. S. McEwen (2012), Seasonal activity and morphological changes in martian gullies, *Icarus*, *220*(1), 124–143, doi:10.1016/j.icarus.2012.04.005.

Dundas, C. M., S. Diniega, and A. S. McEwen (2015), Long-term monitoring of martian gully formation and evolution with MRO/HiRISE, *Icarus*, *251*, 244–263, doi:10.1016/j.icarus.2014.05.013.

Edgett, K. S. (2009), MRO CTX and MGS MOC observations regarding small impact craters and substrate resistance to erosion on Mars, *Bull. Am. Astron. Soc.*, *4*(3), 1113.

Edgett, K. S., M. C. Malin, R. M. E. Williams, and S. D. Davis (2003), Polar and middle-latitude martian gullies: A view from MGS MOC after two Mars years in the mapping orbit, in *Lunar and Planetary Science XXXIV*, abstract 1038.

Edgett, K. S., B. A. Cantor, T. N. Harrison, M. R. Kennedy, L. J. Lipkaman, M. C. Malin, L. V. Posiolova, and D. E. Shean (2010), Active and Recent Volcanism on Mars, in *Bulletin of the American Astronomical Society*, abstract 34.06.

Erismann, T. H. (1979), Mechanics of large landslides, *Rock Mech.*, *12*, 15–46.

Feldman, W. C. (2004), Global distribution of near-surface hydrogen on Mars, *J. Geophys. Res.*, *109*(E9), E09006, doi:10.1029/2003JE002160.

Forget, F., R. M. Haberle, F. Montmessin, B. Levrard, and J. W. Head (2006), Formation of glaciers on Mars by atmospheric precipitation at high obliquity., *Science*, *311*(5759), 368–71, doi:10.1126/science.1120335.

French, H. M. (2007), *The Periglacial Environment*, 3rd ed., John Wiley and Sons, Hoboken.

Gaidos, E. (2001), Cryovolcanism and the recent flow of liquid water on Mars, *Icarus*, *153*(1), 218–223, doi:10.1006/icar.2001.6649.

Gallagher, C., M. R. Balme, S. J. Conway, and P. M. Grindrod (2011), Sorted clastic stripes, lobes and associated gullies in high-latitude craters on Mars: Landforms

indicative of very recent, polycyclic ground-ice thaw and liquid flows, *Icarus*, *211*(1), 458–471, doi:10.1016/j.icarus.2010.09.010.

Gauer, P., K. Lied, and K. Kristensen (2008), On avalanche measurements at the Norwegian full-scale test-site Rvggfonn, *Cold Reg. Sci. Technol.*, *51*(2-3), 138–155, doi:10.1016/j.coldregions.2007.05.005.

Geldart, D., and A. C. Y. Wong (1984), Fluidization of Powders Showing Degrees of Cohesiveness—1. Bed Expansion, *Chem. Eng. Sci.*, *39*(10), 1481–1488.

Gilmore, M. S., and E. L. Phillips (2002), Role of aquicludes in formation of Martian gullies, *Geology*, *30*(12), 1107, doi:10.1130/0091-7613(2002)030<1107:ROAIFO>2.0.CO;2.

Glade, T. (2005), Linking debris-flow hazard assessments with geomorphology, *Geomorphology*, *66*(1-4 SPEC. ISS.), 189–213, doi:10.1016/j.geomorph.2004.09.023.

Gougel, J. (1978), Scale-dependent rockslide mechanisms, with emphasis on the role of pore fluid vaporization, in *Rockslides and Avalanches*, edited by B. Voight, pp. 693–706, Elsevier, Amsterdam, Netherlands (NLD).

Haberle, R. M., C. P. Mckay, J. Schaeffer, N. A. Cabrol, E. A. Grin, A. P. Zent, and R. Quinn (2001), On the possibility of liquid water on present-day Mars, *J. Geophys. Res.*, *106*(E10), 23317–23326, doi:10.1029/2000JE001360.

Habib, P. (1975), Production of gaseous pore pressure during rock slides, *Rock Mech. Rock Eng.*, *7*, 193–197.

Hansen, C. J. et al. (2011), Seasonal erosion and restoration of Mars' northern polar dunes, *Science*, *331*(February), 575–578, doi:10.1126/science.1197636.

Hansen, C. J., S. Byrne, G. Portyankina, M. Bourke, C. Dundas, A. McEwen, M. Mellon, A. Pommerol, and N. Thomas (2013), Observations of the northern seasonal polar cap on Mars: I. Spring sublimation activity and processes, *Icarus*, *225*(2), 881–897, doi:10.1016/j.icarus.2012.09.024.

Harrison, T. N., M. C. Malin, and K. S. Edgett (2009a), Present-day activity, monitoring, and documentation of gullies with the Mars Reconnaissance Orbiter (MRO) Context Camera (CTX), in *Geological Society of America Abstracts with Programs*, p. 267.

Harrison, T. N., M. C. Malin, and K. S. Edgett (2009b), Present-day gully activity

observed by the Mars Reconnaissance Orbiter (MRO) Context Camera (CTX), in *Bulletin of the American Astronomical Society, DPS Meeting #41*, p. 1113.

Harrison, T. N., G. R. Osinski, and L. L. Tornabene (2015), Global Documentation of Gullies With the Mars Reconnaissance Orbiter Context Camera (CTX) and Implications for Their Formation, *Icarus*, *252*, 236–254, doi:http://dx.doi.org/10.1016/j.icarus.2015.01.022.

Hartmann, W. K., and G. Neukum (2001), Cratering chronology and the evolution of Mars, *Space Sci. Rev.*, *96*(1-4), 165–194, doi:10.1023/A:1011945222010.

Hartmann, W. K., T. Thorsteinsson, and F. Sigurdsson (2002), Comparison of Icelandic and Martian hillside gullies, *Lunar Planet. Sci. XXXIII*, 1904.

Hartmann, W. K., T. Thorsteinsson, and F. Sigurdsson (2003), Martian hillside gullies and Icelandic analogs, *Icarus*, *162*(2), 259–277, doi:10.1016/S0019-1035(02)00065-9.

Head, J. W., J. F. Mustard, M. a Kreslavsky, R. E. Milliken, and D. R. Marchant (2003), Recent ice ages on Mars, *Nature*, *426*(6968), 797–802, doi:10.1038/nature02114.

Head, J. W., D. R. Marchant, and M. a. Kreslavsky (2008), Formation of gullies on Mars: Link to recent climate history and insolation microenvironments implicate surface water flow origin, *Proc. Natl. Acad. Sci.*, *105*(36), 13258–13263, doi:10.1073/pnas.0803760105.

Hecht, M. (2002), Metastability of liquid water on Mars, *Icarus*, *156*(2), 373–386, doi:10.1006/icar.2001.6794.

Heim, A. (1932), *Bergsturz und Menschenleben*, Fretz and Wasmuth, Zürich.

Heldmann, J. L. (2005), Formation of Martian gullies by the action of liquid water flowing under current Martian environmental conditions, *J. Geophys. Res.*, *110*(E5), E05004, doi:10.1029/2004JE002261.

Heldmann, J. L., and M. T. Mellon (2004), Observations of martian gullies and constraints on potential formation mechanisms, *Icarus*, *168*(2), 285–304, doi:10.1016/j.icarus.2003.11.024.

Heldmann, J. L., E. Carlsson, H. Johansson, M. T. Mellon, and O. B. Toon (2007), Observations of martian gullies and constraints on potential formation mechanisms II. The northern hemisphere, *Icarus*, *188*(2), 324–344,

doi:10.1016/j.icarus.2006.12.010.

Heldmann, J. L., C. A. Conley, A. J. Brown, L. Fletcher, J. L. Bishop, and C. P. McKay (2010), Possible liquid water origin for Atacama Desert mudflow and recent gully deposits on Mars, *Icarus*, *206*(2), 685–690, doi:10.1016/j.icarus.2009.09.013.

Hétu, B., and J. T. Gray (2000), Effects of environmental change on scree slope development throughout the postglacial period in the Chic-Choc Mountains in the northern Gaspé Peninsula, Québec, *Geomorphology*, 335–355.

Hétu, B., H. Van Steijn, and P. Vandelac (1994), Les coulées de pierres glacées : un nouveau type de coulées de pierraille sur les talus d'éboulis, *Géographie Phys. Quat.*, *48*(1), 3–22, doi:10.7202/032969ar.

Hoffman, N. (2002), Active polar gullies on Mars and the role of carbon dioxide, *Astrobiology*, *2*(3), 313–323, doi:10.1089/153110702762027899.

Holstein-Rathlou, C., H. P. Gunnlaugsson, J. J. Iversen, P. Nornberg, L. K. Tamppari, P. Smith, and the Phoenix Science Team (2014), Mars wind as seen by the NASA Phoenix lander telltale, *8th International Conference on Mars*, abstract 1247.

Holt, J. W. et al. (2008), Radar Sounding Evidence for Buried Glaciers in the Southern Mid-Latitudes of Mars, *Science*, *322*, 1235–1238.

Hsu, K. J. (1975), Catastrophic debris streams (sturzstroms) generated by rock falls, *Bull. Geol. Soc. Am.*, *86*(129-140).

Hugenholtz, C. H. (2008), Frosted granular flow: A new hypothesis for mass wasting in martian gullies, *Icarus*, *197*, 65–72, doi:10.1016/j.icarus.2008.04.010.

Hungr, O., S. G. Evans, M. J. Bovis, and J. N. Hutchinson (2001), A review of the classification of landslides of the flow type, *Environ. Eng. Geosci.*, *VII*(3), 221–238.

Hutchinson, J. N. (1988), General Report: morphological and geotechnical parameters of landslides in relation to geology and hydrogeology, in *Proceedings, Fifth International Symposium on Landslides, Vol. 1*, edited by C. Bonnard, pp. 3–36, A. A. Balkema, Rotterdam.

Hutter, K., Y. Wang, and S. P. Pudasaini (2005), The Savage-Hutter avalanche model: How far can it be pushed?, *Philos. Trans. A. Math. Phys. Eng. Sci.*, *363*(June), 1507–1528, doi:10.1098/rsta.2005.1594.

Ishii, T., and S. Sasaki (2004), Formation of recent martian gullies by avalanches of CO2

frost, *Lunar and Planetary Science XXXV*, abstract #1556.

Iverson, R. M., J. E. Costa, and R. G. LaHusen (1992), Debris-flow flume at H.J. Andrews Experimental Forest, Oregon, *USGS Open-File Rep. 92–483*.

Iverson, R. M., M. E. Reid, and R. G. Lahusen (1997), Debris-flow mobilization from landslides, *Annu. Rev. Earth Planet. Sci.*, *25*, 85–138.

Iverson, R. M., M. Logan, and R. P. Denlinger (2004), Granular avalanches across irregular three-dimensional terrain: 2. Experimental tests, *J. Geophys. Res.*, *109*(F01015), doi:10.1029/2003JF000084.

Iverson, R. M., M. Logan, R. G. LaHusen, and M. Berti (2010), The perfect debris flow? Aggregated results from 28 large-scale experiments, *J. Geophys. Res.*, *115*(F3), F03005, doi:10.1029/2009JF001514.

Jakob, M., M. Bovis, and M. Oden (2005), The significance of channel recharge rates for estimating debris-flow magnitude and frequency, *Earth Surf. Process. Landforms*, *30*(6), 755–766, doi:10.1002/esp.1188.

Jakosky, B. M., and E. S. Barker (1984), Comparison of ground-based and Viking Orbiter measurements of Martian water vapor: Variability of the seasonal cycle, *Icarus*, *57*(3), 322–334, doi:10.1016/0019-1035(84)90121-0.

Jakosky, B. M., and C. B. Farmer (1982), The seasonal and global behavior of water vapor in the Mars atmosphere: Complete global results of the Viking atmospheric water detector experiment, *J. Geophys. Res.*, *87*(B4), 2999–3019, doi:10.1029/JB087iB04p02999.

Jaumann, R. et al. (2007), The high-resolution stereo camera (HRSC) experiment on Mars Express: Instrument aspects and experiment conduct from interplanetary cruise through the nominal mission, *Planet. Space Sci.*, *55*(7-8), 928–952, doi:10.1016/j.pss.2006.12.003.

Johnson, A. M. (1970), *Physical Processes in Geology*, Freeman, Cooper & Co., San Francisco, CA.

Johnson, K. L., K. Kendall, and A. D. Roberts (1971), Surface energy and the contact of elastic solids, *Proc. R. Soc. A Math. Phys. Eng. Sci.*, *324*(1558), 301–313, doi:10.1098/rspa.1971.0141.

Klein, S. P., and B. R. White (1988), Dynamic shear of granular material under variable

gravity conditions, *AIAA 26th Aerospace Sciences Meeting*, abstract AIAA–88–0648.

Kleinhans, M. G., H. Markies, S. J. De Vet, A. C. In't Veld, and F. N. Postema (2011), Static and dynamic angles of repose in loose granular materials under reduced gravity, *J. Geophys. Res. Planets*, *116*(11), 1–13, doi:10.1029/2011JE003865.

Kneissl, T., D. Reiss, S. van Gasselt, and G. Neukum (2010), Distribution and orientation of northern-hemisphere gullies on Mars from the evaluation of HRSC and MOC-NA data, *Earth Planet. Sci. Lett.*, *294*(3-4), 357–367, doi:10.1016/j.epsl.2009.05.018.

Kolb, K. J., J. D. Pelletier, and A. S. McEwen (2010), Modeling the formation of bright slope deposits associated with gullies in Hale Crater, Mars: Implications for recent liquid water, *Icarus*, *205*, 113–137, doi:10.1016/j.icarus.2009.09.009.

Kossacki, K. J., and W. J. Markiewicz (2004), Seasonal melting of surface water ice condensing in martian gullies, *Icarus*, *171*(2), 272–283, doi:10.1016/j.icarus.2004.05.018.

Kostama, V. P., M. A. Kreslavsky, and J. W. Head (2006), Recent high-latitude icy mantle in the northern plains of Mars: Characteristics and ages of emplacement, *Geophys. Res. Lett.*, *33*, L11201, doi:10.1029/2006GL025946.

Kreslavsky, M. A., and J. W. Head (2000), Kilometer-scale roughness of Mars: Results from MOLA data analysis, *J. Geophys. Res.*, *105*(E11), 26695–26711.

Landis, G. A. (2007), Observation of frost at the equator of Mars by the Opportunity rover, *38th Annual Lunar and Planetary Science Conference*, abstract 2433.

Lanza, N. L., G. a. Meyer, C. H. Okubo, H. E. Newsom, and R. C. Wiens (2010), Evidence for debris flow gully formation initiated by shallow subsurface water on Mars, *Icarus*, *205*(1), 103–112, doi:10.1016/j.icarus.2009.04.014.

Laskar, J., a. C. M. Correia, M. Gastineau, F. Joutel, B. Levrard, and P. Robutel (2004), Long term evolution and chaotic diffusion of the insolation quantities of Mars, *Icarus*, *170*(2), 343–364, doi:10.1016/j.icarus.2004.04.005.

Lee, P. (2002), Slope Gullies on Devon Island, Canadian Arctic: Possible Analogs for Gullies on Mars and Evidence for Recent Transient Environmental Change on Mars, *Am. Geophys. Union, Fall Meet. 2002*, abstract #P12A–0362.

Lee, P., C. P. McKay, and J. Matthews (2002), Gullies on Mars: Clues to their formation

timescale from possible analogs from Devon Island, Nunavut, Arctic Canada, *Lunar Planet. Sci. XXXIII*, abstract 2050.

Levrard, B., F. Forget, F. Montmessin, and J. Laskar (2004), Recent ice-rich deposits formed at high latitudes on Mars by sublimation of unstable equatorial ice during low obliquity, *Nature*, *431*, 1072–1075, doi:10.1038/nature03006.1.

Levy, J., J. Head, and D. Marchant (2009a), Thermal contraction crack polygons on Mars: Classification, distribution, and climate implications from HiRISE observations, *J. Geophys. Res.*, *114*, E01007, doi:10.1029/2008JE003273.

Levy, J. S., J. W. Head, and D. R. Marchant (2008), The role of thermal contraction crack polygons in cold-desert fluvial systems, *Antarct. Sci.*, *20*(06), 565–579, doi:10.1017/S0954102008001375.

Levy, J. S., J. W. Head, D. R. Marchant, J. L. Dickson, and G. A. Morgan (2009b), Geologically recent gully-polygon relationships on Mars: Insights from the Antarctic Dry Valleys on the roles of permafrost, microclimates, and water sources for surface flow, *Icarus*, *201*, 113–126, doi:10.1016/j.icarus.2008.12.043.

Logan, M., and R. M. Iverson (2013), Video documentation of experiments at the USGS debris-flow flume 1992–2006 (amended to include 2007–2013), *U.S. Geol. Surv. Open-File Rep. 2007–1315 v. 1.3*, http://pubs.usgs.gov/of/2007/1315/.

Lucas, A., and A. Mangeney (2007), Mobility and topographic effects for large Valles Marineris landslides on Mars, *Geophys. Res. Lett.*, *34*(10), 1–5, doi:10.1029/2007GL029835.

Madeleine, J.-B., F. Forget, J. W. Head, B. Levrard, F. Montmessin, and E. Millour (2009), Amazonian northern mid-latitude glaciation on Mars: A proposed climate scenario, *Icarus*, *203*(2), 390–405, doi:10.1016/j.icarus.2009.04.037.

Malin, M. C. (1998), Early Views of the Martian Surface from the Mars Orbiter Camera of Mars Global Surveyor, *Science*, *279*(5357), 1681–1685, doi:10.1126/science.279.5357.1681.

Malin, M. C., and K. S. Edgett (1999), Oceans or seas in the Martian northern lowlands: High resolution imaging tests of proposed coastlines, *Geophys. Res. Lett.*, *26*(19), 3049–3052, doi:10.1029/1999GL002342.

Malin, M. C., and K. S. Edgett (2000a), Evidence for recent groundwater seepage and

surface runoff on Mars, *Science*, *288*(5475), 2330–2335, doi:10.1126/science.288.5475.2330.

Malin, M. C., and K. S. Edgett (2000b), Sedimentary rocks of early Mars, *Science*, *290*(5498), 1927–1937, doi:10.1126/science.290.5498.1927.

Malin, M. C., K. S. Edgett, L. V Posiolova, S. M. Mccolley, and E. Z. N. Dobrea (2006), Present-day impact cratering rate and contemporary gully activity on Mars, *Science*, *314*(5805), 1573–1577.

Malin, M. C. et al. (2007), Context Camera Investigation on board the Mars Reconnaissance Orbiter, *J. Geophys. Res.*, *112*(E5), E05S04, doi:10.1029/2006JE002808.

Manzella, I., and V. Labiouse (2007), Rock avalanches: Experimental study of the main parameters influencing propagation, in *11th Congress of the International Society for Rock Mechanics (ISRM)*, edited by L. Ribeiro e Sousa, C. Olalla, and N. Grossman, pp. 657–660, TAYLOR & FRANCIS INC, Lisbon.

Márquez, A., M. Á. de Pablo, R. Oyarzun, and C. Viedma (2005), Evidence of gully formation by regional groundwater flow in the Gorgonum-Newton region (Mars), *Icarus*, *179*(2), 398–414, doi:10.1016/j.icarus.2005.07.020.

Martínez, G. M., and N. O. Renno (2013), Water and brines on Mars: Current evidence and implications for MSL, *Space Sci. Rev.*, *175*(1-4), 29–51, doi:10.1007/s11214-012-9956-3.

Maruyama, M., M. Bienfait, J. G. Dash, and G. Coddens (1992), Interfacial melting of ice in graphite and talc powders, *J. Cryst. Growth*, *118*(33-40).

Massé, M. et al. (2016), Transport processes resulting from metastable boiling water under Mars surface conditions, *Nat. Geosci.*, (May), 5–9, doi:10.1038/ngeo2706.

McClung, D., and P. A. Schaerer (2006), *The Avalanche Handbook: 3rd Edition*, The Mountaineers Books, Seattle.

McConnochie, T. H., I. F. Bell, D. Savransky, G. Mehall, M. Caplinger, P. R. Christensen, L. Cherednik, K. Bender, and A. Dombovari (2006), Calibration and in-flight performance of the Mars Odyssey Thermal Emission Imaging System visible imaging subsystem (THEMIS VIS), *J. Geophys. Res. Planets*, *111*(6), 1–32, doi:10.1029/2005JE002568.

McEwen, A., L. Ojha, C. Dundas, S. Mattson, S. Byrne, J. Wray, S. Cull, S. Murchie, and N. Thomas (2011), Seasonal flows on warm martian Slopes, *Science*, *333*(6043), 740–743.

McEwen, A. S., and E. B. Bierhaus (2006), The importance of secondary cratering to age constraints on planetary surfaces, *Annu. Rev. Earth Planet. Sci.*, *34*, 535–567, doi:10.1146/annurev.earth.34.031405.125018.

Mcewen, A. S., M. C. Malin, M. H. Carr, and W. K. Hartmann (1999), Voluminous volcanism on early Mars revealed in Valles Marineris, *Nature*, *397*(8003), 584–586, doi:10.1038/17539.

McEwen, A. S. et al. (2007), Mars Reconnaissance Orbiter's High Resolution Imaging Science Experiment (HiRISE), *J. Geophys. Res.*, *112*(E5), E05S02, doi:10.1029/2005JE002605.

McEwen, A. S., C. M. Dundas, S. S. Mattson, A. D. Toigo, L. Ojha, J. J. Wray, M. Chojnacki, S. Byrne, S. L. Murchie, and N. Thomas (2014), Recurring slope lineae in equatorial regions of Mars, *Nat. Geosci.*, *7*, 53–58, doi:10.1038/ngeo2014.

McKay, C. P., and W. L. Davis (1991), Duration of liquid water habitats on early Mars, *Icarus*, *90*(2), 214–221, doi:10.1016/0019-1035(91)90102-Y.

Mellon, M. T., and R. J. Phillips (2001), Recent gullies on Mars and the source of liquid water, *J. Geophys. Res.*, *106*(E10), 23165–23179, doi:10.1029/2000JE001424.

Melosh, H. J. (1979), Acoustic fluidization - A new geologic process?, *J. Geophys. Res.*, *84*(9), 7513–7520, doi:10.1029/JB084iB13p07513.

Milliken, R. E., and J. F. Mustard (2003), Erosional morphologies and characteristics of latitude-dependent surface mantles on Mars, *Sixth Int. Conf. Mars, Pasadena, Calif.*, 3240.

Mischna, M. A. (2003), On the orbital forcing of Martian water and CO2 cycles: A general circulation model study with simplified volatile schemes, *J. Geophys. Res.*, *108*(E6), 5062, doi:10.1029/2003JE002051.

Montgomery, D. R., and W. E. Dietrich (1988), Where do channels begin?, *Nature*, *336*(6196), 232–234, doi:10.1038/336232a0.

Montgomery, D. R., and W. E. Dietrich (1994), Landscape dissection and drainage area-slope thresholds, in *Process Models and Theoretical Geomorphology*, edited by M.

J. Kirkby, pp. 221–246, John Wiley and Sons, Hoboken.

Moore, D. P., and W. H. Matthews (1978), The Rubble Creek Landslide, *Can. J. Earth Sci.*, *15*, 1039–1052.

Morishige, K., and K. Kawano (2000), Freezing and melting of methanol in a single cylindrical pore: Dynamical supercooling and vitrification of methanol, *J. Chem. Phys.*, *112*(24), 11023–11029, doi:10.1063/1.481742.

Musselwhite, D. S., T. D. Swindle, and J. I. Lunine (2001), Liquid CO2 breakout and the formation of recent small gullies on Mars, *Geophys. Res. Lett.*, *28*(7), 1283–1285.

Mustard, J. F., C. D. Cooper, and M. K. Rifkin (2001), Evidence for recent climate change on Mars from the identification of youthful near-surface ground ice, *Nature*, *412*, 411–414, doi:10.1038/35086515.

Naaim, M., T. Faug, and F. Naaim-Bouvet (2003), Dry granular flow modelling including erosion and deposition, *Surv. Geophys.*, *24*(5-6), 569–585, doi:10.1023/B:GEOP.0000006083.47240.4c.

Neukum, G., B. A. Ivanov, and W. K. Hartmann (2001), Cratering records in the inner solar system in relation to the lunar reference system, *Space Sci. Rev.*, *96*, 55–86, doi:10.1023/A:1011989004263.

Nicoletti, P. G., and M. Sorriso-Valvo (1991), Geomorphic controls of the shape and mobility of rock avalanches, *Geol. Soc. Am. Bull.*, *103*(10), 1365–1373, doi:10.1130/0016-7606(1991)103<1365:GCOTSA>2.3.CO.

Núñez, J. I., O. S. Barnouin, F. P. Seelos, and S. L. Murchie (2016), Compositional constraints on martian gully formation as seen by CRISM on MRO, *47th Lunar and Planetary Science Conference*, abstract 3034.

O'Brien, J. S., and P. Y. Julien (1988), Laboratory analysis of mudflow properties, *J. Hydraul. Eng.*, *114*(8), 877–887.

Ojha, L., M. B. Wilhelm, S. L. Murchie, A. S. McEwen, J. J. Wray, J. Hanley, M. Massé, M. Chojnacki, M. Masse, and M. Chojnacki (2015), Spectral evidence for hydrated salts in recurring slope lineae on Mars, *Nat. Geosci.*, *8*, 829–832, doi:10.1038/NGEO2546.

Parsons, J. D., K. X. Whipple, and A. Simoni (2001), Experimental Study of the Grain-Flow, Fluid- Mud Transition in Debris Flows, *J. Geol.*, *109*(4), 427–447,

doi:10.1086/320798.

Patton, J. S. (1987), Shear flows of rapidly flowing granular materials, *J. Appl. Mech.*, *54*(4), 801–805.

Pelletier, J. D., K. J. Kolb, A. S. McEwen, and R. L. Kirk (2008), Recent bright gully deposits on Mars: Wet or dry flow?, *Geology*, *36*(3), 211, doi:10.1130/G24346A.1.

Picardi, G. et al. (2004), Performance and surface scattering models for the Mars Advanced Radar for Subsurface and Ionosphere Sounding (MARSIS), *Planet. Space Sci.*, *52*(1-3), 149–156, doi:10.1016/j.pss.2003.08.020.

Pilorget, C., and F. Forget (2016), Formation of gullies on Mars by debris flows triggered by CO2 sublimation, *Nat. Geosci.*, *9*(1), 65–69, doi:10.1038/ngeo2619.

Piqueux, S., S. Byrne, and M. I. Richardson (2003), Sublimation of Mars's southern seasonal CO2 ice cap and the formation of spiders, *J. Geophys. Res.*, *108*(E8), 5084, doi:10.1029/2002JE002007.

Platzer, K., P. Bartelt, and C. Jaedicke (2007), Basal shear and normal stresses of dry and wet snow avalanches after a slope deviation, *Cold Reg. Sci. Technol.*, *49*(1), 11–25, doi:10.1016/j.coldregions.2007.04.003.

Plaut, J. J., A. Safaeinili, J. W. Holt, R. J. Phillips, J. W. Head, R. Seu, N. E. Putzig, and A. Frigeri (2009), Radar evidence for ice in lobate debris aprons in the mid-northern latitudes of Mars, *Geophys. Res. Lett.*, *36*(2), L02203, doi:10.1029/2008GL036379.

Pouliquen, O., and N. Renaut (1996), Onset of granular flows on an inclined rough surface: Dilatancy effects, *J. Phys. II*, *6*(6), 923–935.

Pouliquen, O., and J. W. Vallance (1999), Segregation induced instabilities of granular fronts, *Chaos*, *9*(3), 621–630, doi:10.1063/1.166435.

Pouliquen, O., J. Delour, and S. B. Savage (1997), Fingering in granular flows, *Nature*, *386*, 816–817, doi:10.1038/386816a0.

Presley, M. A., and P. R. Christensen (1997), Thermal conductivity measurements of particulate materials 2. Results, *J. Geophys. Res.*, *102*(E3), 6551–6566.

Raack, J., D. Reiss, and H. Hiesinger (2012), Gullies and their relationships to the dust–ice mantle in the northwestern Argyre Basin, Mars, *Icarus*, *219*(1), 129–141, doi:10.1016/j.icarus.2012.02.025.

Raack, J., D. Reiss, T. Appéré, M. Vincendon, O. Ruesch, and H. Hiesinger (2015),

Present-day seasonal gully activity in a south polar pit (Sisyphi Cavi) on Mars, *Icarus*, *251*, doi:10.1016/j.icarus.2014.03.040.

Rafkin, S. C. R., M. R. V. S. Maria, and T. I. Michaels (2002), Simulation of the atmospheric thermal circulation of a martian volcano using a mesoscale numerical model, *Nature*, *420*(6911), 106–106, doi:10.1038/nature01206.

Reiss, D., S. van Gasselt, G. Neukum, and R. Jaumann (2004), Absolute dune ages and implications for the time of formation of gullies in Nirgal Vallis, Mars, *J. Geophys. Res. E Planets*, *109*(6), 1–9, doi:10.1029/2004JE002251.

Rodine, J. D., and A. M. Johnson (1976), Ability of debris, heavily freighted with coarse clastic materials, to flow on gentle slopes, *Sedimentology*, *23*, 213–234.

Roesli, U., and C. Schindler (1990), Debris flows 1987 in Switzerland : geological and hydrogeological aspects, in *Hydrology in Mountainous Regions II—Artificial Reservoirs; Water and Slopes*, pp. 379–386.

Russell, P. et al. (2008), Seasonally active frost-dust avalanches on a north polar scarp of Mars captured by HiRISE, *Geophys. Res. Lett.*, *35*(23), 1–5, doi:10.1029/2008GL035790.

Ryan, J. A., and R. M. Henry (1979), Mars atmospheric phenomena during major dust storms, as measured at surface, *J. Geophys. Res.*, *84*, doi:10.1029/JB084iB06p02821.

Schon, S. C., and J. W. Head (2012), Gasa impact crater, Mars: Very young gullies formed from impact into latitude-dependent mantle and debris-covered glacier deposits?, *Icarus*, *218*(1), 459–477, doi:10.1016/j.icarus.2012.01.002.

Schon, S. C., J. W. Head, and R. E. Milliken (2009), A recent ice age on Mars: Evidence for climate oscillations from regional layering in mid-latitude mantling deposits, *Geophys. Res. Lett.*, *36*(15), L15202, doi:10.1029/2009GL038554.

Schon, S. C., J. W. Head, and C. I. Fassett (2012), Recent high-latitude resurfacing by a climate-related latitude-dependent mantle: Constraining age of emplacement from counts of small craters, *Planet. Space Sci.*, *69*(1), 49–61, doi:10.1016/j.pss.2012.03.015.

Schorghofer, N., and K. S. Edgett (2006), Seasonal surface frost at low latitudes on Mars, *Icarus*, *180*(2), 321–334, doi:10.1016/j.icarus.2005.08.022.

Seu, R., D. Biccari, R. Orosei, L. V. Lorenzoni, R. J. Phillips, L. Marinangeli, G. Picardi, A. Masdea, and E. Zampolini (2004), SHARAD: The MRO 2005 shallow radar, *Planet. Space Sci.*, *52*(1-3), 157–166, doi:10.1016/j.pss.2003.08.024.

Shinbrot, T., N.-H. Duong, L. Kwan, and M. M. Alvarez (2004), Dry granular flows can generate surface features resembling those seen in Martian gullies., *Proc. Natl. Acad. Sci. U. S. A.*, *101*(23), 8542–8546, doi:10.1073/pnas.0308251101.

Shreve, R. I. (1966), Sherman landslide, Alaska, *Science*, *154*, 1639–1643.

Shreve, R. L. (1968), Leakage and fluidization in air-layer lubricated avalanches, *Bull. Geol. Soc. Am.*, *79*(5), 653–658, doi:10.1130/0016-7606(1968)79[653:LAFIAL]2.0.CO;2.

Smith, P. H., and the Phoenix Science Team (2009), Water at the Phoenix landing site, *40th Lunar Planet. Sci. Conf.*, abstract 1329, doi:10.1029/2004GL021326.

Squyres, S. W. (1978), Martian fretted terrain: Flow of erosional debris, *Icarus*, *34*, 600–613.

Squyres, S. W. (1979), The distribution of lobate debris aprons and similar flows on Mars, *J. Geophys. Res.*, *84*(B14), 8087–8096, doi:10.1029/JB084iB14p08087.

Squyres, S. W., and M. H. Carr (1986), Geomorphic evidence for the distribution of ground ice on Mars, *Science*, *231*, 249–252.

Squyres, S. W. et al. (2006), Two years at Meridiani Planum: Results from the Opportunity Rover, *Science*, *313*(5792), 1403–1407, doi:10.1126/science.1130890.

Stewart, S. T., and F. Nimmo (2002), Surface runoff features on Mars: Testing the carbon dioxide formation hypothesis, *J. Geophys. Res.*, *107*(E9), 5069, doi:10.1029/2000JE001465.

Stillman, D., and R. E. Grimm (2009), SHARAD penetrates only the youngest geological units on Mars, *American Geophysical Union Fall Meeting 2009*, abstract #P31B–1276.

Stock, J. D., and W. E. Dietrich (2006), Erosion of steepland valleys by debris flows, *Bull. Geol. Soc. Am.*, *118*(9-10), 1125–1148, doi:10.1130/B25902.1.

Straub, S. (2001), Bagnold revisited: Implications for the rapid motion of high-concentration sediment flows, in *Particulate Gravity Currents*, edited by W. McCaffrey, B. Kneller, and J. Peakall, pp. 91–109, Publications of the International

Association of Sedimentologists.

Stuurman, C. M., T. C. Brothers, J. W. Holt, M. Kerrigan, and G. R. Osinski (2013), SHARAD Detection of Subsurface Interfaces in Southern-Central Utopia Planitia, *American Geophysical Union, Fall Meeting 2013*, abstract #P43D–06.

Stuurman, C. M., G. R. Osinski, T. C. Brothers, J. W. Holt, and M. Kerrigan (2014), SHARAD reflectors in Utopia Planitia, Mars consistent with widespread, thick subsurface ice, *45th Lunar and Planetary Science Conference*, abstract 2262.

Tamppari, L. K., and M. T. Lemmon (2014), Vertical water vapor distribution at Phoenix, *8th International Conference on Mars*, abstract 1092.

Treiman, A. H. (2003), Geologic settings of Martian gullies: Implications for their origins, *J. Geophys. Res.*, *108*(E4), 8031, doi:10.1029/2002JE001900.

Valverde, J. M., A. Castellanos, and A. Ramos (2000), Avalanches in fine, cohesive powders, *Phys. Rev. E*, *62*(5), 6851–6860, doi:10.1103/PhysRevE.62.6851.

Varnes, D. J. (1978), Slope movement types and processes, in *Landslides, Analysis and Control*, edited by R. L. Schuster and R. J. Krizek, pp. 11–33, Special Report 176: Transportation Research Board, National Academy of Sciences, Washington, DC, United States (USA).

Vincendon, M., J. Mustard, F. Forget, M. Kreslavsky, A. Spiga, S. Murchie, and J. P. Bibring (2010a), Near-tropical subsurface ice on Mars, *Geophys. Res. Lett.*, *37*(1), 1–8, doi:10.1029/2009GL041426.

Vincendon, M., F. Forget, and J. Mustard (2010b), Water ice at low to midlatitudes on Mars, *J. Geophys. Res. E Planets*, *115*(10), 1–13, doi:10.1029/2010JE003584.

Walton, O. R., C. P. Moor, and K. S. Gill (2007), Effects of gravity on cohesive behavior of fine powders: implications for processing Lunar regolith, *Granul. Matter*, *9*(5), 353–363, doi:10.1007/s10035-006-0029-8.

Wang, G., and K. Sassa (2003), Pore-pressure generation and movement of rainfall-induced landslides: effects of grain size and fine-particle content, *Eng. Geol.*, *69*(1-2), 109–125, doi:10.1016/S0013-7952(02)00268-5.

Whipple, K. X., and T. Dunne (1992), The influence of debris-flow rheology on fan morphology, Owens Valley, California, *Geol. Soc. Am. Bull.*, *104*, 887–900.

White, B. R., and S. P. Klein (1990), Dynamic shear of granular material under variable

gravity conditions, *AIAA J.*, *28*(10), 1701–1702, doi:10.2514/3.10461.

White, O. L., and E. R. Stofan (2010), An estimation of the theoretical MARSIS aquifer detection depth, *41st Lunar Planet. Sci. Conf.*, abstract 1220.

Wieland, M., J. M. N. T. Gray, and K. Hutter (1999), Channelized free-surface flow of cohesionless granular avalanches in a chute with shallow lateral curvature, *J. Fluid Mech.*, *392*, 73–100, doi:10.1017/S0022112099005467.

Williams, K. E., O. B. Toon, J. L. Heldmann, and M. T. Mellon (2009), Ancient melting of mid-latitude snowpacks on Mars as a water source for gullies, *Icarus*, *200*, 418–425, doi:10.1029/2003JE002051.

Williams, R., R. Shao, and R. A. Overfelt (2008), The flowability of fine powders in reduced gravity conditions, *Granul. Matter*, *10*(2), 139–144, doi:10.1007/s10035-007-0068-9.

Chapter 2: Global documentation of gullies with the Mars Reconnaissance Orbiter Context Camera and implications for their formation

Tanya N. Harrison[1], Gordon R. Osinski[1,2], Livio L. Tornabene[1], and Eriita Jones[1]

[1]*Centre for Planetary Science and Exploration, Department of Earth Sciences, University of Western Ontario*

[2]*Department of Physics and Astronomy, University of Western Ontario*

2.1. Introduction

Gullies in the mid- and high-latitudes of Mars were first observed in Mars Global Surveyor (MGS) Mars Orbiter Camera (MOC) images in 1997 [*Malin and Edgett*, 2000]. Appearing to be geologically young based on superposition relationships with aeolian features and the lack of impact craters observed on the majority of gullies [*Malin and Edgett*, 2000], they quickly became a feature of interest for the Mars science community because of the implication of liquid water in their formation. This interpretation is based on the distinct morphological characteristics of gullies, including incised channels, many with banked and sinuous morphologies with terraces and streamlined features indicative of fluid flow [e.g., *Malin and Edgett*, 2000; *Edgett et al.*, 2003; *McEwen et al.*, 2007]. The possibility of liquid water on Mars in the geologically recent past—and possibly even today with the observation of present-day gully activity [*Malin et al.*, 2006; *Harrison et al.*, 2009; *Dundas et al.*, 2010, 2012; *Reiss et al.*, 2010; *Raack et al.*, 2015]—is significant as it has implications for the past and present habitability of Mars.

While the morphology of gully channels was initially interpreted as requiring liquid water for their formation [*Malin and Edgett*, 2000], the difficulty in sustaining water on the surface in the recent martian climate [e.g., *Mellon and Phillips*, 2001] led to the proposal of a number of models to explain the formation of gullies, including: 1) "dry" mass movement processes [*Treiman*, 2003; e.g., *Shinbrot et al.*, 2004] and CO_2-related processes [e.g., *Musselwhite et al.*, 2001; *Ishii and Sasaki*, 2004; *Cedillo-Flores*

et al., 2011], and 2) "wet" mechanisms such as the release of liquid water/brine from shallow [*Malin and Edgett*, 2000] or deep [*Gaidos*, 2001] subsurface aquifers, or through the melting of snowpacks [e.g., *Christensen*, 2003; *Williams et al.*, 2008a] or near-surface ground ice [*Costard et al.*, 2002] emplaced during periods of higher obliquity [e.g., *Laskar et al.*, 2004; *Levrard et al.*, 2004].

Previous surveys of gully distribution have been conducted using either MOC narrow-angle (NA) images [*Heldmann and Mellon*, 2004; *Heldmann et al.*, 2007], or MOC NA images combined with Mars Odyssey Thermal Emission Imaging System visible subsystem data (THEMIS VIS, ~18 m/pixel) [*Bridges and Lackner*, 2006] and Mars Express High Resolution Stereo Camera (HRSC, 12.5–50 m/pixel) data [*Balme et al.*, 2006; *Kneissl et al.*, 2010]. However, surveys utilizing only MOC NA suffered from low spatial coverage (<1% of the planet) and possible sampling biases due to the narrow image footprint typically only covering portion(s) of individual craters. While lower resolution datasets provided larger spatial coverage (~6% of the surface by Balme et al. [2006] and ~42% of the surface by Kneissl et al. [2010]), many gullies are not resolvable at THEMIS VIS and HRSC scale. Kneissl et al. [2010] noted that ~42% of the gullies imaged with MOC NA in their survey could not be detected by HRSC due to their small size, in addition to poor atmospheric conditions and unfavourable illumination angles at the time of image acquisition.

The Mars Reconnaissance Orbiter Context Camera (CTX) provides large areal coverage at relatively high resolution (~6 m/pixel) [*Malin et al.*, 2007] and was specifically targeted to search for gullies during ideal illumination and atmospheric conditions [*Harrison et al.*, 2009]. We have conducted an extensive study utilizing the CTX dataset to map out the global distribution of martian gullies, document variations in gully morphology, and to investigate the relationship of gullies to other landforms and regional thermophysical properties. The goal of this effort is to narrow down the range of possible gully formation mechanisms on Mars and determine whether liquid water played—or may still play—a role in their formation and evolution over time.

2.2. Methods

As of the end of February 2013, CTX has covered ~85% of the surface of Mars at a resolution of ~6 m/pixel (Figure 1). CTX provides spatial resolution capable of resolving >95% of martian gullies (in our survey, all gullies documented by Malin et al. [2010] from MOC NA images were resolvable by CTX) and large areal coverage (up to 9,390 km^2 in a single image), improving any sampling bias from previous studies [*Harrison et al.*, 2009]. Landforms potentially hosting gullies were specifically targeted by CTX during optimum seasonal illumination and atmospheric (weather) conditions to maximize slope visibility [*Harrison et al.*, 2009].

As can be seen in Figure 2.1, CTX provides excellent global coverage. However, there are notable gaps in coverage in the higher mid-latitudes, arising from poor atmospheric conditions throughout much of the martian year. In the northern hemisphere the majority of the gaps occur over the plains; however, over 90% of the craters in these regions large enough for gullies to be resolved with CTX are covered. In the southern hemisphere, the gaps occur over areas of low surface roughness [*Kreslavsky and Head*, 2000] blanketed with the mantle characteristic of the higher latitudes [*Mustard et al.*, 2001]. Gullies are rarely found in these areas based on previous surveys [*Heldmann and Mellon*, 2004; *Balme et al.*, 2006], and in our survey the occurrence of gullies is indeed sparse in the areas of the high latitudes that have coverage with CTX. As such, the documentation effort and the trends presented here are globally representative, and are not expected to change significantly with additional areal coverage by CTX.

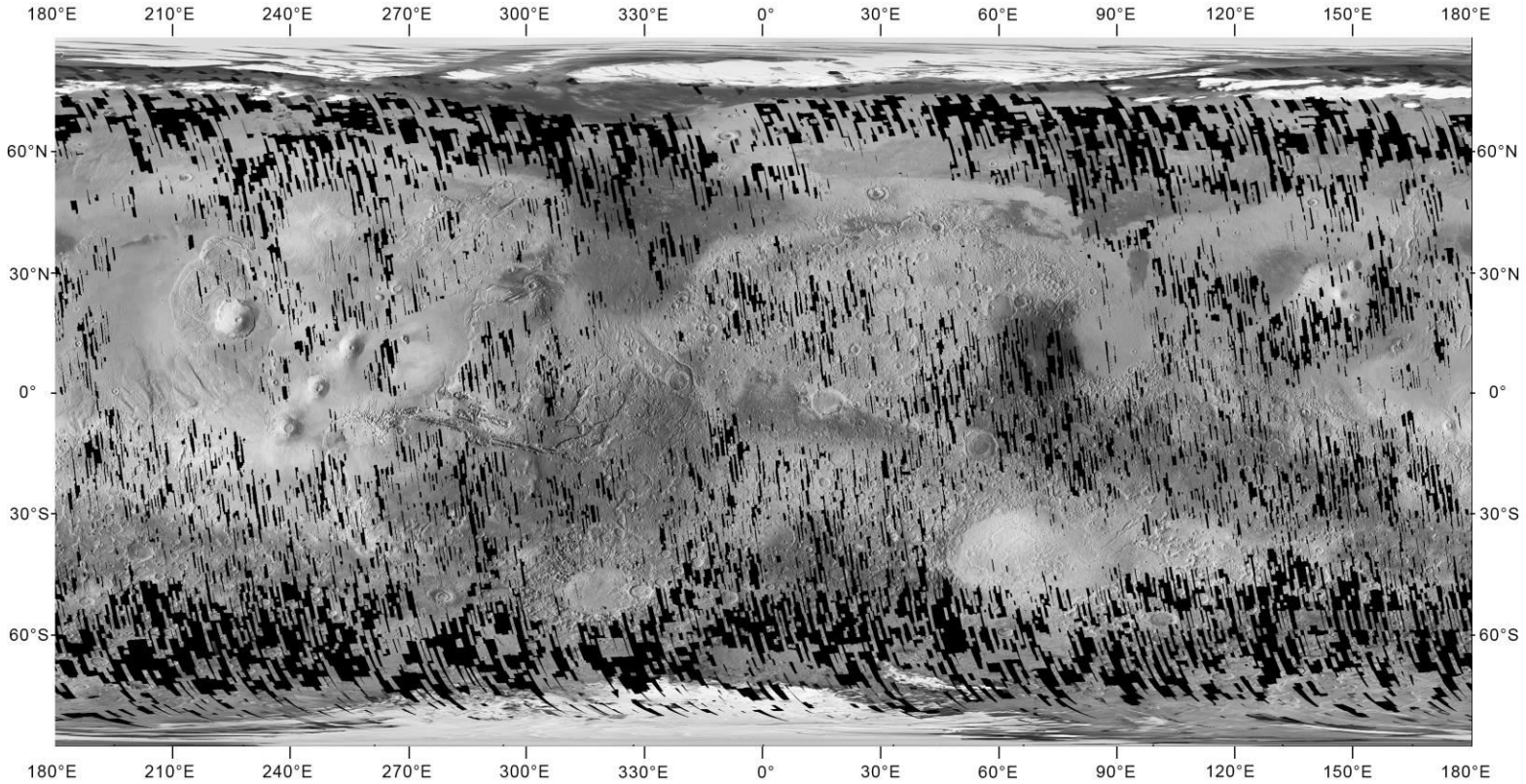

Figure 2.1. Map of CTX global coverage through the end of phase D09 (February 2013), constituting ~85% coverage of the planet at ~6 m/pixel resolution. Coverage is overlaid atop the TES albedo map of Christensen et al. [2001].

We inspected all 54,023 CTX images acquired during phases T01–D09 planet-wide (90°S–90°N) to search for occurrences of gullies, documenting their setting (e.g., crater wall, massif, scarp wall, etc.), the geographic coordinates of each gullied landform (e.g., crater center coordinates), and the orientations of the gullies present at each location. Images were analyzed using the Java Mission-Planning and Analysis for Remote Sensing (JMARS) software package [*Christensen et al.*, 2009] combined with Map a Planet on the Web (POW) [*Hare et al.*, 2013], Planetary Image LOCator Tool (PILOT), and ArcGIS.

Malin and Edgett [*2000*] define gullies as consisting of three characteristic features: alcove, channel, and apron. However, not all gullies have distinctive alcoves and/or aprons (Figure 2). Features in the equatorial regions classified as gullies by some authors [e.g., *Treiman*, 2003; *Shinbrot et al.*, 2004] (Figure 2.2A–D) host alcoves and aprons (which are characteristic of multiple mass movement processes [*Hungr et al.*, 2001]) but lack the incised channels of mid- to high-latitude gullies, which often display fluvial characteristics such as tributaries, streamlined features, and terraces [*McEwen et al.*, 2007]. Therefore, these equatorial features that lack incised channels are not considered gullies in this study, as the terrestrial definition of a "gully" is a type of incised channel morphology [*Bull and Kirkby*, 1997]. It is important to note that the term "gully" describes only a morphologic feature, and not a specific genetic process [*Hungr et al.*, 2001; *Lanza et al.*, 2010]. Typically on Earth, multiple processes contribute to gully formation and evolution—even within a single gully system [e.g., *Decaulne and Sæmundsson*, 2007]—and many different types of mass movements can occur within a pre-existing gully channel (see Hungr et al. [2001] for a comprehensive discussion of terrestrial landslide classifications).

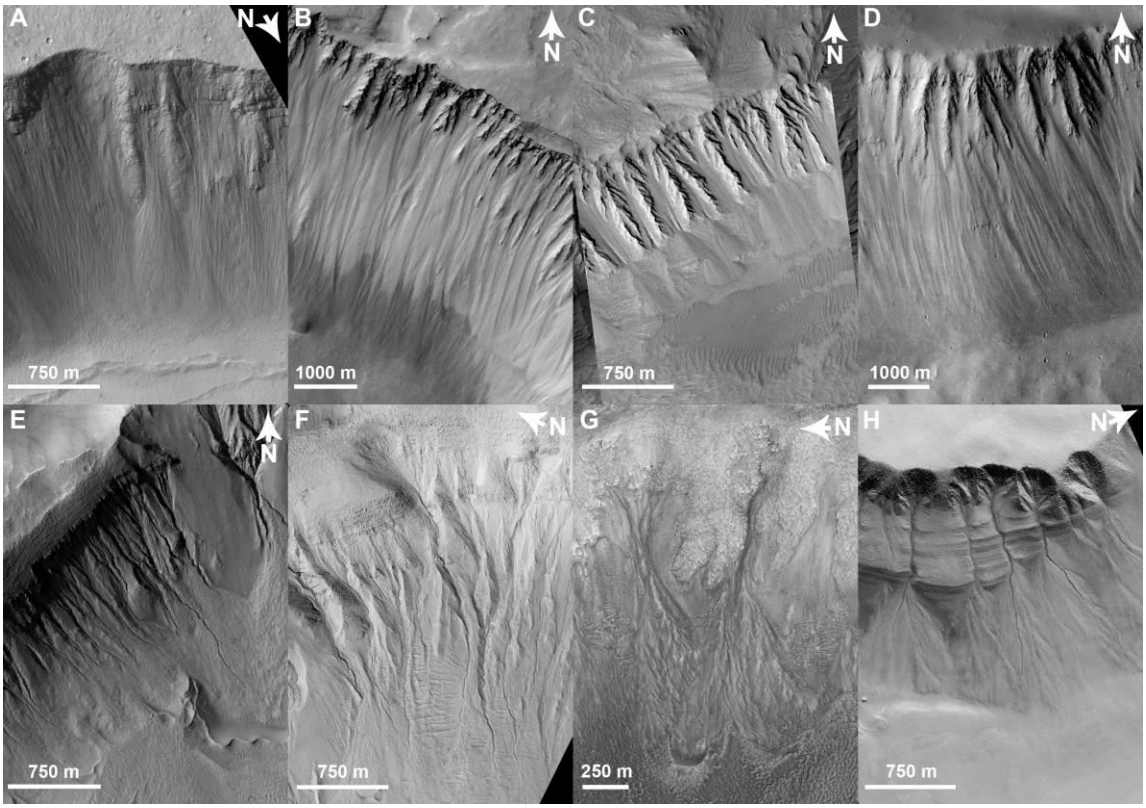

Figure 2.2. Comparison of equatorial mass movement features (A–C cited as gullies by Treiman [2003], D cited as gullies by Shinbrot et al. [2004]) and mid- to high-latitude gullies (E–H). The equatorial features lack the sinuous, deeply incised channels characteristic of martian mid- to high-latitude gullies, and are thus not counted as gully features in this study. (A) Northern wall of the Tharsis Tholus caldera, 13.94°N, 90.92°W, subframe of MOC E03-01974. (B) Northwestern wall of the Olympus Mons caldera, 18.64°N, 133.94°W, subframe of HiRISE PSP_004821_1985. (C) Northern wall of the Pavonis Mons caldera, 0.85°N, 112.81°W, subframe of MOC M18-01192. (D) Mass movement chutes on light-toned layered material in East Candor Chasma, 7.25°S, 69.04°W, subframe of MOC M11-02514. (E) Gullies on the northeastern wall of Niquero Crater, 39.05°S, 166.12°W, subframe of MOC E11-04033. (F) Gullies on the eastern wall of a crater southwest of Acidalia Mensa, 44.59°N, 26.22°W, subframe of HiRISE PSP_006953_2245. (G) Gullies on the northeastern wall of Palikir Crater, 41.83°S, 157.83°W, subframe of HiRISE PSP_005943_1380. (H) South polar pit gullies near Sisyphi Cavi, 68.65°S, 358.79°W, subframe of HiRISE ESP_013585_1115. North is up in all images. *Image credits: NASA/JPL-Caltech/MSSS/University of Arizona.*

2.3. Observations

2.3.1 Geographic Distribution

We documented 4,861 separate gullied landforms (e.g., individual craters, massifs, pits, valleys, etc.), hosting tens of thousands of individual gullies (Figure 2.3). These gullied landforms are confined to ~27–83°S and ~28–72°N and span all longitudes. While the general distribution of gullies observed in our study is consistent with the results of Balme et al. [2006] and Kneissl et al. [2010], there are a few notable differences. In particular, we observed gullies on the floors of both the Hellas and Argyre basins (Figure 2.4), which have not been documented in any previous gully surveys. The lack of detection previously is likely due to unfavourable atmospheric conditions in these basins throughout much of the martian year. More gullies are also observed poleward of ~45°S in our study relative to that of Balme et al. [2006], as well as along the Hellas and Argyre rim complexes. In the northern hemisphere, the only notable difference relative to Kneissl et al. [2010] is the presence of gullies in Arcadia Planitia. This is again likely due to poor atmospheric conditions in the northern higher latitudes throughout much of the year and CTX being specifically targeted to image around those conditions.

Regional clusters of gullied landforms are observed in both hemispheres. In the southern hemisphere, three distinct peaks in gully density (number of gullied landforms per unit area) are observed: central-eastern Terra Cimmeria/western Terra Sirenum (peaking near Gorgonum Chaos), in the vicinity of 36°S, 204°W in Terra Cimmeria, and the Argyre rim complex (Nereidum and Charitum Montes) (Figure 2.5). These clusters are consistent with the results of Balme et al. [2006], although the cluster at Gorgonum Chaos is more prominent in the CTX mapping results.

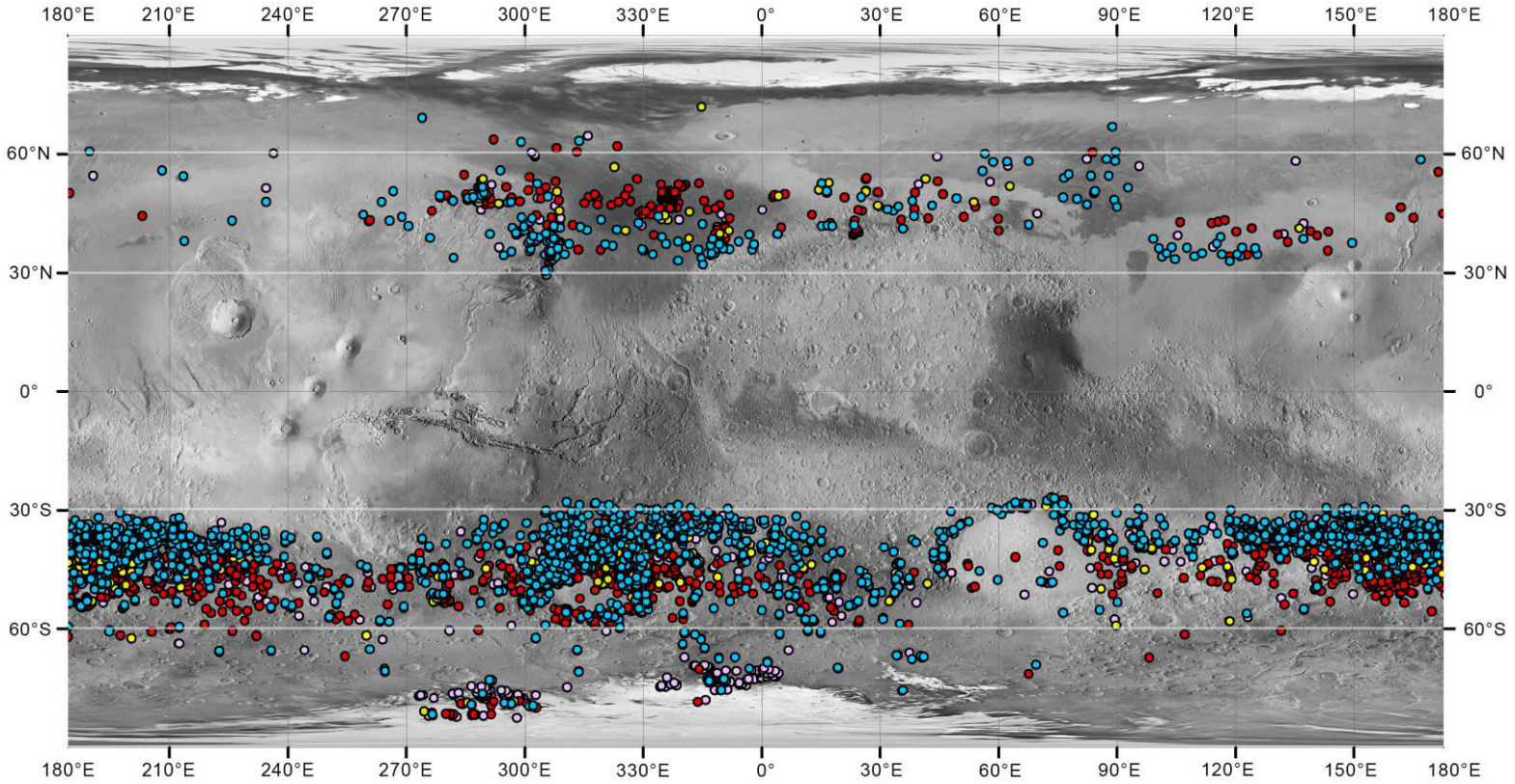

Figure 2.3. Global distribution of gullied landforms as mapped using CTX data plotted atop the Mars Global Surveyor (MGS) Mars Orbiter Camera Wide Angle (MOC WA) global mosaic overlaid on MGS Mars Orbiter Laser Altimeter (MOLA) topographic data. Colors indicate orientation preference at each landform. Blue = poleward-facing, yellow = east/west, red = equatorward, purple = no preference. *Basemap image credit: NASA/JPL-Caltech/MSSS.*

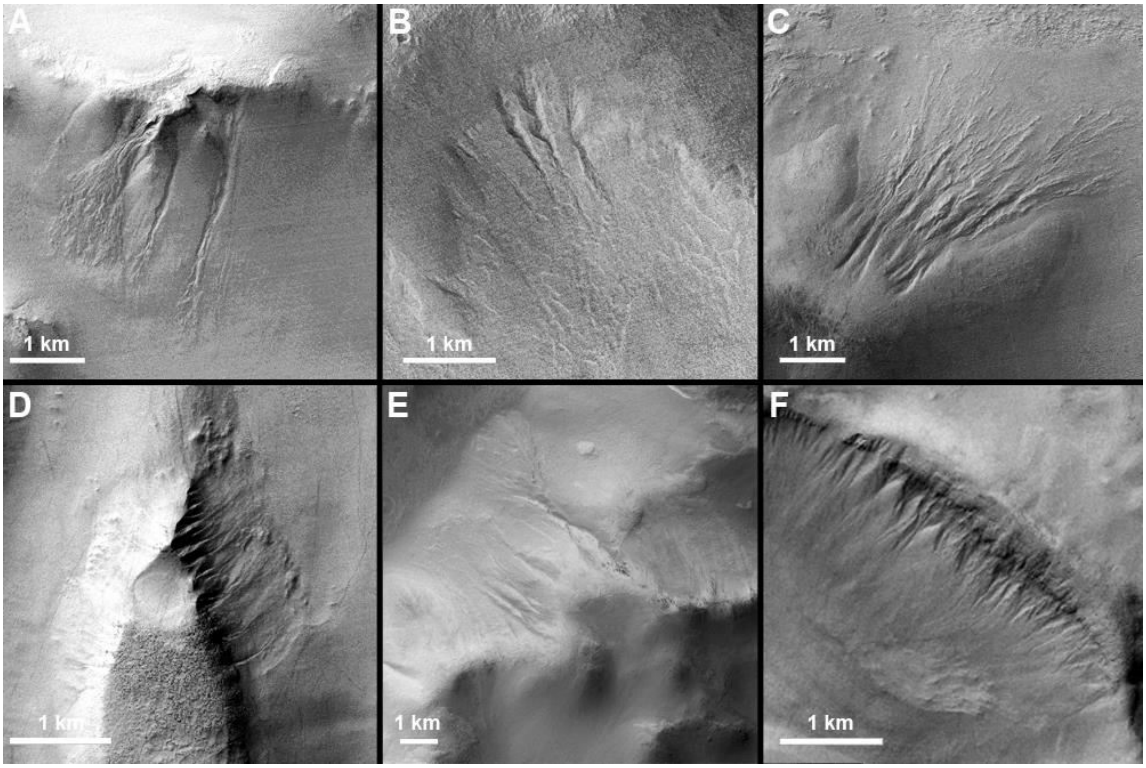

Figure 2.4. Examples of gullies discovered on the floors of Hellas (A–C) and Argyre (D–F) in our study. North is up in all images. Sub-frames of CTX images: **(A)** B19_017077_1336; **(B)** B21_017684_1383; **(C)** B18_016642_1371; **(D)** P13_006242_1327; **(E)** G15_023990_1287; **(F)** G15_024201_1323. *Image credit: NASA/JPL-Caltech/MSSS.*

In the northern hemisphere, regional clustering of gullies is observed in Tempe Terra near the boundary with Acidalia Planitia, the fretted terrain along the dichotomy boundary, and Acidalia and Utopia Planitiae. A relative lack of gullies is observed in the northern high latitudes (>55°N), on the southern flanks of Alba Patera, and in the areas of Tempe and Arabia Terrae north of 30°N until reaching the boundary with Acidalia Planitia and the fretted terrain, respectively (Figs. 2.3, 2.5). The decrease in gully density in both hemispheres roughly correlates with the lowest latitudinal extent of subdued terrain as mapped by Kreslavsky and Head [2000] [c.f., *Dickson and Head*, 2009], neglecting the effects of the steep mountain slopes of the Argyre rim complex.

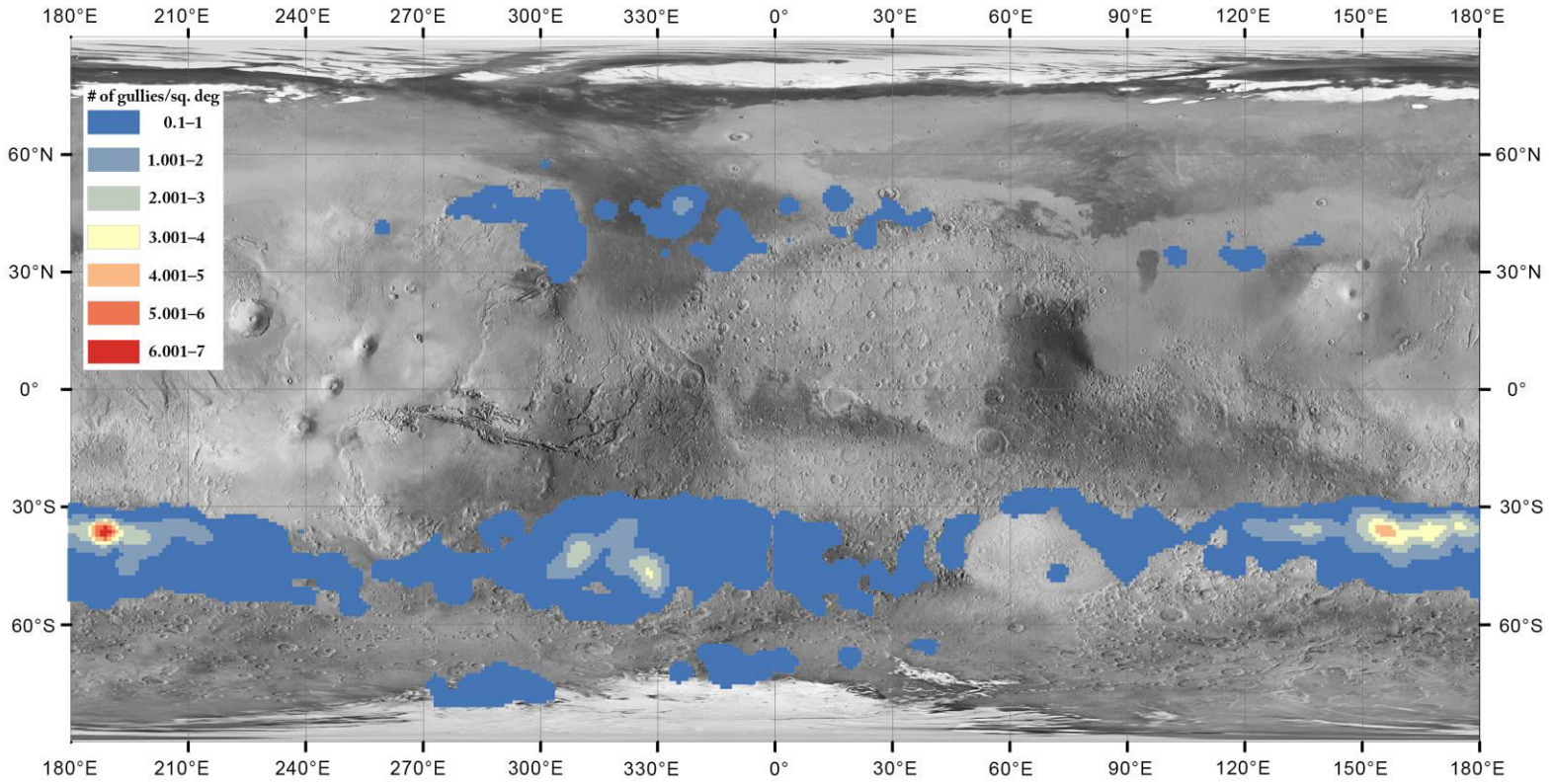

Figure 2.5. Density map of gullied landforms (number of gullied landforms per square degree). Red denotes areas of highest density. The break at 0° longitude over Noachis Terra is an artefact introduced in ArcMap. *Basemap image credit: NASA/JPL-Caltech/MSSS.*

A clear transition in dominant gully orientation is observed in the southern hemisphere, moving from poleward-facing preference in the lower mid-latitudes to equator-facing at ~45°S (Figure 2.3). The only exception is the highest latitude occurrence of gullies, in the south polar pits of Sisyphi Cavi and Cavi Angusti, which show no orientation preference. The transition of pole-facing to equator-facing preference with increasing latitude is also roughly observed in the northern hemisphere, most clearly in Acidalia, at ~40°N. Poleward of 50°N, no dominant orientation preference is observed. These observations in both hemispheres are broadly consistent with previous studies utilizing less areally extensive coverage [*Heldmann and Mellon*, 2004; *Balme et al.*, 2006; *Heldmann et al.*, 2007; *Kneissl et al.*, 2010].

Crater wall gullies occur in craters with diameters ranging from 0.07–258 km, with ~98% occurring in craters < 50 km (57% in craters < 7 km, the average simple-to-complex crater transition diameter for Mars [*Pike*, 1980])(Figure 2.6A–C). While this initially appears to show a preference for gullies to occur in small craters, normalizing the number of gullied craters by the total number of craters both planet-wide (Figure 2.6D) and in the gullied latitude bands in each hemisphere (Figure 2.6E–F) shows that the relationship is due to the greater number of smaller craters on Mars.

Gullies are found at elevations from -7,500 m to +5,700 m, with a strong preference for the -500 m to +2,500 m range (Figure 2.7). This range is larger than that of the MOC NA-based surveys of Heldmann and Mellon [2004] and Heldmann et al. [2007], although the elevation range preference is relatively consistent. A simple histogram plot of gully occurrence vs. elevation shows a distinct peak in gully occurrence at 500–1,000 m elevation globally, following the general elevation trend of the planet in the mid to high latitudes (Figure 2.7A). However, if the number of gullied landforms in each elevation bin is normalized by the surface area covered by each elevation bin in the gullied latitudes, the peak shifts to 0–500 m globally and becomes less distinct (Figure 2.7B). Looking at each hemisphere individually, the northern hemisphere peak occurs at -6,000–5,500 m when normalized for area, but this peak is

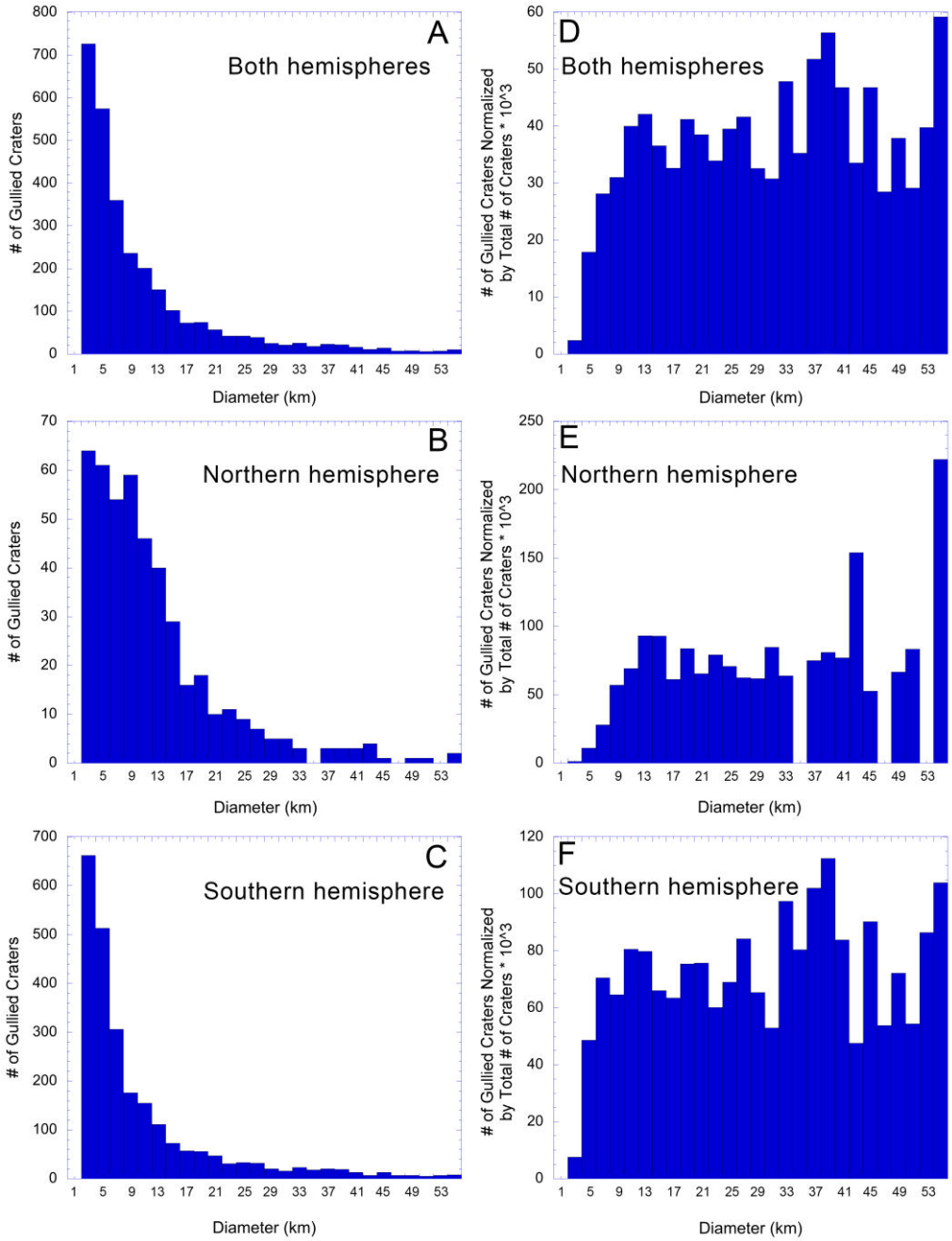

Figure 2.6. Histogram plot of the number of gullied craters vs. crater diameter (A–C) and number of gullied craters vs. crater diameter normalized by the total number of craters in each diameter bin (from Robbins and Hynek [2012]) multiplied by a factor of 10^3. X-axis labels denote the lower bound of each bin. Fewer than 20 craters are >55 km; these have been omitted from the plot. The apparent preference for gullies to occur in smaller craters in the original plots disappears upon normalization.

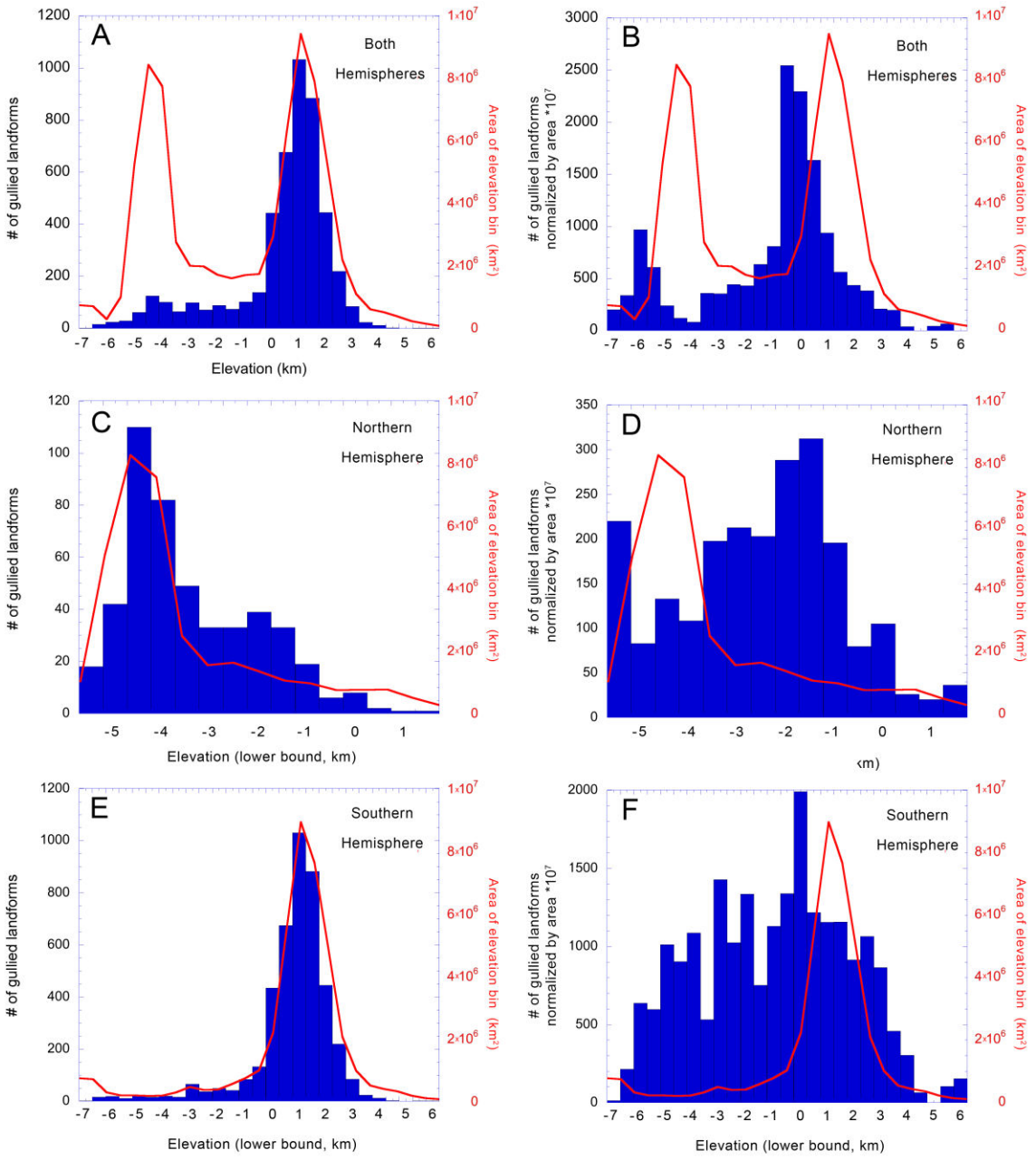

Figure 2.7. Histogram of the elevations (derived from MOLA MEGDR data) of gullied landforms for the gullied latitude bands in both hemispheres (A–B), the northern hemisphere (C–D), and southern hemisphere (E–F). The left column shows the number of gullied landforms vs. elevation, while the right column shows the number of gullied landforms normalized by the surface area covered by each elevation bin in the gullied latitude range in the corresponding hemisphere(s) vs. elevation. The red curve in each graph represents the area of each elevation bin vs. elevation, showing that the relationship between gully occurrence and latitude is not purely a result of the general elevation trends once normalized by area.

strongly influenced by the fact that this elevation bin is extremely small in area (~16,500 km^2, whereas all of the other elevation bins are ~275,000–8,300,000 km^2) (Figure 2.8). If this anomalous bin is removed from the plot, the peak occurs at -1,000–1,500 m, despite most surfaces in the northern mid to high latitudes lying at lower elevation (peaking around -4,500 m). In the southern hemisphere, the peak after normalizing for area of each elevation bin occurs at 0–500 m (Figure 2.8F) while the elevation trend of the southern gullied latitudes peaks at 1,000–2,000 m.

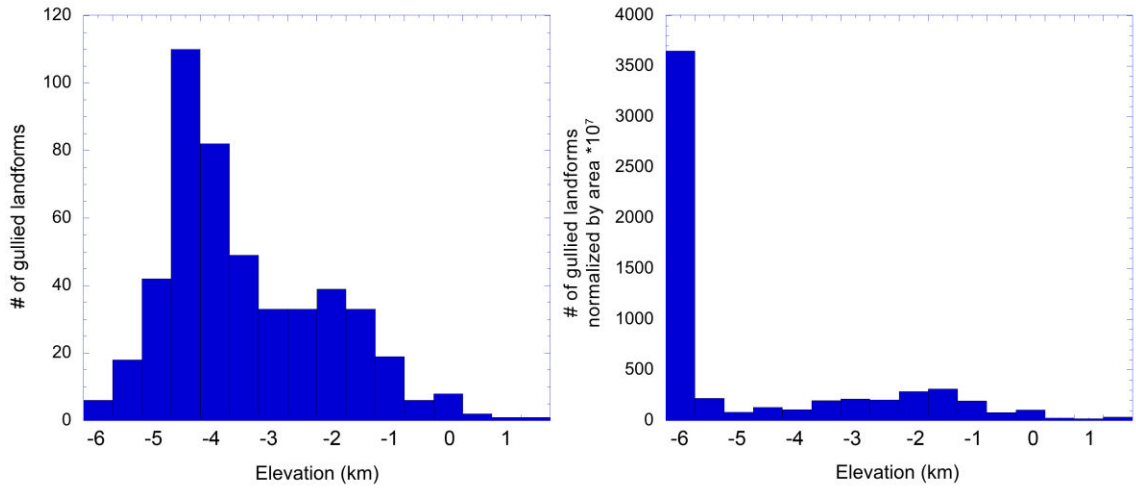

Figure 2.8. Histogram plot of the number of gullied landforms in the northern hemisphere normalized by the area of each elevation bin, with the -6–5.5 km bin included (see text for discussion).

2.3.2 Relationship of gullies to other landforms

The latitudinal distribution of gullies in both hemispheres corresponds with the distribution of surface features indicative of past and/or present near-surface ground ice such as mid-latitude ("concentric") crater fill (CCF) [*Squyres*, 1979], lobate debris aprons [*Squyres*, 1979], viscous flow features [*Milliken and Mustard*, 2003], lineated valley fill (LVF) [*Squyres*, 1979], and the latitude dependent mantle (LDM) [*Head et al.*, 2003]. In multiple craters in both hemispheres, gully channels and/or aprons are observed that both superpose and are cut by fractures associated with the removal of

mid-latitude fill material [Shean, 2010] (Figure 2.9). The LDM superposes CCF [*Head et al.*, 2003] and is dissected by gullies [*Dickson et al.*, 2013], providing information about the relative timing of formation and modification of these landforms.

In all locations we observed where dunes are co-located with crater wall/massif slope gullies poleward of ~45°S, the gullies are superposed by the dunes. From ~30–45°S, gullies incise into the dunes, with the exception of the Nereidum Montes around Argyre, where gullies are superposed by dunes (in the case of Argyre, this was previously noted by Raack et al. [2012]). Our observations indicate that gully formation and/or activity has occurred in at least portions of the mid-latitudes after the cessation of major dune activity in these latitudes. This is significant as martian dunes typically lack many superposed craters, suggesting they are relatively geologically youthful. In contrast, the partial burial of gullies by dunes at higher latitudes suggests that gully activity in these locations ceased before the accumulation of the dunes. These observations demonstrate that the timeframe for gully formation is generally modern. However, the variability in relative gully ages as compared to dunes suggests that optimal conditions for gully formation have not remained constant over time in individual locations.

2.3.3 Relationship to Thermal Properties

Jones et al. [2014] conducted global thermophysical mapping of Mars using combined albedo and nighttime thermal inertia values derived from the Mars Global Surveyor Thermal Emission Spectrometer (TES), refining the previous mapping of Putzig et al. [2005]. They defined 7 classes of surface materials, distinguished by their dominant grain size, degree of induration, and albedo (correlated with mineralogy). We find that martian gullies show a strong association with thermophysical units interpreted to be consistent with areas of low dust cover, low albedo, and grain sizes in the 60 μm–3 mm range, corresponding with the class 1 and 2 terrains of Jones et al. [2014] (Figs. 2.10 and 2.11; Table 2.1) and units B, C, and E of Putzig et al. [2005]. Some gullies occur in

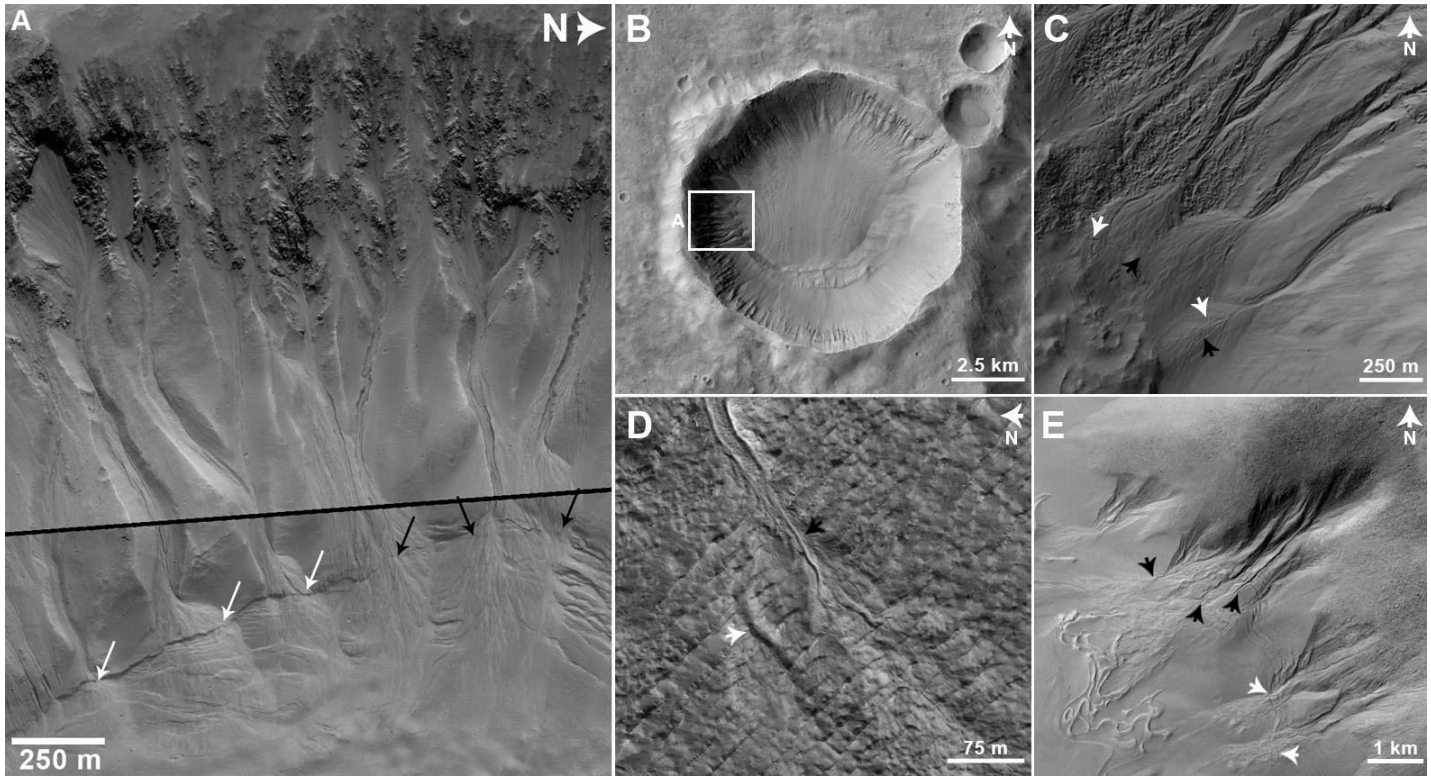

Figure 2.9. Gullies and their relationship to mid-latitude crater fill. White arrows denote fill margin cracks cutting gully channels and/or aprons, while black arrows denote gully channels or aprons cutting and/or superposing fill margin cracks. The presence of both of these relationships demonstrates that gully activity in these locations occurred both before and after (and/or during) the retreat of the mid-latitude crater fill. **(A)** Mosaic of subframes of HiRISE ESP_02294_1435 and ESP_022216_1435. **(B)** White box marks context for (A), showing the greater extent of the evidence for fill retreat (terraces and marginal cracks). Subframe of CTX B12_014357_1440. **(C)** Subframe of HiRISE ESP_016504_1410. **(D)** Subframe of HiRISE ESP_019157_1430 showing a highly eroded gully channel cut by fill marginal cracks adjacent to a more youthful gully, which cuts through the cracks. **(E)** Gullies in the Nereidum Montes. Subframe of CTX P14_006572_1367. *Image credits: NASA/JPL-Caltech/University of Arizona/MSSS.*

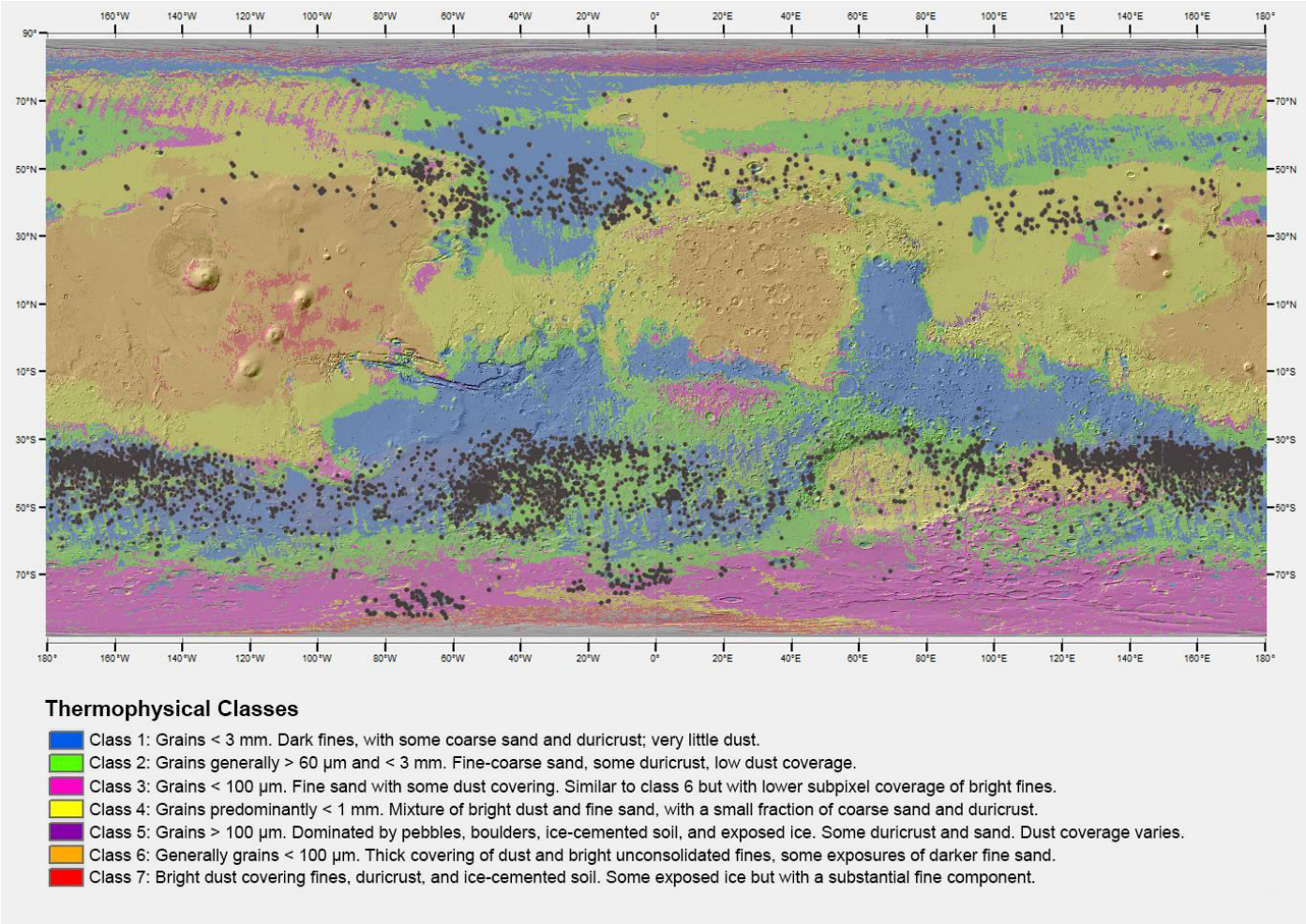

Figure 2.10. Locations of gullied landforms (black dots) plotted atop the global thermophysical map of Jones et al. [2014]. Gullies are strongly associated with class 1 and 2 terrains (see Fig. 2.11), which both consist of low dust cover, low albedo, and a grain size in the 60 µm–3 mm range. See Table 2.1 for a comparison between these units and those of Putzig et al. [2005].

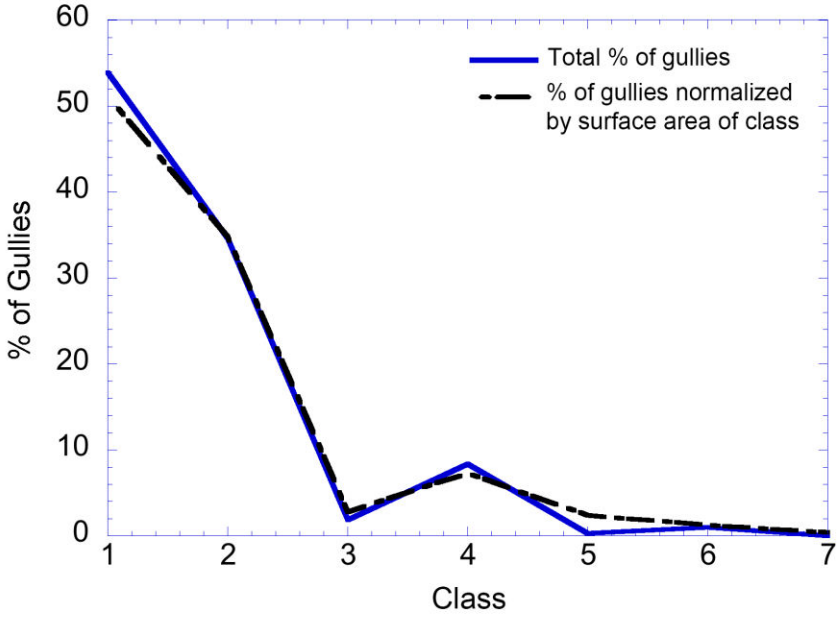

Figure 2.11. Plot of the percentage of gullied landforms located within each thermophysical surface class of Jones et al. [2014] (solid line) and the percentage normalized by the total surface area covered by each class (dashed line). Gullies show a strong correlation with classes 1 and 2. See Fig. 2.10 and Table 2.1 for details.

class 4 terrain, which is interpreted to be dustier terrain than classes 1 and 2 but similar in grain size; most of these cases occur in the northern hemisphere. Gullies are rare in units interpreted to be dominated by very fine (< 100 μm) or very coarse (pebbles/boulders) grains and in units of thick dust cover. This is in contrast to the MOC NA-based gully surveys by Heldmann and Mellon [2004] and Heldmann et al. [2007], who stated that gullies in both hemispheres were typically found in areas of higher albedo and lower thermal inertia relative to global trends. The Heldmann and Mellon [2004] and Heldmann et al. [2007] studies utilized thermal inertia studies derived by Mellon et al. [2000, 2002] from Mars Years (MY) 24 and 25, whereas the thermal inertia and albedo dataset derived by Putzig et al. [2005] contains a significantly larger number of observations than previous maps, and spans MY24–27. The Jones et al. [2014] maps utilized derived thermal inertia from MY24–27 and albedo values from

Jones et al. [2014] Class	Color on Map (Fig. 10)	Dust Cover	Dominant Grain Size	General Interpretation of Dominant Surface Grains from Jones et al. [2014]	Unit from Putzig et al. [2005]	Thermal Inertia	Albedo	% Surface [Putzig et al. 2005]	Interpretation from Putzig et al. [2005]
Class 1*	Blue	Low	< 3 mm	Dark fines with some coarse sand and duricrust; very little dust.	E	High	Very low	0.3	As B, but little or no fines
Class 2*	Green	Low	60 μm–3 mm	Fine-coarse sand, some duricrust, and low dust coverage.	B	High	Low	36	Sand, rocks, and bedrock; some duricrust
Class 3	Fuchsia	Some	< 100 μm	Fine sand with some dust covering. Similar to Class 6 but with a lower subpixel coverage of fines,	D	Low	Low-med	2	Low-density mantle or dark dust?
Class 4*	Yellow	Mix	< 1 mm	Mixture of bright dust and fine sand, with a small fraction of coarse sand and duricrust,	C	High	Med	23	Duricrust; some sand, rocks, and bedrock
Class 5	Purple	Mix	> 100 μm	Dominated by pebbles, boulders, ice-cemented soil, and exposed ice. Some duricrust and sand. Dust coverage varies.	F	Very high	All	4	Rocks, bedrock, duricrust, and polar ice
Class 6	Orange	Thick	< 100 μm	Thick covering of dust and bright, unconsolidated fines, some exposures of darker fine sand.	A	Low	High	19	Bright unconsolidated fines
Class 7	Red	Thick		Bright dust covering fines, duricrust, and ice-cemented soil. Some exposed ice but with a substantial fine component.	G	Low-high	Very high	0.7	As A, thermally thin at higher inertia

Table 2.1. Terrain class descriptions from Jones et al. [2014] and Putzig et al. [2005]. Asterisks denote classes in which gullies are concentrated.

MY24. Dust storm activity and dust optical depth of the atmosphere were lowest in MY24 compared to the rest of the years analyzed by Putzig et al. [2005] [*Cantor et al.*, 2002; *Smith*, 2004; *Tamppari et al.*, 2008]; therefore, MY24 albedo values should be the most representative of average martian surface materials [*Jones et al.*, 2014]. The different datasets used may thus account for the differences in our observations versus those of Heldmann and Mellon [2004] and Heldmann et al. [2007].

2.3.4 Morphology

Figures 2.12 and 2.13 show examples of "typical" gullies in the mid and high latitudes across both hemispheres. Northern hemisphere gullies tend to be much less developed (e.g., shorter channels and smaller aprons with lobes suggestive of fewer periods of activity) and more heavily eroded than their southern hemisphere counterparts [c.f., *Heldmann et al.*, 2007]. We find that, in general, pole-facing gullies tend to be better developed than equator-facing gullies in both hemispheres, indicating gully activity occurred more frequently or for longer periods of time on pole-facing slopes [c.f., *Dickson and Head*, 2009]. Mid-latitude gullies in both hemispheres are also generally better developed than those at higher latitudes [c.f., *Bridges and Lackner*, 2006], suggesting that gullies in the mid-latitudes were more active than those in the higher latitudes.

The substrate material through which gully channels incise plays a significant role in overall gully morphology [e.g., *Rowntree*, 1991; *Harrison et al.*, 2013]. Figure 14A–B shows examples of gullies with channels in crater walls that incise into aeolian dunes that have superposed the crater walls, while Figure 14C shows dune gullies in Russell Crater. The morphologies of all three examples are nearly identical, with low-sinuosity channels lacking debris aprons commonly seen with typical crater/valley/scarp wall gullies. Alcoves, which are typically (but not always) associated with crater wall gullies, are not present in these examples.

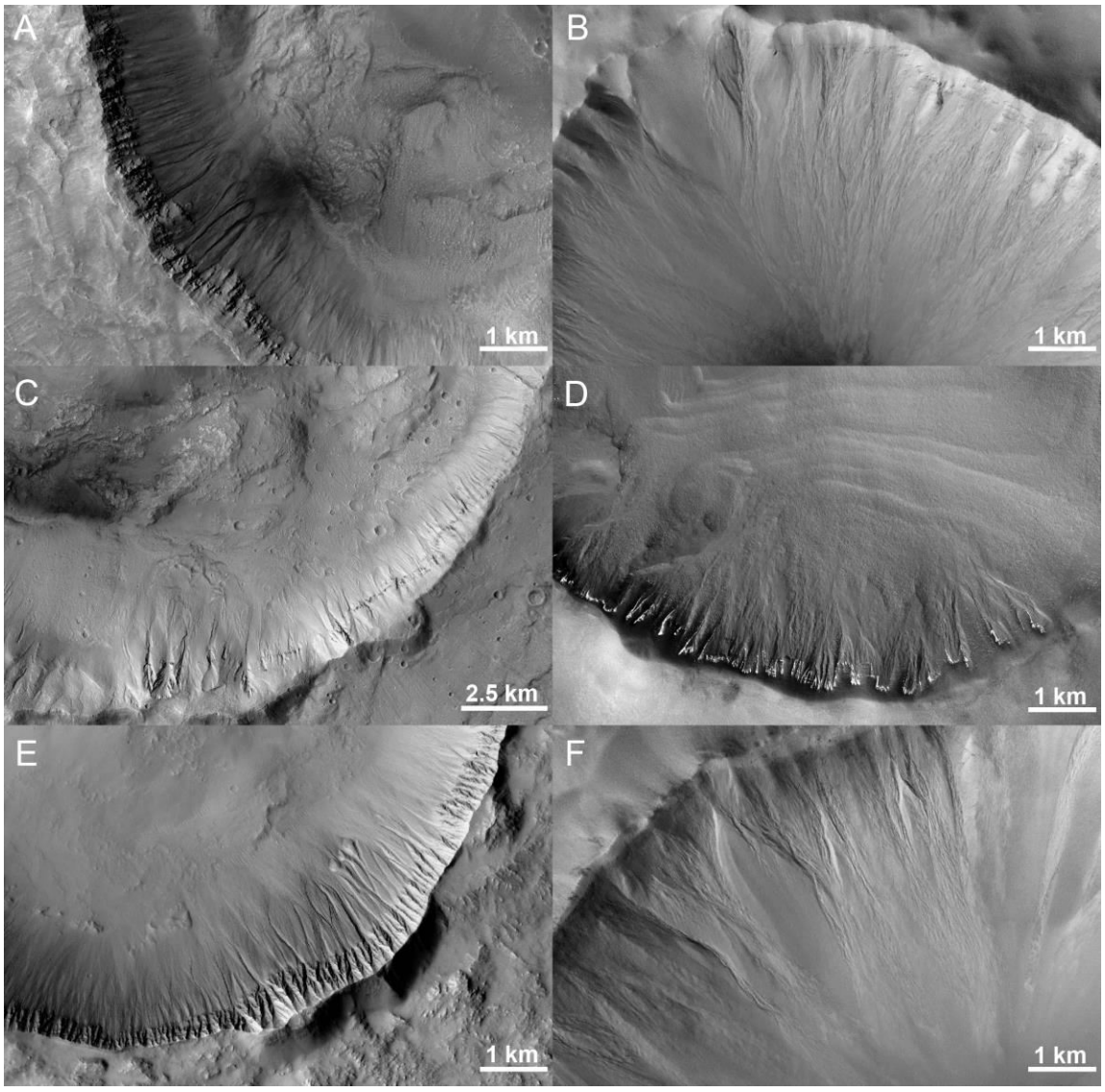

Figure 2.12. Mid-latitude (left column) vs. high-latitude (right column) gullies in the northern hemisphere. High-latitude gullies typically display deeper alcoves, incising into thicker mantling material than at lower latitudes, and are often localized to fewer slopes within single craters than mid-latitude gullied craters. Gullies at high latitudes also tend to be much less developed than mid-latitude gullies, with smaller aprons and lobes suggestive of fewer periods of activity. Subframes of CTX images: **(A)** G12_022808_1426 (Triolet Crater), **(B)** B12_014299_1184, **(C)** G15_024241_1402, **(D)** B09_013162_1261, **(E)** B11_013962_1429, and **(F)** G14_023621_1189. North is up in all images. *Image credit: NASA/JPL-Caltech/MSSS.*

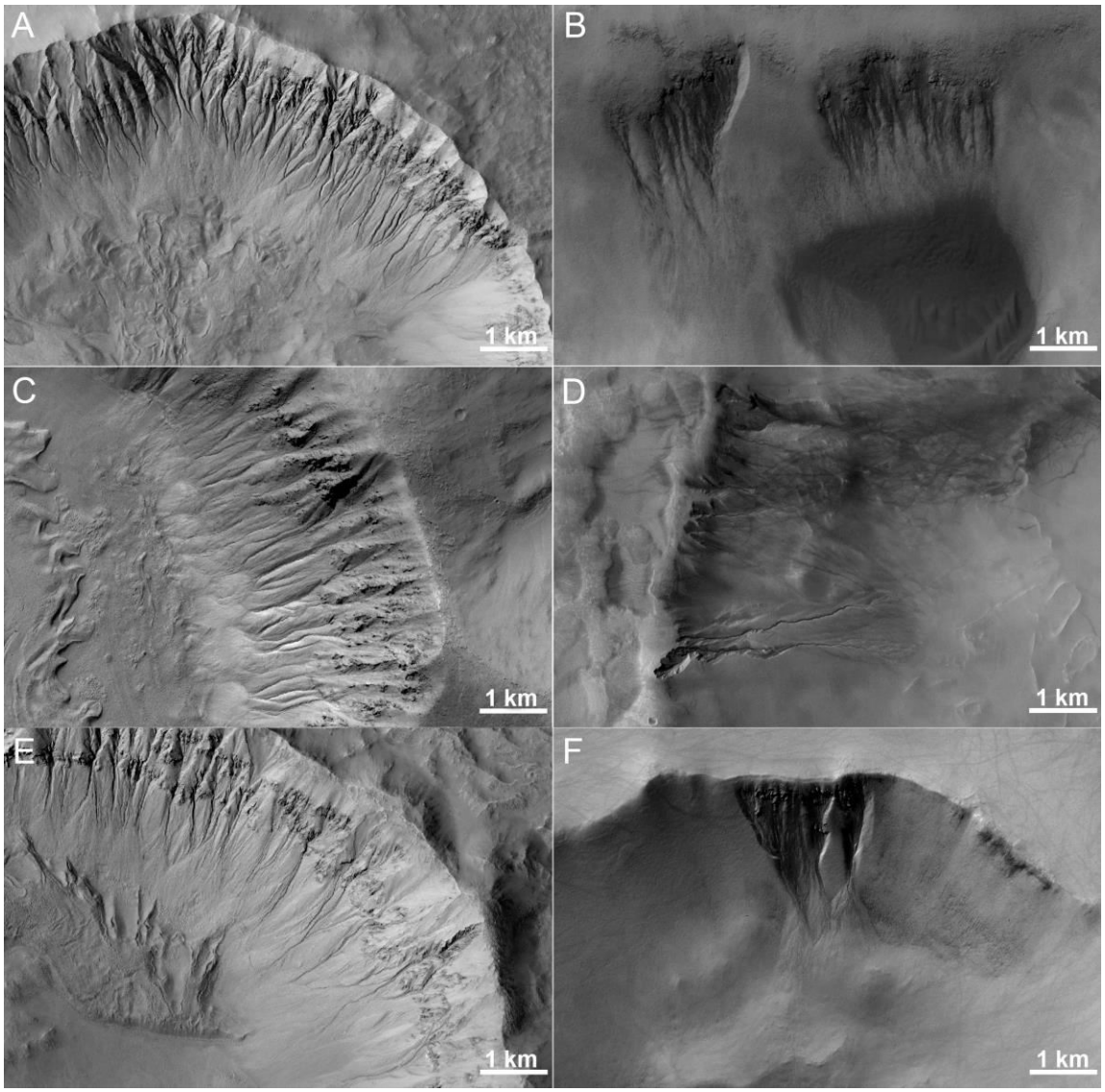

Figure 3.13. Mid-latitude (left column) vs. high-latitude (right column) gullies in the southern hemisphere. As observed in the northern hemisphere, southern high-latitude gullies typically display deeper alcoves, incising into thicker mantling material than at lower latitudes. High-latitude gullies in the southern hemisphere also tend to be much less developed than mid-latitude gullies, with smaller aprons and lobes suggestive of fewer periods of activity. Subframes of CTX images: **(A)** B21_017805_2149, **(B)** G23_027128_2448, **(C)** B22_018187_2189, **(D)** B19_016917_2471, **(E)** B22_018096_2186, and **(F)** G23_027274_2461. North is up in all images. *Image credit: NASA/JPL-Caltech/MSSS.*

Changes in morphology of a single gully system as it cuts through different lithologies are also observed. Figure 14D–E shows an example of a gully channel (38.7°S, 181.8°E) that originates in a relatively bare portion of exposed rock in a crater wall. Mantling ("pasted on") material [*Christensen*, 2003] is present downslope on the crater wall. The alcove/gully walls abruptly become deeper where the channel intersects this material.

Differences in gully morphology within individual craters are observed as well. Figure 14F shows an example of gullies occurring on two walls of a crater (39.5°S, 176.9°E) where the northern wall is covered by mantling material and the eastern wall appears to be mantle-free. The gullies on the western wall display fine channels lacking large alcoves, whereas the gullies on the northern wall are larger with significantly deeper alcoves. Both sets of gullies have relatively small debris aprons. These differences in morphology suggest that substrate properties play a significant a role in controlling the morphology of gullies.

2.4. Interpretations and Discussion

Despite many previous studies, there remains considerable debate about what physical (e.g., slope, substrate, etc.) and environmental conditions are required for gully formation [e.g., *Malin and Edgett*, 2000; *Costard et al.*, 2002; *Christensen*, 2003; *Treiman*, 2003; *Hugenholtz*, 2008]. We suggest that the latitudinal distribution, shift in orientation preference with increasing latitude, strong correlation with regions of distinct thermophysical characteristics, and location relative to areas of documented glacial features and to areas of present-day near-surface ground ice all point towards insolation and atmospheric conditions (e.g., temperature) playing key roles in martian gully formation. Many of the characteristic morphologic features of gully channels, such as banked/sinuous channels, terraces, streamlined features in some examples, and occurrence on slopes well below the angle of repose [e.g., *Malin and Edgett*, 2000; *Heldmann and Mellon*, 2004; *McEwen et al.*, 2007], require formation by a process other than dry granular flow (contrary to Treiman [2003] and Shinbrot et al. [2004]).

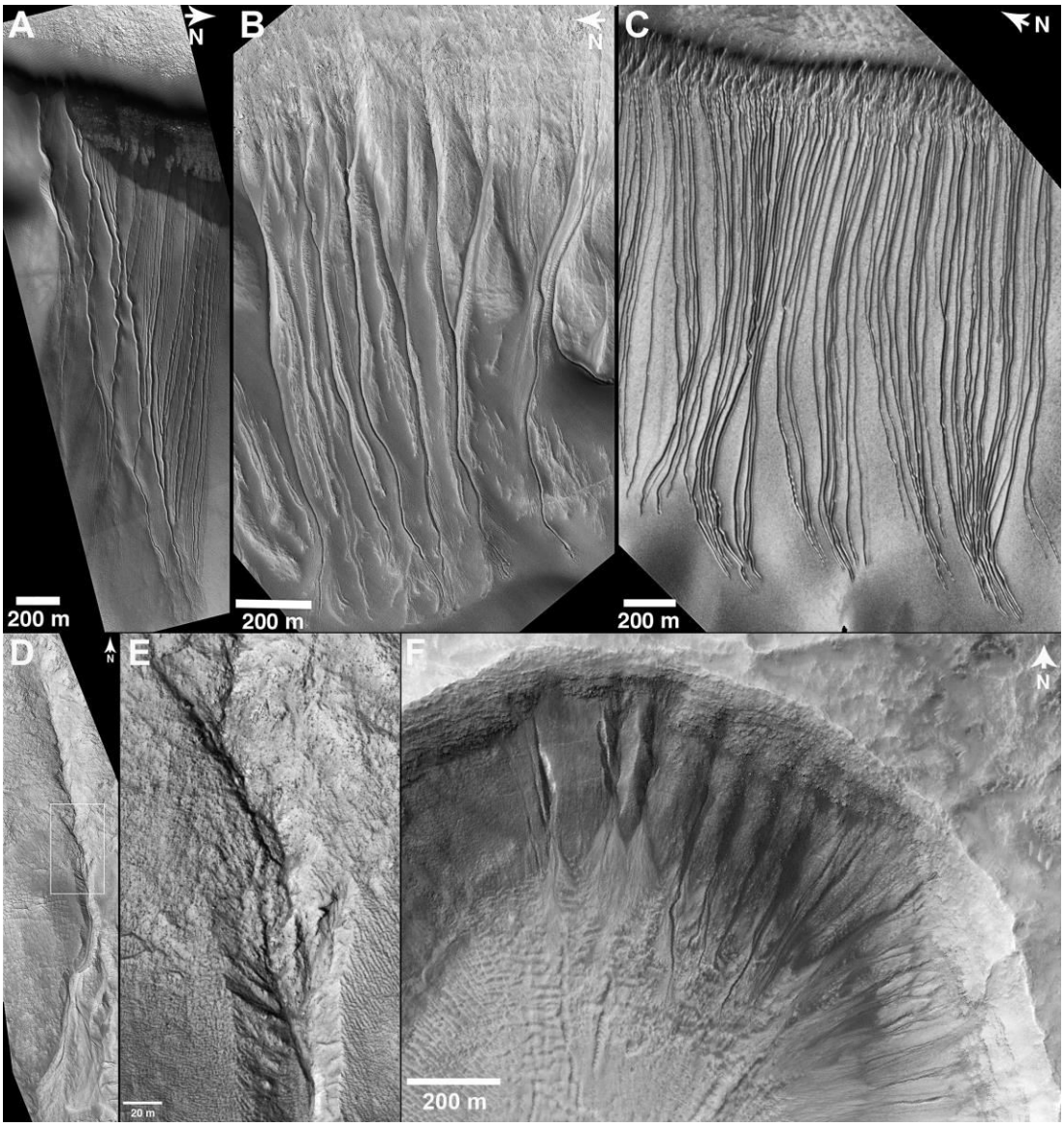

Figure 2.14. Relationships between gully morphology and substrate properties. **(A)** Crater wall gullies in an unnamed crater near 52.7°S, 351.8°E. The gullies originate in the crater wall and then incise into aeolian dunes that have superposed the crater wall. Subframe of HiRISE image PSP_006821_1270. **(B)** Crater wall gullies in Avire Crater in HiRISE ESP_012206_1390 that incise into dunes superposed on the crater wall. **(C)** Dune gullies in Russell Crater. Subframe of MOC NA M19-01170. **(D)** HiRISE PSP_003979_1410 showing a gully incised into both a crater wall and mantling material. White box denotes the location of Figure 2.13E. **(E)** Higher resolution view of the change in gully morphology at the crater wall/mantle contact. **(F)** Gullies in the wall of a crater near 38.5°S, 194.5°E displaying differing morphologies in the northern wall, which is mantled by pasted on material, and the northeastern wall, which hosts dark, possibly sandy material. Subframe of HiRISE ESP_023665_1410. *HiRISE image credits: NASA/JPL-Caltech/University of Arizona. MOC NA image credit: NASA/JPL-Caltech/MSSS.*

Here we discuss proposed formation mechanisms based on the observations made in this study.

2.4.1 Frost-related processes

Frost (predominantly CO_2 over a small amount of H_2O) can accumulate as far north as 24°S in the southern hemisphere [*Schorghofer and Edgett*, 2006] and has been observed within gully alcoves on Mars today [e.g., *Costard et al.*, 2007], leading to the suggestion of its involvement in gully formation. Ishii and Sasaki [2004] propose CO_2 frost avalanches during periods of defrosting as a formation mechanism for martian gullies. Avalanches initiated by seasonal defrosting likely play a role in the development of gully systems [e.g., observations by *Costard et al.*, 2007], but are unlikely to be the primary formation mechanism as they do not explain the morphological characteristics of gully channels suggestive of fluid flow. Diniega et al. [2013] propose that the "linear" dune gullies in Russell Crater (Figure 2.14C) were carved by CO_2 frost blocks dislodging near the dune crest and moving downhill. However, these linear gullies are morphologically distinct from typical crater wall-type gullies (with the exception of those in 2.14A–B); this process would not result in the channel morphologies observed in the majority of gullies.

Other authors have suggested sublimation of CO_2 frost initiating gas-fluidized mass movement to form gullies [*Hoffman*, 2002; *Cedillo-Flores et al.*, 2011; *Raack et al.*, 2015]. However, these models require frost accumulation on pole-facing slopes at high latitudes, making it difficult to explain lower mid-latitude and equator-facing gullies. Raack et al. [2015] note that while they prefer the CO_2 gas fluidization hypothesis for their observations of present-day activity within a gully in Sisyphi Cavi, this process is not necessarily linked to the overall gully formation process.

Hugenholtz [2008] proposes frosted granular flow as a gully formation mechanism on Mars. Frosted granular flow—terrestrially referred to as "frost coated clast flow," or FCCF—is a rare type of landslide on Earth where downslope movement is facilitated by thin frost coatings on grains, permitting flow across slopes as low as 24° [*Hétu et al.*, 1994]. They are found in periglacial environments on slopes with platy or friable lithologies, frequent freeze-thaw cycles, and limited snow cover over the course of

the seasons [*Hétu et al.*, 1994]. Flow initiation requires some kind of triggering mechanism upslope—in the case of Mars, these could include rockfalls [*Hétu et al.*, 1994], point-source defrosting [*Costard et al.*, 2007], vapour-induced instability [*Hoffman*, 2002], or avalanching of CO_2 frost [*Ishii and Sasaki*, 2004]. Locations of repeated flows often either follow pre-existing channels or, when diverted by obstacles, create new channels. FCCFs exhibit levees, straight to sinuous channels, concave profiles, and digitate termination [*Hétu et al.*, 1994; *Hétu and Gray*, 2000], similar to debris flows, but the channels are very shallow (0.5–1.5 m) and wide [*Hétu et al.*, 1994; *Hétu and Gray*, 2000] and do not resemble those of martian or terrestrial gullies (Figure 2.15). The observation of fluvial characteristics in some martian gullies channels such as terraces and streamlined landforms [*Malin and Edgett*, 2000; *McEwen et al.*, 2007] also argues against this hypothesis as these are not observed in FCCFs. These types of features are also not observed in dry avalanches [*Hungr et al.*, 2001]. Therefore, while FCCFs or frost/defrosting avalanches may play a role in gully development on Mars, they are not likely to be exclusively responsible for the initial formation of gully channels.

Melting of frost under favourable conditions has also been proposed as a possible formation mechanism for martian gullies [*Hecht*, 2002; *Hecht and Bridges*, 2003], as has been observed in gullies in the Antarctic Dry Valleys on Earth [*Marchant and Head*, 2007]. In martian gully alcoves, after the sublimation of seasonal CO_2 frost, the underlying H_2O frost could potentially melt due to heating rapid enough to avoid sublimation [*Hecht and Bridges*, 2003; *Kossacki and Markiewicz*, 2004]. Sufficient meltwater could have potentially been generated to lead to mass movement activity under past martian climate conditions, but while melting could occur under present-day conditions [*Kossacki and Markiewicz*, 2004], the low H_2O frost abundance on Mars today would not likely generate enough meltwater to explain the present-day gully activity observed [*Hecht and Bridges*, 2003; *Kossacki and Markiewicz*, 2004]. However, the occurrence of gullies on equator-facing slopes is difficult to explain with this model, as frost accumulation would only be expected on pole-facing slopes [e.g., *Schorghofer and Edgett*, 2006].

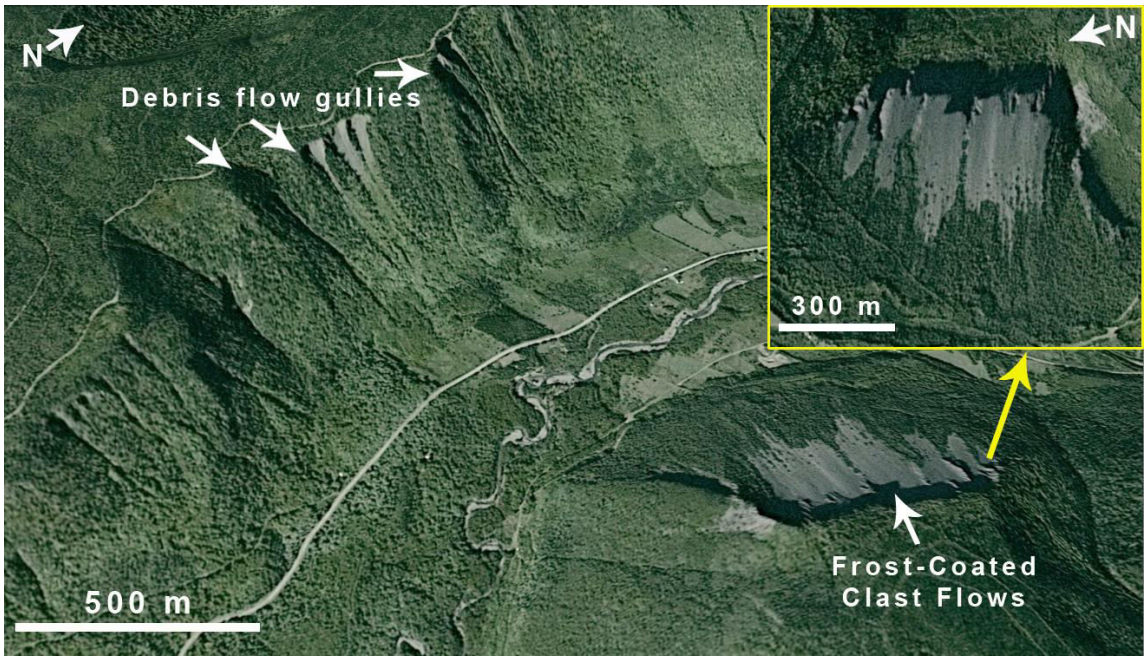

Figure 2.15. Gully channels carved by debris flows compared to a slope that has experienced frost-coated clast flow (FCCF) in Mont-Saint-Pierre, Quebec (slope T3 from Hétu et al. [1994]). The debris flow-carved gullies exhibit deep alcoves and incised channels, similar to many martian gully systems, while the FCCF slope displays a very different morphology, lacking clearly incised channels at this scale. *Image credit: Google Earth/CNES/Spot Image.*

2.4.2 Groundwater release

Malin and Edgett [2000] first proposed that gullies formed via the release of groundwater from shallow subsurface aquifers, while Gaidos [2001] proposed a deeper aquifer source. Heldmann and Mellon [2004] supported the subsurface aquifer hypothesis as only 9% of the gullied locations they inspected had alcoves that were occupied by pasted on material, citing this as evidence against a snowmelt water source if the pasted on material represents remnants of a dusty snowpack [*Christensen*, 2003]. The lack of detection of gullies on the floor of Hellas in previous studies was used as evidence against the groundwater hypothesis as groundwater would be expected to flow toward low elevations [e.g., *Dickson and Head*, 2009], and the low elevation of the basin floor provides a temperature and pressure environment where water could persist for longer periods of time on the surface relative to the rest of the planet [*Haberle et al.*, 2001]. While we have now documented gullies on the floors of both Hellas and Argyre, there are still observations that do not support the shallow groundwater hypothesis.

Shallow subsurface aquifers would not be sustainable under Late Amazonian hyperarid conditions of low atmospheric temperature, pressure [e.g., *Carr*, 1996], and soil temperatures (<196 K in gullied latitudes [e.g., *Mellon and Jakosky*, 1993])—where subsurface ice would sublime before ever reaching the melting point—when gullies formed [*Mellon and Phillips*, 2001]. The Mars Reconnaissance Orbiter Shallow Radar (SHARAD) instrument, with a maximum penetration depth of ~1 km depending on subsurface material properties [*Carter et al.*, 2009], has also found no evidence of subsurface reflections indicative of liquid water beneath gullied regions [*Nunes et al.*, 2010]. Many example of gullies thought to originate from a specific rock layer in MOC NA images, one of the key observations used to support the shallow subsurface aquifer hypothesis [e.g., *Malin and Edgett*, 2000; *Heldmann and Mellon*, 2004], have small tributary channels originating higher in the crater wall visible at HiRISE resolution [c.f., *Dickson and Head*, 2009]. This observation demonstrates that these gullies do not originate at a specific rock layer. The occurrence of gullies on sand dunes and isolated peaks such as the central peaks of impact craters and the mountains in the Argyre rim complex is difficult to explain with a groundwater model, as confined aquifers located within these isolated settings are unlikely [e.g., *Costard et al.*, 2002].

2.4.3 Melting of snow

A top-down snowmelt model has been suggested by previous authors [*e.g.,* [*Christensen*, 2003; *Bridges and Lackner*, 2006; *Williams et al.*, 2008a; *Dickson and Head*, 2009; *Heldmann et al.*, 2012]. Models show that snowfall is possible in the mid to high latitudes at higher obliquity [*Mischna*, 2003; *Madeleine et al.*, 2009], which could then be concentrated into topographic hollows to create snowpacks thicker than the annual average precipitation. Subsequent melting of these snowpacks via direct solar insolation would then lead to gully formation and activity, as observed in the Antarctic Dry Valleys [e.g., *Dickson et al.*, 2007; *Morgan et al.*, 2008]. Gully activity and channel incision initiated entirely by snowmelt has also been documented in northern and northwestern Iceland, where sudden rapid snowmelt is the primary control on debris flow initiation [*Decaulne and Sæmundsson*, 2007]. Flows here were observed in association

with rapid (~10°C) temperature increases, leading to saturation of superficial loose debris on slope faces [*Decaulne and Sæmundsson*, 2007].

The effect of microclimates on the development of gullies has been documented in the Antarctic Dry Valleys [*Marchant and Head*, 2007]. Flow in gullies on slopes where the regional average conditions would lead to sublimation rather than melting of snow has been directly observed in summer, largely driven by melting of snowpacks on locally warmer slopes that accumulated in sheltered areas due to katabatic winds [*Morgan et al.*, 2007, 2008], demonstrating the importance of local over regional conditions. Significant microclimate control is also observed in the Mont-Saint-Pierre region of Quebec, where the aforementioned FCCFs documented by Hétu et al. [1994] are located. This area (Figure 2.15) consists of a steep glacial valley that terminates at the St. Lawrence River. The east-facing slopes of the valley experience deep snow cover in winter, leading to the formation of gullies via debris flows from snowmelt [*Hétu and Gray*, 2000]. The west-facing slopes, ~1.5 km away, remain relatively snow-free, and FCCFs are "almost exclusively" responsible for downslope mass movement on these faces [*Hétu and Gray*, 2000]. The effect of microclimates on gully formation on Mars is illustrated in examples of adjacent craters of similar preservation states (or in some cases, formed simultaneously (Figure 2.16)) where some bear gullies while others do not. If a larger-scale regional control were responsible, the distribution of gullies in a given region would be expected to be more homogenous. Heldmann and Mellon [2004] cite the lack of homogeneity as a strike against the snowmelt hypothesis, but their argument neglects the effects of microclimates.

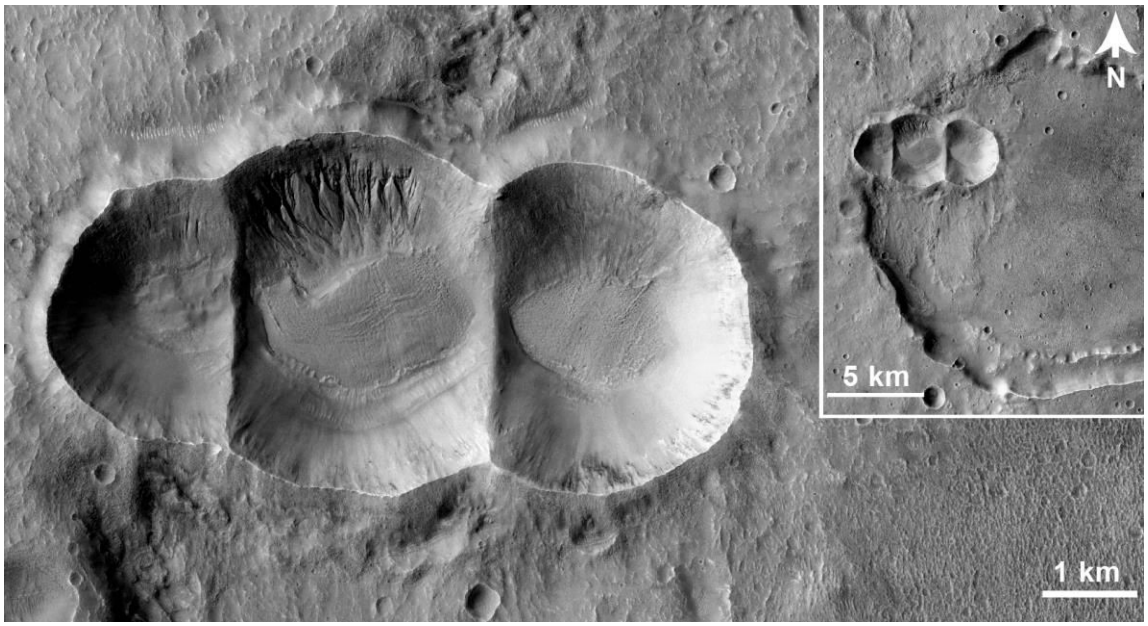

Figure 2.16. Example of adjacent craters, all of which exhibit pasted on material and crater fill material, but not all contain gullies. These three craters in Terra Sirenum must have formed simultaneously due to the lack of ejecta within them, and have therefore been exposed to identical climatic conditions for the same length of time since their formation, but only the western two craters exhibit gullies. Subframe of CTX B12_014329_1430. Inset shows the context of these craters, which formed upon the wall of a larger, older crater. *Image credit: NASA/JPL-Caltech/MSSS.*

The global distribution of gullies on Mars relative to the areas of predicted mid-latitude ice accumulation at higher obliquity may lend support to the snowmelt hypothesis [*Harrison et al.*, 2014]. Gullies are clustered around the margins of mid-latitudes ice sheets modeled by Madeleine et al. [2009] (Figure 2.17). Storm activity would be expected along the margins of these ice sheets due to katabatic winds, as is observed along the margins of the seasonal caps in spring and summer (when the temperature gradient between the frost-covered and frost-free ground is greatest)—and to a lesser extent along the edges of the permanent caps in winter—on Mars today [*Malin et al.*, 2007]. These storms on Mars today consist of dust and water ice clouds. If the martian atmosphere were thicker and capable of holding more water vapour in the past, these storms would have deposited dust and snow on the surface. Dust deposited

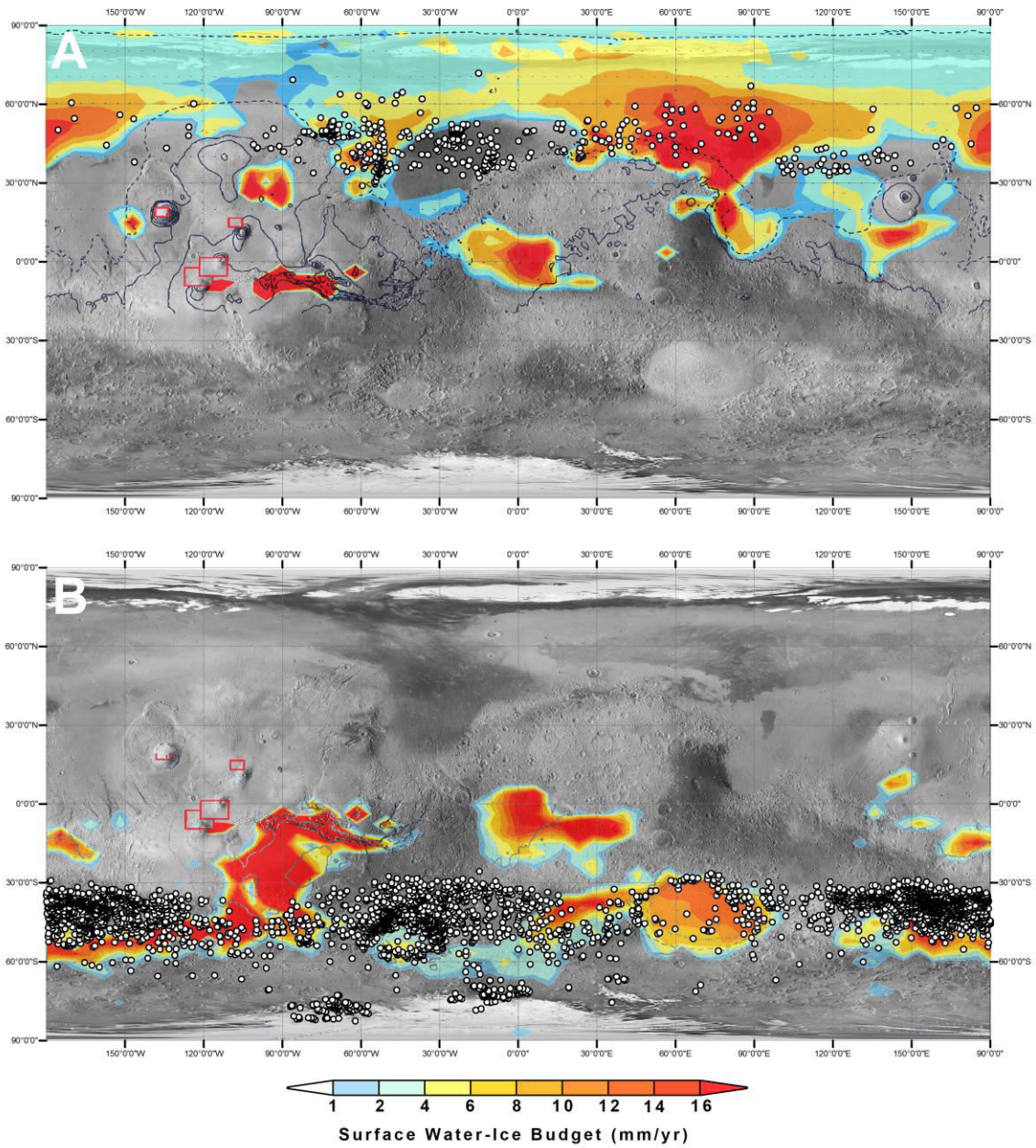

Figure 2.17. Global distribution of gullied landforms relative to the modeled locations of peak mid-latitude glaciation (obliquity = 35°, eccentricity = 0.1) in the northern **(A)** and southern **(B)** hemispheres from Madeleine et al. [2009]. Red boxes denote the locations of ice at 45° obliquity from which the mid-latitude ice sheets are sourced. *Basemap image credit: NASA/JPL-Caltech/MSSS.*

atop snowpacks would help to preserve them across multiple seasons or years, and in favourable locations melting could occur via solar insolation, resulting in erosion to slowly form gullies over time [e.g., *Christensen*, 2003; *Williams et al.*, 2008a; *Morgan et*

al., 2010]. As the mid-latitude ice sheets retreated as obliquity decreased, the areas of storm activity would migrate to follow the edges of the retreating ice, resulting in deposition of snow and dust in previously ice-covered areas, allowing for eventual gully formation.

This sequence of events explains the global distribution of gullies in terms of the latitudinal dependence and regional clustering, as well as the greater maturity of mid- versus high-latitude gullies. The observation of mid-latitude gullies being generally more well-developed than those at higher latitudes [e.g., *Bridges and Lackner*, 2006] is explained by this model, as more melting would be expected at the warmer mid-latitudes. It also explains the greater evolution of pole-facing versus equator-facing gullies: snowpacks should be better preserved on pole-facing slopes [e.g., *Christensen*, 2003], providing a source of meltwater for longer periods of time. Greater erosion rates lead to a positive feedback loop, creating larger alcoves in which snow can accumulate, and hence a larger contributing area for the gully system. Lanza et al. [2010] found that the relationship between contributing area and slope gradient for martian gullies indicates a shallow and broadly distributed water source, such as melting snow or ground ice (discussed in the following section), as opposed to a concentrated source such as release of groundwater from an aquifer, also lending support to this hypothesis.

2.4.4 Melting of near-surface ground ice

Costard et al. [2002] were the first to propose meltwater from near-surface ground ice as the water source for the formation of martian gullies. Their modeling found that the only locations on Mars where the daily mean temperature was above the melting point of water during the past obliquity cycle are poleward of 30°, where melting would have been permitted to depths of ~10–50 cm depending on the thermal conductivity parameters used for the subsurface. Accumulation of ground ice to such depths is expected at obliquities greater than ~30° based on modeling [*Mellon and Jakosky*, 1995], and is present even today in the northern hemisphere poleward of ~40°N [e.g., *Boynton*, 2002; *Feldman*, 2004; *Byrne et al.*, 2009]. Surface melting would only occur on poleward-facing slopes in the 28–40°S range, and on all slopes south of 60°S in the Costard et al. [2002] models. The concentration of gullies in the south polar pits can be

explained in this model by increased insolation over the pole at high obliquity, although this is predicted for pole-facing slopes and gullies are found at all orientations in the pits.

Modeling by Mellon and Phillips [2001] shows that ground ice as shallow as 5 cm never reaches the melting point, even at high obliquity (50°) unless the ice is composed of 15–40% salts. Measurements from Viking [*Clark*, 1981], Pathfinder [*Wänke et al.*, 2001], the Mars Exploration Rovers [*Vaniman et al.*, 2004], and Phoenix [*Hecht et al.*, 2009] indicate that the salt content of martian regolith varies between 8–30% by mass, in the range where melting could occur. Modeling by Mellon and Jakosky [1995] predicts that near-surface ground ice should be present globally at obliquities >32°, which Heldmann and Mellon [2004] suggest implies gullies should not be restricted to areas poleward of 30°. However, climate modeling by Levrard [2004] and Madeleine et al. [2009] found that surface ice accumulates on the flanks of the large volcanoes and in Terra Sabaea, the only two equatorial regions where glacial/ice-related features have been observed [e.g., *Shean et al.*, 2005; *Schon and Head*, 2012]. If ground ice were also concentrated in these regions, it could explain the general lack of gullies at the equator, but does not explain the lack of gullies in areas of predicted equatorial ice accumulation.

Gilmore and Phillips [2002] and Lanza and Gilmore [2006] note that if shallow subsurface ice is the source of liquid for gully formation globally, gullies should emanate from lower along slopes closer to the equator due to the relationship between ground ice stability and latitude. A weak relationship between gully head depth and latitude has been documented in previous studies [*Heldmann and Mellon*, 2004; *Lanza and Gilmore*, 2006; *Heldmann et al.*, 2007], which may suggest ground ice plays a role in gully formation in at least some locations, although a more broad survey utilizing HiRISE digital terrain models (DTMs) may be in order to confirm this observation as Jones et al. [2007] found the relationship to be statistically insignificant. Lanza et al. [2010] also determined that area-slope relationship in some gullies (measured using HiRISE DTMs) indicates that the source of the liquid involved in their formation must be shallow and broadly distributed, such as ground ice or snow, as release of water from a subsurface aquifer would only result in saturation of the regolith at a discrete point and would therefore not be expected to form debris flows with an area-slope relationship. The observation of polygonal terrain in association with some gullies [*Bridges and Lackner*, 2006; *Levy et al.*, 2008; *Lanza et*

al., 2010], as well as the inference of subsurface ice from the Mars Odyssey Gamma Ray Spectrometer (GRS) [*Boynton*, 2002; *Feldman*, 2004], the direct observation of shallow subsurface ice in the northern mid-latitudes within polygonal terrain by Phoenix [*Arvidson et al.*, 2008] and MRO [*Byrne et al.*, 2009], and the detection of possible nearly pure water ice by SHARAD in the northern mid-latitudes [*Bramson et al.*, 2014; *Stuurman et al.*, 2014] may also lend support to the ground ice hypothesis.

Measurements of insolation properties of gullied vs. non-gullied slopes in the northern hemisphere by Lanza and Gilmore [2006] found that gullied slopes have a thermal environment conducive to the formation of gullies, receiving a consistent amount of insolation throughout the year due to their latitude and aspect. Ollila and Gilmore [2007] and Ollila et al. [2008] expanded upon this, examining temperatures of gullied vs. non-gullied slopes in both hemispheres. They found that while daytime temperatures of gullied vs. non-gullied slopes did not differ significantly from each other throughout the seasons, nighttime temperatures on gullied slopes were higher in spring and summer than non-gullied slopes. This supports our interpretation based on the large-scale (3 km) TES thermal units from Jones et al. [2014] that gullies occur in higher thermal inertia environments relative to non-gullied slopes, as units with higher thermal inertia will retain warmer nighttime temperatures.

Our observation of a correlation between gullies and units of high thermal inertia and low albedo supports the shallow ground ice hypothesis. Surface materials with low albedo and high thermal inertia provide the warmest subsurface thermal environment within the top tens of meters of the subsurface, with the temperature-depth profile dependent on the thermophysical properties of the surface and subsurface materials [*Jakosky et al.*, 2000; *Mellon et al.*, 2000]. High albedo low thermal inertia materials on the other hand act as good insulators, providing a more stable but colder subsurface profile. Therefore, subsurface melting would be more likely to occur in the high thermal inertia low albedo units. TES thermal inertia measurements show that the mid-latitudes of Mars, where gullies are generally found, appear to be dominated by upper layers of higher thermal inertia and the polar regions by lower thermal inertia [*Putzig and Mellon*, 2007], which may play a role in decreasing gully density with latitude if thermal inertia is playing a role in gully formation.

The correlation of gullies with terrains of specific thermophysical characteristics (low dust cover and 60 μm–3 mm grain size) suggest that although thermal inertia and albedo provide information only on surficial materials (on the order of centimeters), there may be an association between the surface grain size distribution and the presence of past volatile-rich materials in the subsurface. This may be related to the shallow subsurface thermal environment, which is known to be largely dominated by the heat-conduction characteristics of surface materials [*Turcotte and Shubert*, 1982; *Pollack and Huang*, 2000]; hence, the surface materials in gullied regions may have the ideal thermal characteristics to insulate and promote the stability of subsurface ground ice. This is a potentially significant insight that should be investigated in further detail in future work.

2.4.5 Present-day gully activity

The observation of present-day gully activity in both crater wall gullies [*Malin et al.*, 2006; *Harrison et al.*, 2009; *Dundas et al.*, 2010] and dune gullies [*Diniega et al.*, 2010; *Reiss et al.*, 2010] suggests that whatever processes formed gullies initially may still be active today. Therefore, this must be taken into account when looking at possible formation processes. Some active processes in gullies today are clearly dry—for example, boulder tracks from rockfalls observed in gully alcoves (Figure 2.18)—but other newly-formed features observed such as the formation of new apron deposits (e.g., Figure 19B) [*Malin et al.*, 2006; *Harrison et al.*, 2009; *Diniega et al.*, 2010; *Dundas et al.*, 2010; *Reiss et al.*, 2010] and channels [*Dundas et al.*, 2014], require another explanation.

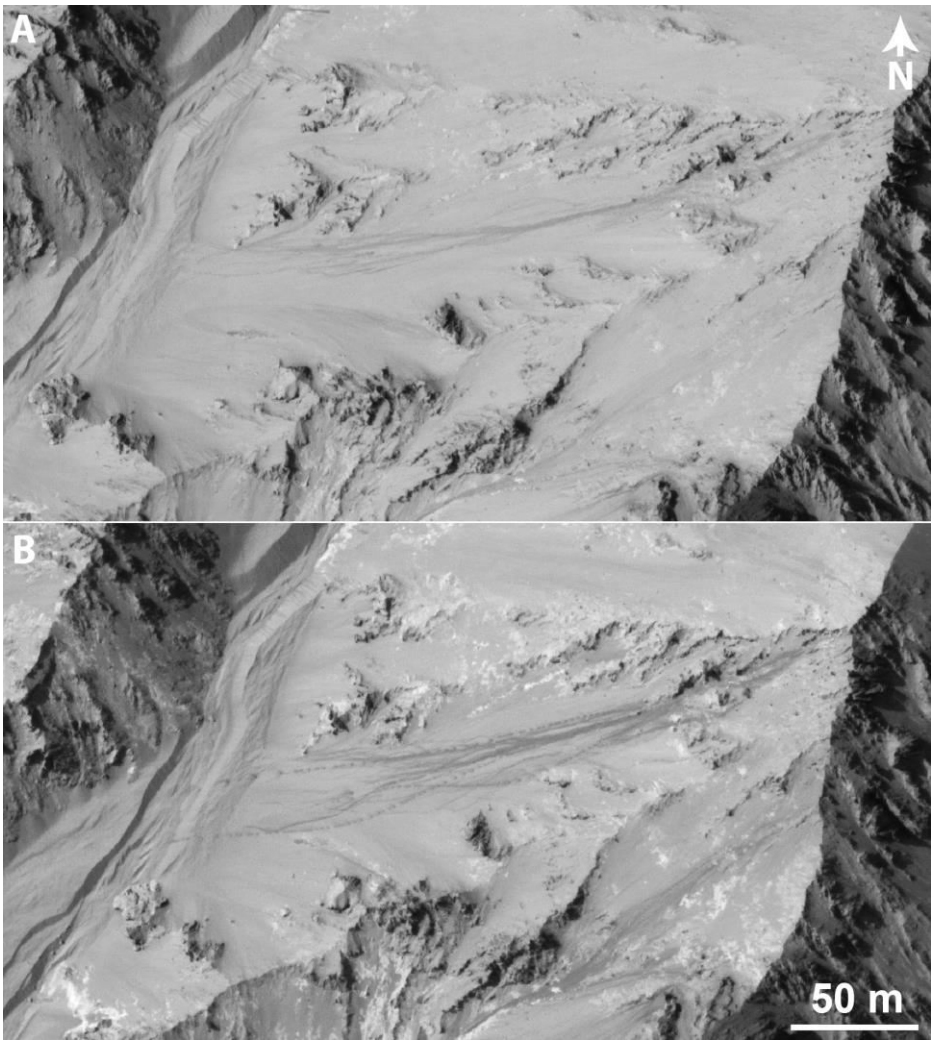

Figure 2.18. Before **(A)** and after **(B)** images of boulder tracks from rockfalls in a gully alcove in Gasa Crater. Subframes of HiRISE images **(A)** PSP_004060_1440 and **(B)** PSP_005550_1440. *Image credit: NASA/JPL-Caltech/University of Arizona.*

Present-day gully activity is concentrated outside of summer [*Harrison et al.*, 2009; *Diniega et al.*, 2010; *Dundas et al.*, 2012], with dune gully activity in particular appearing to occur preferentially in winter during periods of active defrosting [*Diniega et al.*, 2010; *Dundas et al.*, 2012]. This activity appears to occur later seasonally in the higher latitudes than in the mid-latitudes [*Dundas et al.*, 2012]. The concentration of activity in winter led to the suggestion of frost-related processes as the trigger [*Diniega et al.*, 2010; *Dundas et al.*, 2012]. As noted in section 4.1, melting of H_2O frost in the current martian climate would be unlikely to generate enough meltwater to account for the scale of the observed gully activity [*Kossacki and Markiewicz*, 2004]. The new gully

flows are observed on slopes as low as 10° [*Dundas et al.*, 2012], much lower than both the typical angle of repose (26°–35° depending on climate and material properties [*Ritter*, 1986]) and slopes on which FCCFs have been observed on Earth (≥24°) [*Hétu et al.*, 1994; *Hétu and Gray*, 2000]. This is significant as experiments aboard the NASA KC-135 spacecraft found that with decreasing gravity the dynamic angle of repose increases, scaling as a factor of $\sqrt{g}$ [*White and Klein*, 1990; *Brucks et al.*, 2007], while the fluidization decreases [*Walton et al.*, 2007; *Williams et al.*, 2008b]. For example, well-rounded 1.35 mm diameter glass beads under terrestrial gravity were found to have an angle of repose of 30° in terrestrial gravity and 34° under martian gravity in experiments by White and Klein (1990). Therefore, entirely dry flows and FCCFs are highly unlikely to be responsible for at least some the new gully flows.

Pelletier et al. [2008] modeled the new gully flow in Penticton Crater (from Malin et al. [2006]) and stated that the flow was "more likely" to be dry than a purely liquid water flow, although they did note that debris flows—which require water by definition [e.g., *Hungr et al.*, 2001]—were also consistent with their models and observations. One of their key arguments was that dry flow was required to produce the fingering observed in the Penticton flow. However, increasing the viscosity of the flow (i.e., a debris flow rather than purely water) would produce fingers, as fingering requires lateral flow instability [*Pouliquen et al.*, 1997]. Their liquid water model assumes a volume of 2500 m^3, taken from Malin and Edgett [2000], but this volume was specified for a gully system in Avire Crater with a morphology significantly different from that of the Penticton gully in which the new flow is observed (Figure 2.19). The Pelletier et al. [2008] model results do not definitively rule in favour of either wet or dry flow (which were also the results of follow-up work by Kolb et al. [2010]), but the authors rule in favour of dry flow, stating that liquid water to produce the flow would not be stable (e.g., Mellon and Phillips [2001]) despite numerous models indicating that liquid water would be stable on the martian surface for up to a few hours under present-day conditions [e.g., *Carr*, 1983; *McKay and Davis*, 1991; *Haberle et al.*, 2001; *Hecht*, 2002; *Kossacki and Markiewicz*, 2004; *Heldmann*, 2005]. Therefore, at least some of the characteristics of present-day gully activity are consistent with water-related mass movement processes.

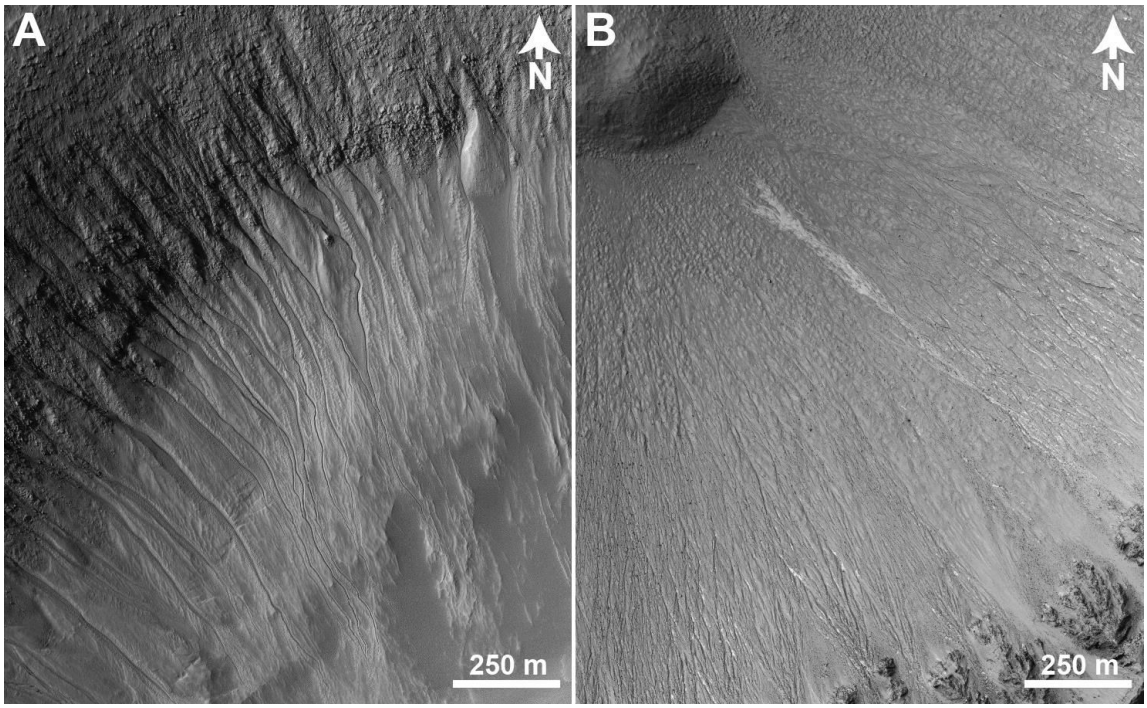

Figure 2.19. (A) The gully system for which Malin and Edgett [2000; see their note #36] estimated a water volume required for its formation of 2500 m^3, in Avire Crater. **(B)** The new gully flow in Penticton Crater. *Image credit: NASA/JPL-Caltech/University of Arizona.*

2.5. Conclusions

The latitudinal distribution, shift in orientation preference with increasing latitude, and location relative to documented glacial features and areas of present-day near-surface ground ice all point towards insolation and atmospheric conditions playing key roles in martian gully formation. The strong correlation between gullies and regions of distinct thermophysical properties (sand to small pebble grain sizes, low albedo, and higher thermal inertia) indicate that substrate properties are also a significant factor in gully formation. The correlation based on TES thermal inertia measurements is a potentially significant insight that we plan to investigate in future work utilizing THEMIS thermal inertia for a higher resolution study of this relationship.

Our results support either melting snow or melting of near-surface ground ice (or potentially a combination of the two) as the source for liquid involved in martian gully formation, but we are unable to favour one over the other based on the current

observations. The occurrence of gullies in terrains where ground ice has been inferred or detected by SHARAD, CRISM, and GRS, correlation with thermophysical units providing the highest shallow subsurface temperature profile, and geographic location relative to surface features indicative of ice such as polygonal terrain, CCF, and LVF lend support to a ground ice origin for gullies, while the correlation between gully locations and predicted areas of ice accumulation at high obliquity and relationship to pasted on material support the snowmelt hypothesis. Either way, these results have significant implications for both past and present habitability of Mars as they suggest that 1) the gully channels were carved by water, and 2) some characteristics of present-day gully activity suggest the involvement of water on Mars today.

It is important to note that while melting of snow or near-surface ground ice was likely responsible for the initial formation of martian gully channels, terrestrial gullies develop by the action of a number of processes after channel formation, ranging from fluvial activity to wet debris flows to dry rockfalls. Therefore, martian gullies have likely been subject to multiple types of mass movement processes over time, as suggested by the observation of multiple types of mass movement activity in gully systems on Mars today. The morphology of their channels and the global distribution of gullies suggest a common control on their formation; however, not all of their discrete formation mechanisms or evolution are necessarily the same. This study has provided an unprecedented census of martian gullies that has considerably narrowed down the range of possible gully formation mechanisms on Mars.

Acknowledgments

We thank Nina Lanza and an anonymous reviewer for their helpful comments and suggestions for improving this manuscript. T. N. Harrison acknowledges funding for this project by the Vanier Canada Graduate Scholarship, the National Science and Engineering Research Council of Canada Collaborative Research and Training Experience (NSERC CREATE) Technologies and Techniques for Space Exploration Fellowship, the NSERC CREATE Canadian Astrobiology Training Program (CATP), and the Amelia Earhart Fellowship.

References

Arvidson, R. et al. (2008), Mars Exploration Program 2007 Phoenix landing site selection and characteristics, *J. Geophys. Res.*, *113*, E00A03, doi:10.1029/2007JE003021.

Balme, M., N. Mangold, D. Baratoux, F. Costard, M. Gosselin, P. Masson, P. Pinet, and G. Neukum (2006), Orientation and distribution of recent gullies in the southern hemisphere of Mars: Observations from High Resolution Stereo Camera/Mars Express (HRSC/MEX) and Mars Orbiter Camera/Mars Global Surveyor (MOC/MGS) data, *J. Geophys. Res.*, *111*(E5), E05001, doi:10.1029/2005JE002607.

Boynton, W. V. (2002), Distribution of hydrogen in the near surface of Mars: Evidence for subsurface ice deposits, *Science*, *297*(5578), 81–85, doi:10.1126/science.1073722.

Bramson, A. M., S. Byrne, N. E. Putzig, J. J. Plaut, and J. W. Holt (2014), Thick excess water ice in Arcadia Planitia, Mars, *45th Lunar and Planetary Science Conference*, abstract 2120.

Bridges, N. T., and C. N. Lackner (2006), Northern hemisphere Martian gullies and mantled terrain: Implications for near-surface water migration in Mars' recent past, *J. Geophys. Res.*, *111*(E9), E09014, doi:10.1029/2006JE002702.

Brucks, A., T. Arndt, J. Ottino, and R. Lueptow (2007), Behavior of flowing granular materials under variable g, *Phys. Rev. E*, *75*(3), 032301, doi:10.1103/PhysRevE.75.032301.

Bull, L. J., and M. J. Kirkby (1997), Gully processes and modelling, *Prog. Phys. Geogr.*, *21*(3), 354–374, doi:10.1177/030913339702100302.

Byrne, S. et al. (2009), Distribution of mid-latitude ground ice on Mars from new impact craters, *Science*, *325*(5948), 1674–1676.

Cantor, B., M. Malin, and K. S. Edgett (2002), Multiyear Mars Orbiter Camera (MOC) observations of repeated Martian weather phenomena during the northern summer season, *J. Geophys. Res.*, *107*(E3), 5014.

Carr, M. H. (1983), Stability of streams and lakes on Mars, *Icarus*, *56*, 476–495, doi:10.1016/0019-1035(83)90168-9.

Carr, M. H. (1996), *Water on Mars*, Oxford University Press, New York, N.Y., United States (USA).

Carter, L. M. et al. (2009), Shallow radar (SHARAD) sounding observations of the Medusae Fossae Formation, Mars, *Icarus*, *199*(2), 295–302, doi:10.1016/j.icarus.2008.10.007.

Cedillo-Flores, Y., A. H. Treiman, J. Lasue, and S. M. Clifford (2011), CO2 gas fluidization in the initiation and formation of Martian polar gullies, *Geophys. Res. Lett.*, *38*(L21202), doi:10.1029/2011GL049403.

Christensen, P. R. (2003), Formation of recent martian gullies through melting of extensive water-rich snow deposits, *Nature*, *422*(6927), 45–48, doi:10.1038/nature01436.

Christensen, P. R. et al. (2001), Mars Global Surveyor Thermal Emission Spectrometer experiment: Investigation description and surface science results, *J. Geophys. Res.*, *106*(2000), 23823–23871.

Christensen, P. R., E. Engle, S. Anwar, S. Dickenshied, D. Noss, N. Gorelick, and M. Weiss-Malik (2009), JMARS – A Planetary GIS, *American Geophysical Union, Fall Meeting 2009*, abstract IN22A–06.

Clark, B. (1981), The salts of Mars, *Icarus*, *45*(2), 370–378, doi:10.1016/0019-1035(81)90041-5.

Costard, F., F. Forget, N. Mangold, and J. P. Peulvast (2002), Formation of recent martian debris flows by melting of near-surface ground ice at high obliquity, *Science*, *295*(5552), 110–113, doi:10.1126/science.1066698.

Costard, F., N. Mangold, D. Baratoux, and F. Forget (2007), Current gullies activity: Dry avalanches at seasonal defrosting as seen on HiRISE images, *Seventh International Conference on Mars*, abstract 3133.

Decaulne, A., and P. Sæmundsson (2007), Spatial and temporal diversity for debris-flow meteorological control in subarctic oceanic periglacial environments in Iceland, *Earth Surf. Process. Landforms*, *32*, 1971–1983, doi:10.1002/esp.

Dickson, J., J. W. Head, and L. Barbieri (2013), Martian gullies as stratigraphic markers for latitude-dependent mantle emplacement and removal, *44th Lunar and Planetary Science Conference*, abstract 1012.

Dickson, J. L., and J. W. Head (2009), The formation and evolution of youthful gullies on Mars: Gullies as the late-stage phase of Mars' most recent ice age, *Icarus*, *204*(1),

63–86, doi:10.1016/j.icarus.2009.06.018.

Dickson, J. L., J. W. Head, and M. Kreslavsky (2007), Martian gullies in the southern mid-latitudes of Mars: Evidence for climate-controlled formation of young fluvial features based upon local and global topography, *Icarus*, *188*(2), 315–323, doi:10.1016/j.icarus.2006.11.020.

Diniega, S., S. Byrne, N. T. Bridges, C. M. Dundas, and A. S. McEwen (2010), Seasonality of present-day Martian dune-gully activity, *Geology*, *38*(11), 1047–1050, doi:10.1130/G31287.1.

Diniega, S., C. J. Hansen, J. N. McElwaine, C. H. Hugenholtz, C. M. Dundas, A. S. McEwen, and M. C. Bourke (2013), A new dry hypothesis for the formation of martian linear gullies, *Icarus*, *225*, 526–537, doi:10.1016/j.icarus.2013.04.006.

Dundas, C. M., A. S. McEwen, S. Diniega, S. Byrne, and S. Martinez-Alonso (2010), New and recent gully activity on Mars as seen by HiRISE, *Geophys. Res. Lett.*, *37*(7), L07202, doi:10.1029/2009GL041351.

Dundas, C. M., S. Diniega, C. J. Hansen, S. Byrne, and A. S. McEwen (2012), Seasonal activity and morphological changes in martian gullies, *Icarus*, *220*(1), 124–143, doi:10.1016/j.icarus.2012.04.005.

Dundas, C. M., S. Diniega, and A. S. McEwen (2014), Long-term monitoring of martian gully activity with HiRISE, *45th Lunar and Planetary Science Conference*, abstract 2204.

Edgett, K. S., M. C. Malin, R. M. E. Williams, and S. D. Davis (2003), Polar and middle-latitude martian gullies: A view from MGS MOC after two Mars years in the mapping orbit, *Lunar and Planetary Science XXXIV*, abstract 1038.

Feldman, W. C. (2004), Global distribution of near-surface hydrogen on Mars, *J. Geophys. Res.*, *109*(E9), E09006, doi:10.1029/2003JE002160.

Gaidos, E. (2001), Cryovolcanism and the recent flow of liquid water on Mars, *Icarus*, *153*(1), 218–223, doi:10.1006/icar.2001.6649.

Gilmore, M. S., and E. L. Phillips (2002), Role of aquicludes in formation of Martian gullies, *Geology*, *30*(12), 1107, doi:10.1130/0091-7613(2002)030<1107:ROAIFO>2.0.CO;2.

Haberle, R. M., C. P. Mckay, J. Schaeffer, N. A. Cabrol, E. A. Grin, A. P. Zent, and R.

Quinn (2001), On the possibility of liquid water on present-day Mars, *J. Geophys. Res.*, *106*(E10), 23317–23326, doi:10.1029/2000JE001360.

Hare, T. M., S. W. Akins, R. M. Sucharski, M. S. Bailen, and J. A. Anderson (2013), Map projection web service for PDS images, *44th Lunar and Planetary Science Conference*, abstract 2068.

Harrison, T. N., M. C. Malin, and K. S. Edgett (2009), Present-day gully activity observed by the Mars Reconnaissance Orbiter (MRO) Context Camera (CTX), *Bulletin of the American Astronomical Society, DPS Meeting #41*, p. 1113.

Harrison, T. N., G. R. Osinski, and L. L. Tornabene (2013), Relationship between host material and gully morphology on Mars, *44th Lunar and Planetary Science Conference*, abstract 1420.

Harrison, T. N., G. R. Osinski, and L. L. Tornabene (2014), Global documentation of gullies with the Mars Reconnaissance Orbiter Context Camera (CTX) and implications for their formation, *45th Lunar and Planetary Science Conference*, abstract 2124.

Head, J. W., J. F. Mustard, M. a Kreslavsky, R. E. Milliken, and D. R. Marchant (2003), Recent ice ages on Mars, *Nature*, *426*(6968), 797–802, doi:10.1038/nature02114.

Hecht, M. (2002), Metastability of liquid water on Mars, *Icarus*, *156*(2), 373–386, doi:10.1006/icar.2001.6794.

Hecht, M. H., and N. T. Bridges (2003), A mechanism for recent production of liquid water on Mars, *Lunar and Planetary Science XXXIV*, abstract 2073.

Hecht, M. H. et al. (2009), Detection of perchlorate and the soluble chemistry of martian soil at the Phoenix lander site, *Science*, *325*(5936), 64–67, doi:10.1126/science.1172466.

Heldmann, J. L. (2005), Formation of Martian gullies by the action of liquid water flowing under current Martian environmental conditions, *J. Geophys. Res.*, *110*(E5), E05004, doi:10.1029/2004JE002261.

Heldmann, J. L., and M. T. Mellon (2004), Observations of martian gullies and constraints on potential formation mechanisms, *Icarus*, *168*(2), 285–304, doi:10.1016/j.icarus.2003.11.024.

Heldmann, J. L., E. Carlsson, H. Johansson, M. T. Mellon, and O. B. Toon (2007),

Observations of martian gullies and constraints on potential formation mechanisms II. The northern hemisphere, *Icarus*, *188*(2), 324–344, doi:10.1016/j.icarus.2006.12.010.

Heldmann, J. L., M. Marinova, K. E. Williams, D. Lacelle, C. P. Mckay, a. Davila, W. Pollard, and D. T. Andersen (2012), Formation and evolution of buried snowpack deposits in Pearse Valley, Antarctica, and implications for Mars, *Antarct. Sci.*, *24*(03), 299–316, doi:10.1017/S0954102011000903.

Hétu, B., and J. T. Gray (2000), Effects of environmental change on scree slope development throughout the postglacial period in the Chic-Choc Mountains in the northern Gaspé Peninsula, Québec, *Geomorphology*, 335–355.

Hétu, B., H. Van Steijn, and P. Vandelac (1994), Les coulées de pierres glacées : un nouveau type de coulées de pierraille sur les talus d'éboulis, *Géographie Phys. Quat.*, *48*(1), 3–22, doi:10.7202/032969ar.

Hoffman, N. (2002), Active polar gullies on Mars and the role of carbon dioxide, *Astrobiology*, *2*(3), 313–323, doi:10.1089/153110702762027899.

Hugenholtz, C. H. (2008), Frosted granular flow: A new hypothesis for mass wasting in martian gullies, *Icarus*, *197*, 65–72, doi:10.1016/j.icarus.2008.04.010.

Hungr, O., S. G. Evans, M. J. Bovis, and J. N. Hutchinson (2001), A review of the classification of landslides of the flow type, *Environ. Eng. Geosci.*, *VII*(3), 221–238.

Ishii, T., and S. Sasaki (2004), Formation of recent martian gullies by avalanches of CO_2 frost, *Lunar and Planetary Science XXXV*, abstract 1556.

Jakosky, M., T. Mellon, H. Kieffer, R. Christensen, E. S. Varnes, and S. W. Lee (2000), The thermal inertia of Mars from the Mars Global Surveyor Thermal Emission Spectrometer, *J. Geophys. Res.*, *105*, 9643–9652.

Jones, E., G. Caprarelli, F. Mills, B. Doran, and J. Clarke (2014), An alternative approach to mapping thermophysical units from martian thermal inertia and albedo data using a combination of unsupervised classification techniques, *Remote Sens.*, *6*(6), 5184–5237, doi:10.3390/rs6065184.

Jones, E. G., and C. H. Lineweaver (2007), Identifying the potential biosphere of Mars, *Proceedings from the 7th Australian Space Conference*, pp. 60–72.

Kneissl, T., D. Reiss, S. van Gasselt, and G. Neukum (2010), Distribution and orientation

of northern-hemisphere gullies on Mars from the evaluation of HRSC and MOC-NA data, *Earth Planet. Sci. Lett.*, *294*(3-4), 357–367, doi:10.1016/j.epsl.2009.05.018.

Kolb, K. J., J. D. Pelletier, and A. S. McEwen (2010), Modeling the formation of bright slope deposits associated with gullies in Hale Crater, Mars: Implications for recent liquid water, *Icarus*, *205*, 113–137, doi:10.1016/j.icarus.2009.09.009.

Kossacki, K. J., and W. J. Markiewicz (2004), Seasonal melting of surface water ice condensing in martian gullies, *Icarus*, *171*(2), 272–283, doi:10.1016/j.icarus.2004.05.018.

Kreslavsky, M. A., and J. W. Head (2000), Kilometer-scale roughness of Mars: Results from MOLA data analysis, *J. Geophys. Res.*, *105*(E11), 26695–26711.

Lanza, N. L., and M. S. Gilmore (2006), Depths, orientation, and slopes of martian hillside gullies in the northern hemisphere, in *Lunar and Planetary Science XXXVII*, vol. 06459, p. 2412.

Lanza, N. L., G. A. Meyer, C. H. Okubo, H. E. Newsom, and R. C. Wiens (2010), Evidence for debris flow gully formation initiated by shallow subsurface water on Mars, *Icarus*, *205*(1), 103–112, doi:10.1016/j.icarus.2009.04.014.

Laskar, J., A. C. M. Correia, M. Gastineau, F. Joutel, B. Levrard, and P. Robutel (2004), Long term evolution and chaotic diffusion of the insolation quantities of Mars, *Icarus*, *170*(2), 343–364, doi:10.1016/j.icarus.2004.04.005.

Levrard, B., F. Forget, F. Montmessin, and J. Laskar (2004), Recent ice-rich deposits formed at high latitudes on Mars by sublimation of unstable equatorial ice during low obliquity, *Nature*, *431*, 1072–1075, doi:10.1038/nature03006.1.

Levy, J. S., J. W. Head, and D. R. Marchant (2008), The role of thermal contraction crack polygons in cold-desert fluvial systems, *Antarct. Sci.*, *20*(06), 565–579, doi:10.1017/S0954102008001375.

Madeleine, J.-B., F. Forget, J. W. Head, B. Levrard, F. Montmessin, and E. Millour (2009), Amazonian northern mid-latitude glaciation on Mars: A proposed climate scenario, *Icarus*, *203*(2), 390–405, doi:10.1016/j.icarus.2009.04.037.

Malin, M. C., and K. S. Edgett (2000), Evidence for recent groundwater seepage and surface runoff on Mars, *Science*, *288*(5475), 2330–2335, doi:10.1126/science.288.5475.2330.

Malin, M. C., K. S. Edgett, L. V Posiolova, S. M. Mccolley, and E. Z. N. Dobrea (2006), Present-day impact cratering rate and contemporary gully activity on Mars, *Science*, *314*(5805), 1573–1577.

Malin, M. C. et al. (2007), Context Camera Investigation on board the Mars Reconnaissance Orbiter, *J. Geophys. Res.*, *112*(E5), E05S04, doi:10.1029/2006JE002808.

Malin, M. C., K. S. Edgett, B. A. Cantor, M. A. Caplinger, G. E. Danielson, E. H. Jensen, M. A. Ravine, J. L. Sandoval, and K. D. Supulver (2010), An overview of the 1985-2006 Mars Orbiter Camera science investigation, *Mars J.*, *5*, 1–60, doi:10.1555/mars.2010.0001.

Marchant, D. R., and J. W. Head (2007), Antarctic dry valleys: Microclimate zonation, variable geomorphic processes, and implications for assessing climate change on Mars, *Icarus*, *192*(1), 187–222, doi:10.1016/j.icarus.2007.06.018.

McEwen, A. S. et al. (2007), Mars Reconnaissance Orbiter's High Resolution Imaging Science Experiment (HiRISE), *J. Geophys. Res.*, *112*(E5), E05S02, doi:10.1029/2005JE002605.

McKay, C. P., and W. L. Davis (1991), Duration of liquid water habitats on early Mars, *Icarus*, *90*(2), 214–221, doi:10.1016/0019-1035(91)90102-Y.

Mellon, M. T., and B. M. Jakosky (1993), Geographic variations in the thermal and diffusive stability of ground ice on Mars, *J. Geophys. Res.*, *98*(E2), 3345, doi:10.1029/92JE02355.

Mellon, M. T., and B. M. Jakosky (1995), The distribution and behavior of Martian ground ice during past and present epochs, *J. Geophys. Res.*, *100*(E6), 11781–11799, doi:10.1029/95JE01027.

Mellon, M. T., and R. J. Phillips (2001), Recent gullies on Mars and the source of liquid water, *J. Geophys. Res.*, *106*(E10), 23165–23179, doi:10.1029/2000JE001424.

Mellon, M. T., B. M. Jakosky, H. H. Kieffer, and P. R. Christensen (2000), High-resolution thermal inertia mapping from the Mars Global Surveyor Thermal Emission Spectrometer, *Icarus*, *148*, 437–455, doi:10.1006/icar.2000.6503.

Mellon, M. T., K. A. Kretke, M. D. Smith, and S. M. Pelkey (2002), A global map of thermal inertia from Mars Global Surveyor Mapping-Mission data, *Lunar and*

Planetary Science XXXIII, abstract 1416.

Milliken, R. E., and J. F. Mustard (2003), Erosional morphologies and characteristics of latitude-dependent surface mantles on Mars, *Sixth Int. Conf. Mars, Pasadena, Calif.*, 3240.

Mischna, M. A. (2003), On the orbital forcing of Martian water and CO2 cycles: A general circulation model study with simplified volatile schemes, *J. Geophys. Res.*, *108*(E6), 5062, doi:10.1029/2003JE002051.

Morgan, G. A., J. W. Head, D. R. Marchant, J. . Dickson, and J. S. Levy (2007), Gully formation on Mars: Testing the snowpack hypothesis from analysis of analogs in the Antarctic Dry Valleys, *Lunar and Planetary Science XXXVIII*, abstract 1656.

Morgan, G. A., J. W. Head, D. R. Marchant, J. . Dickson, and J. S. Levy (2008), Gully formation and evolution in the Antarctic Dry Valleys: Implications for Mars, *Workshop on Martian Gullies: Theories and Tests*, abstract 8015.

Morgan, G. A., J. W. Head, F. Forget, J.-B. Madeleine, and A. Spiga (2010), Gully formation on Mars: Two recent phases of formation suggested by links between morphology, slope orientation and insolation history, *Icarus*, *208*(2), 658–666, doi:10.1016/j.icarus.2010.02.019.

Musselwhite, D. S., T. D. Swindle, and J. I. Lunine (2001), Liquid CO2 breakout and the formation of recent small gullies on Mars, *Geophys. Res. Lett.*, *28*(7), 1283–1285.

Mustard, J. F., C. D. Cooper, and M. K. Rifkin (2001), Evidence for recent climate change on Mars from the identification of youthful near-surface ground ice, *Nature*, *412*, 411–414, doi:10.1038/35086515.

Nunes, D. C., S. E. Smrekar, A. Safaeinili, J. Holt, R. J. Phillips, R. Seu, and B. Campbell (2010), Examination of gully sites on Mars with the shallow radar, *J. Geophys. Res.*, *115*(E10), E10004, doi:10.1029/2009JE003509.

Ollila, A. M., and M. S. Gilmore (2007), Thermophysical properties of gullied and non-gullied slopes in Acidalia Planitia, Mars, *Lunar and Planetary Science XXXVIII*, abstract 1861.

Ollila, A. M., M. S. Gilmore, and H. E. Newsom (2008), Temperature analysis of gullied and non-gullied slopes on Mars: Evidence for a thermal control on gully formation, *Workshop on Martian Gullies: Theories and Tests*, abstract 8037.

Pelletier, J. D., K. J. Kolb, A. S. McEwen, and R. L. Kirk (2008), Recent bright gully deposits on Mars: Wet or dry flow?, *Geology*, *36*(3), 211, doi:10.1130/G24346A.1.

Pike, R. J. (1980), Control of crater morphology by gravity and target type: Mars, Earth, Moon, *Proc. Lunar Planet. Sci. Conf.*, *11*, 2159–2190.

Pollack, H. N., and S. Huang (2000), Climate reconstruction from subsurface temperatures, *Annu. Rev. Earth Planet. Sci.*, *28*, 339–365.

Pouliquen, O., J. Delour, and S. B. Savage (1997), Fingering in granular flows, *Nature*, *386*, 816–817, doi:10.1038/386816a0.

Putzig, N., and M. Mellon (2007), Apparent thermal inertia and the surface heterogeneity of Mars, *Icarus*, *191*(1), 68–94, doi:10.1016/j.icarus.2007.05.013.

Putzig, N., M. Mellon, K. Kretke, and R. Arvidson (2005), Global thermal inertia and surface properties of Mars from the MGS mapping mission, *Icarus*, *173*(2), 325–341, doi:10.1016/j.icarus.2004.08.017.

Raack, J., D. Reiss, and H. Hiesinger (2012), Gullies and their relationships to the dust–ice mantle in the northwestern Argyre Basin, Mars, *Icarus*, *219*(1), 129–141, doi:10.1016/j.icarus.2012.02.025.

Raack, J., D. Reiss, T. Appéré, M. Vincendon, O. Ruesch, and H. Hiesinger (2015), Present-day seasonal gully activity in a south polar pit (Sisyphi Cavi) on Mars, *Icarus*, *251*, 226–243, doi:10.1016/j.icarus.2014.03.040.

Reiss, D., G. Erkeling, K. E. Bauch, and H. Hiesinger (2010), Evidence for present day gully activity on the Russell crater dune field, Mars, *Geophys. Res. Lett.*, *37*(L06203), doi:10.1029/2009GL042192.

Ritter, D. F. (1986), *Process Geomorphology*, W. C. Brown, Dubuque, Iowa.

Rowntree, K. M. (1991), Morphological characteristics of gully networks and their relationship to host materials, Baringo District, Kenya, *GeoJournal*, *23*(1), 19–27.

Schon, S. C., and J. W. Head (2012), Decameter-scale pedestal craters in the tropics of Mars: Evidence for the recent presence of very young regional ice deposits in Tharsis, *Earth Planet. Sci. Lett.*, *317-318*, 68–75, doi:10.1016/j.epsl.2011.09.005.

Schorghofer, N., and K. S. Edgett (2006), Seasonal surface frost at low latitudes on Mars, *Icarus*, *180*(2), 321–334, doi:10.1016/j.icarus.2005.08.022.

Shean, D. E. (2010), Evidence for widespread removal of martian mid-latitude “fill”

material, *41st Lunar and Planetary Science Conference*, abstract 1509.

Shean, D. E., J. W. Head, and D. R. Marchant (2005), Origin and evolution of a cold-based tropical mountain glacier on Mars: The Pavonis Mons fan-shaped deposit, *J. Geophys. Res.*, *110*(E5), E05001, doi:10.1029/2004JE002360.

Shinbrot, T., N.-H. Duong, L. Kwan, and M. M. Alvarez (2004), Dry granular flows can generate surface features resembling those seen in Martian gullies., *Proc. Natl. Acad. Sci. U. S. A.*, *101*(23), 8542–8546, doi:10.1073/pnas.0308251101.

Smith, M. D. (2004), Interannual variability in TES atmospheric observations of Mars during 1999–2003, *Icarus*, *167*, 148–165, doi:10.1016/j.icarus.2003.09.010.

Squyres, S. W. (1979), The distribution of lobate debris aprons and similar flows on Mars, *J. Geophys. Res.*, *84*(B14), 8087–8096, doi:10.1029/JB084iB14p08087.

Stuurman, C. M., G. R. Osinski, T. C. Brothers, J. W. Holt, and M. Kerrigan (2014), SHARAD reflectors in Utopia Planitia, Mars consistent with widespread, thick subsurface ice, in *45th Lunar and Planetary Science Conference*, p. abstract 2262.

Tamppari, L. K., M. D. Smith, D. S. Bass, and A. S. Hale (2008), Water-ice clouds and dust in the north polar region of Mars using MGS TES data, *Planet. Space Sci.*, *56*, 227–245, doi:10.1016/j.pss.2007.08.011.

Treiman, A. H. (2003), Geologic settings of Martian gullies: Implications for their origins, *J. Geophys. Res.*, *108*(E4), 8031, doi:10.1029/2002JE001900.

Turcotte, D. L., and G. Shubert (1982), *Geodynamics*, Cambridge University Press, Cambridge, UK.

Vaniman, D. T., D. L. Bish, S. J. Chipera, C. I. Fialips, J. W. Carey, and W. C. Feldman (2004), Magnesium sulphate salts and the history of water on Mars, *Nature*, *431*, 663–665, doi:10.1038/nature02973.

Walton, O. R., C. P. Moor, and K. S. Gill (2007), Effects of gravity on cohesive behavior of fine powders: implications for processing Lunar regolith, *Granul. Matter*, *9*(5), 353–363, doi:10.1007/s10035-006-0029-8.

Wänke, H., Brückner, G. Dreibus, R. Rieder, and I. Ryabchikov (2001), Chemical composition of rocks and soils at the Pathfinder site, *Space Sci. Rev.*, *96*, 317–330.

White, B. R., and S. P. Klein (1990), Dynamic shear of granular material under variable gravity conditions, *AIAA J.*, *28*(10), 1701–1702, doi:10.2514/3.10461.

Williams, K., O. Toon, J. Heldmann, C. Mckay, and M. Mellon (2008a), Stability of mid-latitude snowpacks on Mars, *Icarus*, *196*(2), 565–577, doi:10.1016/j.icarus.2008.03.017.

Williams, R., R. Shao, and R. A. Overfelt (2008b), The flowability of fine powders in reduced gravity conditions, *Granul. Matter*, *10*(2), 139–144, doi:10.1007/s10035-007-0068-9.

Chapter 3: Late Amazonian geologic history of Western Utopia Planitia, Mars

Tanya N. Harrison[1], Gordon R. Osinski[1,2], Livio L. Tornabene[1], and Cassie Stuurman[3]

[1]*Centre for Planetary Science and Exploration, Department of Earth Sciences, University of Western Ontario*

[2]*Department of Physics and Astronomy, University of Western Ontario*

[3]*University of Texas at Austin Institute for Geophysics, Austin, TX, USA.*

3.1 Introduction

Western Utopia Planitia has long been an area of intrigue based on the presence of potential glacial and periglacial features. In particular, the high concentration of so-called scalloped depressions in Utopia relative to the rest of the planet has led to a debate on the geologic history of the area in the Late Amazonian. Some authors have suggested that these features formed via subsurface ice melting [*Costard and Kargel*, 1995; *Soare et al.*, 2008, 2012, 2013], while others propose ice sublimation [*Morgenstern et al.*, 2007; *Lefort et al.*, 2009; *Ulrich et al.*, 2010]. It has also been suggested that the terrain hosting the scalloped depressions is a distinct, unique geologic unit [*Soare et al.*, 2010, 2012; *Capitan et al.*, 2012; *Kerrigan et al.*, 2012; *Kerrigan*, 2013]. Utopia also hosts other features whose formation is thought to be related to changes in climate driven by orbital oscillations over the past ~100 Ma [*Head et al.*, 2003; *Laskar et al.*, 2004; *Levrard et al.*, 2004; *Madeleine et al.*, 2009]. These changes included a migration in the surface ice distribution, with ice being removed from the current polar regions and depositing in the mid-latitudes [*Head et al.*, 2003; *Levrard et al.*, 2004; *Madeleine et al.*, 2009]. Evidence of this ice is present in a suite of landforms exclusive to the middle and high latitudes of Mars such as mid-latitude ("concentric") crater fill [e.g., *Squyres*, 1979; *Squyres and Carr*, 1986; *Levy et al.*, 2009b, 2010a; *Pedersen and Head*, 2010], lobate debris aprons, lineated valley fill [*Squyres*, 1979], viscous flow features [*Milliken and Mustard*, 2003], and the latitude-dependent mantle [*Mustard et al.*, 2001; *Head et al.*, 2003; *Milliken and Mustard*, 2003]. Large near-surface deposits of nearly pure ice in the northern mid-latitudes of Utopia [*Stuurman et al.*, 2014] and Arcadia Planitiae [*Bramson et al.*, 2015] have been interpreted from

results from the Mars Reconnaissance Orbiter (MRO) Shallow Radar (SHARAD) instrument. Newly-formed impact craters in the northern mid-latitudes have also been observed to excavate near-surface ice [*Byrne et al.*, 2009]. In Utopia specifically, pingo-like mounds have also been cited as additional evidence for near-surface ice [*Seibert and Kargel*, 2001; *Soare et al.*, 2005; *Dundas et al.*, 2008].

Here we investigate the geologic history of western Utopia Planitia based on the stratigraphic relationships between the scalloped depression-bearing terrain, gullies, and mid-latitude crater fill. This will help to inform on the relative timing of the glacial, periglacial, and potentially fluvial processes in the region in the Late Amazonian, and how Utopia Planitia is evolving under present-day conditions.

3.2. Background

Utopia Planitia, in the northern plains of Mars, is thought to be a ~3,300 km diameter Noachian impact basin [*McGill*, 1989; *Thomson and Head*, 2001] (Figure 3.1A). Since its formation, the basin has been subjected to infilling by Early Hesperian lava flows, Late Hesperian outflow sediments comprising the Vastitas Borealis Formation, and Early Amazonian lava flows and lahar deposits from Elysium volcanism [*Thomson and Head*, 2001, and references therein]. Obliquity shifts during the Late Amazonian resulted in deposition of ice in the region as ice migrated from the poles to the mid-latitudes [*Head et al.*, 2003; *Levrard et al.*, 2004; *Madeleine et al.*, 2009], with some of this ice preserved today within the subsurface [*Stuurman et al.*, 2014]. Evidence of this change in climate remains in surface landforms found in the region, including gullies, mid-latitude crater filling material, scalloped depressions, and the latitude-dependent mantle.

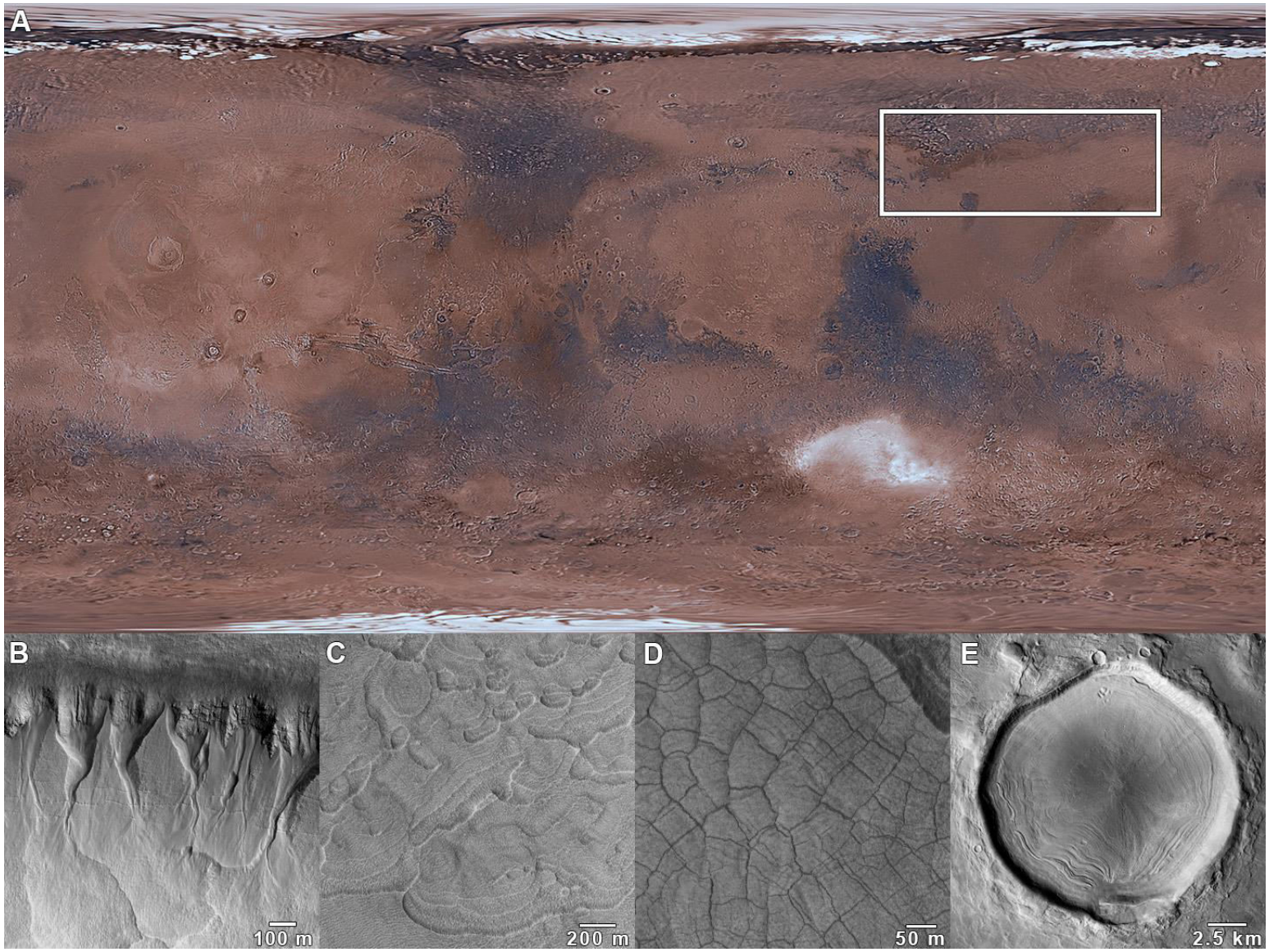
A
B
100 m
C
200 m
D
50 m
E
2.5 km

Figure 3.1. **(A)** Context map of Utopia atop the Viking MDIM 2.1 basemap, with example landforms described in this paper shown below in B–E. **(B)** Gullies incising into pasted-on material. Subframe of HiRISE ESP_028297_2270. **(C)** Example of scalloped depressions. Subframe of HiRISE ESP_028297_2270. **(D)** Polygonal fractures. Subframe of HiRISE ESP_036499_2240. **(E)** Concentric crater fill (CCF). Subframe of CTX P20_008755_2164. North is up in all images.

3.2.1. Gullies

Gullies are very recent geologic features on Mars, having formed in only the last few million years [*Malin and Edgett*, 2000; *Reiss et al.*, 2004; *Schon et al.*, 2009b] and still experiencing activity at present [*Malin et al.*, 2006; *Harrison et al.*, 2009; *Diniega et al.*, 2010; *Dundas et al.*, 2010, 2012, 2015; *Raack et al.*, 2015] (Figure 3.1B). They typically consist of a source alcove, channel, and depositional apron [*Malin and Edgett*, 2000]. Gullies are found on features such as the walls of craters and valleys, as well as on the slopes of massifs and central peaks, in the middle and high latitudes (~30–80°) in both hemispheres [*Malin and Edgett*, 2000; *Heldmann and Mellon*, 2004; *Balme et al.*, 2006; *Heldmann et al.*, 2007; *Kneissl et al.*, 2010; *Harrison et al.*, 2015b]. Their morphology is highly suggestive of formation involving liquid water. Multiple water-related mechanisms have been proposed, including formation via groundwater release from subsurface aquifers [*Malin and Edgett*, 2000; *Gaidos*, 2001], or melting of snow [*Christensen*, 2003; *Williams et al.*, 2008] or near-surface ground ice [*Costard et al.*, 2002; *Gilmore and Phillips*, 2002]. Mechanisms involving H_2O frost [*Kossacki and Markiewicz*, 2004; *Hugenholtz*, 2008] and CO_2 frost have also been proposed [e.g., *Dundas et al.*, 2010, 2012, 2015], as well as dry mass wasting [*Treiman*, 2003; *Shinbrot et al.*, 2004]. At the time of writing, present-day gully activity has been observed at ~40 separate locations on Mars [*Malin et al.*, 2006; *Harrison et al.*, 2009; *Diniega et al.*, 2010; *Dundas et al.*, 2010, 2012, 2015; *Raack et al.*, 2015]. Only two of these locations are in the northern hemisphere, but one of the two is near western Utopia Planitia (58.7°N, 82.3°E) [*Dundas et al.*, 2015]. While the process(es) controlling gully activity at present may be different than that which formed them originally, it is something that

should be taken into account when considering possible gully formation hypotheses. It is also important to note that gullies on Mars did not necessarily all form via the same mechanism; on Earth, gullies form by many different (and combinations of) processes (see Chapters 1 and 2 of this thesis for further discussion). However, observations of gullies in western Utopia and their relationship to other Amazonian landforms may help to inform us on the local formation of gullies.

3.2.2 Latitude-dependent mantle (LDM)

Terrain softening observed in middle and high latitudes of Mars has been attributed to partial (~30–45° N/S) or full (≳45° N/S) draping by a unit referred to as the latitude-dependent mantle (LDM) [*Head et al.*, 2003]. This unit is interpreted to be a weakly cemented mixture of ice and dust deposited over the course of multiple obliquity cycles [*Kreslavsky and Head*, 2002; *Head et al.*, 2003] based on the following observations: 1) its latitudinal restriction, and degraded ("dissected") appearance at lower latitudes [*Mustard et al.*, 2001], 2) polygonal surface texture in some locations [*Mustard et al.*, 2001; *Head et al.*, 2003; *Milliken and Mustard*, 2003], and 3) internal metre-scale layering [*Kreslavsky and Head*, 2002; *Milliken et al.*, 2003; *Schon et al.*, 2009a; *Dickson et al.*, 2015]. Crater dating of the LDM in Utopia Planitia yields a modelled age of ~1.5 Ma [*Levy et al.*, 2009b]. LDM thicknesses in Utopia are typically 10–20 m, extending up to 40 m thick in some locations based on Mars Global Surveyor (MGS) Mars Orbiter Laser Altimeter (MOLA) shots [*Levy et al.*, 2009b]. Localized "pasted on" deposits found on many mid-latitude (typically pole-facing) slopes such as crater walls [*Christensen*, 2003] may be related to the LDM [*Levy et al.*, 2010b] but this is unclear at present; these deposits often occur in association with gullies [*Christensen*, 2003; *Dickson et al.*, 2015] (Figure 3.1B). Intact LDM displays a characteristic "basketball" texture at higher latitudes, which is removed in dissected LDM in the lower mid-latitudes [*Kreslavsky and Head*, 2002; *Head et al.*, 2003]. It has been suggested that as the LDM desiccates due to ice instability under present-day conditions in the middle and high latitudes [e.g., *Mellon and Jakosky*, 1993], a surface lag of the remnant dust

would form [*Marchant et al.*, 2002]. Such a surface lag would protect underlying ice from sublimation, but would also be easily removed by aeolian processes, because it is no longer cemented by ice. Once this protective layer is removed, sublimation would resume. However, it has been suggested that the duration of low obliquity periods (i.e., when ice is unstable in the mid-latitudes) are insufficient for the LDM to desiccate completely [*Head et al.*, 2003]. Thus, some fraction of ice may still be preserved within the LDM today.

3.2.3. Scalloped Depressions

Scalloped depressions are a common feature in western Utopia [e.g., *Costard and Kargel*, 1995; *Kreslavsky and Head*, 2000; *Soare et al.*, 2007] (Figure 3.1C). Similar depressions have also been observed in Tempe Terra in the northern hemisphere, and in Malea Planum and the Charitum Montes in the southern hemisphere [*Lefort et al.*, 2010; *Zanetti et al.*, 2010; *Soare et al.*, 2016]. Scalloped depressions are rimless and exhibit flat floors with steep pole-facing walls and gently graded, equator-facing terraced walls that sometimes expose internal layering [*Costard and Kargel*, 1995; *Milliken and Mustard*, 2003; *Morgenstern et al.*, 2007; *Soare et al.*, 2007, 2008; *Lefort et al.*, 2009]. They are typically metres to tens of metres deep and ~100–3,000 metres wide, and in many cases, adjacent scalloped depressions appear to have coalesced [*Milliken and Mustard*, 2003; *Lefort et al.*, 2009; *Zanetti et al.*, 2010]. The scalloped depressions have been proposed to be the product of thermokarst (i.e., degradation of permafrost), either from the thaw of massive or interstitial ice [*Soare et al.*, 2007, 2008, 2012] or from sublimation of interstitial ice [e.g., *Morgenstern et al.*, 2007; *Lefort et al.*, 2009, 2010; *Zanetti et al.*, 2010; *Séjourné et al.*, 2011]. In the thaw model, melting of ground ice leads to collapse, with ponding of meltwater in the resulting depression. Over time, this water is lost via infiltration into the regolith, evaporation, and/or sublimation, leaving the empty collapse pits (alases) behind [*Costard and Kargel*, 1995; *Soare et al.*, 2007, 2008]. However, it is difficult to explain the sustenance of lakes-worth of water under Mars' recent climate conditions [*Costard et al.*, 2002; *Hecht*, 2002]. In the

sublimation model, scalloped depressions initiate at locations of uneven terrain where slight differences in solar insolation lead to differential removal of interstitial ice, with enhanced removal on the warmer equator-facing slopes, eventually leading to collapse [*Morgenstern et al.*, 2007; *Lefort et al.*, 2009]. Regardless of whether scalloped depressions form by thaw or melting, they are indicative of excess ice, where the volumetric occurrence of frozen water exceeds the available sedimentary pore-space [*French*, 2007].

The scalloped-depression-bearing terrain in Utopia (Figures 3.2 and 3.3) displays polygonal fractures (Figure 3.1D), interpreted to be thermal contraction polygons indicative of the presence of subsurface ice [*Lefort et al.*, 2009; *Levy et al.*, 2009a]. Some authors have proposed that the scalloped-depression-bearing terrain in western Utopia represents a distinct geomorphic unit separate from the LDM (Soare et al [2012], which has been referred to as the "Periglacial Unit" by Kerrigan et al. [2012] or more recently as Amazonian Basin Periglacial Unit "ABp" as mapped by Kerrigan [2013]). Others suggest the scallops occur within or as part of the LDM with the latitudinal restriction of the scallops controlled by insolation [*Lefort et al.*, 2009]. For the rest of this study, we refer to the material hosting the scalloped depressions as the "Scalloped Depression Bearing Terrain" (SDBT) to avoid any preference to genetic interpretations with naming, unless specifically referring to the mapped ABp boundary from Kerrigan [2013].

3.2.4. Post-impact crater fill material

Many mid-latitude craters on Mars exhibit a morphologically distinct post-impact deposit commonly referred to in the literature as "fill" on their floors [e.g., *Squyres*, 1979; *Levy et al.*, 2010a; *Pedersen and Head*, 2010; *Pearce et al.*, 2011] (Figure 3.1E). This material is inferred to be (or have been) ice-rich based on morphological characteristics such as evidence for flow and removal, as well as their morphologic similarity to lineated valley fill and lobate debris aprons [e.g., *Squyres*, 1979]. These latter features have been effectively sounded with ground-penetrating

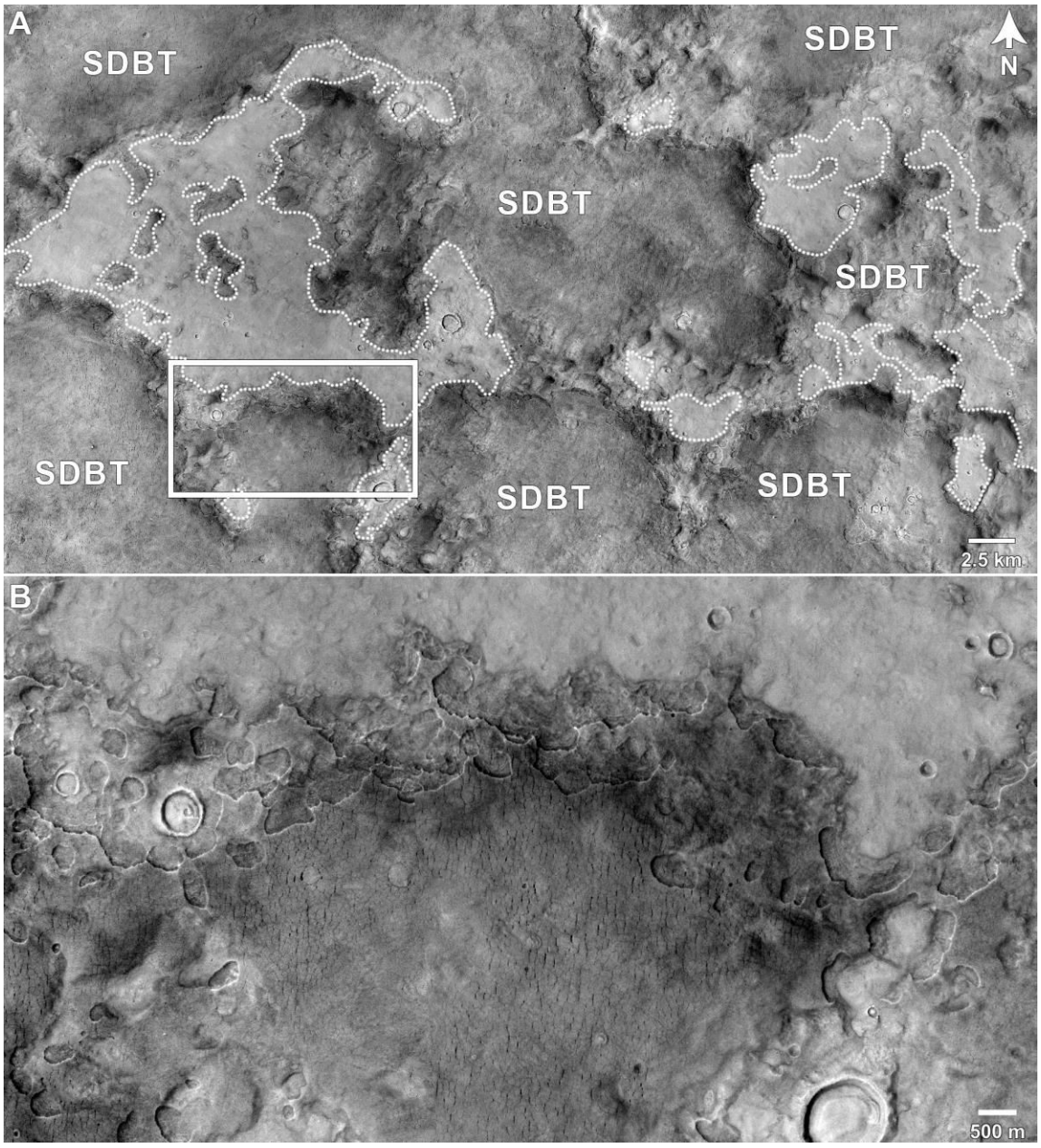

Figure 3.2. Example of the scalloped depression bearing terrain (SDBT) in western Utopia Planitia at 42.3°N, 85.8°E. **(A)** CTX mosaic showing the SDBT and the contact with the underlying light-toned unit (dotted white lines). White box denotes the location of B. **(B)** Close view of the SDBT, showing polygonal fractures and scallops. Subframe of CTX G02_018948_2237.

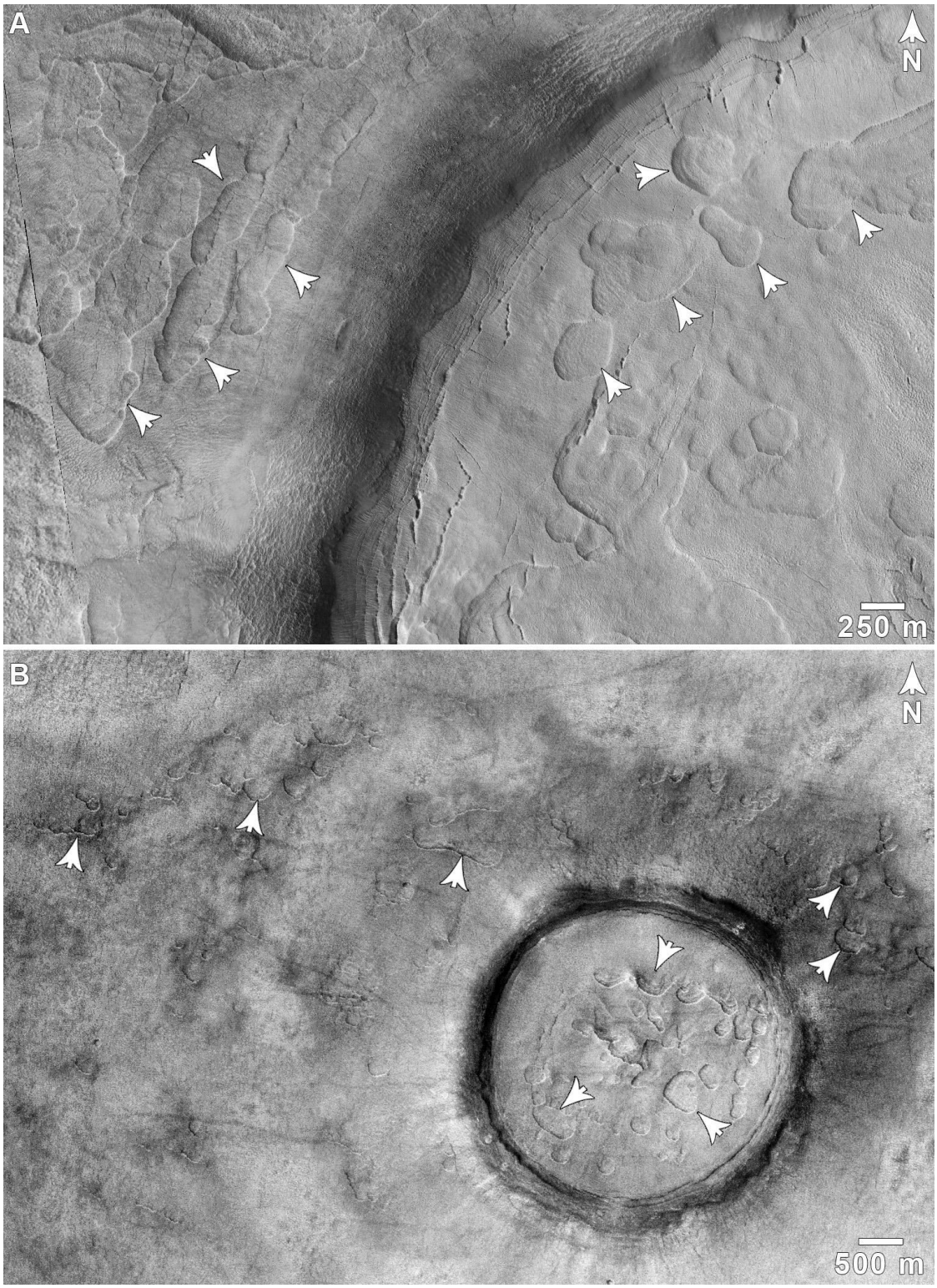

Figure 3.3. Scalloped depression bearing terrain (SDBT) inside craters and atop their ejecta blankets. Example of scallops denoted by white arrows. **(A)** Subframe of HiRISE ESP_028416_2260. **(B)** Subframe of CTX B17_016350_2314.

radar, and exhibit dielectric properties consistent with nearly pure water ice based on results from SHARAD [*Holt et al.*, 2008; *Plaut et al.*, 2009]. Morphological markers indicative of removal of this fill material over time such as "brain terrain" and concentric fractures observed at the margins of mid-latitude crater fill deposits interpreted as late-stage mechanical failure [*Levy et al.*, 2009b; *Shean*, 2010b] are also consistent with a significant fraction of ice (either past or present). The ability to sound fill-bearing craters using SHARAD techniques is limited by their size. While SHARAD ideally has a horizontal resolution of ~0.3–3 km on smooth surfaces [*Seu et al.*, 2007], the characteristic bowl-shaped topography of crater rims creates abundant noise (or "clutter") that masks any potential subsurface signal [*Holt et al.*, 2006]. Thus, crater-fill morphology is the prime indicator for inferring the composition of the deposit. In Utopia, crater dating of "brain terrain" surfaces of the crater fill material yield a modelled age of ~10–100 Ma [*Levy et al.*, 2009b].

3.3. Methods

Mapping and image analysis were completed using MRO Context Camera (CTX) [*Malin et al.*, 2007] and HiRISE images in the Java Mission-planning and Analysis for Remote Sensing (JMARS) software package [*Christensen et al.*, 2009] spanning 30–60°N and 70–150°E. Gully locations were taken from the global gully database in Chapter 2 of this thesis. Crater fill was mapped using a modification of the classification scheme proposed by Harrison et al. [2015a] (Figure 3.4). We distinguished 4 primary classes of mid-latitude post-impact crater fill material in western Utopia based on morphology. The goal of creating such a classification scheme is to look for any relationships in morphology with latitude/longitude. The four crater fill types used in this work are:

Concentric class. This class displays the classical "concentric crater fill" (CCF) morphology, with ridges concentric to the crater rim (Figure 3.4A). CCF class typically occupies the entire crater floor. Regional mapping by Levy et al. [2010a] shows that in at least portions of the northern hemisphere, the occurrence

of CCF is strongly latitude-dependent, with preference for latitudes poleward of 40°. Higher latitude examples of CCF are sometimes observed to be partially or fully draped by the LDM (Figure 3.4B); in these cases, the LDM is thin enough that the concentric features of the CCF are still identifiable, but often the characteristic brain terrain texture is obscured (Figure 3.5). In and near the scalloped-depression-bearing terrain, some craters of this class display CCF features overprinted by material exhibiting scalloped depressions (Figure 3.4C). In our mapping, we distinguish between non-mantled CCF, CCF mantled by scalloped-depression-bearing material, and CCF mantled by material exhibiting no scalloped depressions.

Flow Class. This class displays surficial lineations suggesting flow in a preferential direction—typically toward the pole in either hemisphere [*Pearce et al.*, 2011; *Dickson et al.*, 2012] (Figure 3.4D). It may occupy part or the majority of a crater floor. Levy et al. [2010a] refer to this class as "low-definition CCF" in their work.

Smooth Class. The surfaces of fill deposits of this class are relatively smooth compared to other classes, displaying neither distinctive flow lines nor concentric features (Figure 3.4E). This type typically only occupies a portion of a crater floor, often with evidence for fill removal (see Shean [2010b]).

Irregular Class. These fill deposits display a crenulated texture covering portions of or their entire surface with possible modification by sublimation pits (Figure 3.4F). This type often occurs with evidence for fill removal (see Shean [2010b]).

3.4. Results and Discussion

3.4.1 Post-impact crater fill

The distribution of crater fill classes observed in western Utopia Planitia is shown in Figure 3.6. A mix of all fill classes occur south of ~40°N, but poleward of that only concentric class (CCF) is observed. Around 30°N, irregular and smooth fill classes are dominant. Craters lacking fill entirely are also concentrated at these lower latitudes.

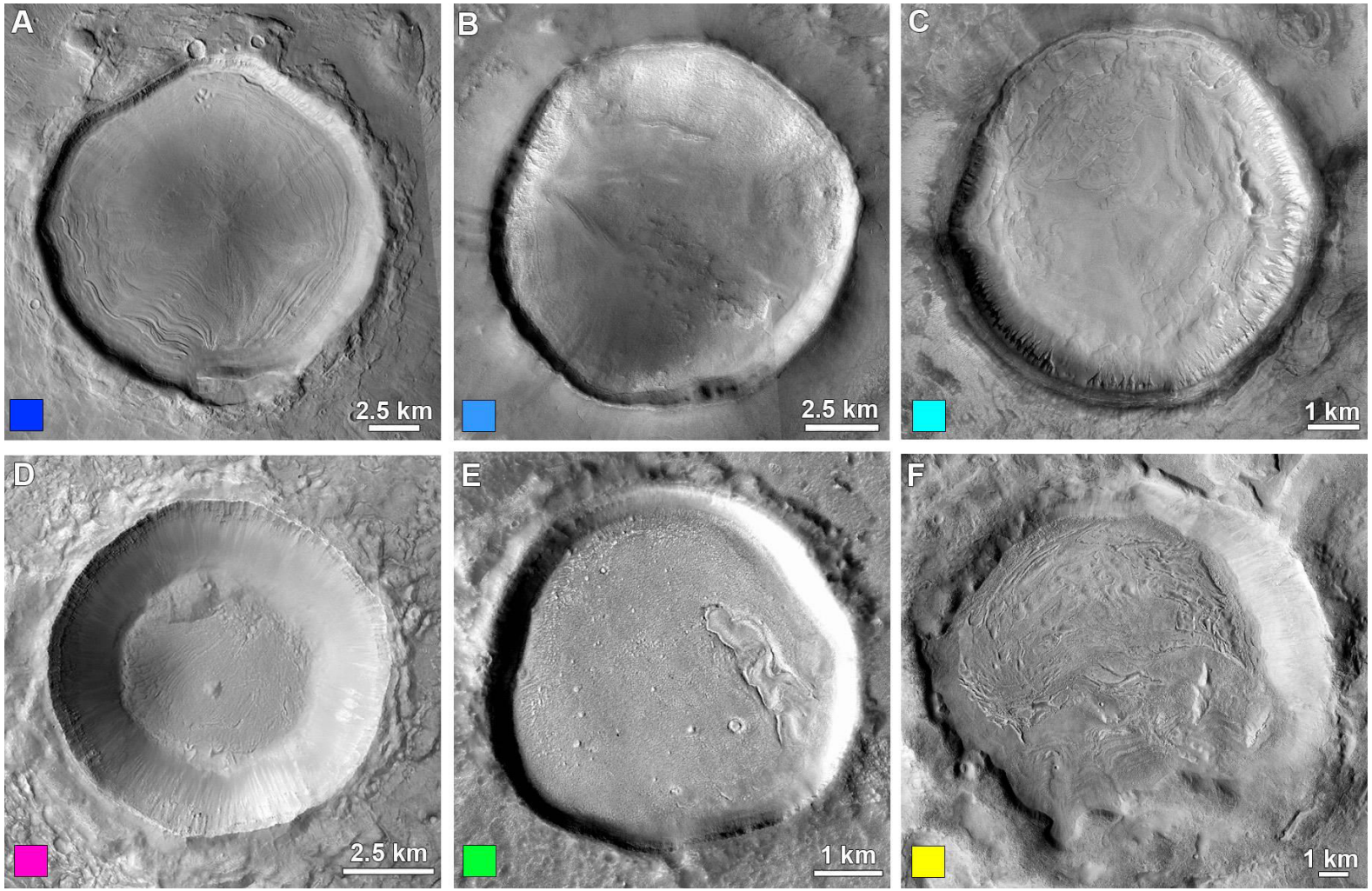
A
2.5 km
B
2.5 km
C
1 km
D
2.5 km
E
1 km
F
1 km

Figure 3.4. Crater fill classification chart. Coloured boxes correspond to the map in Figure **3.4.** A–C are the concentric crater fill (CCF) classes. **(A)** "Classical" concentric crater fill. Subframes of CTX images P20_008755_2164 and B01_010100_2165. **(B)** High-latitude mantled concentric crater fill. Subframes of CTX images G01_018512_2346 and B16_01588_2346. **(C)** Concentric crater fill superposed by scalloped-depression-bearing material. Subframe of CTX B20_017405_2270. **(D)** Flow class fill. Subframe of CTX G21_026477_2111. **(E)** Smooth class fill. Subframe of CTX P22_009465_2144. **(F)** Irregular class fill. Subframe of CTX G16_024500_2129. North is up in all images.

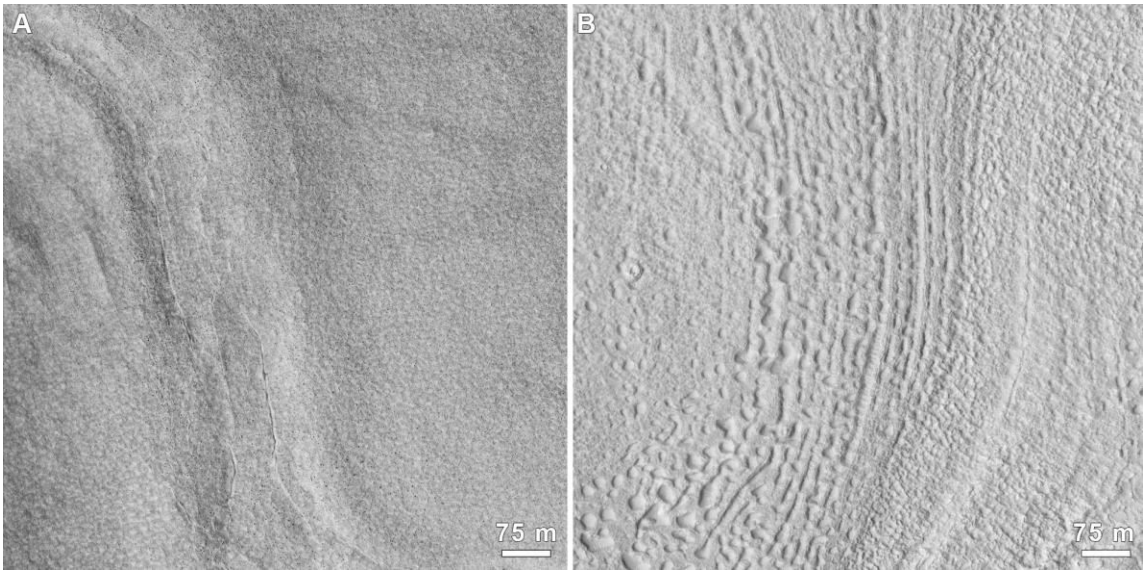

Figure 3.5. Examples of mantled (A) and non-mantled (B) concentric crater fill. The mantled fill, within a crater at 58.7°N, 82.4°W, displays polygonal fracturing characteristic of the latitude-dependent mantle (and is not observed on CCF surfaces [*Levy et al.*, 2009b]). This obscures the brain terrain texture typically observed on CCF surfaces [*Levy et al.*, 2009b] shown in B, within a crater at 36.6°N, 95.8°E.

Flow class fill becomes dominant at ~33°N, but tapers off at ~36°N and is no longer observed poleward of ~42°N. Fill of all classes exhibit evidence for removal, such as fill-facing scarps and concentric extensional fractures at the fill margins [i.e., *Shean*, 2010b].

CCF-bearing craters mantled by scalloped-depression-bearing material (the SDBT) are strongly localized to the "Periglacial Unit" ABp of Kerrigan [2013], with a few outliers. This is to be expected, as the presence of scalloped depressions was the

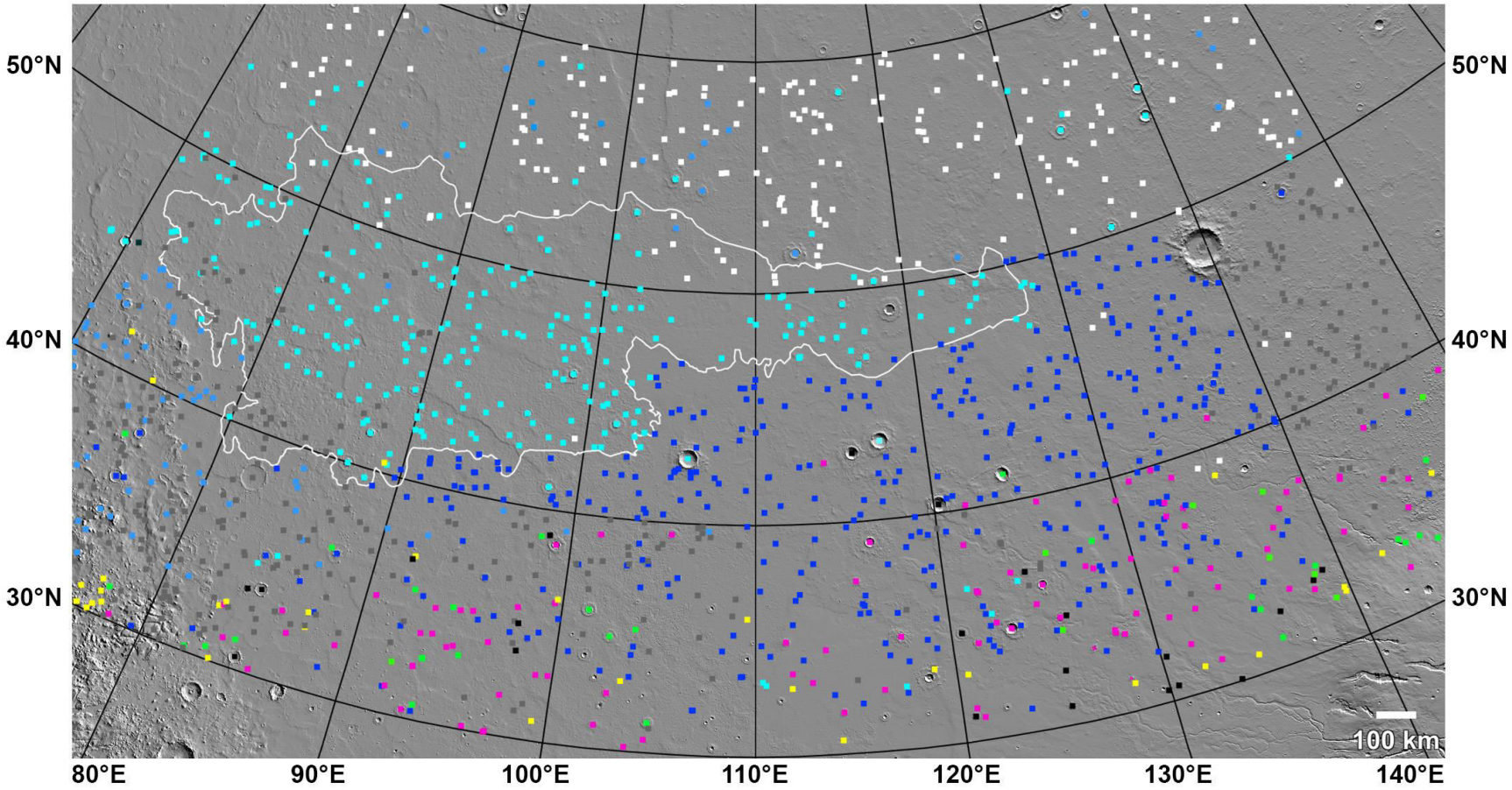

Figure 3.6. Crater fill class map. See Figure 3.4 for examples and text for description. Black = no fill (of the types classified in this paper), dark blue = "classical" CCF, light blue = CCF superposed by LDM, teal = CCF superposed by SDBT, pink = flow, green = smooth, yellow = irregular, grey = other, white = entirely draped/filled with LDM. Size of dots denotes crater outline (diameter). White outline denotes the "Periglacial Unit" ABp as mapped by Kerrigan [2013].

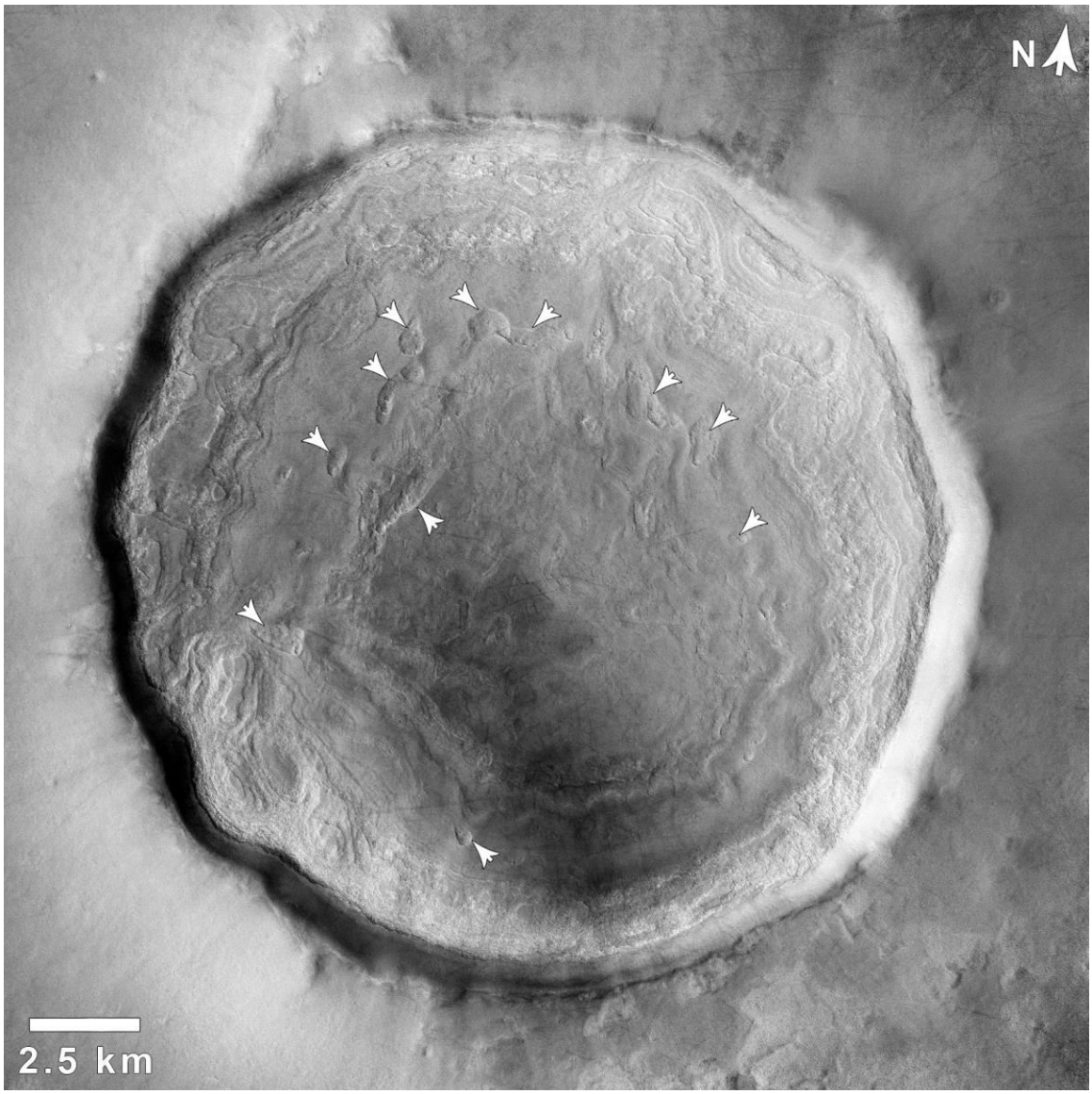

Figure 3.7. Example of possible early stage scalloped depressions (white arrows) within material filling a crater at 55°N, 133°E. Subframe of CTX G19_025803_2355.

identifying factor for mapping the proposed Periglacial Unit; the presence of outliers can also be explained by the greater areal coverage of Utopia with CTX at present. Poleward of 50°N, CCF becomes increasingly mantled by material without scalloped depressions, or with possible signs of scalloped depressions in very early stages of development (Figure 3.7). The interiors of many craters smaller than ~3 km poleward of ~50°N are completely mantled with no clearly visible signs of buried CCF (Figure 3.8). Larger craters as far north as 66°N, however, show clear evidence for mantled CCF (some of which are not included in the Levy et al. [2014] crater fill survey). This may indicate that

the mantle is sufficiently thick within smaller craters at these latitudes to obscure the concentric features. Mantled CCF is also observed immediately to the west of Utopia in the area in/around Nilosyrtis Mensae, but as far south as 30°N. These occurrences taper off at ~85–90°E latitude, transitioning to scalloped-depression-bearing mantles at the mapped boundary of the Periglacial Unit, and to non-mantled CCF and flow/smooth/irregular fill class deposits in Utopia south of the Periglacial Unit. Few craters without fill are observed; these likely post-date the last period of mid-latitude crater fill emplacement.

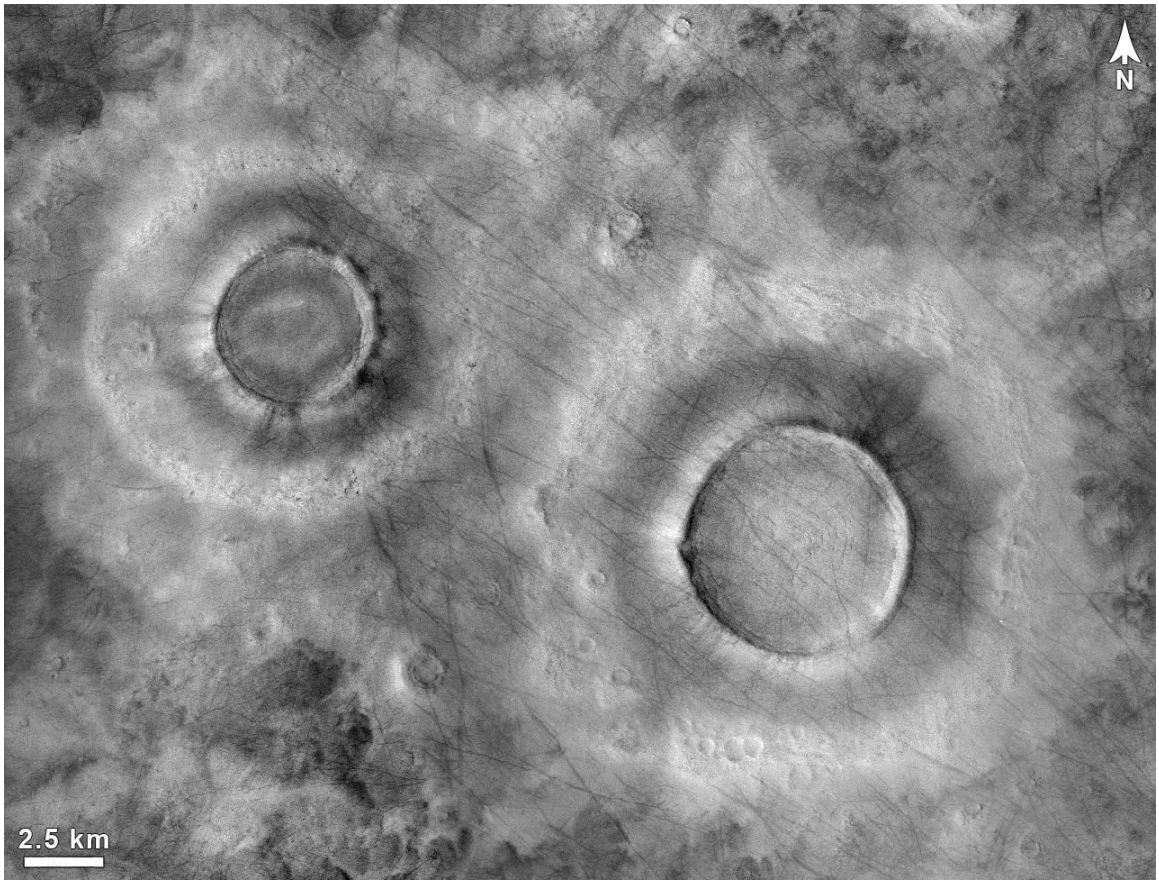

Figure 3.8. Two craters at 57.6°N, 114.9°E, with entirely filled/mantled interiors displaying no scalloped depressions, and little to no evidence of buried CCF textures. Mosaic of subframes of CTX D02_028085_2388 and D01_027452_2360.

3.4.2 Gullies

In western Utopia, gullies are concentrated south of ~43°N (Figure 3.9). Within and near the SDBT, gullies are sparse, only occurring within craters with heavily eroded scalloped depressions, while the non-gullied craters host no scallops (Figure 3.10A–C). In craters where both mid-latitude fill (the types described in Section 3) and gullies are observed in contact with each other, gullies always superpose the fill. Where the fill exhibits extensional fracturing at the margins, gully fans are observed that both cover the fractures and are cut by fractures up to 60°N. These two relationships are sometimes observed within a single gully system, and other times the relationship differs across multiple gullies along a given slope (Figures 3.11–3.12). This implies that gully formation post-dates mid-latitude crater fill emplacement, and has occurred coincident with fill retreat and removal.

Features characterized as "sinuous downslope ridges" found in association with southern hemisphere gullies by Dickson et al. [2015] are observed in association with gullies in Utopia from 37–50°N, consistent with the latitudes of highly dissected LDM [*Mustard et al.*, 2001; *Head et al.*, 2003; *Milliken and Mustard*, 2003] (Figures 3.13–3.14). These downslope ridges are sometimes observed with associated degraded debris aprons. In some cases, the debris aprons appear to be thinly mantled, displaying polygonal fractures across their surfaces that are not observed in younger apron lobes on the same slope (Figure 3.10). We agree with the interpretation of Dickson et al. [2015] that the sinuous downslope ridges represent inverted gully channels from older periods of gully activity that are now being exhumed from within degrading ice-rich pasted-on deposits, as ice is unstable at those latitudes in Mars' present climate [e.g., *Mellon and Jakosky*, 1993]. If these are indeed inverted gully channels, it requires that tens of metres of pasted-on material (considered to be part of the LDM by Levy et al. [2010b] and Dickson et al. [2015]) on crater wall slopes has been removed [i.e., *Dickson et al.*, 2015]. In western Utopia within craters hosting SDBT, the pasted-on mantle on the crater walls appears to form a single continuous unit with the SDBT (e.g., Figures 3.11–3.12). This could have larger implications as to whether the pasted-on material globally

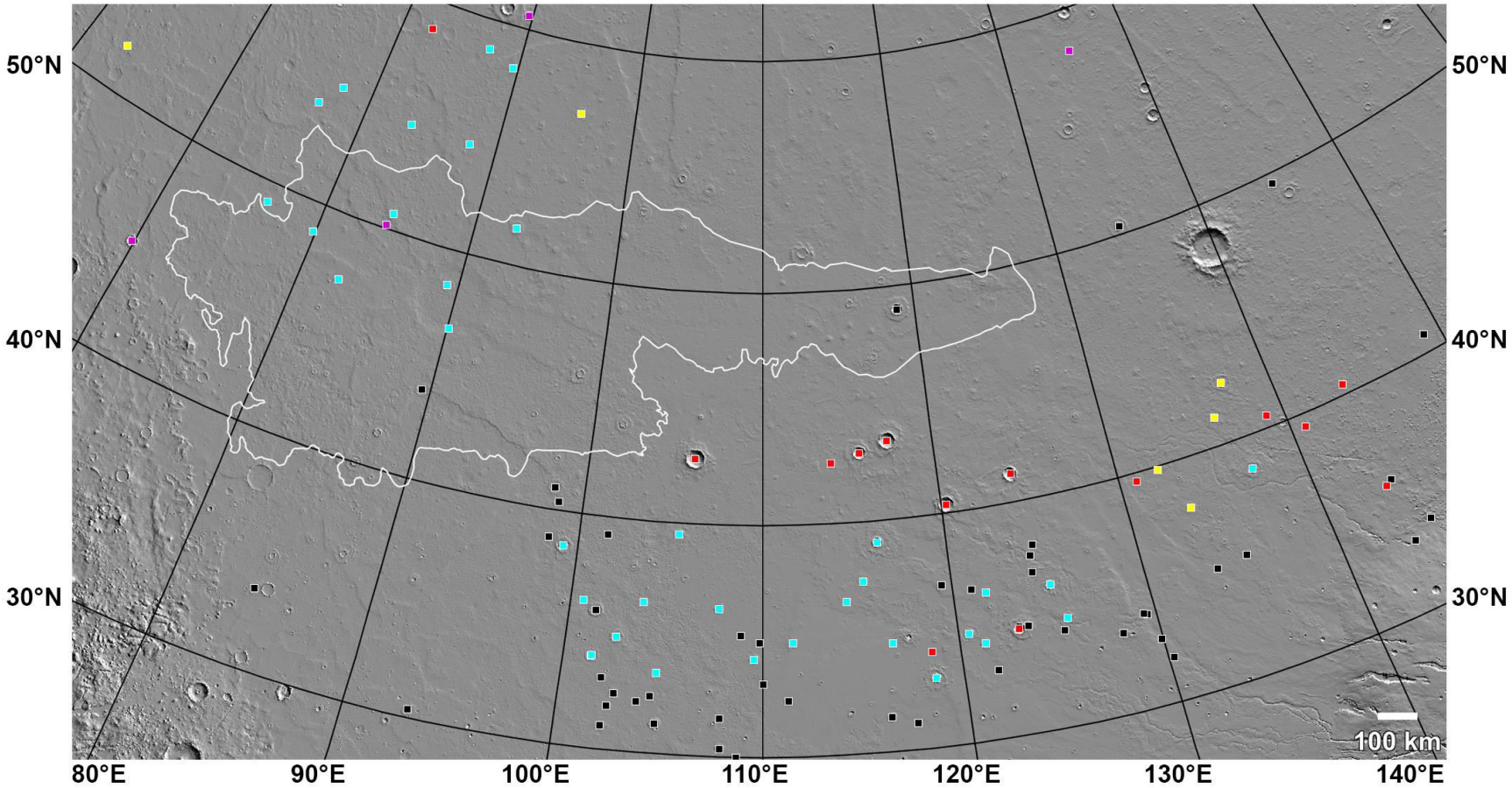

Figure 3.9. Gullies (coloured dots) and gully-like features (black dots). For gullies, teal = pole-facing preference, red = equator-facing, yellow = east/west, and purple = no preference. White outline denotes the "Periglacial Unit" ABp as mapped by Kerrigan [2013].

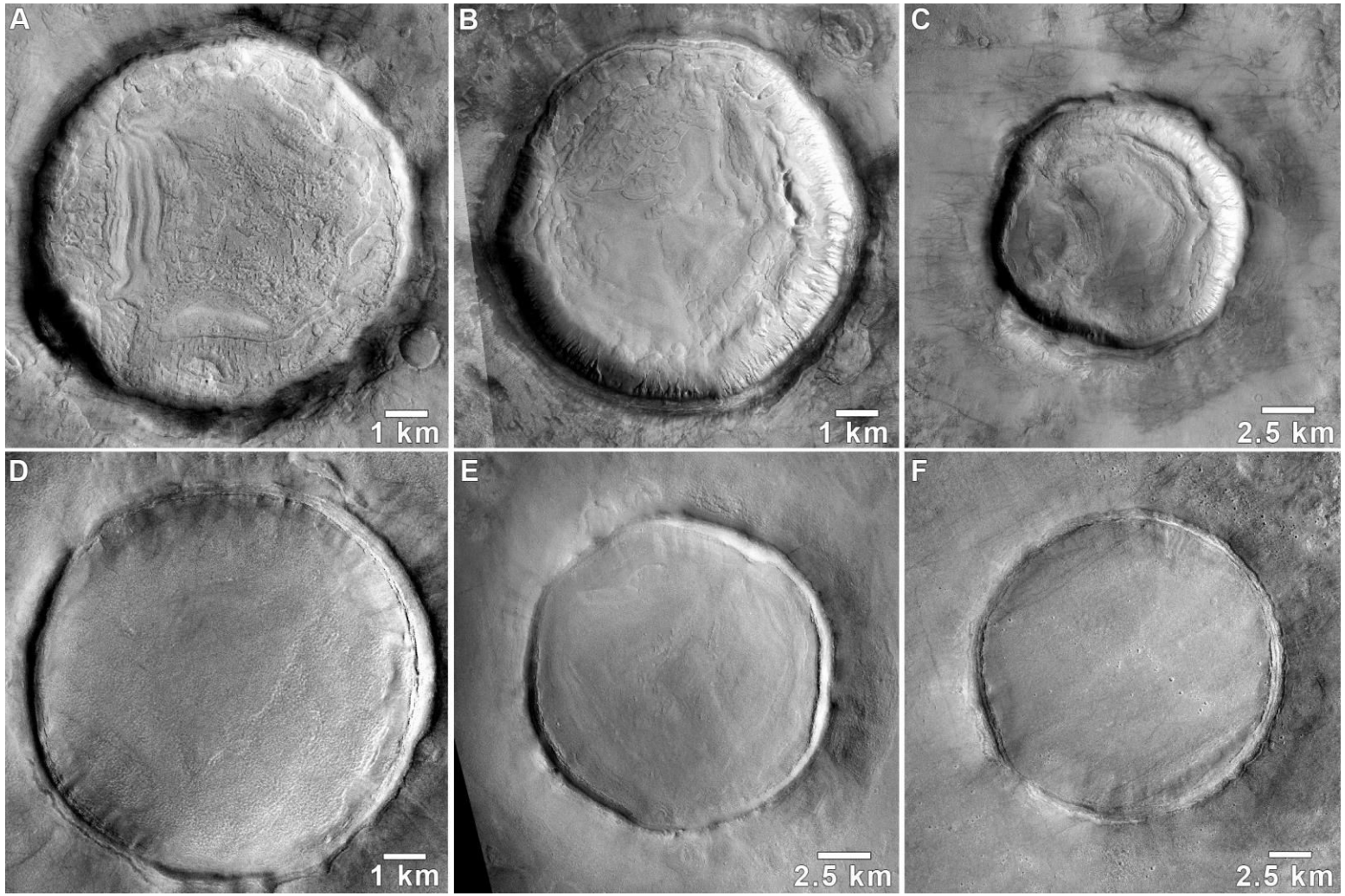

Figure 3.10. Examples of gullied (A–C) and non-gullied (D–F) craters within the SDBT. Subframes of CTX: **(A)** B18_016746_2252, **(B)** F05_037646_2275 and F02_036446_2267, **(C)** F05_037646_2275, **(D)** D01_027544_2299, **(E)** B18_016837_2289, and **(F)** B18_01675_2277. North is up in all images.

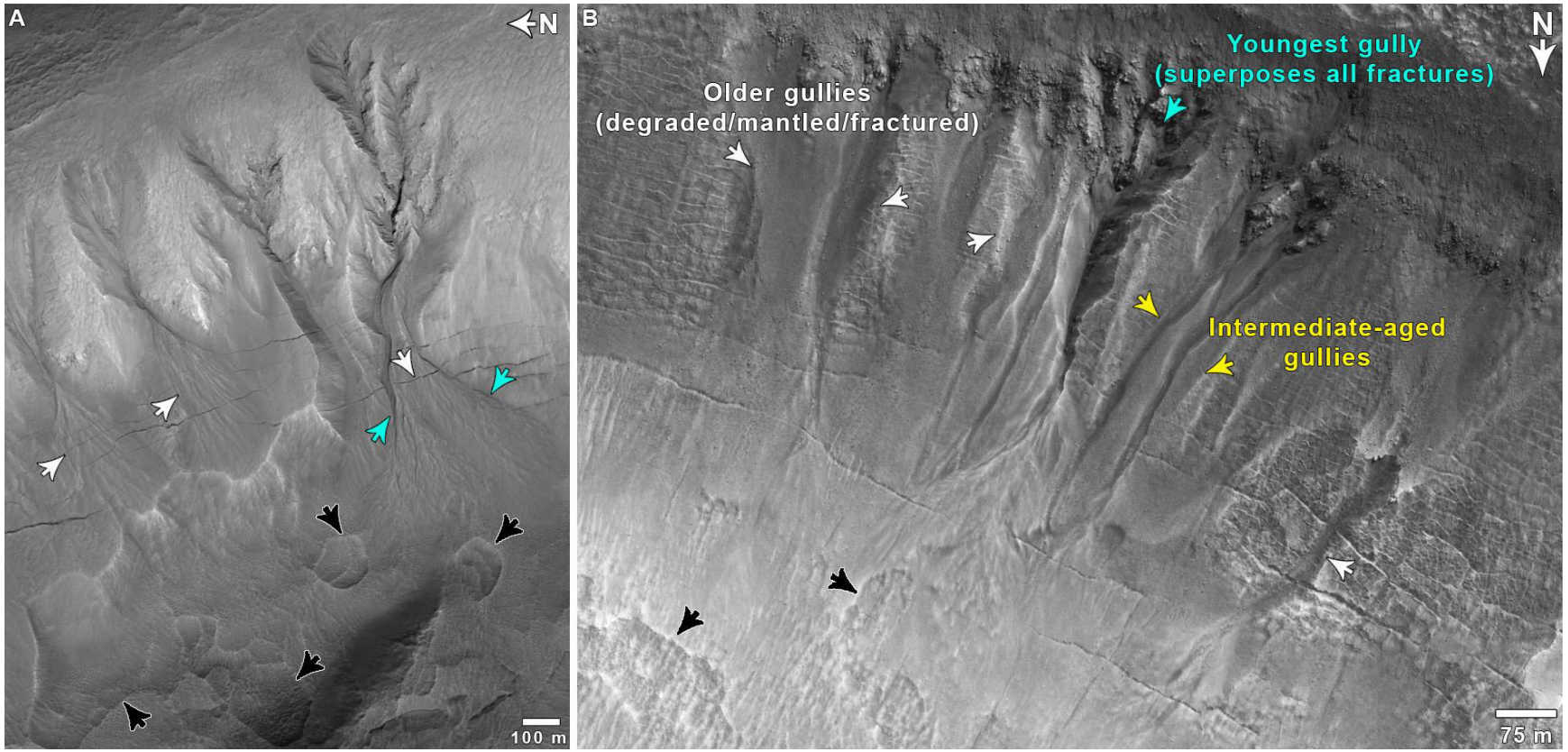

Figure 3.11. Relationships between gully fans and fractures from crater fill retreat. **(A)** Fans cut by (white arrows) and superposing (teal arrows) fractures. Subframe of HiRISE ESP_028719_2290. **(B)** Multiple generations of gullies on a single crater wall. Some gullies are partially filled with pasted-on material, with fractured aprons (white arrows). Intermediate-aged gullies (yellow arrows) have fans that are crosscut by some fractures, but superpose others. The youngest—or at least the most recently active—gully superposes all fractures. Subframe of HiRISE ESP_041866_2290.

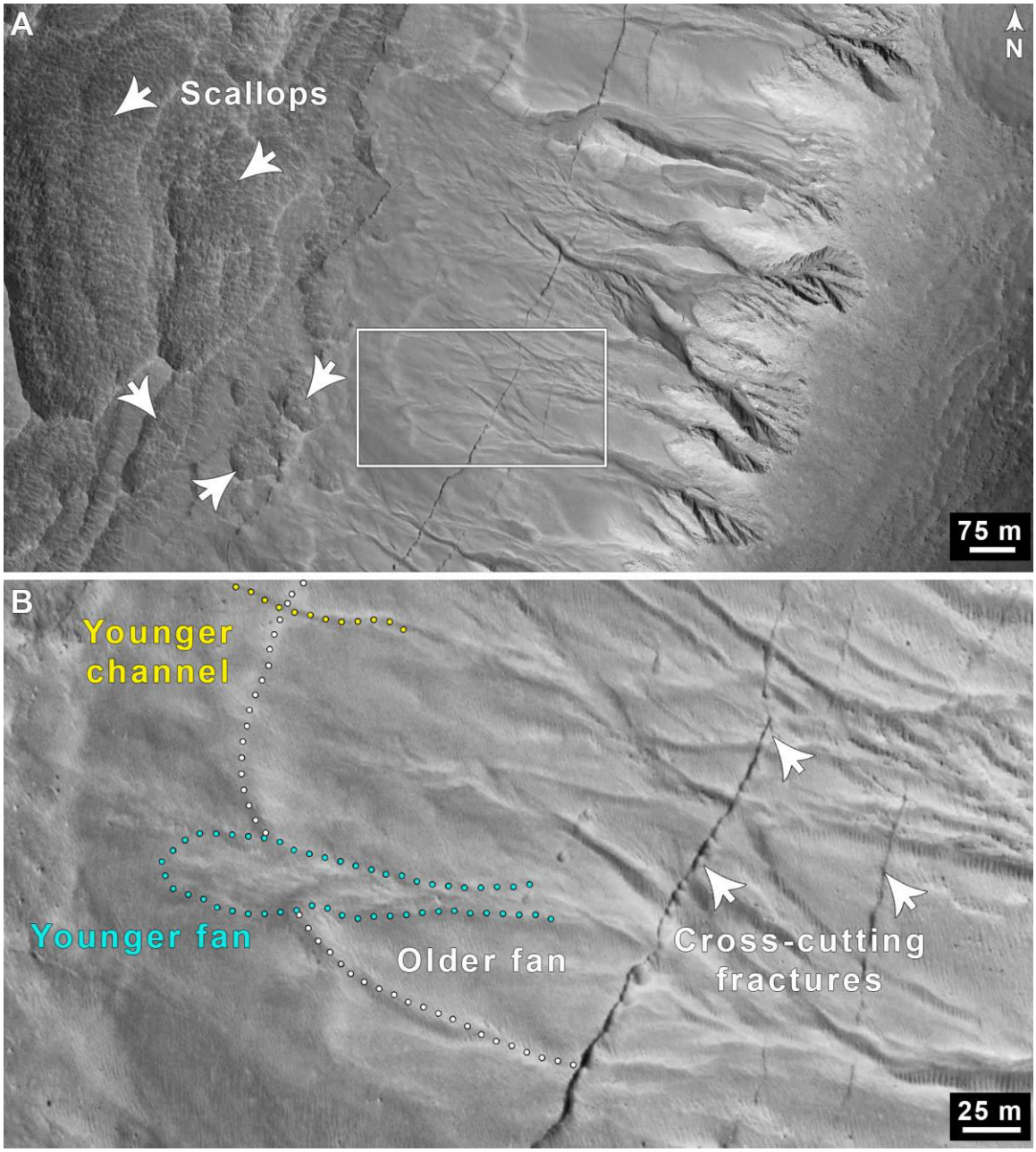

Figure 3.12. **(A)** Multiple generations of gully activity on a crater wall. White box denotes the location of B. Subframe of HiRISE ESP_028719_2290. **(B)** A large older gully fan (white dotted outline) is crosscut by younger channels (yellow dotted outline) and superposed by younger aprons (teal dotted outline), all of which pre-date the formation of the fractures upslope (white arrows). Subframe of HiRISE ESP_028719_2290.

and/or SDBT locally in Utopia constitutes part of the LDM. Future work will investigate the global nature of the LDM—and what middle- and high-latitude morphologies do and do not constitute LDM—as it goes beyond the scope of this particular study.

We interpret the mantled gully aprons (i.e., Figure 3.13) to be representative of older periods of gully activity that pre-date the most recent episode of SDBT emplacement and have been draped by subsequent SDBT deposition. Younger gully aprons terminate farther upslope than the relict aprons (Figure 3.13), possibly reflecting a reduction in the availability of liquid water for gully activity over time. This would be consistent with a meltwater source (from either the crater wall mantling deposits [*Christensen*, 2003] or near-surface ground ice [*Costard et al.*, 2002]) where the source material is/was undergoing desiccation.

Dickson et al. [2015] found that in the southern hemisphere, gullies in the ~30–40°S latitude band were most likely to be degraded and completely removed over time compared to gullies in the ~40–50°S range, which exhibit multiple episodes of burial and inversion. Our observations find this relationship holds for gullies in western Utopia as well. Also consistent with the southern hemisphere observations of Dickson et al. [2015], we find that there is a clear relationship between pasted-on material, and gully formation and preservation. This lends support to the hypothesis of Christensen [2003] that gullies can form via melting of snow/ice within the pasted-on deposits. The snowmelt hypothesis is also supported by the distribution of gullies globally relative to the locations of mid-latitude ice deposits at high obliquity (see Chapter 2). The observed relationship between gullies and pasted-on material may also explain the lack of gullies in the equatorial regions; if any mantling deposits were ever present at those latitudes, they have since eroded away, likely removing evidence of gullies formed within the deposits. Climate models predict ice deposition in the equatorial regions under high obliquity (>45°) conditions [e.g., *Levrard et al.*, 2004], and crater filling material that is morphologically similar to that found in the mid-latitudes has been observed in the equatorial region of Terra Sabaea [*Shean*, 2010a], supporting the climate model results.

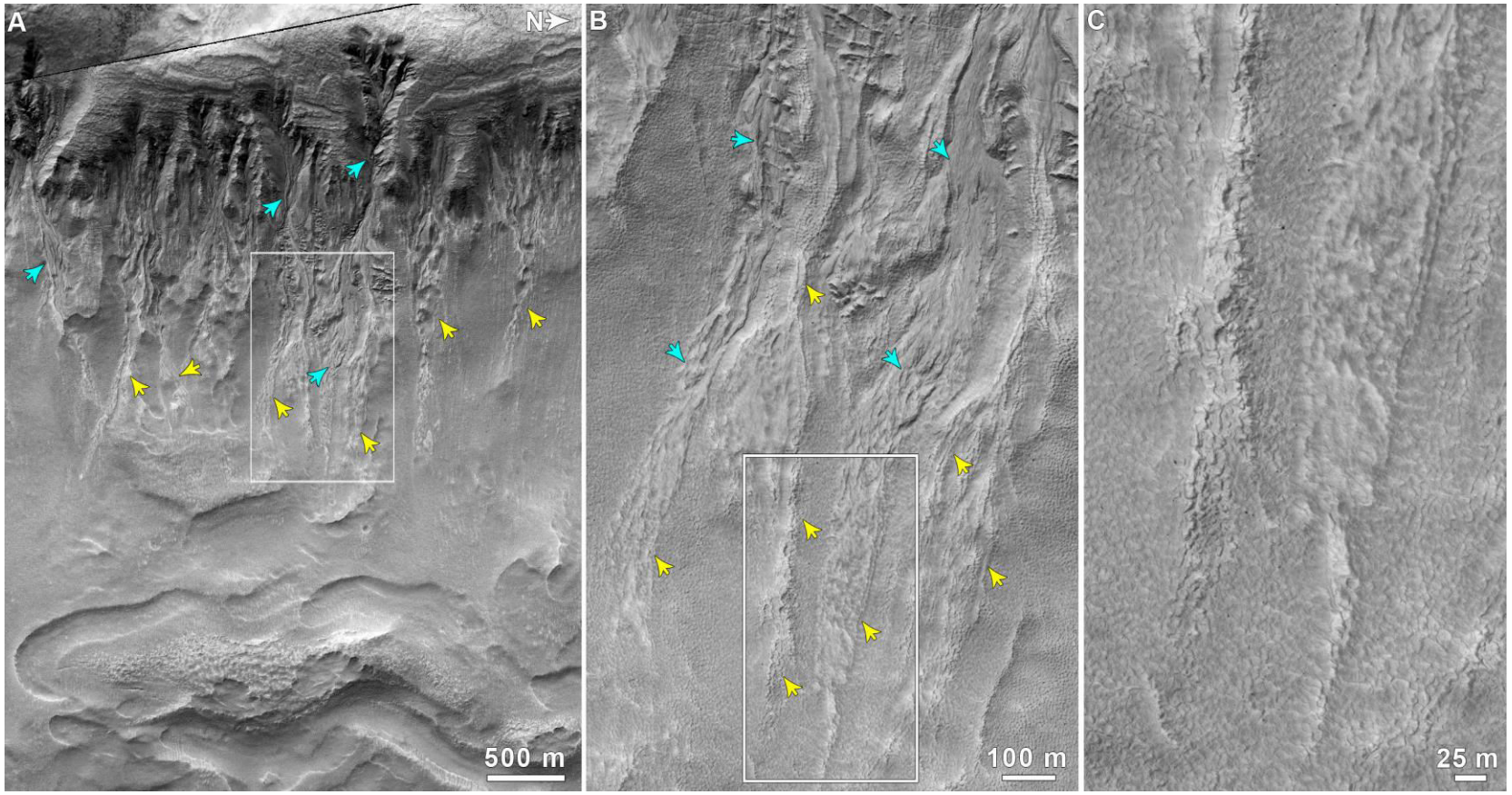

Figure 3.13. Multiple generations of gullies on a mantled crater wall. Teal arrows denote younger gully deposits. Yellow arrows mark older buried/inverted gully segments. **(A)** Wide view, with white box marking the extent of B. **(B)** Closer view of older, mantled (yellow arrows) and younger, non-mantled (teal) gully deposits. White box denotes the extent of C. **(C)** Mantled gully deposits. Note how they have the same surface texture as the surrounding crater wall mantling (pasted-on) material. Subframes of HiRISE ESP_025659_2230.

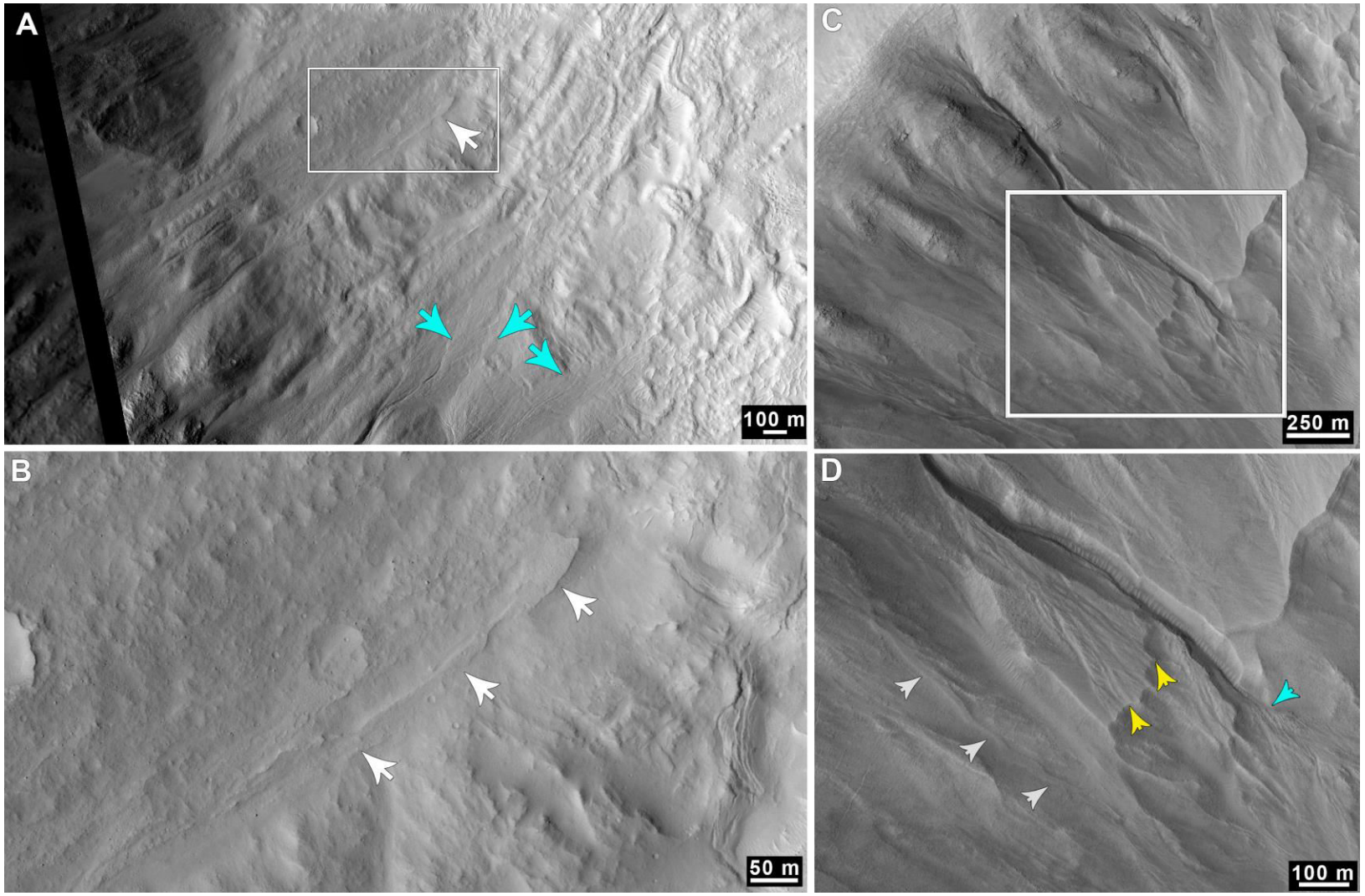
A
100 m
C
250 m
B
50 m
D
100 m

Figure 3.14. Multiple generations of gullies on mantled crater walls. **(A)** Wide view of a potential inverted (white arrow) gully channel on a crater wall, with younger gullies to the south (teal arrows). White box denotes the extent of B. Subframes of HiRISE PSP_009796_2145. **(B)** Closer view of the potential inverted gully channel. Subframe of HiRISE PSP_009796_2145. **(C)** Wide view of gullies on a crater wall, with white box marking the extent of D. Subframe of HiRISE ESP_022561_2305. **(D)** An inverted gully channel (white arrows) adjacent to an older gully fan truncated by a scalloped depression (yellow arrows) and a gully that post-dates the most recent episode of scallop development (teal arrow). Subframe of HiRISE ESP_022561_2305.

However, no evidence for either gullies (i.e., relict alcoves) or pasted-on crater wall deposits are observed within fill-bearing craters in Terra Sabaea [*Shean*, 2010a; *Harrison et al.*, 2014, 2015b].

From ~30–40°N, 139 craters containing "gully-like" features are observed (Figure 3.15A–C). Analysis during the creation of the global gully database presented in Chapter 2 revealed these features to be highly localized to Utopia. The gully-like features typically consist of alcoves and aprons with predominantly linear, poorly defined channels or mass movement chutes. In some cases, wide, eroded channels are observed that start mid-slope with no clearly associated alcoves and/or aprons preserved (Figure 3.15D–E) In other cases, mantled alcoves are observed without any visible evidence of associated preserved channels and/or depositional aprons (Figure 3.15F). The gully-like features typically superpose extensional fractures suggestive of crater fill removal; however, older disconnected fans that are crosscut by fill retreat fractures are observed (Figure 3.16). These older fans often show evidence of eroded leveed flows and channel segments, and are much broader than the stratigraphically younger lobes upslope. Based on the morphologies and stratigraphic relationships, we interpret the disconnected fan segments to represent periods of gully activity where the pasted-on mantle upslope has either partially or entirely (depending on the individual crater) eroded away, with the gully-like features representing more youthful periods of mass movement activity involving very little to no water.

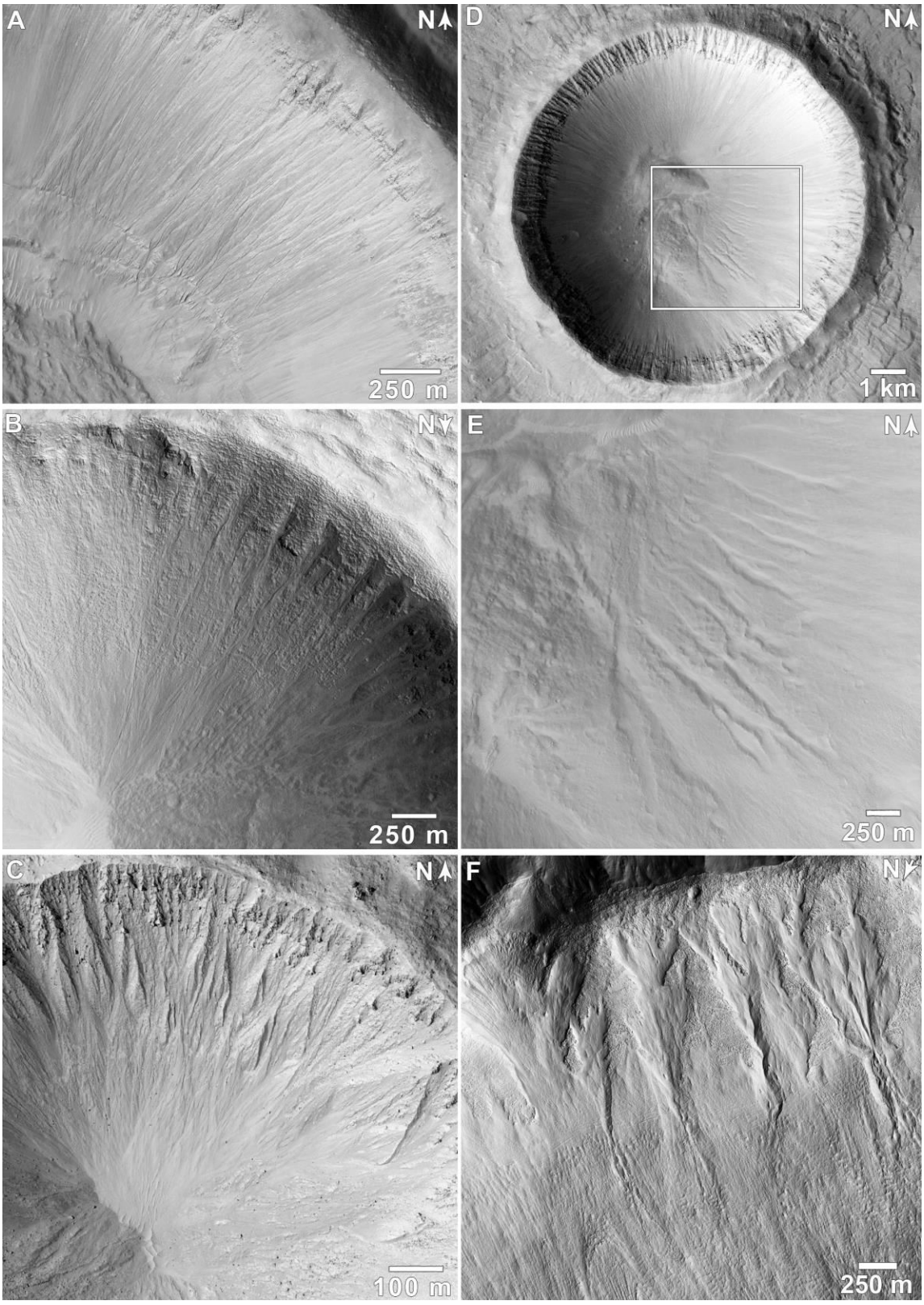
A
N
250 m
D
N
1 km
B
N
250 m
E
N
250 m
C
N
100 m
F
N
250 m

Figure 15. (A–C) Gully-like features in southern Utopia. Subframes of HiRISE ESP_025118_2115, ESP_016244_2150, and ESP_026331_2179, respectively. (D) Crater with wide channels on southeastern wall. White box denotes the location of E. Subframe of CTX P15_006816_2100. (E) Closer view of the wide channels from E. Subframe of HiRISE PSP_006816_2120. (F) Alcoves filled (mantled) with LDM-related pasted-on material. Subframe of HiRISE PSP_009056_2180.

3.4.3 Scalloped-Depression-Bearing Terrain

The SDBT extends from ~38–54°N and 70–128°E. We observe occurrences of scalloped depressions within craters out to ~60°N and ~150°E (Figure 3.6), and poleward of 50°N some craters exhibit possible signs of scalloped depressions in very early stages of formation (Figure 3.7). The SDBT gradually becomes discontinuous near the margins of the possible "Periglacial Unit" ABp mapped by Kerrigan [2013] at its southern boundary before no visible evidence of it is preserved. Near its southern extent, the SDBT is typically darker toned than the surrounding terrain (i.e., Figure 3.2). Along the northern boundary, the tone of the SDBT is comparable to that of the surrounding terrain (Figure 3.17). Within the ABp boundaries mapped by Kerrigan [2013], the tone of the SDBT is highly variable. However, the tonal differences between the SDBT and the underlying/surrounding units do not appear to be a primary feature of the unit. The mottled tonal differences across the SDBT appear to arise from differences in dust cover based on observations in areas of concentrated dust devil tracks, revealing darker-toned material amidst lighter-toned (interpreted as dusty) areas (Figure 3.18). The occurrence of scallops gradually tapers off with increasing latitude, consistent with the observations of Morgenstern et al. [2007].

A reflector coinciding with the base of the layered scarps of the SDBT has been detected using SHARAD. The dielectric properties of the SDBT are consistent with porous, slightly dirty H_2O ice (50–85% ice by volume) ranging in thickness from ~80–170 m [*Stuurman et al., accepted*]. Using the ice accumulation rate for this region of

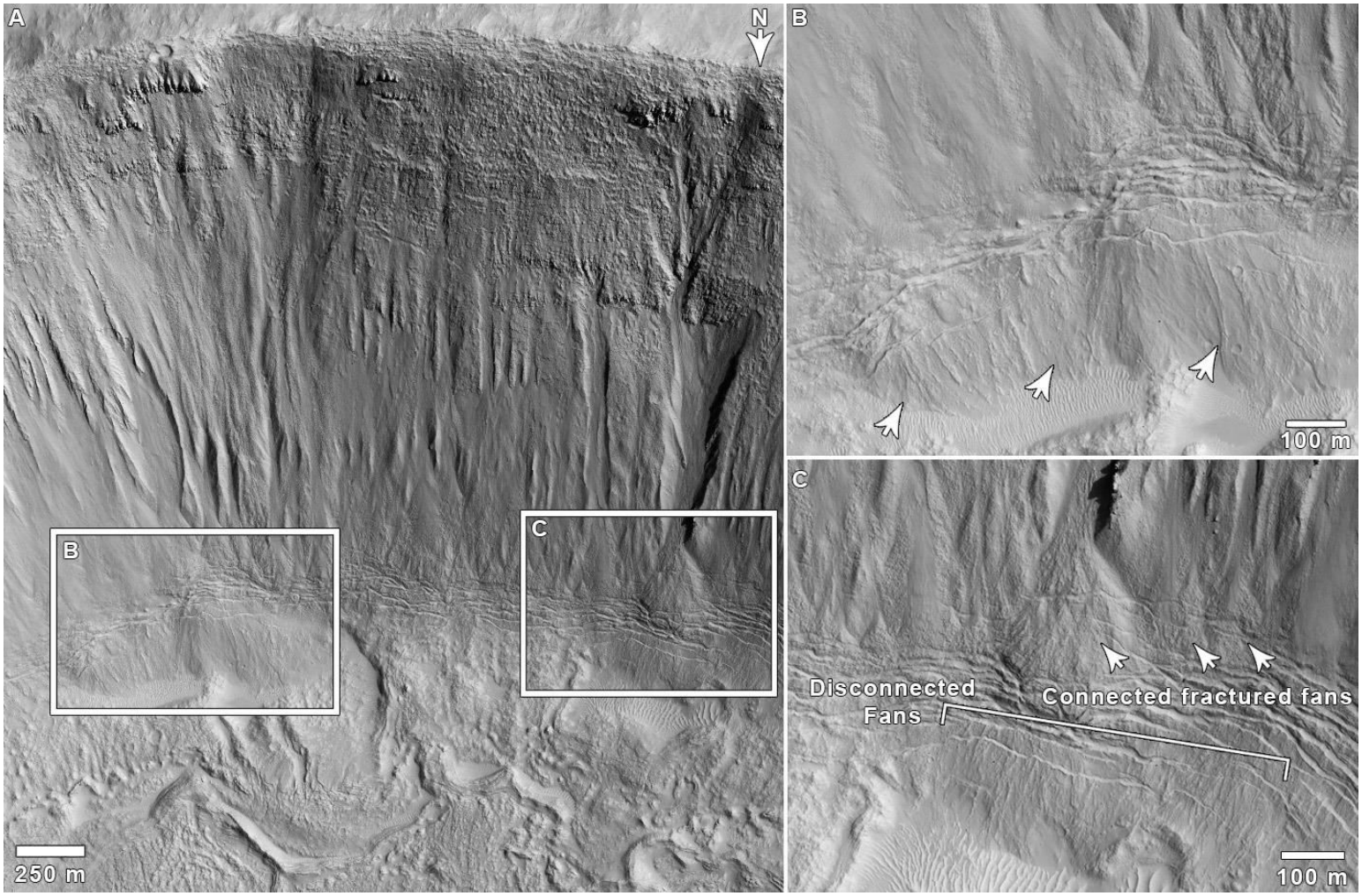

Figure 3.16. **(A)** Example of gully-like features on a crater wall at 32.4°N, 102.7°E. **(B)** Disconnected fans at the base of the crater wall. **(C)** Fans connected to the gully-like features fractured by crater fill retreat, along with fractured disconnected fans that show evidence of old leveed flows. Subframes of HiRISE ESP_028745_2130.

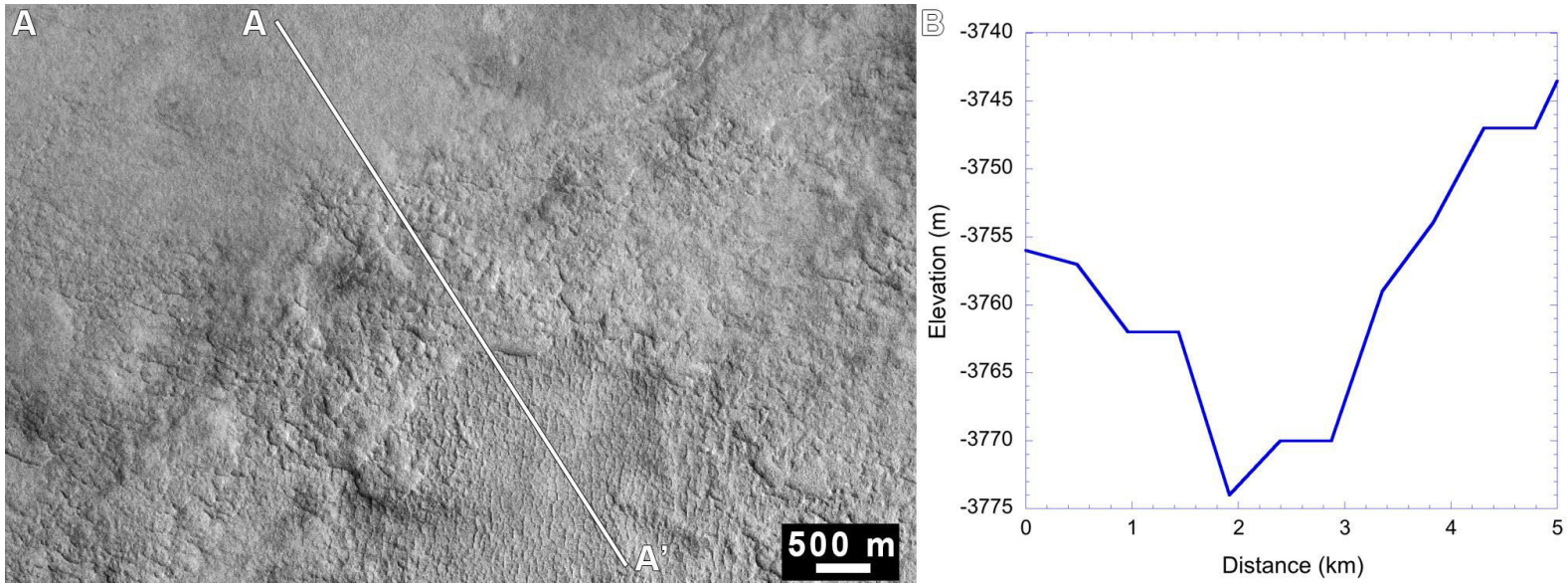

Figure 3.17. (A) Comparison of the SDBT tonality to surrounding terrain along the northern mapped boundary of the "Periglacial Unit." Subframe of CTX D20_035220_2269. **(B)** MOLA profile across the SDBT from A to A', highlighting the steep scarps characteristic of the terrain.

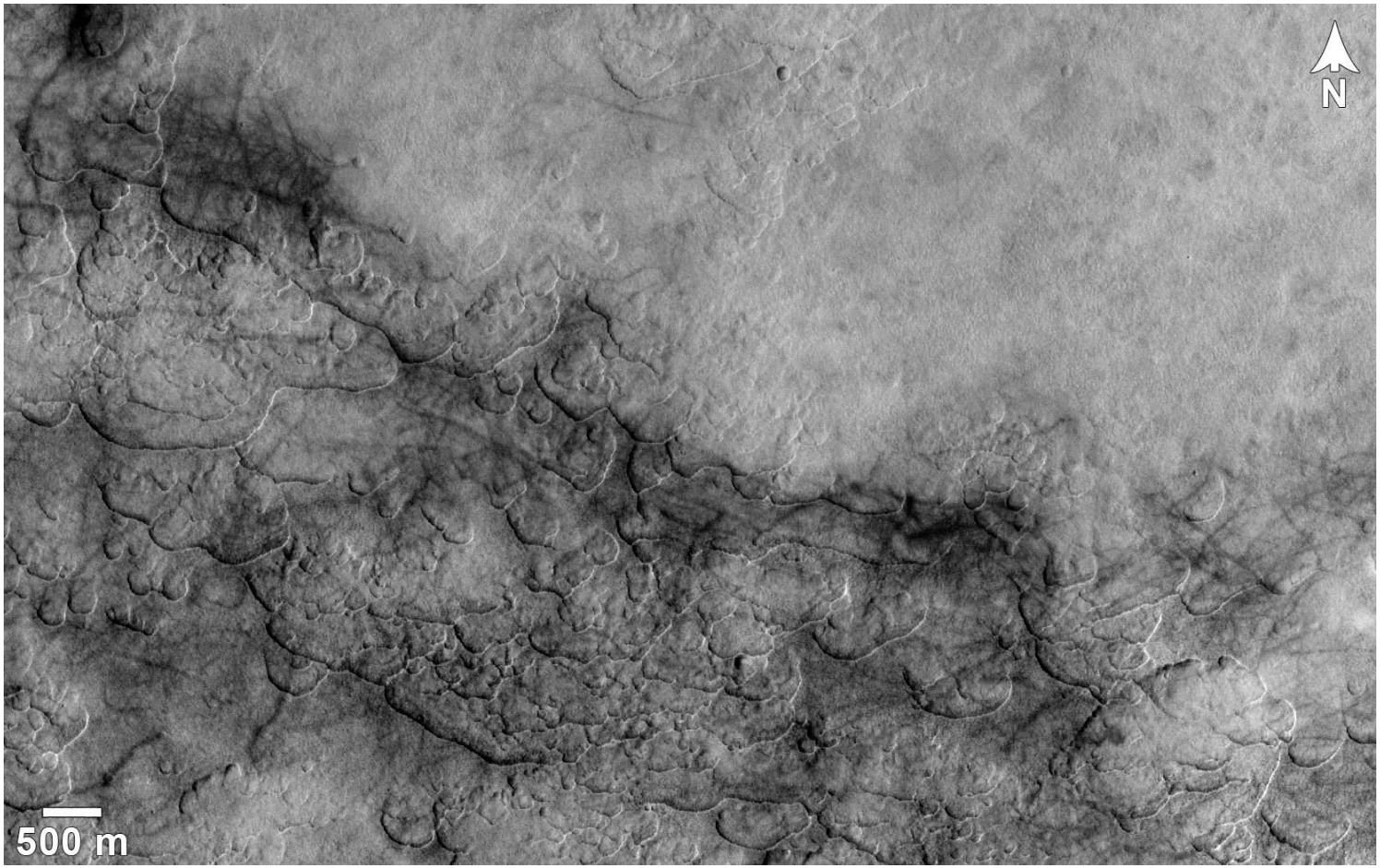

Figure 3.18. Heavily scalloped scarp (sloping downward from SW to SE in the frame) within the SDBT, showing tonal differences across various areas. Note the numerous dark-toned dust devil tracks where surface dust has been cleared, revealing the darker underlying material.

Utopia in the climate model of Madeleine et al. [2009] of 8–14 mm/year, Stuurman et al. [*accepted*] calculate that it would take ~100,000 years to deposit a 100 m thick layer of ice. A large ice component in the SDBT is also supported by the lack of talus along scarp edges within the unit. If the SDBT is composed of ice-cemented dust, then any dust left behind upon sublimation of the ice would be easily transported by wind and thereby largely removed over time. This could explain both the lack of debris along scallop/scarp slopes, as well as the dark tone of the SDBT relative to the terrain to the south. In this region of Utopia under current martian conditions, west-to-east storm activity is common during certain times of the year. This storm activity is predominantly driven by a combination of topography and temperature differentials between the seasonal north polar cap and the adjacent frost-free ground [*Cantor*, 2007]. Therefore, it is expected that this pattern would hold during past climate conditions that are similar to the present, and these winds could mobilize dust off the surface of the SDBT. This creates a positive feedback cycle for erosion of the SDBT; that is, removal of the protective surface lag exposes more near-surface ice to sublimation, resulting in desiccation and a new non-cohesive surface lag of dust, which is then removed by aeolian activity over time, with the process repeating itself with the cyclic variations in martian obliquity.

Kreslavsky and Head [2002] and Soare et al. [2012] state that based on observations with MOC NA and HiRISE, respectively, the LDM overlies the SDBT in Utopia. However, other workers propose that the locations that Soare et al. [2012] interpret to be LDM deposited within depressions in the SDBT are actually "gaps" in the SDBT that expose an underlying lighter-toned unit [*Capitan et al.*, 2012; *Osinski et al.*, 2012; *Stuurman et al.*, 2014] (Figure 3.19). Inspecting the two units using both HiRISE images and anaglyphs, our observations support the hypothesis that the light-toned unit underlies the SDBT. The light-toned unit is heavily cratered relative to the nearly crater-free SDBT and lacks the polygonal fracturing observed on the SDBT (Figures 3.19–3.21). Craters within the light-toned unit are often partially filled with material that is morphologically identical to the surrounding SDBT scarps (Figure 3.20C), suggesting

they are the same unit. Depressions that appear to be eroding atop the light-toned unit are also observed, with the SDBT displaying a pitted texture rather than (or in addition to) polygonal fracturing atop places where the light-toned unit appears to be thinly buried (Figures 3.20A–B). SHARAD-derived SDBT thicknesses are consistent with the change in elevation (based on MOLA) from the polygonally fractured SDBT to the pitted-texture SDBT (Figure 3.22), supporting our interpretation that the pitted-texture areas represent thin SDBT deposits atop the lighter-toned underlying unit. These deposits are thin enough that the reflectors, if present, are not resolvable by SHARAD (thinner than ~10 m). Within larger craters that are partially buried by the SDBT, the crater wall mantling material appears to be continuous with the crater-filling material hosting scalloped depressions, suggesting they are a single depositional unit. Along the crater wall contact, evidence for retreat of the SDBT is sometimes visible (Figure 3.23). The SDBT is thin enough within some craters that underlying CCF patterns are visible, but thick enough in other craters that even when highly eroded, the surface patterns of the underlying CCF are not visible. All of these observations suggest that the SDBT was once more areally extensive, burying the light-toned unit (and CCF-bearing craters within it). Subsequently, the SDBT eroded to exhume the underlying light-toned unit, with deposits of the SDBT preserved within formerly buried craters. Based on the morphology, stratigraphic relationships, and SHARAD results of Stuurman et al. [2014; *accepted*], we interpret the SDBT to be ice-rich layered deposits emplaced at periods of high obliquity [i.e., *Morgenstern et al.*, 2007; *Lefort et al.*, 2009]. The typical lack of mass movement features along scalloped depression walls, despite slopes up to ~80° based on MOLA shots (Figure 3.17), combined with the relative lack of impact craters preserved on the SDBT surface (i.e., Figure 3.21) supports the hypothesis that the scallops/scarps are rapidly degrading [*Stuurman et al., accepted*].

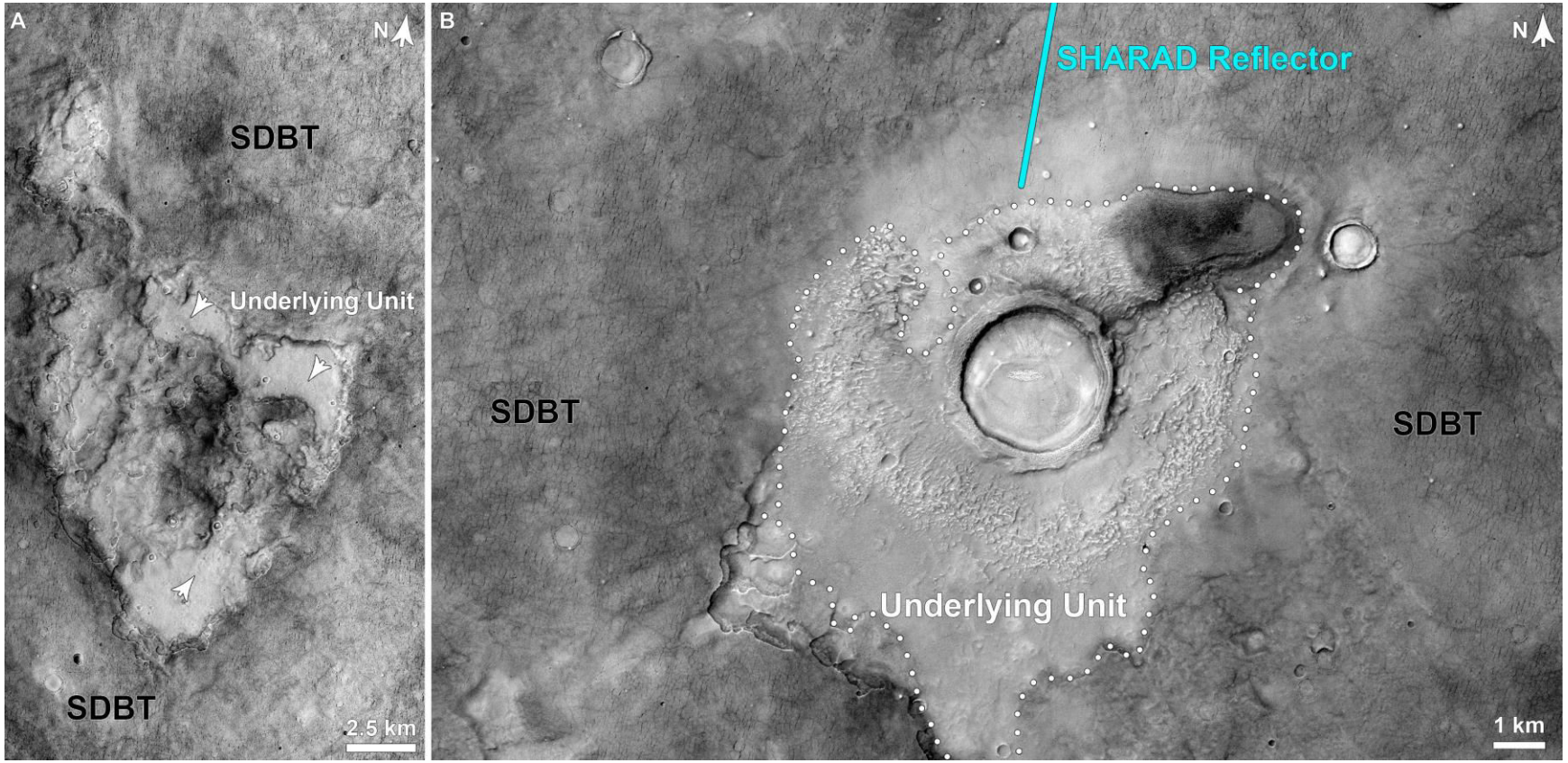

Figure 3.19. Examples of "gaps" in the SDBT, exposing a lighter-toned underlying unit. **(A)** Darker-toned, polygonally fractured SDBT atop the lighter-toned unit (white arrows). Subframe of CTX G22_026873_2201. **(B)** Darker-toned, polygonally fractured SDBT atop the lighter-toned unit (outlined by the white dotted line). Note the smaller craters to the NW of the large crater at the centre, which is partially buried by the SDBT. Blue line denotes the location of the subsurface reflector within the SDBT detected by SHARAD with dielectric properties consistent with water ice as documented by Stuurman et al. [2014]. Subframe of CTX G22_026662_2201.

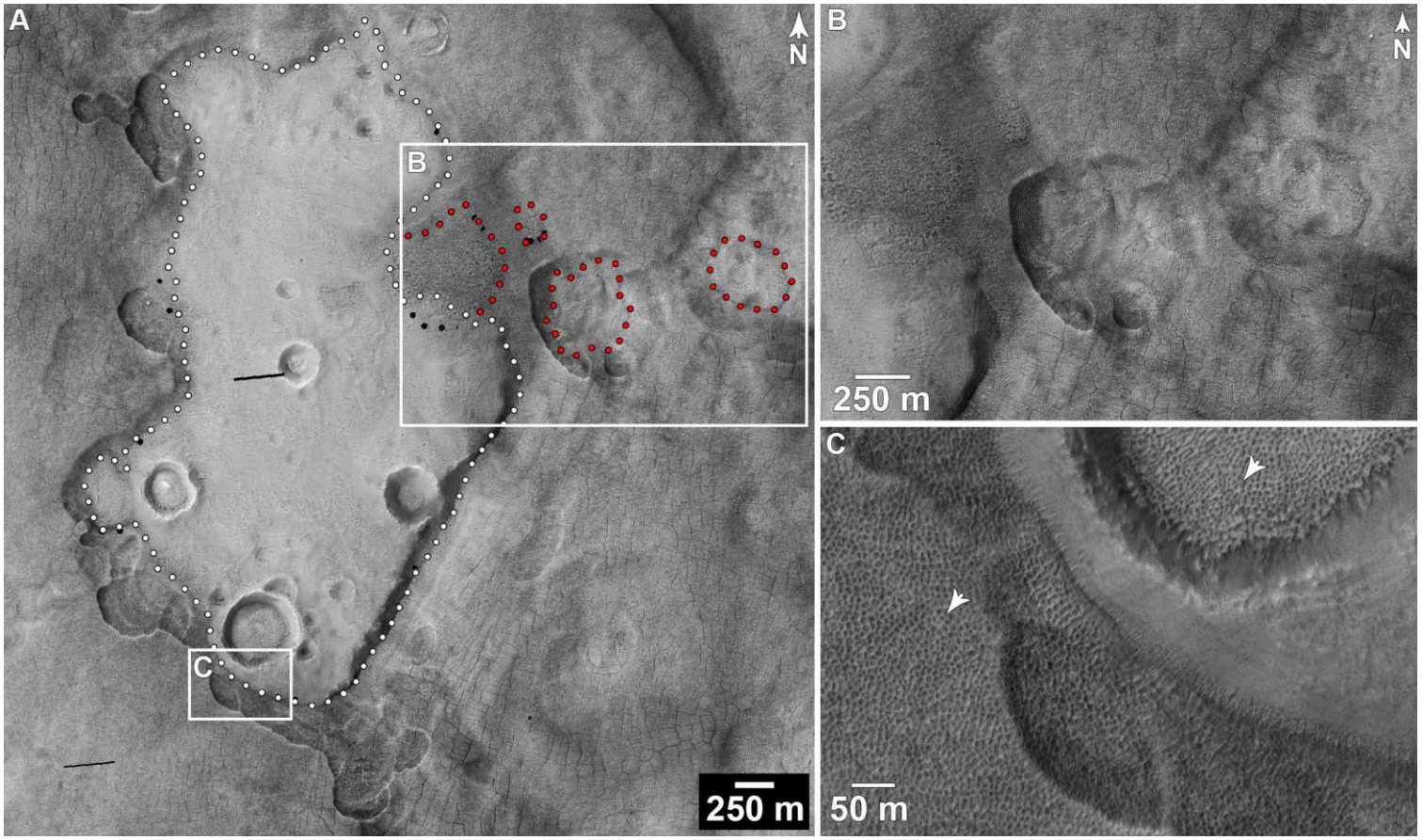

Figure 3.20. (A) Light-toned basement exposed within gaps in the SDBT (darker-toned terrain). White dotted line denotes the extent of the basement exposure. Red outlines denote areas of potentially thinly buried basement material. White boxes mark the locations of B and C. **(B)** Closer view of the potentially thinly buried basement material. Note the pitted texture of the SDBT within and to the west of the depressions. **(C)** Contact between the SDBT and the light-toned basement unit, showing a portion of a crater within the basement unit. The crater is partially filled with material that displays the same pitted texture as the scarp wall of the SDBT to the southwest. Subframes of HiRISE PSP_009467_2225.

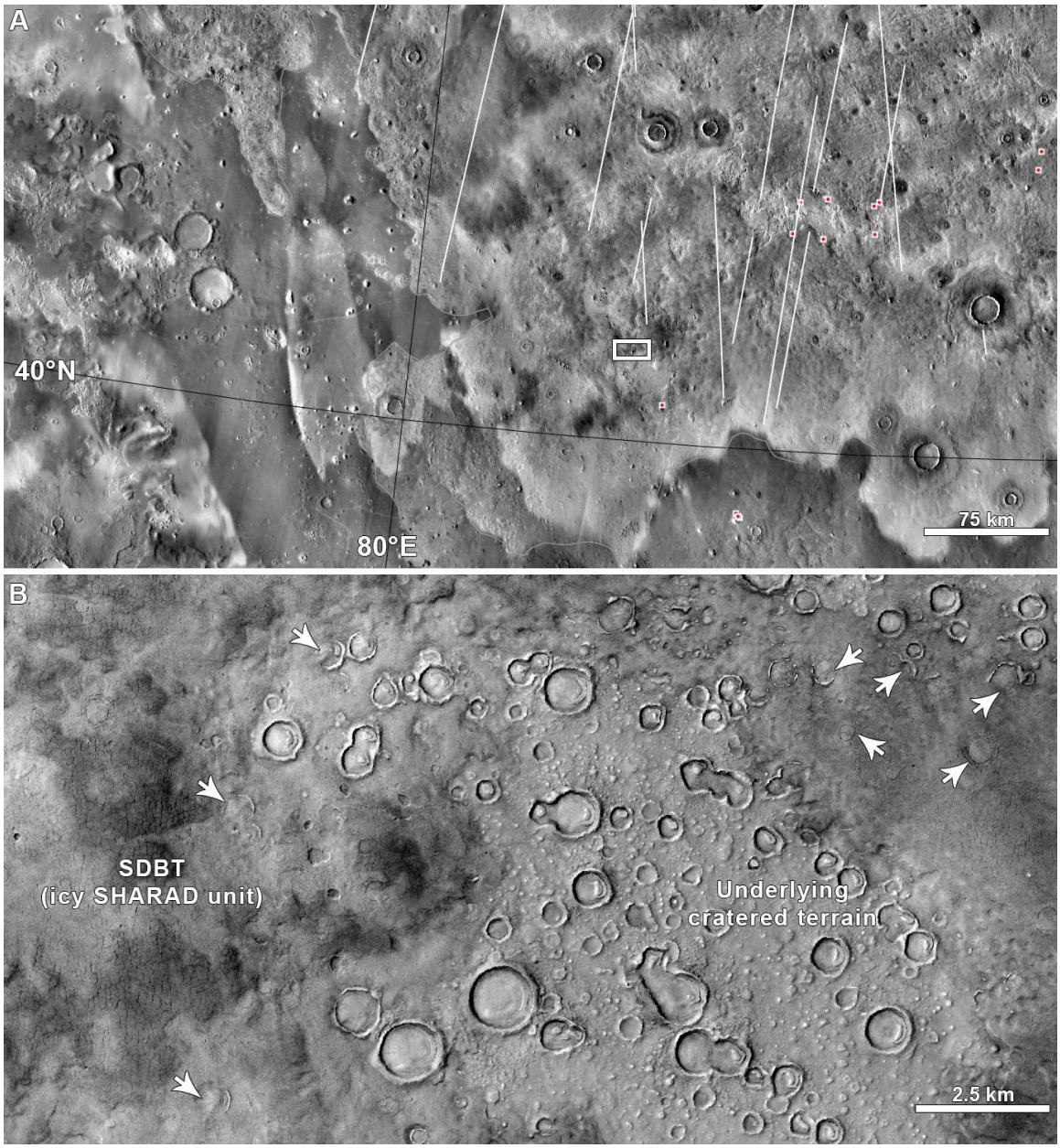

Figure 3.21. (A) THEMIS daytime IR view of the western portion of the SDBT. White lines and red dots represent SHARAD reflectors with dielectric properties consistent with water ice from Stuurman et al. [2014]. White box denotes the location of B. **(B)** The polygonally fractured SDBT, appears to be 50–85% ice by volume based on SHARAD results. The underlying lighter-toned unit retains many more craters than the SDBT, implying that the lighter-toned unit is older. White arrows mark partially buried craters within the SDBT. Subframe of CTX P18_008162_2207.

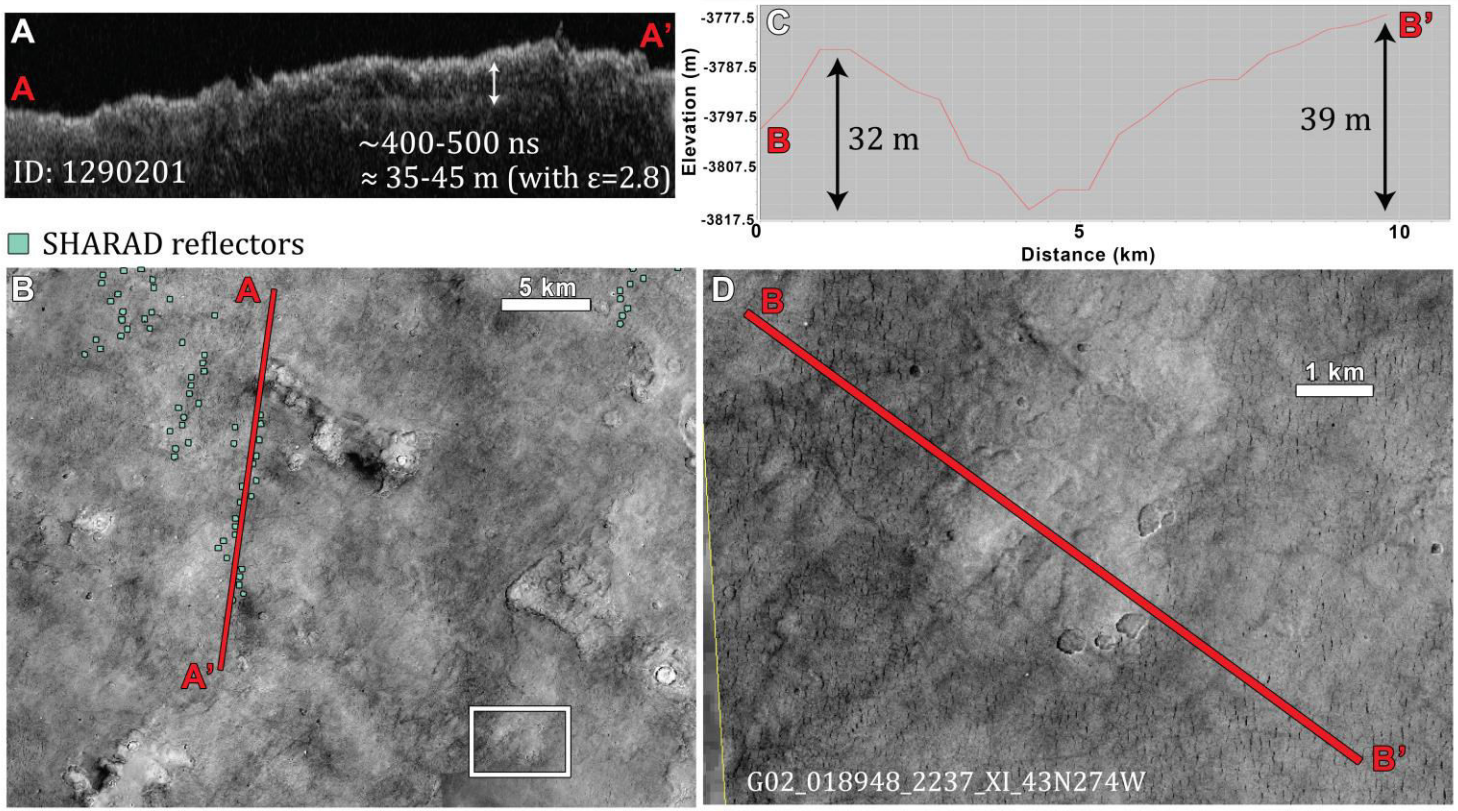

Figure 3.22. SHARAD-derived thicknesses of the SDBT. **(A)** SHARAD radargram covering A–A' as marked in B. The delay time is consistent with a reflector depth of ~35–45 m. Stuurman et al. [2014] found that the reflector depths correspond to the contact between the SDBT and the underlying light-toned, cratered unit (pictured in Figure 3.21). **(B)** CTX context view showing the location of D (white box). Subframe of CTX G02_018948_2237. **(C)** MOLA profile covering B–B' as marked in D. This area spans two areas of dark-toned, polygonally-fractured SDBT separated by a lighter toned portion which we interpret to be a thin mantle of SDBT atop the underlying light-toned cratered unit. The heights of the dark-toned scarps are consistent with SHARAD reflector depths measured ~10 km to the northwest, supporting the interpretation that the SDBT is very thin in the lighter-toned portion of the B–B' transect. **(D)** Subframe of CTX G02_018948_2237.

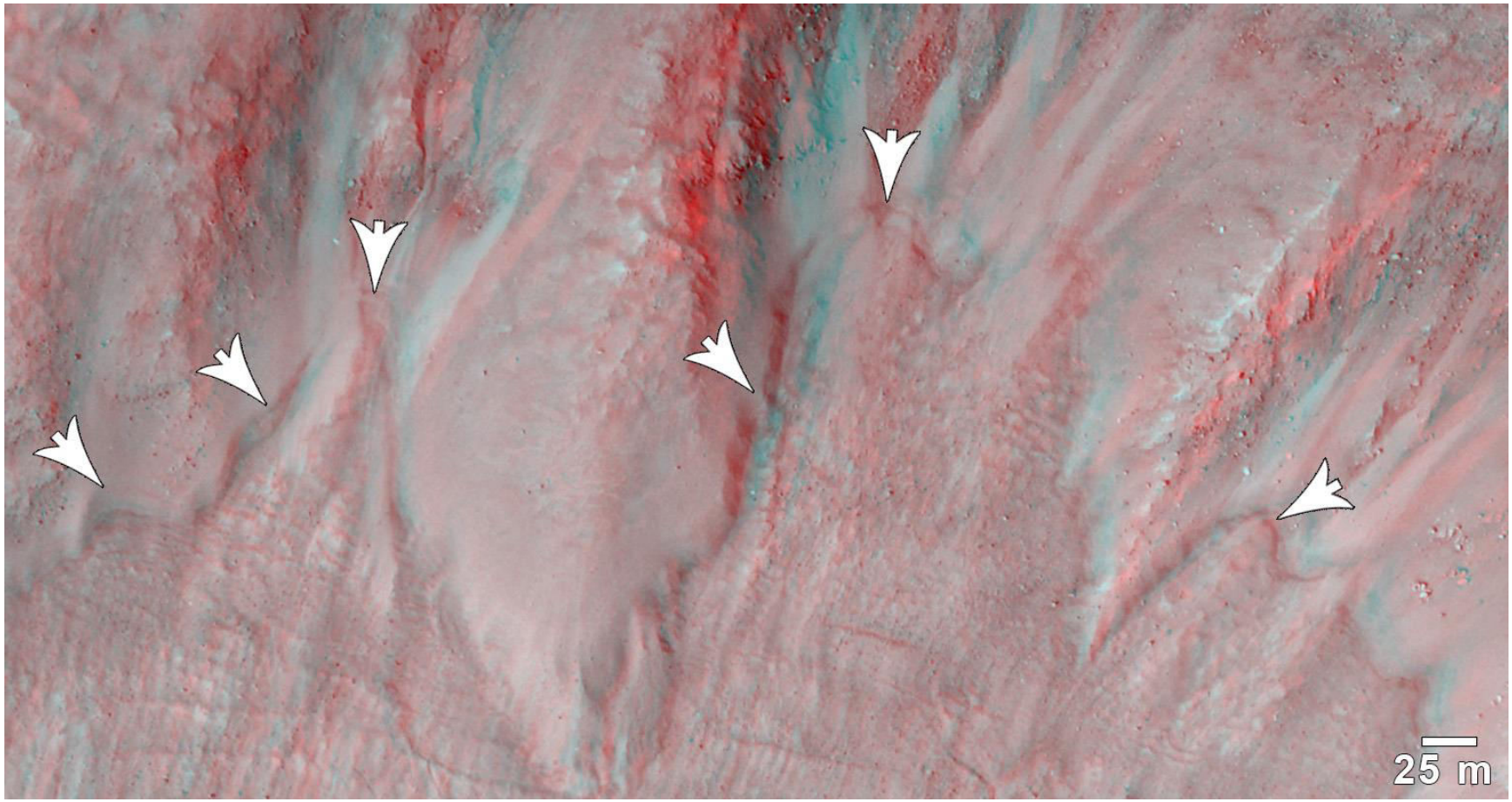

Figure 3.23. HiRISE anaglyph of small scarps (marked with white arrows) suggestive of retreat of the SDBT down a crater wall. North is up. Subframe of anaglyph from ESP_037646_2290 and ESP_028719_2290.

3.5. Late Amazonian History of Western Utopia Planitia

Based on our observations, we propose the following scenario for the history of western Utopia (Figure 3.24):

1. Ice is redistributed from the poles to the mid-latitudes during periods of high mean obliquity (>35°), resulting in the formation of large regional ice sheets at ~10–100 Ma.
2. As obliquity decreases, ice becomes unstable in the mid-latitudes, with ice being redistributed back to the polar regions. The mid-latitude ice sheets retreat, with remnants preserved in topographically protected areas such as crater interiors (i.e., CCF).
3. Ice instability in the mid-latitudes increases with decreasing obliquity, leading to cold desert ("interglacial") conditions [*Head et al.*, 2003] and the retreat of CCF/mid-latitude crater fill as ice within it sublimates. This leaves behind characteristic morphological markers as described by Shean [2010b]: longitudinal ridges and characteristic surface textures continuous across topographic protrusions in the fill; fill-facing scarps, extensional features, and ridges near the fill margins; "bathtub-ring" circumferential ridges on protrusions within the fill and on crater walls; and extensional fractures/faults that crosscut gully fans superposed atop the fill.
4. Obliquity increases yet again, but only to a maximum of ~35° as Mars transitions into a period of lower mean obliquity (25°). Atmospheric conditions during this period were such that several centimetres of ice could have accumulated poleward of ~30° each winter [*Madeleine et al.*, 2009]. Dust storm activity peaking in summer deposits a semi-protective layer of dust atop the ice. Jet streams moving across Arabia Terra predicted by the models of Madeleine et al. [2009] lead to deposition of dust and ice—or possibly volcanic ash [*Soare et al.*, 2015]—in Utopia in particular [i.e., *Kerrigan*, 2013] which has the highest average ice cloud content in the northern hemisphere at ~35° obliquity under conditions of high atmospheric

opacity. Some of this dust and ice deposition results in the formation of pasted-on crater wall deposits. During spring/summer under favourable conditions, melting of ice within the pasted-on deposits leads to episodes of gully formation.

5. As obliquity decreases, the jet stream moving across Arabia Terra weakens, leading to a reduction in ice and dust deposition in Utopia over time [*Kerrigan*, 2013]. Conditions conducive to melting become more temporally restricted, leading to a reduction in gully activity, and in some cases complete burial by subsequent deposition of the dust- and ice-rich material comprising the SDBT (in which scallops have not yet formed at this stage). Sublimation begins to occur again, resulting in continued retreat of CCF/mid-latitude crater fill.
6. When obliquity drops below 30°, sublimation processes become dominant as ice becomes even more unstable in the mid-latitudes. This results in the formation of periglacial features within the dust- and ice-rich material comprising the SDBT (polygonal fracturing and scalloped depressions). Sublimation also results in the continued retreat of CCF/mid-latitude crater fill material. Under favourable conditions, enough melting within the pasted-on deposits may occur for gully activity to continue, but in a very limited capacity.
7. At present-day obliquity (~25°), deposition of dust and ice effectively ceases in Utopia. Sublimation of ice from within the SDBT and CCF may slow due to protection from an increasingly thick desiccated dust layer. However, the desiccated dust—no longer cemented by ice—can now be transported by wind. This may explain the dark tone of portions of the SDBT in western Utopia relative to the surrounding and underlying terrain. Dust transport and removal would result in exposing deeper ice within the SDBT to sublimation, leading to continued erosion of the SDBT. In extremely limited cases, gully

activity possibly continues into the present day in the region [*Dundas et al.*, 2015].

3.6. Conclusions

The geologic history of western Utopia Planitia in the Late Amazonian is a dynamic one, intimately linked to glacial and periglacial processes controlled by changes in obliquity. CCF deposits represent the period of peak mid-latitude glaciation, temporally separated from the emplacement of the SDBT by a period of periglacial, cold desert conditions. These deposits appear to be geologically youthful and/or rapidly degrading based on the relative lack of superposed craters and sharp scarp morphology within the SDBT. Thus far no evidence for present-day scarp retreat within the SDBT has been documented; long-term monitoring, via repeated high-resolution imaging, is needed to determine whether or not the scarps are actively degrading. Gully formation and activity has occurred repeatedly across a range of obliquity and climate conditions in western Utopia, after the cessation of glacial conditions. The stratigraphic and crosscutting relationships between gullies and the SDBT clearly show that gully formation and activity coincided with the formation and growth of scalloped depressions, as well as the retreat of CCF. The observation of inverted gullies within pasted-on deposits on crater walls, combined with observations of inverted gullies in the southern hemisphere by Dickson et al. [2015], supports the hypothesis of Christensen [2003] that gully formation is linked to melting of ice within the pasted-on material. Gully activity persists in an extremely limited capacity in Utopia today, documented thus far in only a single gully, although this appears to be controlled by frost-related processes [*Dundas et al.*, 2015] and may not be the same process as that by which gullies originally formed.

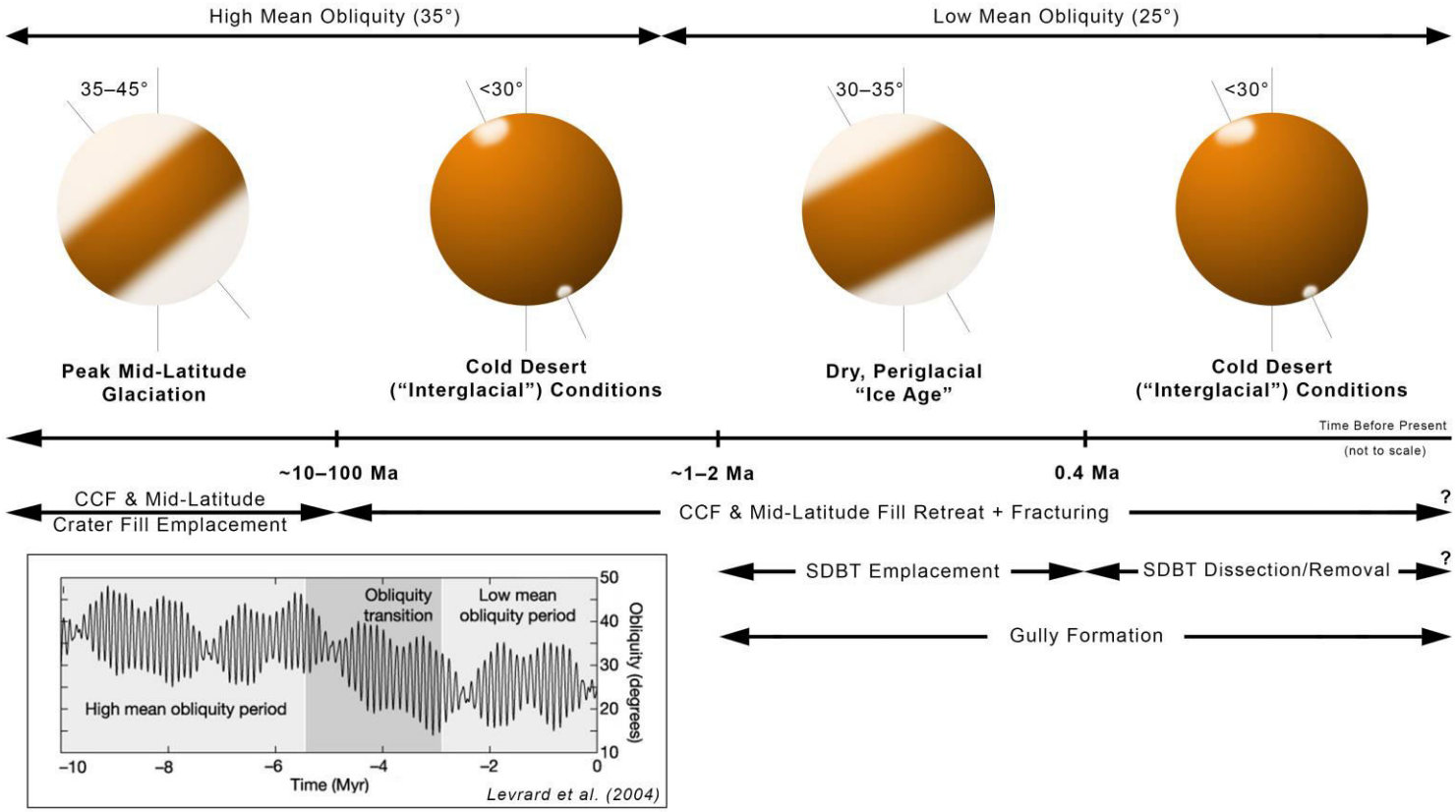

Figure 3.24. The Late Amazonian history of Utopia Planitia. Inset: Martian obliquity shifts over the past 10 Ma from Laskar et al. [2004].

References

Balme, M., N. Mangold, D. Baratoux, F. Costard, M. Gosselin, P. Masson, P. Pinet, and G. Neukum (2006), Orientation and distribution of recent gullies in the southern hemisphere of Mars: Observations from High Resolution Stereo Camera/Mars Express (HRSC/MEX) and Mars Orbiter Camera/Mars Global Surveyor (MOC/MGS) data, *J. Geophys. Res.*, *111*(E5), E05001, doi:10.1029/2005JE002607.

Bramson, A. M., S. Byrne, N. E. Putzig, S. Sutton, J. J. Plaut, T. C. Brothers, and J. W. Holt (2015), Widespread excess ice in Arcadia Planitia, Mars, *Geophys. Res. Lett.*, *42*(16), 6566–6574, doi:10.1002/2015GL064844.

Byrne, S. et al. (2009), Distribution of mid-latitude ground ice on Mars from new impact craters, *Science*, *325*(5948), 1674–1676.

Cantor, B. A. (2007), MOC observations of the 2001 Mars planet-encircling dust storm, *Icarus*, *186*(1), 60–96, doi:10.1016/j.icarus.2006.08.019.

Capitan, R. D., G. R. Osinski, M. J. Van De Wiel, M. Kerrigan, N. Barry, and S. Blain (2012), Mapping Utopia Planitia: Morphometric and Geomorphologic Mapping at a Regional Scale, *43rd Lunar and Planetary Science Conference*, abstract #2237.

Christensen, P. R. (2003), Formation of recent martian gullies through melting of extensive water-rich snow deposits, *Nature*, *422*(6927), 45–48, doi:10.1038/nature01436.

Christensen, P. R., E. Engle, S. Anwar, S. Dickenshied, D. Noss, N. Gorelick, and M. Weiss-Malik (2009), JMARS – A Planetary GIS, in *American Geophysical Union, Fall Meeting 2009*, p. abstract IN22A–06.

Costard, F., and J. S. Kargel (1995), Outwash Plains and Thermokarst on Mars, *Icarus*, *114*, 93–112, doi:10.1006/icar.1995.1046.

Costard, F., F. Forget, N. Mangold, and J. P. Peulvast (2002), Formation of recent martian debris flows by melting of near-surface ground ice at high obliquity, *Science*, *295*(5552), 110–113, doi:10.1126/science.1066698.

Dickson, J. L., J. W. Head, and C. I. Fassett (2012), Patterns of accumulation and flow of ice in the mid-latitudes of Mars during the Amazonian, *Icarus*, *219*(2), 723–732, doi:10.1016/j.icarus.2012.03.010.

Dickson, J. L., J. W. Head, T. A. Goudge, and L. Barbieri (2015), Recent climate cycles

on Mars: Stratigraphic relationships between multiple generations of gullies and the latitude dependent mantle, *Icarus*, *252*, 83–94, doi:10.1016/j.icarus.2014.12.035.

Diniega, S., S. Byrne, N. T. Bridges, C. M. Dundas, and A. S. McEwen (2010), Seasonality of present-day Martian dune-gully activity, *Geology*, *38*(11), 1047–1050, doi:10.1130/G31287.1.

Dundas, C. M., M. T. Mellon, A. S. McEwen, A. Lefort, L. P. Keszthelyi, and N. Thomas (2008), HiRISE observations of fractured mounds: Possible Martian pingos, *Geophys. Res. Lett.*, *35*(4), 1–5, doi:10.1029/2007GL031798.

Dundas, C. M., A. S. McEwen, S. Diniega, S. Byrne, and S. Martinez-Alonso (2010), New and recent gully activity on Mars as seen by HiRISE, *Geophys. Res. Lett.*, *37*(7), L07202, doi:10.1029/2009GL041351.

Dundas, C. M., S. Diniega, C. J. Hansen, S. Byrne, and A. S. McEwen (2012), Seasonal activity and morphological changes in martian gullies, *Icarus*, *220*(1), 124–143, doi:10.1016/j.icarus.2012.04.005.

Dundas, C. M., S. Diniega, and A. S. McEwen (2015), Long-term monitoring of martian gully formation and evolution with MRO/HiRISE, *Icarus*, *251*, 244–263, doi:10.1016/j.icarus.2014.05.013.

French, H. M. (2007), *The Periglacial Environment*, 3rd ed., John Wiley and Sons, Hoboken.

Gaidos, E. (2001), Cryovolcanism and the recent flow of liquid water on Mars, *Icarus*, *153*(1), 218–223, doi:10.1006/icar.2001.6649.

Gilmore, M. S., and E. L. Phillips (2002), Role of aquicludes in formation of Martian gullies, *Geology*, *30*(12), 1107, doi:10.1130/0091-7613(2002)030<1107:ROAIFO>2.0.CO;2.

Harrison, T. N., M. C. Malin, and K. S. Edgett (2009), Present-day gully activity observed by the Mars Reconnaissance Orbiter (MRO) Context Camera (CTX), in *Bulletin of the American Astronomical Society, DPS Meeting #41*, p. 1113.

Harrison, T. N., G. R. Osinski, L. L. Tornabene, and D. K. Zylik (2014), Classification and mapping of mid-latitude post-impact crater fill morphologies on Mars, *Geological Society of America Annual Meeting*, abstract 247055.

Harrison, T. N., G. R. Osinski, L. L. Tornabene, and D. K. Zylik (2015a), Classifying

martian mid-latitude post-impact crater fill morphologies and their preservation states: Insights into climate history on Mars, *46th Lunar and Planetary Science Conference*, abstract 1625.

Harrison, T. N., G. R. Osinski, and L. L. Tornabene (2015b), Global Documentation of Gullies With the Mars Reconnaissance Orbiter Context Camera (CTX) and Implications for Their Formation, *Icarus*, *252*, 236–254, doi:http://dx.doi.org/10.1016/j.icarus.2015.01.022.

Head, J. W., J. F. Mustard, M. a Kreslavsky, R. E. Milliken, and D. R. Marchant (2003), Recent ice ages on Mars, *Nature*, *426*(6968), 797–802, doi:10.1038/nature02114.

Hecht, M. (2002), Metastability of liquid water on Mars, *Icarus*, *156*(2), 373–386, doi:10.1006/icar.2001.6794.

Heldmann, J. L., and M. T. Mellon (2004), Observations of martian gullies and constraints on potential formation mechanisms, *Icarus*, *168*(2), 285–304, doi:10.1016/j.icarus.2003.11.024.

Heldmann, J. L., E. Carlsson, H. Johansson, M. T. Mellon, and O. B. Toon (2007), Observations of martian gullies and constraints on potential formation mechanisms II. The northern hemisphere, *Icarus*, *188*(2), 324–344, doi:10.1016/j.icarus.2006.12.010.

Holt, J. W., M. E. Peters, S. D. Kempf, D. L. Morse, and D. D. Blankenship (2006), Echo source discrimination in single-pass airborne radar sounding data from the Dry Valleys, Antarctica: Implications for orbital sounding of Mars, *J. Geophys. Res. E Planets*, *111*(6), doi:10.1029/2005JE002525.

Holt, J. W. et al. (2008), Radar Sounding Evidence for Buried Glaciers in the Southern Mid-Latitudes of Mars, *Science*, *322*, 1235–1238.

Hugenholtz, C. H. (2008), Frosted granular flow: A new hypothesis for mass wasting in martian gullies, *Icarus*, *197*, 65–72, doi:10.1016/j.icarus.2008.04.010.

Kerrigan, M. C. (2013), The periglacial landscape of Utopia Planitia; Geologic evidence for recent climate change on Mars, University of Western Ontario.

Kerrigan, M. C., G. R. Osinski, R. D. Capitan, N. Barry, S. Blain, and M. J. Van De Wiel (2012), The distribution and stratigraphy of periglacial landforms in western Utopia Planitia, Mars, *43rd Lunar and Planetary Science Conference*, 2716.

Kneissl, T., D. Reiss, S. van Gasselt, and G. Neukum (2010), Distribution and orientation of northern-hemisphere gullies on Mars from the evaluation of HRSC and MOC-NA data, *Earth Planet. Sci. Lett.*, *294*(3-4), 357–367, doi:10.1016/j.epsl.2009.05.018.

Kossacki, K. J., and W. J. Markiewicz (2004), Seasonal melting of surface water ice condensing in martian gullies, *Icarus*, *171*(2), 272–283, doi:10.1016/j.icarus.2004.05.018.

Kreslavsky, M. A., and J. W. Head (2000), Kilometer-scale roughness of Mars: Results from MOLA data analysis, *J. Geophys. Res.*, *105*(E11), 26695–26711.

Kreslavsky, M. A., and J. W. Head (2002), Mars : Nature and evolution of young latitude-dependent water-ice-rich mantle, *Geophys. Res. Lett.*, *29*(15), 1719, doi:10.1029/2002GL015392.

Laskar, J., A. C. M. Correia, M. Gastineau, F. Joutel, B. Levrard, and P. Robutel (2004), Long term evolution and chaotic diffusion of the insolation quantities of Mars, *Icarus*, *170*(2), 343–364, doi:10.1016/j.icarus.2004.04.005.

Lefort, A., P. S. Russell, N. Thomas, A. S. McEwen, C. M. Dundas, and R. L. Kirk (2009), Observations of periglacial landforms in Utopia Planitia with the High Resolution Imaging Science Experiment (HiRISE), *J. Geophys. Res. E Planets*, *114*(4), 1–18, doi:10.1029/2008JE003264.

Lefort, A., P. S. Russell, and N. Thomas (2010), Scalloped terrains in the Peneus and Amphitrites Paterae region of Mars as observed by HiRISE, *Icarus*, *205*(1), 259–268, doi:10.1016/j.icarus.2009.06.005.

Levrard, B., F. Forget, F. Montmessin, and J. Laskar (2004), Recent ice-rich deposits formed at high latitudes on Mars by sublimation of unstable equatorial ice during low obliquity, *Nature*, *431*, 1072–1075, doi:10.1038/nature03006.1.

Levy, J., J. Head, and D. Marchant (2009a), Thermal contraction crack polygons on Mars: Classification, distribution, and climate implications from HiRISE observations, *J. Geophys. Res.*, *114*, E01007, doi:10.1029/2008JE003273.

Levy, J., J. W. Head, and D. R. Marchant (2010a), Concentric crater fill in the northern mid-latitudes of Mars: Formation processes and relationships to similar landforms of glacial origin, *Icarus*, *209*, 390–404, doi:10.1016/j.icarus.2010.03.036.

Levy, J. S., J. W. Head, and D. R. Marchant (2009b), Concentric crater fill in Utopia

Planitia: History and interaction between glacial “brain terrain” and periglacial mantle processes, *Icarus*, *202*(2), 462–476, doi:10.1016/j.icarus.2009.02.018.

Levy, J. S., J. W. Head, J. L. Dickson, C. I. Fassett, G. A. Morgan, and S. C. Schon (2010b), Identification of gully debris flow deposits in Protonilus Mensae, Mars: Characterization of a water-bearing, energetic gully-forming process, *Earth Planet. Sci. Lett.*, *294*, 368–377, doi:10.1016/j.epsl.2009.08.002.

Levy, J. S., C. I. Fassett, J. W. Head, C. Schwartz, and J. L. Watters (2014), Sequestered glacial ice contribution to the global Martian water budget: Geometric constraints on the volume of remnant, midlatitude debris-covered glaciers, *J. Geophys. Res. Planets*, *119*(10), 2188–2196, doi:10.1002/2014JE004685.

Madeleine, J.-B., F. Forget, J. W. Head, B. Levrard, F. Montmessin, and E. Millour (2009), Amazonian northern mid-latitude glaciation on Mars: A proposed climate scenario, *Icarus*, *203*(2), 390–405, doi:10.1016/j.icarus.2009.04.037.

Malin, M. C., and K. S. Edgett (2000), Evidence for recent groundwater seepage and surface runoff on Mars, *Science*, *288*(5475), 2330–2335, doi:10.1126/science.288.5475.2330.

Malin, M. C., K. S. Edgett, L. V Posiolova, S. M. Mccolley, and E. Z. N. Dobrea (2006), Present-day impact cratering rate and contemporary gully activity on Mars, *Science*, *314*(5805), 1573–1577.

Malin, M. C. et al. (2007), Context Camera Investigation on board the Mars Reconnaissance Orbiter, *J. Geophys. Res.*, *112*(E5), E05S04, doi:10.1029/2006JE002808.

Marchant, D. R., A. R. Lewis, W. M. Phillips, E. J. Moore, R. A. Souchez, G. H. Denton, D. E. Sugden, N. Potter, and G. P. Landis (2002), Formation of patterned ground and sublimation till over Miocene glacier ice Formation of patterned ground and sublimation till over Miocene glacier ice in Beacon Valley , southern Victoria Land , Antarctica, *Geol. Soc. Am. Bull.*, *114*(6), 718–790, doi:10.1130/0016-7606(2002)114<0718.

McGill, G. E. (1989), Buried topography of Utopia, Mars: Persistence of a giant impact depression, *J. Geophys. Res.*, *94*(B3), 2753–2759, doi:10.1029/JB094iB03p02753.

Mellon, M. T., and B. M. Jakosky (1993), Geographic variations in the thermal and

diffusive stability of ground ice on Mars, *J. Geophys. Res.*, *98*(E2), 3345, doi:10.1029/92JE02355.

Milliken, R. E., and J. F. Mustard (2003), Erosional morphologies and characteristics of latitude-dependent surface mantles on Mars, *Sixth Int. Conf. Mars, Pasadena, Calif.*, 3240.

Milliken, R. E., J. F. Mustard, and D. L. Goldsby (2003), Viscous flow features on the surface of Mars: Observations from high-resolution Mars Orbiter Camera (MOC) images, *J. Geophys. Res.*, *108*(E6), 5057, doi:10.1029/2002JE002005.

Morgenstern, A., E. Hauber, D. Reiss, S. van Gasselt, G. Grosse, and L. Schirrmeister (2007), Deposition and degradation of a volatile-rich layer in Utopia Planitia and implications for climate history on Mars, *J. Geophys. Res. E Planets*, *112*(6), 1–11, doi:10.1029/2006JE002869.

Mustard, J. F., C. D. Cooper, and M. K. Rifkin (2001), Evidence for recent climate change on Mars from the identification of youthful near-surface ground ice, *Nature*, *412*, 411–414, doi:10.1038/35086515.

Osinski, G., R. Capitan, M. Kerrigan, N. Barry, and S. Blain (2012), Late Amazonian Glaciations in Utopia Planitia, Mars, *Lunar Planet. Sci. Conf.*, *43*, abstract #1957, doi:10.1029/2006je002852.

Pearce, G., G. R. Osinski, and R. J. Soare (2011), Intra-crater glacial processes in central Utopia Planitia, Mars, *Icarus*, *212*(1), 86–95, doi:10.1016/j.icarus.2010.12.001.

Pedersen, G. B. M., and J. W. Head (2010), Evidence of widespread degraded Amazonian-aged ice-rich deposits in the transition between Elysium Rise and Utopia Planitia, Mars: Guidelines for the recognition of degraded ice-rich materials, *Planet. Space Sci.*, *58*(14-15), 1953–1970, doi:10.1016/j.pss.2010.09.019.

Plaut, J. J., A. Safaeinili, J. W. Holt, R. J. Phillips, J. W. Head, R. Seu, N. E. Putzig, and A. Frigeri (2009), Radar evidence for ice in lobate debris aprons in the mid-northern latitudes of Mars, *Geophys. Res. Lett.*, *36*(2), L02203, doi:10.1029/2008GL036379.

Raack, J., D. Reiss, T. Appéré, M. Vincendon, O. Ruesch, and H. Hiesinger (2015), Present-day seasonal gully activity in a south polar pit (Sisyphi Cavi) on Mars, *Icarus*, *251*, 226–243, doi:10.1016/j.icarus.2014.03.040.

Reiss, D., S. van Gasselt, G. Neukum, and R. Jaumann (2004), Absolute dune ages and

implications for the time of formation of gullies in Nirgal Vallis, Mars, *J. Geophys. Res. E Planets*, *109*(6), 1–9, doi:10.1029/2004JE002251.

Schon, S. C., J. W. Head, and R. E. Milliken (2009a), A recent ice age on Mars: Evidence for climate oscillations from regional layering in mid-latitude mantling deposits, *Geophys. Res. Lett.*, *36*(15), L15202, doi:10.1029/2009GL038554.

Schon, S. C., J. W. Head, and C. I. Fassett (2009b), Unique chronostratigraphic marker in depositional fan stratigraphy on Mars: Evidence for ca. 1.25 Ma gully activity and surficial meltwater origin, *Geology*, *37*(3), 207–210, doi:10.1130/G25398A.1.

Seibert, N. M., and J. S. Kargel (2001), Small scale martain polygonal terrain: Implications for liquid surface water, *Geophys. Res. Lett.*, *28*(5), 899–902.

Séjourné, A., F. Costard, J. Gargani, R. J. Soare, A. Fedorov, and C. Marmo (2011), Scalloped depressions and small-sized polygons in western Utopia Planitia, Mars: A new formation hypothesis, *Planet. Space Sci.*, *59*(5-6), 412–422, doi:10.1016/j.pss.2011.01.007.

Seu, R. et al. (2007), SHARAD sounding radar on the Mars Reconnaissance Orbiter, *J. Geophys. Res. E Planets*, *112*(5), 1–18, doi:10.1029/2006JE002745.

Shean, D. E. (2010a), Candidate ice-rich material within equatorial craters on Mars, *Geophys. Res. Lett.*, *37*(24), L24202, doi:10.1029/2010GL045181.

Shean, D. E. (2010b), Evidence for widespread removal of martian mid-latitude “fill” material, *41st Lunar and Planetary Science Conference*, abstract 1509.

Shinbrot, T., N.-H. Duong, L. Kwan, and M. M. Alvarez (2004), Dry granular flows can generate surface features resembling those seen in Martian gullies., *Proc. Natl. Acad. Sci. U. S. A.*, *101*(23), 8542–8546, doi:10.1073/pnas.0308251101.

Soare, R., J. Kargel, G. Osinski, and F. Costard (2007), Thermokarst processes and the origin of crater-rim gullies in Utopia and western Elysium Planitia, *Icarus*, *191*(1), 95–112, doi:10.1016/j.icarus.2007.04.018.

Soare, R. J., D. M. Burr, and J. M. Wan Bun Tseung (2005), Possible pingos and a periglacial landscape in northwest Utopia Planitia, *Icarus*, *174*, 373–382, doi:10.1016/j.icarus.2004.11.013.

Soare, R. J., G. R. Osinski, and C. L. Roehm (2008), Thermokarst lakes and ponds on Mars in the very recent (late Amazonian) past, *Earth Planet. Sci. Lett.*, *272*(1-2),

382–393, doi:10.1016/j.epsl.2008.05.010.

Soare, R. J., G. D. Pearce, and A. Séjourné (2010), "Wet" periglacial processes, ground ice and a revision of the near-surface stratigraphy in Utopia Planitia, Mars, *41st Lunar and Planetary Science Conference*, p. abstract 1506.

Soare, R. J., F. Costard, G. D. Pearce, and a. Séjourné (2012), A re-interpretation of the recent stratigraphical history of Utopia Planitia, Mars: Implications for late-Amazonian periglacial and ice-rich terrain, *Planet. Space Sci.*, *60*(1), 131–139, doi:10.1016/j.pss.2011.07.007.

Soare, R. J., S. J. Conway, G. D. Pearce, J. M. Dohm, and P. M. Grindrod (2013), Possible crater-based pingos, paleolakes and periglacial landscapes at the high latitudes of Utopia Planitia, Mars, *Icarus*, *225*(2), 971–981, doi:10.1016/j.icarus.2012.08.041.

Soare, R. J., B. Horgan, S. J. Conway, C. Souness, and M. R. El-Maarry (2015), Volcanic terrain and the possible periglacial formation of "excess ice" at the mid-latitudes of Utopia Planitia, Mars, *Earth Planet. Sci. Lett.*, *423*, 182–192, doi:10.1016/j.epsl.2015.04.033.

Soare, R. J., S. J. Conway, C. J. Gallagher, and J. M. Dohm (2016), "Ice-rich" (periglacial) and "icy" (glacial) depressions in the Argyre region, Mars, *47th Lunar and Planetary Science Conference*, abstract 1175.

Squyres, S. W. (1979), The distribution of lobate debris aprons and similar flows on Mars, *J. Geophys. Res.*, *84*(B14), 8087–8096, doi:10.1029/JB084iB14p08087.

Squyres, S. W., and M. H. Carr (1986), Geomorphic evidence for the distribution of ground ice on Mars, *Science*, *231*, 249–252.

Stuurman, C. M., G. R. Osinski, T. C. Brothers, J. W. Holt, and M. Kerrigan (2014), SHARAD reflectors in Utopia Planitia, Mars consistent with widespread, thick subsurface ice, *45th Lunar and Planetary Science Conference*, abstract 2262.

Thomson, B. J., and J. W. I. Head (2001), Utopia Basin, Mars: Characterization of topography and morphology and assessment of the origin and evolution of basin internal structure, *J. Geophys. Res.*, *106*(E10), 23209–23230, doi:10.1029/2000JE001355.

Treiman, A. H. (2003), Geologic settings of Martian gullies: Implications for their

origins, *J. Geophys. Res.*, *108*(E4), 8031, doi:10.1029/2002JE001900.

Ulrich, M., A. Morgenstern, F. Günther, D. Reiss, K. E. Bauch, E. Hauber, S. Rössler, and L. Schirrmeister (2010), Thermokarst in Siberian ice-rich permafrost: Comparison to asymmetric scalloped depressions on Mars, *J. Geophys. Res. E Planets*, *115*(10), 1–22, doi:10.1029/2010JE003640.

Williams, K., O. Toon, J. Heldmann, C. Mckay, and M. Mellon (2008), Stability of mid-latitude snowpacks on Mars, *Icarus*, *196*(2), 565–577, doi:10.1016/j.icarus.2008.03.017.

Zanetti, M., H. Hiesinger, D. Reiss, E. Hauber, and G. Neukum (2010), Distribution and evolution of scalloped terrain in the southern hemisphere, Mars, *Icarus*, *206*, 691–706, doi:10.1016/j.icarus.2009.09.010.

Chapter 4: Thermal inertia variations in Gasa Crater, Mars, driven by gully and mass wasting activity

*Tanya N. Harrison, Livio L. Tornabene, Gordon R. Osinski, and Susan Con*way

4.1 Introduction

Gullies on Mars are incised channel features with source alcoves and depositional fans found on slopes in the middle and high latitudes [*Malin and Edgett*, 2000]. Their morphology is highly suggestive of liquid water having been involved in their initial formation. This includes features such as banked, sinuous, and terraced channels, superelevation of gully deposits, and terminal deposits travelling across slopes much lower than the angle of repose for dry material [e.g., *Malin and Edgett*, 2000; *Heldmann and Mellon*, 2004; *Malin et al.*, 2006; *McEwen et al.*, 2007], although dry and frost-related processes have also been proposed [e.g., *Treiman*, 2003; *Hugenholtz*, 2008; *Cedillo-Flores et al.*, 2011; *Dundas et al.*, 2012, 2015]. They also appear to be geologically youthful, typically lacking craters and superposing recent aeolian features such as transverse aeolian ridges [e.g., *Malin and Edgett*, 2000]. The unexpected observation of new light-toned flows in two pre-existing gully channels with the Mars Global Surveyor (MGS) narrow angle Mars Orbiter Camera (MOC NA) [*Malin et al.*, 2006] led to monitoring efforts to look for gully activity in an attempt to constrain how gullies on Mars may have formed, and how they are evolving today.

Carrying on the monitoring efforts of MOC NA, the Mars Reconnaissance Orbiter (MRO) Context Camera (CTX) [*Malin et al.*, 2007] routinely monitors 617 locations across both hemispheres at a pixel scale of 6 m for present-day gully activity [*Harrison et al.*, 2009]. The High-Resolution Imaging Science Experiment (HiRISE) aboard MRO [*McEwen et al.*, 2007] monitors approximately 500 of these locations at a pixel scale of ~0.25–1 m [*Dundas et al.*, 2016]. Thus far, present-day activity ranging from the movement of boulders [*Dundas et al.*, 2015] to the deposition of material on aprons and incision of new small channel segments [e.g., *Malin et al.*, 2006; *Harrison et al.*, 2009; *Dundas et al.*, 2010] has been observed in 38 separate locations over the past decade. Of

these, Gasa Crater has been the most active site observed on Mars to date, making it of particular interest for studying the process(es) behind gully formation and activity. In this study, we investigate whether differences in thermal inertia across different segments of gully systems, combined with morphological and colour observations with HiRISE, can provide some constraints of the physical characteristics associated with recent activity within gullies in Gasa Crater. We also investigate thermophysical differences between slopes in Gasa dominated by gully activity compared to those predominantly modified by dry mass wasting processes. As thermal inertia can be used as a proxy for grain size and/or induration [e.g., *Fergason et al.*, 2006], utilizing this dataset can help us to better understand the mass movement processes occurring on the slopes within Gasa.

Gasa is a ~7 km-diameter impact crater centred at 35.7°S, 129.4°E (Figure 4.1). It lies within the floor the crater Cilaos, an older ~19 km-diameter impact crater. Morphologically, Gasa appears both youthful and well preserved [e.g., *Tornabene et al.*, 2006, 2012]. Crater counts on the continuous ejecta blanket of Gasa yield a crater retention age of 0.6–2.4 Ma, with a best-fit age of 1.25 Ma, coinciding with Mars' last glacial maximum [*Schon et al.*, 2009]. Unmodified Gasa secondary craters and a lack of evidence for pasted-on deposits on the pole-facing wall of Gasa suggest that Gasa formed after the last major episode of latitude-dependent mantle emplacement in the southern mid-latitudes [*Schon et al.*, 2009; *Schon and Head*, 2012]. This supports the interpretation that Gasa is geologically youthful.

4.2. Methods

Thermal inertia is defined as:

$$I = (k\rho c)^{1/2}$$

where k is the thermal conductivity, ρ is the bulk density of the surface material, and c is the specific heat capacity. Units are in J m^{-2} K^{-1} $s^{-1/2}$, herein shortened to "thermal inertia units" (TIU). On Mars, thermal inertia is most strongly controlled by the bulk thermal conductivity of a material, varying by 3–4 orders of magnitude, while specific heat capacity and density only vary by a factor of ~3 for rocks and soils [e.g., *Wechsler*

and Glaser, 1965; *Neugebauer et al.*, 1971; *Wechsler et al.*, 1972; *Presley and Christensen*, 1997b]. As such, thermal inertia is strongly controlled by the particle size of a material, with bulk conductivity varying as a function of the solid, radiative, and gas conductivity. Solid and gas conductivity play the largest role under martian conditions [*Wechsler et al.*, 1972], predominantly controlled by the relationship between the particle size and the pore size relative to the mean-free path of a gas (~5 μm at martian surface pressures). When grain sizes are small enough that the pore size is about the same or smaller than the mean free gas path, heat transfer becomes inefficient due to a lower frequency of collisions between gas molecules and grains in the material. Thermal conductivity of fine-grained materials is also lowered due to the higher number of grain-to-grain contacts per unit length [*Jakosky*, 1986; *Presley and Christensen*, 1997a]. For larger grains, thermal inertia is controlled by the size of a particle relative to the diurnal thermal skin depth (~1 cm for sand and ~10 cm for rock) [e.g., *Hardgrove et al.*, 2009]. This results in fine-grained, unconsolidated materials exhibiting lower thermal inertia values than coarse-grained and/or well-indurated (cemented) materials [e.g., *Fergason et al.*, 2006 and references therein].

Thermal inertia (TI) values at 100 m per pixel were determined using Thermal Emission Imaging System (THEMIS) night-time IR data [*Christensen et al.*, 2004] with an overall accuracy of ~20%, precision of 10–15%, and relative consistency with MGS Thermal Emission Spectrometer (TES) and the Mars Exploration Rovers mini-TES thermal inertia values [*Fergason et al.*, 2006]. We analysed the 32-bit 100 m/pixel THEMIS thermal inertia images [*Fergason et al.*, 2006; *Christensen et al.*, 2013] using the map sampling function in the Java Mission-planning and Analysis for Remote Sensing (JMARS) software package [*Christensen et al.*, 2009]. Gasa Crater was chosen both based on the size of its gully aprons, and because it is one of the few sites on Mars where present-day gully activity has been observed in multiple locations within the same crater over several Mars years [*Dundas et al.*, 2010, 2015]. Gully fan segments were mapped morphologically using HiRISE images, with the HiRISE and THEMIS TI

datasets each manually georeferenced to the THEMIS daytime IR 100 m global map (version 12) in JMARS. Additional map creation was completed using ArcMap 10.2.

Due to differences in calibration between images and slope effects on absolute THEMIS thermal inertia values [*Fergason et al.*, 2006], we focus this work on the relative differences in thermal inertia between individual gully aprons and lobes within aprons using a single THEMIS TI strips covering Gasa Crater (image ID I09926012, quality rating 5, acquired on 10 March 2004 at L_s 2.48°—near the start of southern autumn when frost is not an issue at these latitudes). Only images with a quality rating of 5 or higher (7 being the highest possible rating), assigned by the THEMIS team, were considered for use. Polygons were drawn covering portions of gully aprons, distinguishing between the youngest (stratigraphically topmost) apron deposits and the underlying older apron deposits (Figure 4.2). These polygons were drawn to intentionally subsample the apron deposits due to the difference in resolution between THEMIS TI and HiRISE in order to minimize sampling from surrounding pixels covering other portion of the apron. Using the map sampling feature in JMARS, the maximum, minimum, average, and standard deviation for the thermal inertia values within each polygon were extracted. This map sampling function works such that if a pixel is more than 50% contained within the sampling polygon, its value is included in calculations; otherwise, the pixel is not counted [*Scott Dickenshied, personal communication*[1]].

[1] Scott Dickenshied a Scientific Software Designer at ASU and one of the lead developers for JMARS.

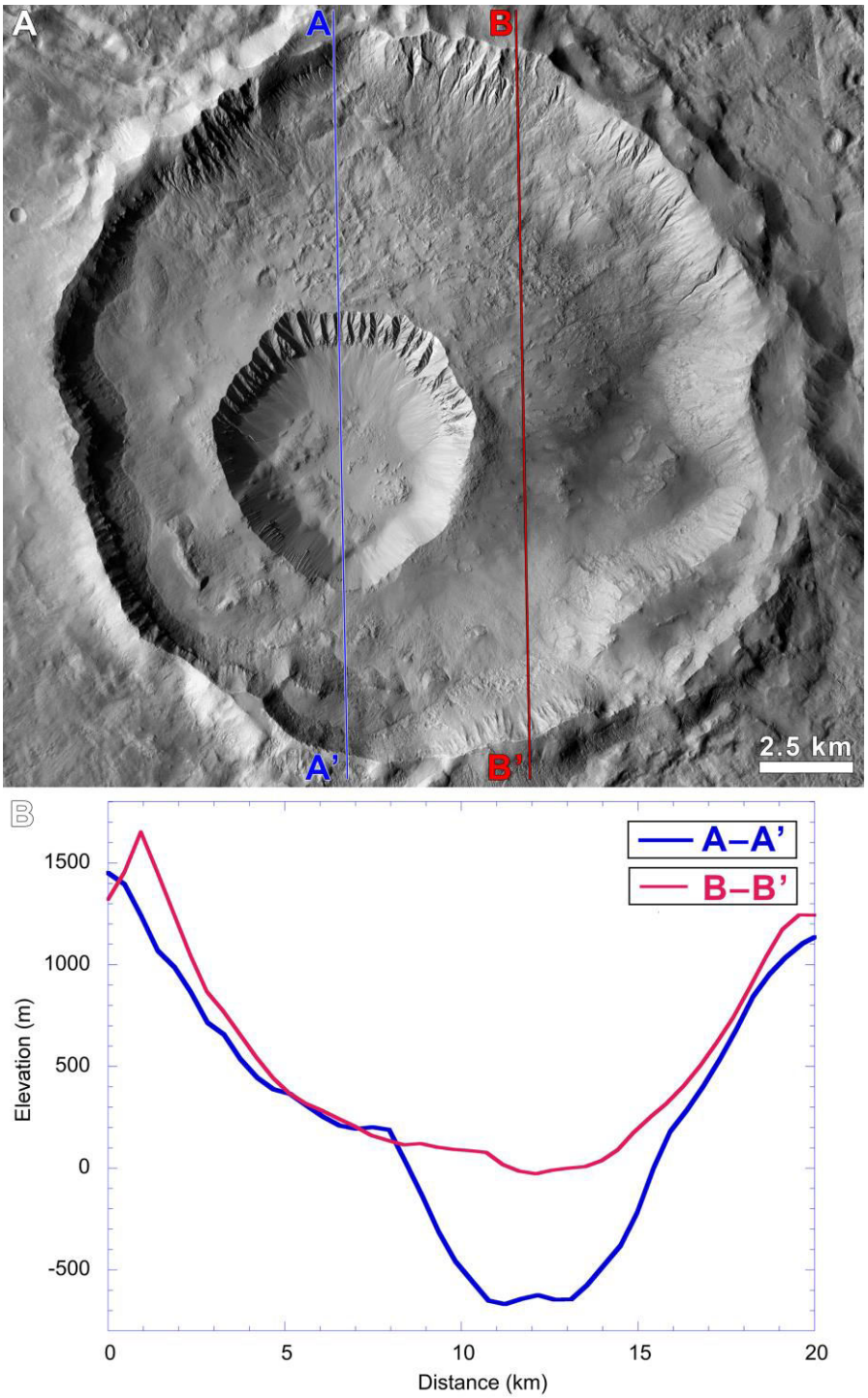

Figure 4.1. (A) CTX mosaic covering Gasa and Cilaos craters. Blue and red lines mark the MOLA elevation transects in B. North is up. **(B)** MOLA elevation profiles across the unnamed crater and Gasa (blue line) and Cilaos (red line).

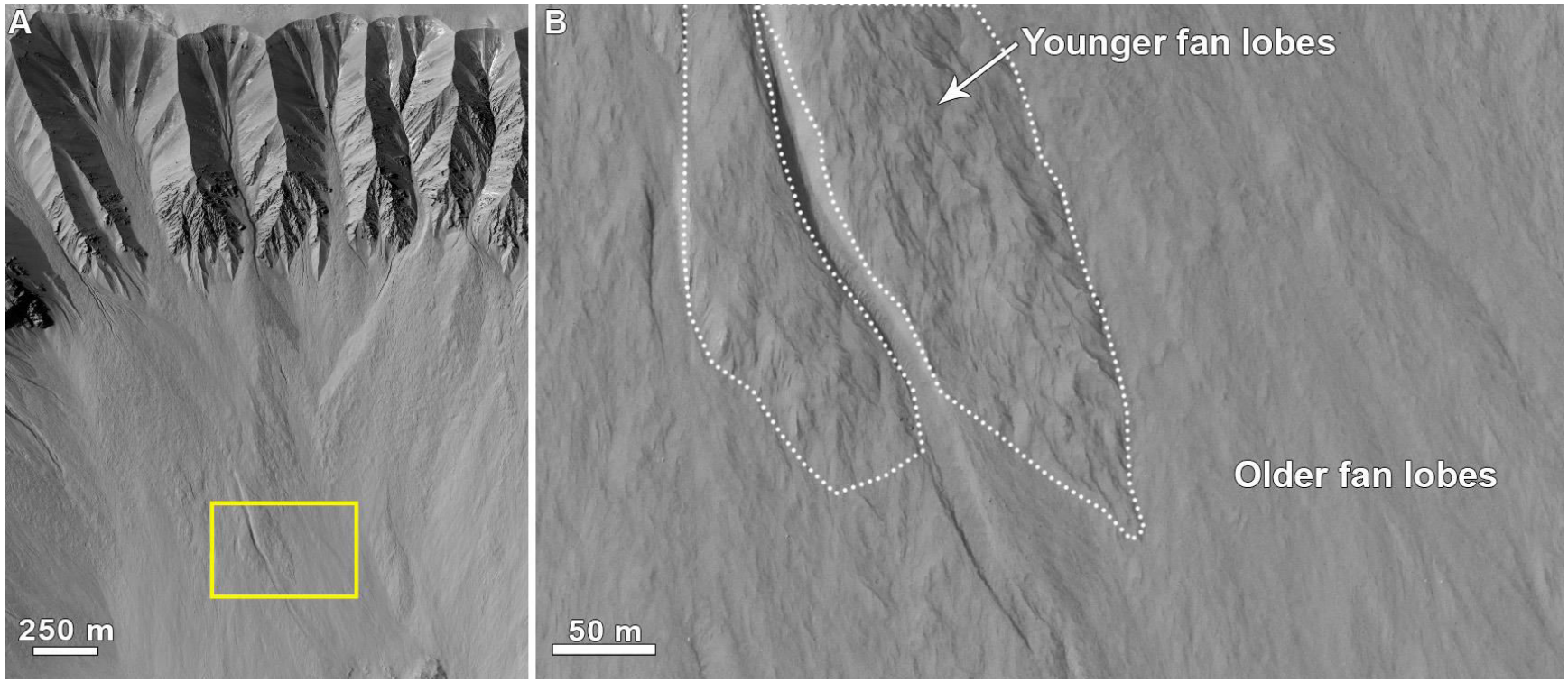

Figure 4.2. Example of younger (stratigraphically higher) and older (underlying) lobes within an individual gully fan in Gasa Crater. Yellow box in A shows context for B. Note the rough surface texture of the younger lobe compared to the underlying older portion of the fan. Subframes of HiRISE ESP_014081_1440.

4.3. Results and Discussion

4.3.1 General thermal inertia conditions within Gasa

The pole-facing walls of Gasa Crater are heavily gullied, while the equator-facing walls are steeper (Figure 4.1B) and display features with morphologies consistent with dry mass wasting processes observed within other well-preserved (non-gullied) craters similar in size to Gasa [e.g., *Tornabene et al.*, 2016]. The larger crater within which Gasa sits hosts gullies on its pole-facing walls. These gullies formed within the pasted-on mantle emplaced before the formation of Gasa. However, in some places the gullies appear to superpose Gasa ejecta that banked up on the walls of the larger crater, suggesting gully activity in the region occurred both before and after the formation of Gasa [c.f., *Schon and Head*, 2012].

The materials within Gasa exhibit a wide range of thermal inertia values (Figure 4.3 and Appendix A). The lowest values, averaging ~312 TIU, correspond with what is likely to be unconsolidated fine-grained deposits that have settled atop of, but not infilling or obscuring pitted materials on the crater floor; pitted materials are consistent with being a primary, crater-related deposits, which are interpreted to form from the interaction of impact melt with volatiles originating from the target [e.g., *Tornabene et al.*, 2012]. The highest TI values correspond with bedrock exposures in the crater walls, particularly along the southwestern (non-gullied) wall and within the gully alcoves of the pole-facing walls. Moderate TI values correspond with coarse-grained, unconsolidated talus on the equator-facing walls, consistent with preliminary morphologic and thermophysical mapping results by Tornabene et al. [2016] in non-gullied well-preserved craters. HiRISE IRB colour imaging of Gasa supports this interpretation. In HiRISE IRB images, yellows correspond to surfaces that are richer in ferric-bearing materials (in many cases due to coatings or the presence of martian “dust”) while blues correspond to ferrous-bearing materials [*Delamere et al.*, 2010]. The gullied walls of Gasa are generally yellower in the HiRISE IRB than the non-gullied walls (Figure 4.4). Thermal inertia values of gully aprons on the pole-facing wall have average thermal inertias ~60–80 TIU lower than the talus from mass wasting on the equator-facing wall (Figure 4.5, Table 4.1, and Appendix A), suggesting the gully aprons are dominated by coarser-grained material than the talus slopes. The gullied walls as a whole have a lower average thermal inertia

than the non-gullied walls, consistent with observations by Lanza et al. [2011] regarding differences in thermal inertia values of gullied vs. non-gullied crater walls.

	Average Thermal Inertia (J m^{-2} K^{-1} $s^{-1/2}$)			
Segment	**NW Wall**	**NE Wall**	**SW Wall**	**SE Wall**
Alcoves	458	488	509	No alcoves
Aprons	375	373	453	436
Alcoves+Aprons	412	436	482	No alcoves

Table 4.1. Average thermal inertia of gullied (NW and NE) and non-gullied (SW and SE) walls in Gasa Crater. *(For a detailed breakdown, see Appendix A.)*

4.3.2 Thermal inertia and recent gully activity

Analysis of 64 individual gully fan segments show that in Gasa, the average thermal inertia values of the youngest apron deposits are systematically ~20–40 TIU higher than the older underlying/surrounding deposits (Figures 4.5 and 4.6). Present-day gully activity has been documented in gullies #10, 12, and 19 (as labelled in Figure 4.3) by Dundas et al. [2010, 2012, 2015]. All three of these have aprons with areas of concentrations of higher TI (yellow patches in Figure 4.3) relative to other fans/fan segments, although they are not the only gullies with high TI fan segments. This suggests additional gullies within Gasa have been recently active, but not in the time period during which it has been actively monitored by CTX and HiRISE. It should be noted that the THEMIS image used in this study was acquired in 2004, before the changes documented by Dundas et al. [2010, 2012, 2015] occurred; therefore, we are not seeing the most recent changes that have occurred within Gasa with the THEMIS dataset.

Thermal mapping of alluvial fans in Death Valley by Hardgrove et al. [2009, 2010] found that older fan deposits had a higher thermal inertia than younger deposits, as their fine-grained component had eroded away from aeolian (i.e., deflation) and fluvial processes. On Mars, the opposite effect appears to be the case. This is likely due to atmospheric deposition of dust, as the rate of dust deposition on Mars greatly exceeds the rate of deflation. THEMIS is sensitive to ~5 thermal skin depths [*Fergason et al.*, 2006]; one thermal skin depth ≈1 cm for sand and increases with increasing grain size [*Hardgrove et al.*, 2009]; therefore, we use a rough estimate of 5 cm for the THEMIS penetration depth in the case of gully aprons. Combining this with the atmospheric dust

deposition rate measured by landed missions, we can obtain a very rough estimate for the time required to deposit enough dust atop a freshly formed gully/landslide deposit for it to be thermally indistinguishable from its surroundings. Using an average dust deposition rate of 0.02–0.06 μm per sol as determined from the Mars Exploration Rovers [*Kinch et al.*, 2015] and Phoenix [*Drube et al.*, 2010] yields a range of ~1,200–3,600 Mars years. These calculations do not take deflation into account; however, deflation rates calculated from the Pathfinder [*Golombek and Bridges*, 2000] and the Mars Exploration Rovers [*Golombek et al.*, 2006, 2014] would be negligible over the time period during which gully formation occurred on Mars (~0.1 nm/Myr in the Amazonian).

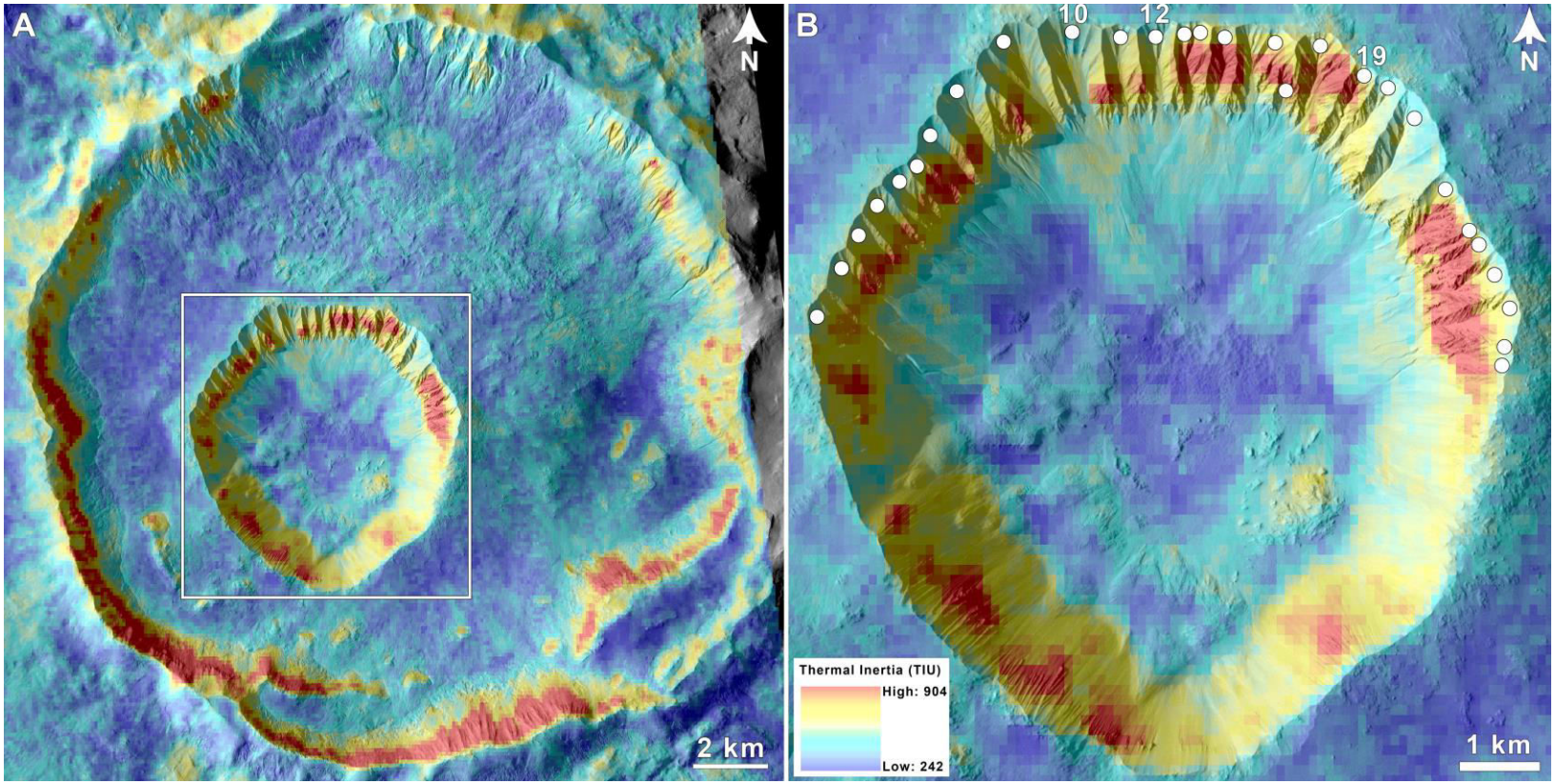

Figure 4.3. (A) CTX mosaic with THEMIS-derived thermal inertia overlaid atop it, centred at 35.7°S, 129.4°E, showing Gasa and Cilaos craters. **(B)** Closer view of Gasa as marked by the white box in A. Numbered gullies indicate locations of activity documented by Dundas et al. [2010, 2012, 2015]. Dots indicate each documented gully (numbered clockwise from the eastern wall from 1–28; individual numbers omitted for space).

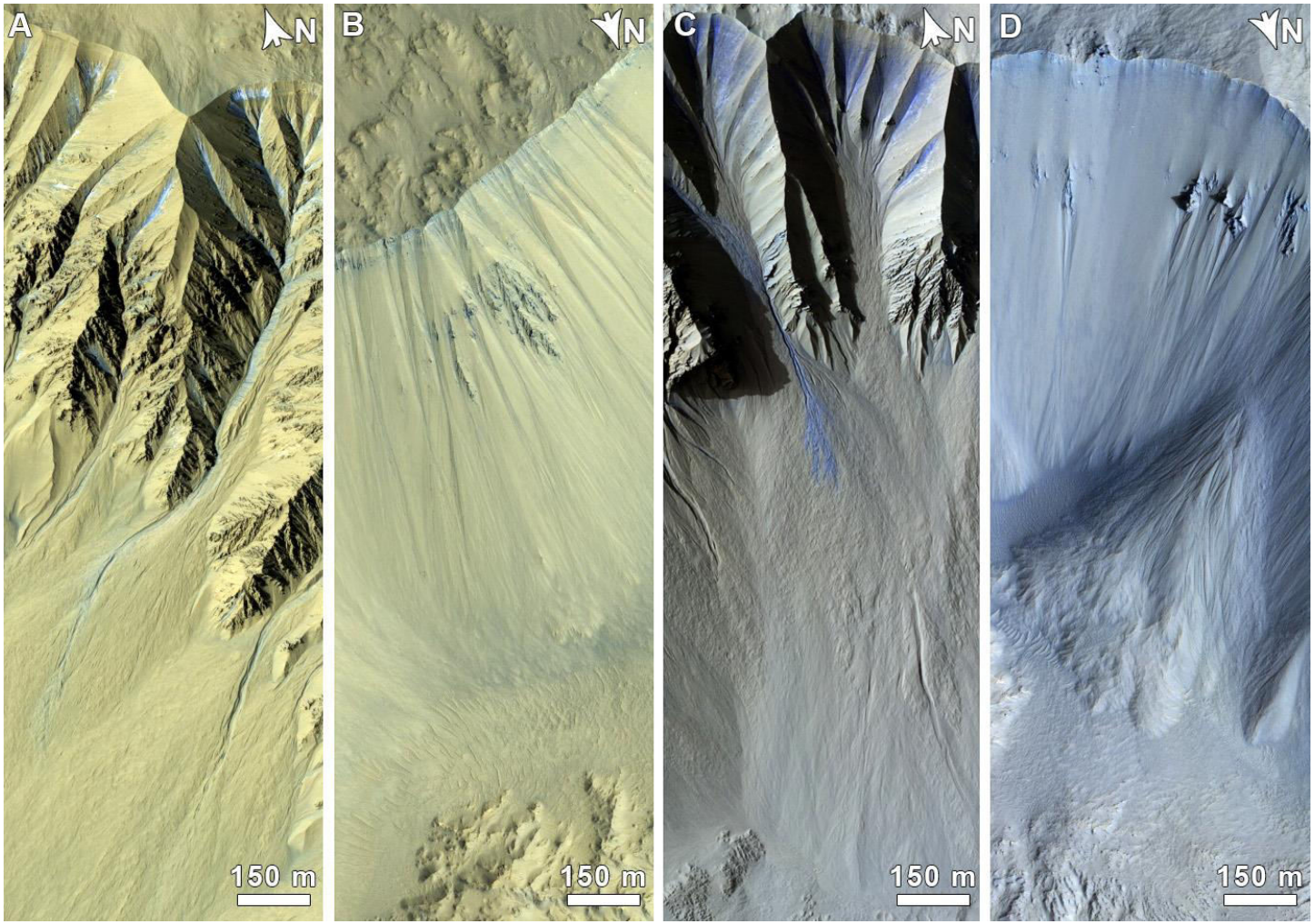

Figure 4.4. HiRISE IRB colour of gullied walls (A and C) and talus on slopes from mass wasting (B and D). A and B and subframes of PSP_004060_1440. C and D are subframes of ESP_020661_1440.

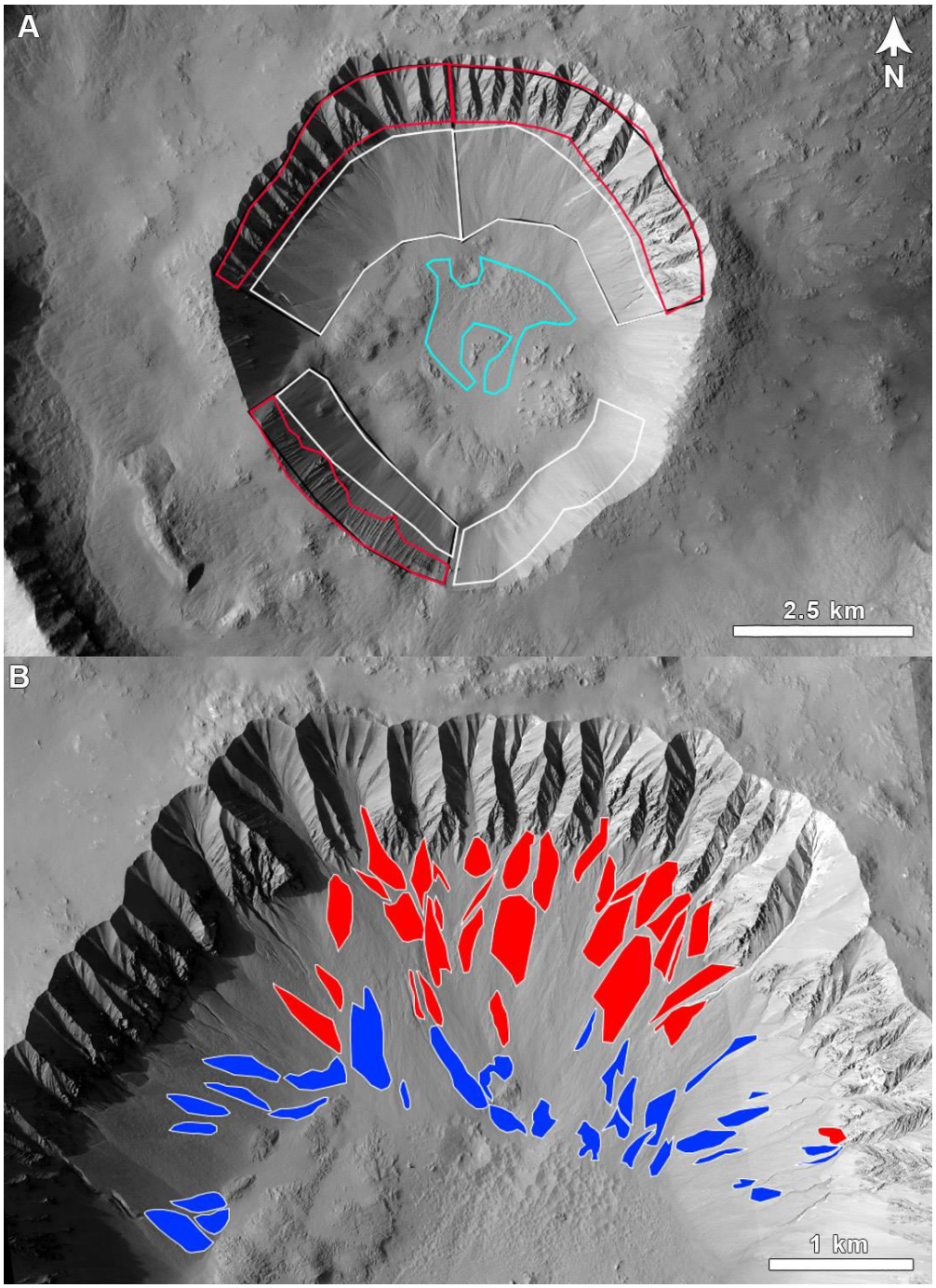

Figure 4.5. (A) Polygons denoting areas sampled for thermal inertia values of gully/talus aprons (white), alcoves (red), and the entire wall (alcoves and aprons, in black but obscured in some places in the figure by the red and white lines). Teal polygon on the crater floor denotes pitted material. Basemap is a subframe of CTX G06_020661_1440. **(B)** Fan segments used for sampling thermal inertia values. Red polygons denote the youngest fans (stratigraphically topmost). Blue polygons denote older underlying fan segments. Basemap consists of subframes of HiRISE ESP_020661_1440 and ESP_021584_1440.

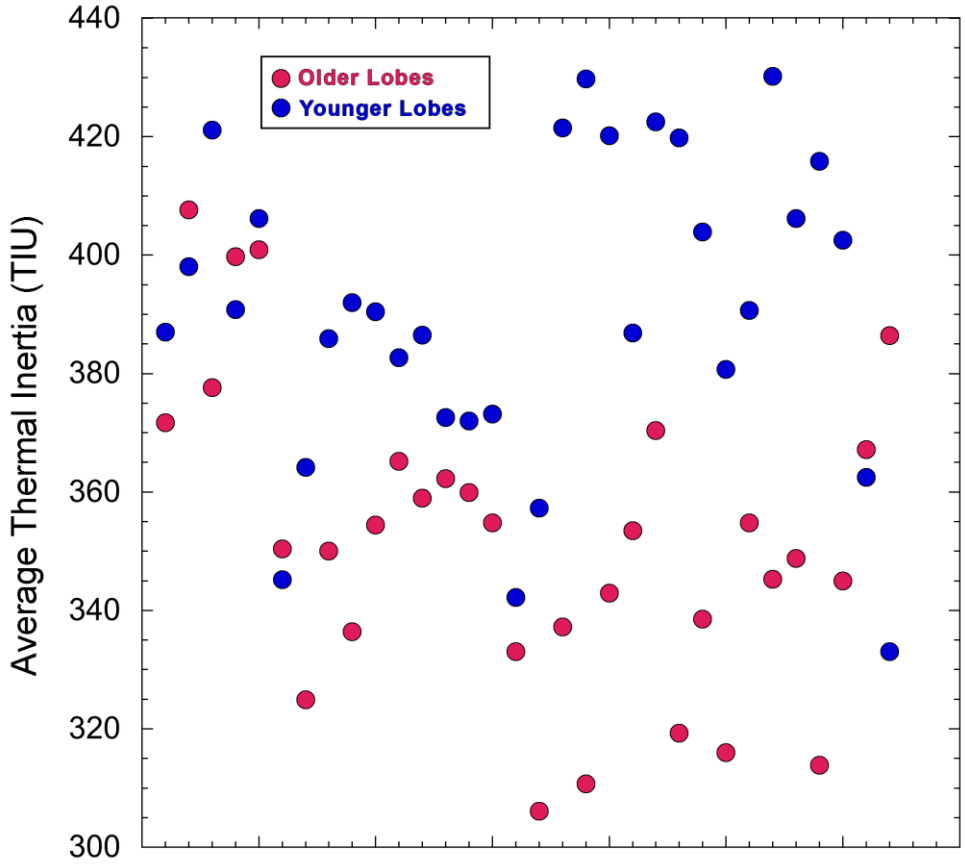

Figure 4.6. Average THEMIS-derived thermal inertia values (in TIU) for young (stratigraphically highest, in blue) and older (superposed, in red) gully fans within Gasa Crater. X-axis has no values; points are separated horizontally to clearly show the range in thermal inertia values along the y-axis. For a detailed breakdown of values for each fan lobe measured, see Appendix A.

4.5. Implications and Future Work

Gasa Crater exhibits clear variations in thermal inertia across its walls, controlled by the material properties and the types of dominant mass movement processes occurring on each wall. The youthful gully fan lobes display thermal inertia values ~20–40 TIU higher than adjacent older eroded and dust-covered lobes. The talus aprons from mass wasting in Gasa have thermal inertia values ~60–80 TIU higher than gully aprons. The results of this study thus suggest that repeated THEMIS day/night IR imaging coordinated with MRO observations could be used for surface change detection. In the case of gullies large

enough to be resolved in the THEMIS IR, acquiring at least 1–2 images (in order to ensure at least 1 of acceptable quality is returned) at the beginning and end of each season in both hemispheres would be ideal as gully activity appears to be seasonally constrained to autumn through early spring [e.g., *Harrison et al.*, 2009; *Diniega et al.*, 2010; *Dundas et al.*, 2010, 2012, 2015]. Analysis of thermal inertia differences could aid in selecting or refining sites for monitoring by CTX and HiRISE, and the 5 m/pixel Colour and Stereo Surface Imaging System (CaSSIS) aboard the European Space Agency's ExoMars Trace Gas Orbiter [*Thomas et al.*, 2014]. Additionally, the thermal imaging of Hardgrove et al. [2009] revealed structure within alluvial fans in Death Valley not distinguishable in visible images. This, combined with the results of our study, may make a case for sending a higher-resolution thermal imager to Mars on a future orbiter, as it could prove to be a valuable asset to study the structure of gullies and deltas/alluvial fans, all of which are found in abundance on the planet.

References

Cedillo-Flores, Y., A. H. Treiman, J. Lasue, and S. M. Clifford (2011), CO_2 gas fluidization in the initiation and formation of Martian polar gullies, *Geophys. Res. Lett.*, *38*(L21202), doi:10.1029/2011GL049403.

Christensen, P. R. et al. (2004), The Thermal Emission Imaging System (THEMIS) for the Mars 2001 Odyssey Mission, *Space Sci. Rev.*, *110*, 85–130, doi:10.1023/B:SPAC.0000021008.16305.94.

Christensen, P. R., E. Engle, S. Anwar, S. Dickenshied, D. Noss, N. Gorelick, and M. Weiss-Malik (2009), JMARS – A Planetary GIS, in *American Geophysical Union, Fall Meeting 2009*, p. abstract IN22A–06.

Christensen, P. R., R. L. Fergason, C. S. Edwards, and J. Hill (2013), THEMIS-derived thermal inertia mosaic of Mars: Product description and science results, *44th Lunar Planet. Sci. Conf.*, abstract 2822.

Delamere, W. A. et al. (2010), Color imaging of Mars by the High Resolution Imaging Science Experiment (HiRISE), *Icarus*, *205*(1), 38–52, doi:10.1016/j.icarus.2009.03.012.

Diniega, S., S. Byrne, N. T. Bridges, C. M. Dundas, and A. S. McEwen (2010), Seasonality of present-day Martian dune-gully activity, *Geology*, *38*(11), 1047–1050, doi:10.1130/G31287.1.

Drube, L. et al. (2010), Magnetic and optical properties of airborne dust and settling rates of dust at the Phoenix landing site, *J. Geophys. Res.*, *115*, E00E23, doi:10.1029/2009JE003419.

Dundas, C. M., A. S. McEwen, S. Diniega, S. Byrne, and S. Martinez-Alonso (2010), New and recent gully activity on Mars as seen by HiRISE, *Geophys. Res. Lett.*, *37*(7), L07202, doi:10.1029/2009GL041351.

Dundas, C. M., S. Diniega, C. J. Hansen, S. Byrne, and A. S. McEwen (2012), Seasonal activity and morphological changes in martian gullies, *Icarus*, *220*(1), 124–143, doi:10.1016/j.icarus.2012.04.005.

Dundas, C. M., S. Diniega, and A. S. McEwen (2015), Long-term monitoring of martian gully formation and evolution with MRO/HiRISE, *Icarus*, *251*, 244–263, doi:10.1016/j.icarus.2014.05.013.

Dundas, C. M., S. Diniega, A. S. McEwen, C. J. Hansen, and S. Byrne (2016), Monitoring martian gullies: Implications for formation and evolution, in *Martian Gullies and Their Earth Analogues*, London, United Kingdom (GBR).

Fergason, R. L., P. R. Christensen, and H. H. Kieffer (2006), High-resolution thermal inertia derived from the Thermal Emission Imaging System (THEMIS): Thermal model and applications, *J. Geophys. Res. E Planets*, *111*(12), 1–22, doi:10.1029/2006JE002735.

Golombek, M. P., and N. T. Bridges (2000), Erosion rates on Mars and implications for climate change: Constraints from the Pathfinder landing site, *J. Geophys. Res.*, *105*, 1841–1853.

Golombek, M. P. et al. (2006), Erosion rates at the Mars Exploration Rover landing sites and long-term climate change on Mars, *J. Geophys. Res.*, *111*(E12), doi:10.1029/2006JE002754.

Golombek, M. P., N. H. Warner, V. Ganti, M. P. Lamb, T. J. Parker, R. L. Fergason, and R. Sullivan (2014), Small crater modification on Meridiani Planum and implications for erosion rates and climate change on Mars, *J. Geophys. Res.*, *119*(12), 2522–2547, doi:10.1002/2014JE004658.

Hardgrove, C., J. Moersch, and S. Whisner (2009), Thermal imaging of alluvial fans: A new technique for remote classification of sedimentary features, *Earth Planet. Sci. Lett.*, *285*(1-2), 124–130, doi:10.1016/j.epsl.2009.06.004.

Hardgrove, C., J. Moersch, and S. Whisner (2010), Thermal imaging of sedimentary features on alluvial fans, *Planet. Space Sci.*, *58*(4), 482–508, doi:10.1016/j.pss.2009.08.012.

Harrison, T. N., M. C. Malin, and K. S. Edgett (2009), Present-day gully activity observed by the Mars Reconnaissance Orbiter (MRO) Context Camera (CTX), in *Bulletin of the American Astronomical Society, DPS Meeting #41*, p. 1113.

Heldmann, J. L., and M. T. Mellon (2004), Observations of martian gullies and constraints on potential formation mechanisms, *Icarus*, *168*(2), 285–304, doi:10.1016/j.icarus.2003.11.024.

Hugenholtz, C. H. (2008), Frosted granular flow: A new hypothesis for mass wasting in martian gullies, *Icarus*, *197*, 65–72, doi:10.1016/j.icarus.2008.04.010.

Jakosky, B. M. (1986), On the thermal properties of Martian fines, *Icarus*, *66*, 117–124, doi:10.1016/0019-1035(86)90011-4.

Kinch, K. M., J. F. Bell III, W. Goetz, J. R. Johnson, J. Joseph, M. B. Madsen, and J. Sohl-Dickstein (2015), Dust deposition on the decks of the Mars Exploration Rovers: 10 years of dust dynamics on the Panoramic Camera calibration targets, *Earth Sp. Sci.*, *2*, 144–172, doi:10.1002/2014EA000073.

Lanza, N. L., H. E. Newsom, and M. M. Osterloo (2011), The systematic effects of martian gravity on hillslope materials and mass movement processes, *42nd Lunar and Planetary Science Conference*, abstract 2383.

Malin, M. C., and K. S. Edgett (2000), Evidence for recent groundwater seepage and surface runoff on Mars, *Science*, *288*(5475), 2330–2335, doi:10.1126/science.288.5475.2330.

Malin, M. C., K. S. Edgett, L. V Posiolova, S. M. Mccolley, and E. Z. N. Dobrea (2006), Present-day impact cratering rate and contemporary gully activity on Mars, *Science*, *314*(5805), 1573–1577.

Malin, M. C. et al. (2007), Context Camera Investigation on board the Mars Reconnaissance Orbiter, *J. Geophys. Res.*, *112*(E5), E05S04, doi:10.1029/2006JE002808.

McEwen, A. S. et al. (2007), Mars Reconnaissance Orbiter's High Resolution Imaging Science Experiment (HiRISE), *J. Geophys. Res.*, *112*(E5), E05S02, doi:10.1029/2005JE002605.

Neugebauer, G., G. Münch, H. H. Kieffer, S. C. Case Jr., and E. Miner (1971), Mariner 1969 infrared radiometer results: Temperatures and thermal properties of the Martian surface, *Astron. J.*, *76*(8), 719–749.

Presley, M. A., and P. R. Christensen (1997a), Thermal conductivity measurements of particulate materials 1. A Review, *J. Geophys. Res.*, *102*(E3), 6535–6549, doi:10.1029/96JE03303.

Presley, M. A., and P. R. Christensen (1997b), Thermal conductivity measurements of particulate materials 2. Results, *J. Geophys. Res.*, *102*(E3), 6551–6566.

Schon, S. C., and J. W. Head (2012), Gasa impact crater, Mars: Very young gullies formed from impact into latitude-dependent mantle and debris-covered glacier

deposits?, *Icarus*, *218*(1), 459–477, doi:10.1016/j.icarus.2012.01.002.

Schon, S. C., J. W. Head, and C. I. Fassett (2009), Unique chronostratigraphic marker in depositional fan stratigraphy on Mars: Evidence for ca. 1.25 Ma gully activity and surficial meltwater origin, *Geology*, *37*(3), 207–210, doi:10.1130/G25398A.1.

Thomas, N. et al. (2014), The Colour and Stereo Surface Imaging System (CaSSIS) for ESA's Trace Gas Orbiter, *8th International Conference on Mars*, abstract 1067.

Tornabene, L. L., J. E. Moersch, H. Y. McSween, A. S. McEwen, J. L. Piatek, K. A. Milam, and P. R. Christensen (2006), Identification of large (2-10 km) rayed craters on Mars in THEMIS thermal infrared images: Implications for possible Martian meteorite source regions, *J. Geophys. Res. E Planets*, *111*(10), 1–25, doi:10.1029/2005JE002600.

Tornabene, L. L., G. R. Osinski, A. S. McEwen, J. M. Boyce, V. J. Bray, C. M. Caudill, J. A. Grant, C. W. Hamilton, S. Mattson, and P. J. Mouginis-Mark (2012), Widespread crater-related pitted materials on Mars: Further evidence for the role of target volatiles during the impact process, *Icarus*, *220*(2), 348–368, doi:10.1016/j.icarus.2012.05.022.

Tornabene, L. L., J. L. Piatek, K. T. Hansen, S. J. Hutchinson, N. G. Barlow, G. R. Osinski, S. J. Robbins, and A. S. McEwen (2016), Visible and thermophysical characteristics of the best-preserved martian craters, part 1: Detailed morphological mapping of Resen and Noord, *LPSC 47*.

Treiman, A. H. (2003), Geologic settings of Martian gullies: Implications for their origins, *J. Geophys. Res.*, *108*(E4), 8031, doi:10.1029/2002JE001900.

Wechsler, A., and P. Glaser (1965), Pressure effects on postulated lunar materials, *Icarus*, *4*, 335–352, doi:10.1016/0019-1035(65)90038-2.

Wechsler, A. E., P. E. Glaser, and J. A. Fountain (1972), Thermal properties of granulated materials, in *Thermal Characteristics of the Moon, Prog. Astron. Aeronaut., vol. 28*, edited by J. W. Lucas, pp. 215–241, MIT Press, Cambridge, MA.

Chapter 5: Discussion and Future Work

By studying martian gullies at global, regional, and local scales, their complex story—regarding their formation and ongoing activity, which appears to be intimately linked to changes in climate in the Late Amazonian—has emerged. Like gullies on Earth, martian gullies most likely form via a range of discrete mechanisms, but their global distribution suggests a common control on their formation. The latitudinal restriction of gullies and the observed shift in dominant orientation from pole-facing to equator-facing with increasing latitude support proposed formation mechanisms involving melting of snow and/or near-surface ground ice[1]. Dry mass movement processes cannot adequately explain these observations or the morphology of most gully systems. While frost-related processes likely play a role in gully evolution and present-day activity based on the observed timing of such activity [*Dundas et al.*, 2010, 2012, 2015], it is difficult to explain the morphology of many gully systems on Mars from these processes alone. As shown in Chapter 2, frost-coasted clast flows (also known as frosted granular flow [*Hugenholtz*, 2008]) on Earth do not produce morphologies resembling most martian (non-dune) gullies. Fan deposits of gullies often contain boulders, which require a fluidized process in order to be entrained and transported downslope [e.g., *Iverson et al.*, 1997; *Stock and Dietrich*, 2006]. Whether a CO_2 gas-fluidized flow would be capable of transporting boulder-sized material remains an open question, as we have no analogous natural process on Earth. Sublimation of CO_2 frost may act as a trigger for mass movement, but whether it could sustain a prolonged fluidized flow down the entire length of a slope is another open question. Laboratory simulations of CO_2 sublimation under martian conditions by Sylvest et al. [2016] found that the process could mobilize unconsolidated fine sediments on slopes $\gtrsim 15°$ under terrestrial gravity. However, the process did not mobilize grains larger than sand-sized well. Additional laboratory experiments are necessary to further our understanding of the possible exotic CO_2-frost-

[1] Distinguishing between meltwater sources is not possible morphologically with the datasets currently available; climate model comparisons are required.

related processes that are likely occurring on Mars today. The most likely scenario is that gullies formed from water-related processes, creating topographic hollows conducive to the subsequent accumulation of frost. Gully alcoves provide sheltered and shadowed areas where frost has been observed to collect through winter and be preserved over longer periods compared to adjacent slope areas outside of the gullies. Avalanching [e.g., *Ishii and Sasaki*, 2004; *Costard et al.*, 2007] and sublimation [e.g., *Dundas et al.*, 2010, 2012, 2015] of this accumulated frost could then trigger activity within these pre-existing gullies.

At the regional scale, multiple generations of gullies are observed in different stages of preservation. On slopes hosting pasted-on material, older inverted (buried and then subsequently exhumed) gully channels observed on the same slopes as younger gully channels and aprons strongly suggest that the process(es) by which gullies formed has been active over the course of multiple obliquity cycles. Gully activity is observed to have occurred coincident with the retreat of mid-latitude crater fill (CCF), a process also driven by changes in climate as ice becomes unstable in the mid-latitudes of Mars [e.g., *Shean*, 2010]. This demonstrates the intimate link between changes in climate and the geomorphology of the martian mid-latitudes, where a suite of landforms indicative of ice deposition and subsequent (partial or complete) removal are concentrated.

On the local scale, thermal variations across gully fans and gullied vs. non-gullied slopes can inform us on geologically recent mass movement activity. Thermal inertia indirectly reveals the relative grain size of materials transported downslope, as well as the amount of dust cover. Deposition of fine-grained atmospheric dust over time should result in a decrease in the thermal inertia of a surface on Mars. Gully apron deposits within Gasa Crater illustrate this effect well: The most youthful (stratigraphically topmost) fan lobes have generally higher thermal inertia values than the older underlying lobes. Therefore, thermal imaging is an additional tool for recognizing geologically recent mass movement activity on martian slopes. Repeated thermal imaging could also be used in present-day change detection efforts, although most gullies are much smaller than the resolution limit of the THEMIS IR dataset. High-resolution thermal imaging,

and/or additional techniques such as interferometric synthetic aperture radar (InSAR), could be valuable assets to look at the physical properties and structure of landslides and other fan deposits, such as putative deltas (i.e., in Eberswalde and Jezero craters) and alluvial fans (i.e., Peace Vallis in Gale Crater) on Mars on future orbiter missions.

Investigating any possible relationship between the formation of gullies and RSL with continued monitoring efforts by HiRISE (and eventually CaSSIS) will be integral in understanding both landforms. Looking at the morphology of possible "small gullies" associated with RSL in the equatorial regions [*McEwen et al.*, 2016] and other so-called equatorial gullies [e.g., *Auld and Dixon*, 2014] and comparing them to the mid-latitude landforms is necessary. These equatorial features are significantly smaller—too small to be confidently identified at CTX resolution (Figure 5.1)—with shorter channels than their potential mid-latitude counterparts according to McEwen et al. [2016]. However, preliminary inspection of these features reveals fan and linear chute-like morphologies more consistent with terrestrial talus slopes than the aprons and incised, erosional channels of martian mid-latitude gullies (Figures 5.2 and 5.3). Because of the lack of incised channels, the equatorial features were not considered as gullies in the global database presented in Chapter 2. Based on their morphology, these equatorial features would not have been considered gullies in that survey even if they were clearly resolvable with CTX. In some cases where the positive identification of gullies was ambiguous with CTX, the location was documented but with a note that the features may not be gullies. These locations are not included in the global map in Chapter 2 in order to be conservative in the identification of "gullies." Updates to the global database—which is publicly available as a shape layer in JMARS—are ongoing with successive releases of CTX and HiRISE data to the NASA PDS. Therefore, as HiRISE coverage is acquired of the ambiguous cases, definitive identifications may become possible for at least some locations.

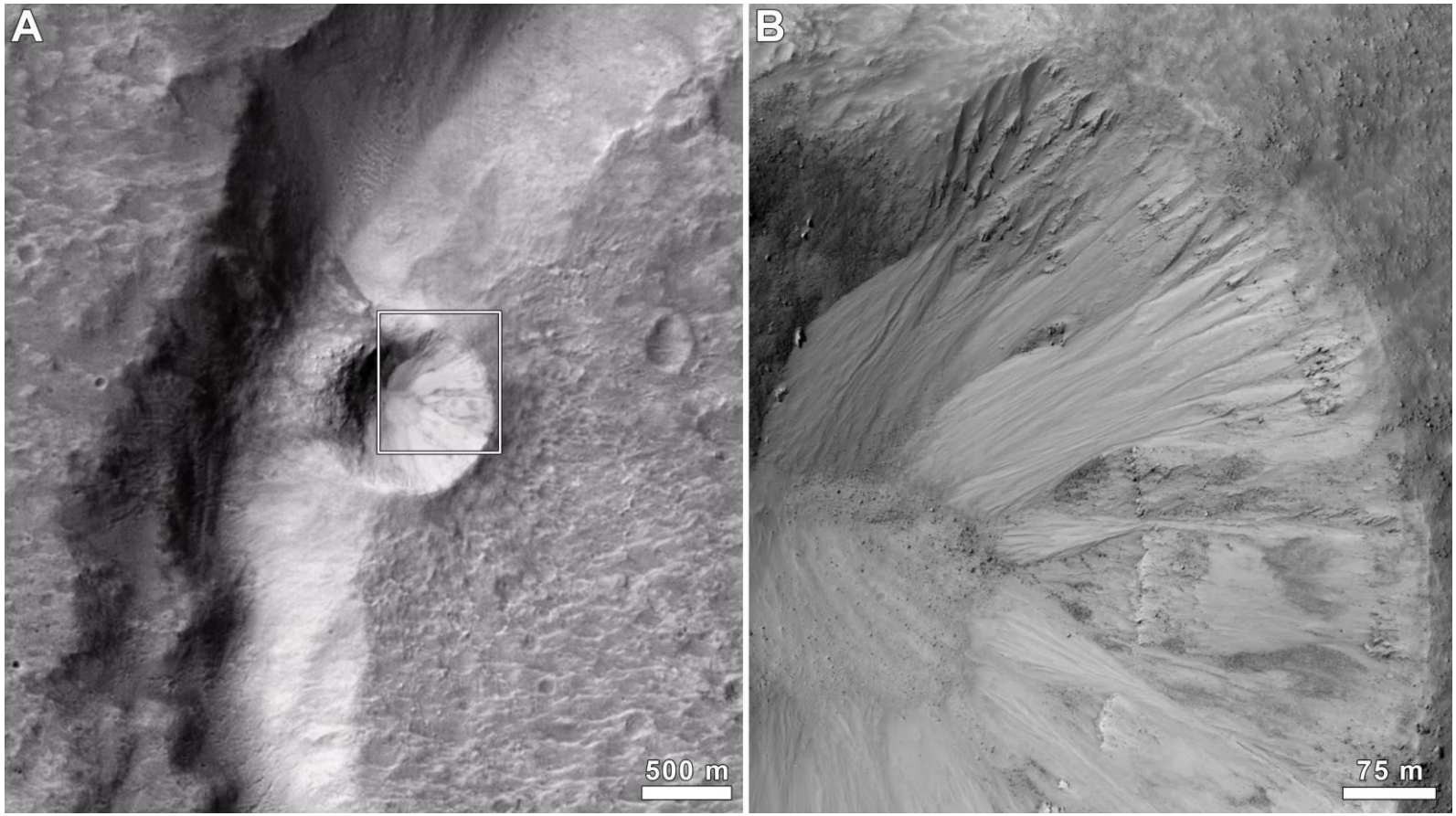

Figure 5.1. "Equatorial gullies" in a crater in the Libya Montes region centred at 2.62°N, 84.64°E. **(A)** Crater at the maximum resolution of CTX (~6 m/pixel). Subframe of B22_018223_1824. **(B)** Portion of the crater denoted by the white box in A, viewed by HiRISE. Note the highly linear chutes of the features compared to mid-latitude gullies (i.e., Figure 2.2 in Chapter 2). Subframe of ESP_034864_1825. North is up in both images.

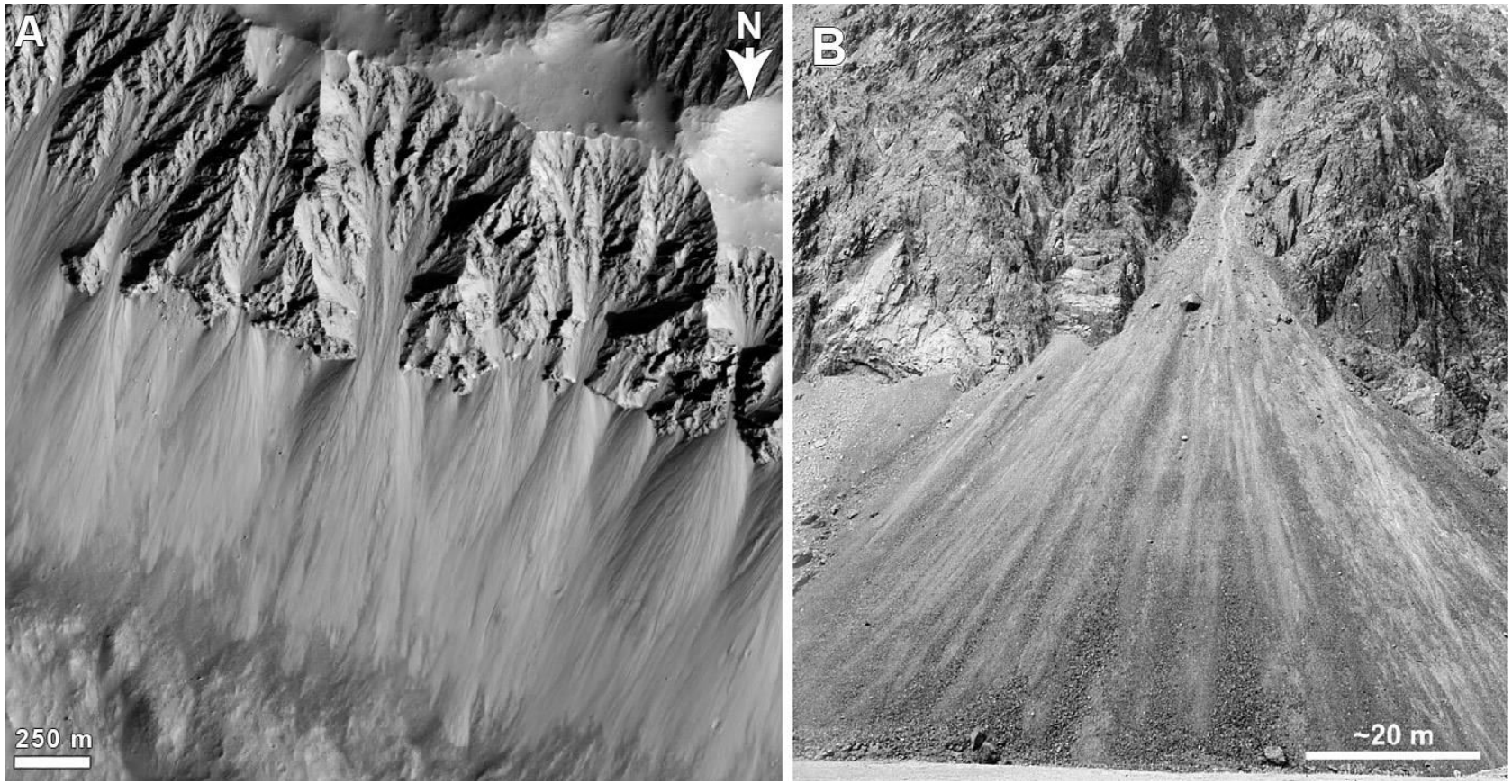

Figure 5.2. (A) "Equatorial gullies" in Coprates Chasma at 12.57°S, 294.68°E. Subframe of HiRISE ESP_018189_1675. **(B)** Example of a talus cone on Earth, in the Punta Vacas, Main Cordillera of the Andes, Argentina. Note the similarity in apron morphology between the terrestrial and martian features. From Gutiérrez [2005] as modified by Johnsson et al. [2014].

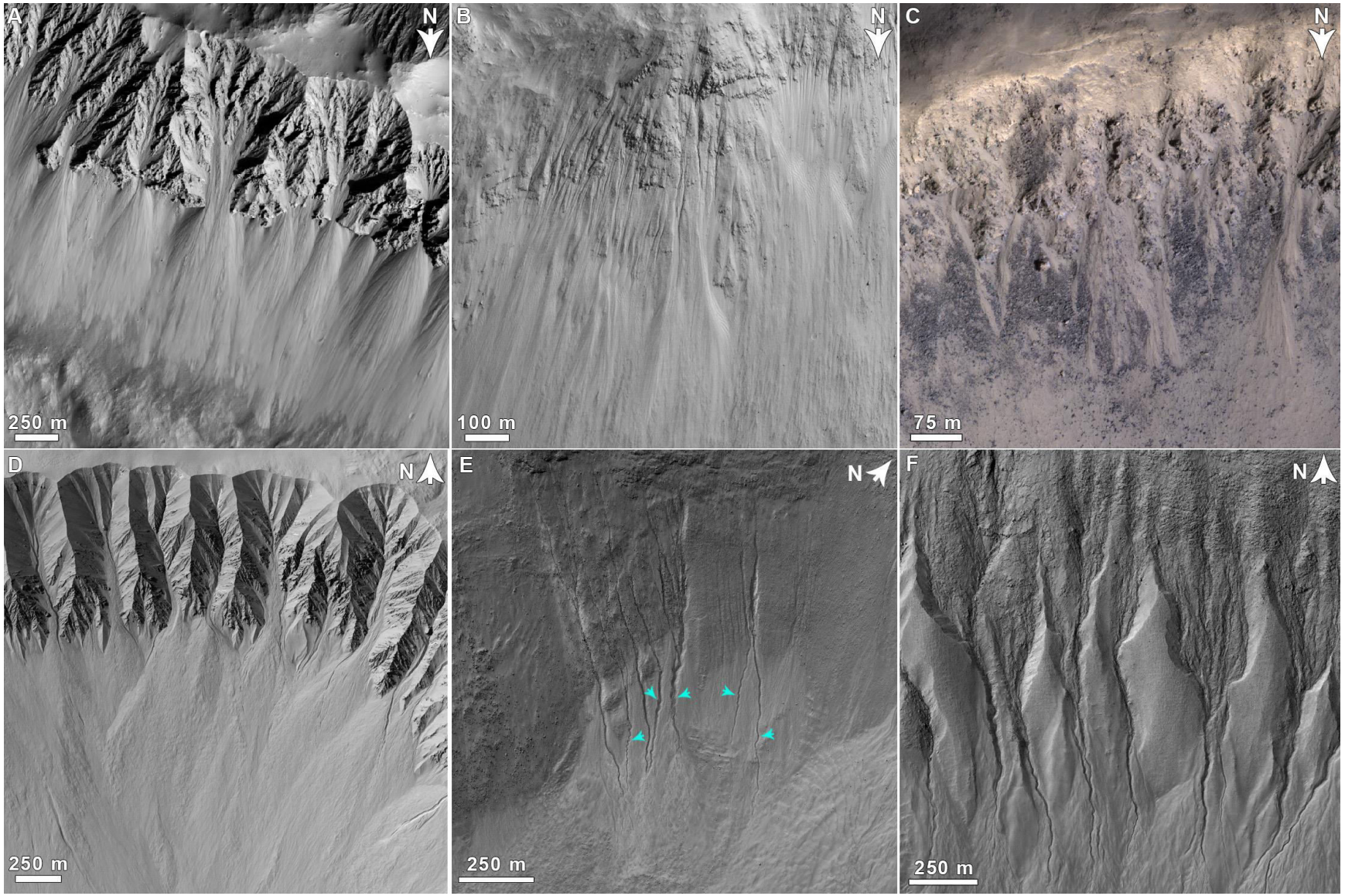
A
N
250 m
B
N
100 m
C
N
75 m
D
N
250 m
E
N
250 m
F
N
250 m

Figure 5.3. HiRISE views of "equatorial gullies" (A–C) and mid-latitude gullies (D–F). **(A)** In Coprates Chasma at 12.57°S, 294.68°E. Subframe of ESP_018189_1675. **(B)** In Juventae Chasma at 4.73°S, 298.60°E. Subframe of ESP_030373_1755. **(C)** IRB colour view of "equatorial gullies" in a crater in Libya Montes at 4.52°S, 92.66°E. Subframe of ESP_035945_1755. **(D)** Gullies in Gasa Crater. Subframe of ESP_032199_1440. **(E)** Gullies with fine channels in Corozal Crater at 38.75°S, 159.38°E. Teal arrows denote sinuous channel segments, a feature characteristic of channels carved by fluid-abetted flow and notably absent from the fine-scale equatorial features pictured in B. Subframe of ESP_013948_1410. **(F)** Gullies incising into pasted-on material on a crater wall at 40.29°S, 196.78°E. Subframe of PSP_005930_1395.

Regardless of the terrestrial definition of a gully (i.e., agricultural[2] vs. the one presented in Chapter 2), the term has been firmly adopted for a specific type of landform on Mars in the 16 years since the canonical description of Malin and Edgett [2000]. As such, consistency in the use of the word "gully" across the literature is required to avoid misinterpretation and conflating disparate landforms. Features consisting of alcoves and aprons without incised channels on the north polar erg [e.g., *Hansen et al.*, 2011, 2013; *Allen et al.*, 2016; *Diniega et al.*, 2016] and on other slopes across Mars [e.g., *Treiman*, 2003; *Shinbrot et al.*, 2004; *Auld and Dixon*, 2014] have been referred to as "gullies" in the literature. As these are morphologically distinct from mid-latitude gullies, the question should be raised as to whether these channel-less features should be classified as something else (the same applies to features termed "gullies" on Vesta [*Scully et al.*, 2015] and the Moon [*Bart*, 2007; *Senthil Kumar et al.*, 2013], which lack clearly incised channels relative to terrestrial and martian gullies (Figure 5.4)). Based on the terrestrial geological definition of Bull and Kirkby [1997] ("an incised channel morphology"), the agricultural definition of Neuendorf et al. [2010][2], and the martian classification of Malin and Edgett [2000], features lacking channels should *not* be considered "gullies." Nearly all mass movement processes—wet or dry—occurring on a slope will form an "alcove" of some type from which the material was sourced, and an apron where the material was deposited at the base of the slope. The incised channel is what sets mid-latitude gullies apart relative to other mass movement landforms observed on Mars and other terrestrial bodies in the Solar System.

---

[2] McEwen et al. [2016] note the agricultural definition of a gully from Neuendorf et al. [2010] as "A small channel with steep sides caused by erosion and cut in unconsolidated materials by concentrated but intermittent flow of water…and too deep (e.g., >0.5 m) to be obliterated by ordinary tillage."

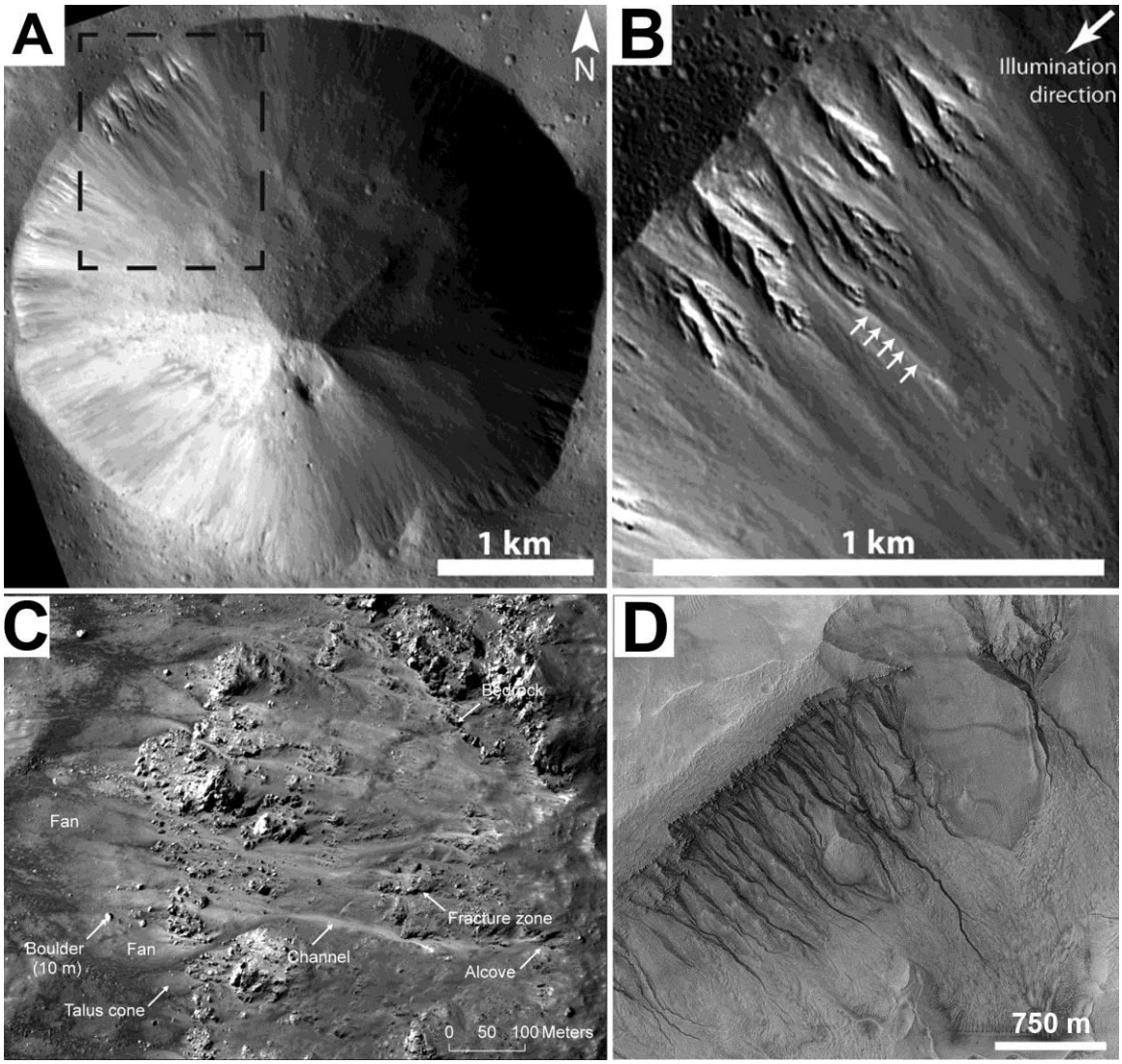

Figure 5.4. Vestan (**A**, with black box denoting the context for **B**) and lunar (**C**) features on crater walls referred to as "gullies" taken from Scully et al. [2015] and Kumar et al. [2013], respectively, compared to martian gullies in Niquero Crater (E11-04033). Note the morphological differences. No clearly incised channels are visible in the Vestan case. The lunar gullies in **C** have light-toned material that has been transported downslope, but without deeply incised channels as observed in terrestrial and martian gullies.

References

Allen, A., S. Diniega, and C. Hansen (2016), Gully and aeolian activity within the "Tleilax" dune field in the Olympia Undae, Mars, *47th Lunar Planet. Sci. Conf.*, abstract 1759, doi:10.1016/j.icarus.2007.12.027.

Auld, K. S., and J. C. Dixon (2014), Classification of martian gullies from HiRISE imagery, *45th Lunar and Planetary Science Conference*, abstract 1270.

Bart, G. D. (2007), Comparison of small lunar landslides and martian gullies, *Icarus*, *187*(2), 417–421, doi:10.1016/j.icarus.2006.11.004.

Bull, L. J., and M. J. Kirkby (1997), Gully processes and modelling, *Prog. Phys. Geogr.*, *21*(3), 354–374, doi:10.1177/030913339702100302.

Costard, F., N. Mangold, D. Baratoux, and F. Forget (2007), Current gullies activity: Dry avalanches at seasonal defrosting as seen on HiRISE images, *Seventh International Conference on Mars*, abstract 3133.

Diniega, S., A. Allen, T. Perez, and C. J. Hansen (2016), Tracking gully activity within the north polar erg, Mars, *47th Lunar and Planetary Science Conference*, abstract 1740.

Dundas, C. M., A. S. McEwen, S. Diniega, S. Byrne, and S. Martinez-Alonso (2010), New and recent gully activity on Mars as seen by HiRISE, *Geophys. Res. Lett.*, *37*(7), L07202, doi:10.1029/2009GL041351.

Dundas, C. M., S. Diniega, C. J. Hansen, S. Byrne, and A. S. McEwen (2012), Seasonal activity and morphological changes in martian gullies, *Icarus*, *220*(1), 124–143, doi:10.1016/j.icarus.2012.04.005.

Dundas, C. M., S. Diniega, and A. S. McEwen (2015), Long-term monitoring of martian gully formation and evolution with MRO/HiRISE, *Icarus*, *251*, 244–263, doi:10.1016/j.icarus.2014.05.013.

Gutiérrez, M. (2005), Climatic geomorphology, in *Earth Surface Processes*, edited by J. Shroder, J. F., p. 760, Elsevier B.V., Amsterdam, Netherlands (NLD).

Hansen, C. J. et al. (2011), Seasonal erosion and restoration of Mars' northern polar dunes, *Science*, *331*(February), 575–578, doi:10.1126/science.1197636.

Hansen, C. J., S. Byrne, G. Portyankina, M. Bourke, C. Dundas, A. McEwen, M. Mellon, A. Pommerol, and N. Thomas (2013), Observations of the northern seasonal polar

cap on Mars: I. Spring sublimation activity and processes, *Icarus*, *225*(2), 881–897, doi:10.1016/j.icarus.2012.09.024.

Hugenholtz, C. H. (2008), Frosted granular flow: A new hypothesis for mass wasting in martian gullies, *Icarus*, *197*, 65–72, doi:10.1016/j.icarus.2008.04.010.

Ishii, T., and S. Sasaki (2004), Formation of recent martian gullies by avalanches of CO2 frost, *Lunar and Planetary Science XXXV*, abstract 1556.

Iverson, R. M., M. E. Reid, and R. G. Lahusen (1997), Debris-flow mobilization from landslides, *Annu. Rev. Earth Planet. Sci.*, *25*, 85–138.

Johnsson, A., D. Reiss, E. Hauber, H. Hiesinger, and M. Zanetti (2014), Evidence for very recent melt-water and debris flow activity in gullies in a young mid-latitude crater on Mars, *Icarus*, *235*, 37–54, doi:10.1016/j.icarus.2014.03.005.

Malin, M. C., and K. S. Edgett (2000), Evidence for recent groundwater seepage and surface runoff on Mars, *Science*, *288*(5475), 2330–2335, doi:10.1126/science.288.5475.2330.

McEwen, A. S., C. M. Dundas, M. Chojnacki, and M. Massé (2016), Small martian gullies associated with recurring slope lineae (RSL), in *Martian Gullies and Their Earth Analogues*, London, United Kingdom (GBR).

Neuendorf, K. K. E., J. P. Mehl, and J. A. Jackson (2010), *The Glossary of Geology*, 5th editio., American Geological Institute, Alexandria, VA.

Scully, J. E. C., C. T. Russell, A. Yin, R. Jaumann, E. Carey, J. Castillo-Rogez, H. Y. McSween, C. A. Raymond, V. Reddy, and L. Le Corre (2015), Geomorphological evidence for transient water flow on Vesta, *Earth Planet. Sci. Lett.*, *411*, 151–163, doi:10.1016/j.epsl.2014.12.004.

Senthil Kumar, P., V. Keerthi, A. Senthil Kumar, J. Mustard, B. Gopala Krishna, Amitabh, L. R. Ostrach, D. A. Kring, A. S. Kiran Kumar, and J. N. Goswami (2013), Gullies and landslides on the Moon: Evidence for dry-granular flows, *J. Geophys. Res. E Planets*, *118*(2), 206–223, doi:10.1002/jgre.20043.

Shean, D. E. (2010), Evidence for widespread removal of martian mid-latitude “fill” material, *41st Lunar and Planetary Science Conference*, abstract 1509.

Shinbrot, T., N.-H. Duong, L. Kwan, and M. M. Alvarez (2004), Dry granular flows can generate surface features resembling those seen in Martian gullies., *Proc. Natl.*

Acad. Sci. U. S. A., *101*(23), 8542–8546, doi:10.1073/pnas.0308251101.

Stock, J. D., and W. E. Dietrich (2006), Erosion of steepland valleys by debris flows, *Bull. Geol. Soc. Am.*, *118*(9-10), 1125–1148, doi:10.1130/B25902.1.

Sylvest, M. E., S. J. Conway, M. R. Patel, J. C. Dixon, and A. Barnes (2016), Controls on sediment transport capacity of carbon dioxide sublimatio under martian conditions: Experimental results, in *Martian Gullies and Their Earth Analogues*, London, United Kingdom (GBR).

Treiman, A. H. (2003), Geologic settings of Martian gullies: Implications for their origins, *J. Geophys. Res.*, *108*(E4), 8031, doi:10.1029/2002JE001900.

Appendix A. Detailed thermal inertia values for Gasa Crater

Table A1. Thermal inertia of Gasa segments as marked in Figure 5A

Portion of Gasa	Average TI	Min TI	Max TI	Standard Deviation
Pitted material	312	281	359	18
NE wall (aprons)	374	282	486	32
NW wall (aprons)	375	275	490	42
SE wall (talus)[1]	436	324	607	54
SW wall (talus)	454	357	537	30
NE wall (alcoves)	488	350	720	76
NW wall (alcoves)	458	345	575	53
SW wall (alcoves)	509	405	722	53
NE wall (all)	436	282	720	84
NW wall (all)	412	275	575	62
SW wall (all)	482	357	722	52

[1]SW wall has no alcoves, so this measurement represents the entire wall.

Table A2. Thermal inertia of Gasa fans as marked in Figure 5B

1	O	306	293	318	10
2	O	311	297	331	13
3	O	314	303	331	10
4	O	316	293	331	13
5	O	319	280	378	27
6	O	325	284	375	29
8	O	333	303	377	30
9	O	336	308	357	18
10	O	337	305	365	20
11	O	339	321	357	18
13	O	343	334	359	10
14	O	345	337	355	9
16	O	345	327	374	18
17	O	349	332	380	15
18	O	350	325	379	18
19	O	350	304	375	29
20	O	353	336	361	11
21	O	354	344	365	15
22	O	355	328	374	19

23	O	355	345	368	8
25	O	359	345	373	10
26	O	360	346	376	12
27	O	362	310	401	30
30	O	365	350	386	11
31	O	367	338	388	18
32	O	370	334	401	19
33	O	372	341	418	31
37	O	378	361	393	15
41	O	386	334	418	27
50	O	400	385	417	13
51	O	401	385	417	12
56	O	408	393	422	10
7	Y	333	288	386	35
12	Y	342	282	401	35
15	Y	345	322	358	11
24	Y	357	340	372	14
28	Y	362	313	376	25
29	Y	364	335	405	21
34	Y	372	365	395	11
35	Y	373	365	380	5
36	Y	373	339	401	16
38	Y	381	362	398	10
39	Y	383	356	401	13
40	Y	386	370	401	9
42	Y	386	356	439	22
43	Y	387	375	401	8
44	Y	387	373	396	8
45	Y	390	384	400	7
46	Y	391	364	427	19
47	Y	391	374	401	11
48	Y	392	370	440	21
49	Y	398	389	414	10
52	Y	403	370	477	32
53	Y	404	402	406	2
54	Y	406	388	422	13
55	Y	406	382	442	26
57	Y	416	388	438	15
58	Y	420	394	468	29

59	Y	420	382	479	31
60	Y	421	383	448	34
61	Y	421	388	466	28
62	Y	423	376	512	50
63	Y	430	382	527	46
64	Y	430	387	525	36

[2]Note that fan number does not correspond in any way to the gully numbers shown in Figure 3.

Curriculum Vitae

Name:	Tanya N. Harrison
Post-secondary Education and Degrees:	University of Washington Seattle, WA, USA 2003–2006 B.Sc. (Astronomy and Physics) Wesleyan University Middletown, CT, USA 2006–2008, M.A. (Earth and Environmental Sciences)
Honours and Awards:	• Geological Society of America Paul Pellas-Graham Ryder Award for Best Student Paper in Planetary Sciences, awarded for papers published in 2015 (2016) • Amelia Earhart Fellowship (2014 & 2015) • Geological Society of America On to the Future Award (2014) • University of Western Ontario Research Western Award (2014) • Vanier Canada Graduate Scholarship (2014) • NASA Group Achievement Award, presented to the MSL Mastcam, MAHLI, & MARDI instruments team (2013) • Lunar and Planetary Institute Career Development Award (2013) • NSERC CREATE Technologies and Techniques for Space Exploration Ph.D. Fellowship (2012) • NSERC CREATE Canadian Astrobiology Training Program Ph.D. Fellowship (2012) • University of Western Ontario Graduate Research Scholarship (2012–2014) • NASA Group Achievement Award, presented to the MRO MARCI/CTX science team (2011) • NASA Connecticut Space Grant Scholar (2008) • Washington Promise Scholar (2003)
Related Work Experience	Research Assistant Department of Geology, Western University 2014–present Web Editor Intern The Planetary Society 2013–present

	Teaching Assistant Department of Geology, Western University 2012–2014 Assistant Staff Scientist Malin Space Science Systems 2008–2012 Researcher Departments of Astronomy and Earth and Space Sciences University of Washington 2006 & 2008 Teaching Assistant Department of Earth and Environmental Sciences Wesleyan University 2006–2008 Student Researcher Department of Earth and Space Sciences University of Washington 2005–2006
Publications	Guallini, L., M. S. Gilmore, L. Marinangeli, N. Thomas, and **T. N. Harrison**, Ancient Martian Lakestands and Fluvial Processes in Iani Chaos: Geology of Light-Toned Layered Deposits and Their Relationship to Ares Vallis Outflow Channels. Accepted to *Journal of Geophysical Research: Planets*. **Harrison, T. N.**, Osinski, G. R., and Tornabene, L. L. (2015), Global Documentation of Gullies with the Mars Reconnaissance Orbiter Context Camera and Implications for Their Formation. *Icarus 252*, 236–324. Williams, R. M. E., Irwin III, R. P., Burr, D. M., **Harrison, T. N.**, and McClelland, P. (2013), Variability in Martian Sinuous Ridge Form: Case Study of Aeolis Serpens in the Aeolis Dorsa, Mars, and Insights from the Mirackina Paleoriver, South Australia. *Icarus* 225, 308–324. **Harrison, T. N.**, M. S. Gilmore, and J. P. Greenwood (2012), Experimental VNIR Reflectance Spectroscopy of Gypsum Dehydration: Investigating the Gypsum to Bassanite Transition. *American Mineralogist* 97*,* 598–

	609. **Harrison, T. N.**, M. C. Malin, K. S. Edgett, D. E. Shean, M. R. Kennedy, L. J. Lipkaman, B. A. Cantor, and L. V. Posiolova (2010), Impact-Induced Overland Fluid Flow and Channelized Erosion at Lyot Crater, Mars. *Geophysical Research Letters* 37, L21201. Byrne, S., C. M. Dundas, M. R. Kennedy, M. T. Mellon, A. S. McEwen, S. C. Cull, I. J. Daubar, D. E. Shean, K. D. Seelos, S. L. Murchie, B A. Cantor, R. E. Arvidson, K. S. Edgett, A. Reufer, N. Thomas, **T. N. Harrison,** L. V. Posiolova, and F. P. Seelos (2009), Distribution of Mid-Latitude Ground Ice on Mars from New Impact Craters, *Science* 325, 1674–1676. Wallerstein, G., **T. Harrison,** U. Munari, and A. Vanture (2008), The Metallicity of Lithium Abundances of the Recurring Novae T CrB and RS Oph, *Publications of the Astronomical Society of the Pacific* 120, 867, 492–497.